THE NAVIGATION POTENTIAL OF SIGNALS OF OPPORTUNITY-BASED TIME DIFFERENCE OF ARRIVAL MEASUREMENTS

DISSERTATION

Kenneth A. Fisher, B.S.E.E., M.S.E.E.
Captain, USAF

AFIT/DS/ENG/05-02

DEPARTMENT OF THE AIR FORCE
AIR UNIVERSITY

AIR FORCE INSTITUTE OF TECHNOLOGY

Wright-Patterson Air Force Base, Ohio

REPORT DOCUMENTATION PAGE

Form Approved
OMB No. 0704-0188

PLEASE DO NOT RETURN YOUR FORM TO THE ABOVE ORGANIZATION.

1. REPORT DATE *(DD-MM-YYYY)*	2. REPORT TYPE	3. DATES COVERED *(From - To)*
05-27-2005	Ph.D. Dissertation	10Sep2005 - 27May2005

4. TITLE AND SUBTITLE

The Navigation Potential of Signals of Opportunity-Based Time Difference of Arrival Measurements

5a. CONTRACT NUMBER

5b. GRANT NUMBER

5c. PROGRAM ELEMENT NUMBER

6. AUTHOR(S)

Kenneth A. Fisher, Captain, USAF
kenneth.fisher@tyndall.af.mil
kapdma@gimail.af.mil

5d. PROJECT NUMBER

5e. TASK NUMBER

5f. WORK UNIT NUMBER

7. PERFORMING ORGANIZATION NAME(S) AND ADDRESS(ES)

Air Force Institute of Technology
2950 Hobson Way
Wright-Patterson AFB, OH 45433

8. PERFORMING ORGANIZATION REPORT NUMBER

AFIT/DS/ENG/05-02

9. SPONSORING/MONITORING AGENCY NAME(S) AND ADDRESS(ES)

Air Force Research Laboratory, Munitions Directorate
Eglin AFB, FL 32542

10. SPONSOR/MONITOR'S ACRONYM(S)

11. SPONSOR/MONITOR'S REPORT NUMBER(S)

12. DISTRIBUTION/AVAILABILITY STATEMENT

Approved for public release; distribution unlimited.

13. SUPPLEMENTARY NOTES

Advisor: John F. Raquet, AFIT/ENG // DSN: 785-3636 ext. 4580 // e-mail: john.raquet@afit.edu

14. ABSTRACT

This research introduces the concept of navigation potential, NP, to quantify the intrinsic ability to navigate using a given signal. NP theory is a new, information theory-like concept that provides a theoretical performance limit on estimating navigation parameters from a received signal that is modeled through a stochastic mapping of the transmitted signal and measurement noise. NP theory is applied to SOP-based TDOA systems in general as well as for the Gaussian case. Furthermore, the NP is found for a received signal consisting of the transmitted signal, multiple delayed and attenuated replicas of the transmitted signal, and measurement noise. Multipath-based NP captures the dominant error source foreseen in SOP-based navigation systems and may be more indicative of actual system performance than non-multipath-based metrics. NP theory applies to signals other than SOP. As an example, NP is used to bound GPS correlation error performance for the multipath and no-multipath case.

15. SUBJECT TERMS

Navigation, Information Theory, GPS, INS, Signals of Opportunity, SOP, Cramer-Rao Lower Bound, Fisher Information Matrix

16. SECURITY CLASSIFICATION OF:			17. LIMITATION OF ABSTRACT	18. NUMBER OF PAGES	19a. NAME OF RESPONSIBLE PERSON
a. REPORT	b. ABSTRACT	c. THIS PAGE			John F. Raquet, AFIT/ENG
U	U	U	SAR	257	19b. TELEPHONE NUMBER *(Include area code)* (937) 255-3636 ext. 4581

The views expressed in this thesis are those of the author and do not reflect the official policy or position of the United States Air Force, Department of Defense, or the U.S. Government.

AFIT/DS/ENG/05-02

THE NAVIGATION POTENTIAL OF SIGNALS OF OPPORTUNITY-BASED TIME DIFFERENCE OF ARRIVAL MEASUREMENTS

DISSERTATION

Presented to the Faculty

Department of Electrical and Computer Engineering

Graduate School of Engineering and Management

Air Force Institute of Technology

Air University

Air Education and Training Command

In Partial Fulfillment of the Requirements for the

Degree of Doctor of Philosophy

Kenneth A. Fisher, B.S.E.E., M.S.E.E.

Captain, USAF

March 2005

AFIT/DS/ENG/05-02

THE NAVIGATION POTENTIAL OF SIGNALS OF OPPORTUNITY-BASED TIME DIFFERENCE OF ARRIVAL MEASUREMENTS

Kenneth A. Fisher, B.S.E.E., M.S.E.E.

Captain, USAF

Approved:

/signed/	_____
Dr. John F. Raquet (Chairman)	Date
/signed/	_____
Dr. Peter S. Maybeck (Member)	Date
/signed/	_____
Dr. Michael A. Temple (Member)	Date
/signed/	_____
Dr. Mark E. Oxley (Member)	Date
/signed/	_____
Major Todd B. Hale, PhD (Member)	Date
/signed/	_____
Dr. Robert A. Canfield (Dean's Representative)	Date

Acknowledgements

There are only three times in a man's life when he screams like that: When he gets married, when he has his first son, and when he finishes a job he was crazy to start.[1] I've now experienced them all. Praise be to God!

Several people enabled me to finish this job. Dr. Raquet, my advisor, kept our eyes on the "big picture" while ensuring each step taken was correct and fruitful. More importantly, there is no substitute for a prayerful advisor! Dr. Maybeck has been an integral part of my entire 8-year Air Force career. This dissertation is no exception — his input was consistent, rigorous, and extensive! His intellect is surpassed only by his faith and compassion. Each member of my committee — Dr. Temple, Dr. Oxley, and Maj. Hale — helped me on a one-to-one level at some point in this process. Dr. Pachter and my sponsor, AFRL/MN, also supported this research. Finally, Dr. Canfield reviewed this research.

I thank my wife for supported me and our family. Without her, I would have never made it. My four children reminded me that AFIT is actually "small-potato stuff." This tour at AFIT will always be remembered with new babies, tumor surgery, Juvenile Rheumatoid Arthritis, football, hunting, John Deere gators, Barbie Jeeps, goats, and chickens.

I thank God for the ability to complete this work and the grace to live. I would offer some words of advice, but the best has already been written:[2]

Except the Lord build the house, they labor in vain that build it:

---

[1] Quoted from James Arness in the movie, *Red River*.

[2] Quoted from Solomon in Psalms 127.

except the Lord keep the city, the watchman waken but in vain. It is vain to for you to rise up early, to sit up late, to eat the bread of sorrows: for so he giveth his beloved sleep. Lo, children are a heritage of the Lord: and the fruit of the womb is His reward. As arrows are in the hand of a mighty man; so are children of the youth. Happy is the man that hath his quiver full of them: they shall not be ashamed, but they shall speak with the enemies in the gate.

Table Of Contents

Page

List of Figures

Page

List of Tables

Page

Abstract

This research introduces the concept of *navigation potential*, *NP*, to quantify the intrinsic ability to navigate using a given signal. In *information theory*, the Shannon Hartley capacity theorem provides the theoretical limit on the amount of information that may be recovered error-free over a bandlimited channel corrupted by Gaussian noise. As developed under this research, *NP* theory is a new, analogous concept that provides a theoretical performance limit on estimating *navigation* parameters from a received signal that is modelled through a stochastic mapping of the transmitted signal and measurement noise. Essentially, *NP* theory is an information theory-like concept applied to navigation systems and is particularly useful when using signals of opportunity (SOP) for navigation.

SOP-based time difference of arrival (TDOA) measurements are a promising positioning alternative when the Global Positioning System (GPS) is not available. SOP are signals that are transmitted for a purpose other than navigation; however, SOP may also be used for positioning if properly exploited. A SOP-based TDOA measurement navigation process, for which the navigation solution may be found using well known GPS techniques, is introduced.

NP theory is applied to SOP-based TDOA systems through the proper selection of a stochastic mapping. When the stochastic mapping assumes a rather simple model, e.g., the received signal is the transmitted signal in additive, Gaussian noise, *NP* results validate previously established performance metrics. In addition, by using a multipath mapping, the *NP* may be found for a received signal consisting of the

transmitted signal, multiple delayed and attenuated replicas of the transmitted signal, and measurement noise. This innovative development captures the dominant error source foreseen in SOP-based navigation systems; consequently, multipath-based *NP* may be considered a better predictor of actual system performance than metrics based on the transmitted signal in measurement noise alone.

The general nature of *NP* theory accommodates its application to signals other than SOP. As an example, *NP* is used to predict GPS correlation error performance. *NP* provides novel theoretical performance bounds on GPS correlation error for the case in which the stochastic mapping is chosen to be a multipath mapping. Prior to this research, no theoretical performance bounds on GPS correlation error were available that address multipath. When the mapping is chosen to be the transmitted signal in measurement noise alone (i.e., no multipath), *NP* provides additional insight beyond, yet consistent with, previously developed GPS correlation error performance bounds.

The Navigation Potential of Signals of Opportunity-Based Time Difference of Arrival Measurements

Chapter 1 - Introduction

This research introduces the concept of *navigation potential* to quantify the intrinsic ability to navigate from a given signal. In *information theory*, the Shannon Hartley capacity theorem provides the theoretical limit on the amount of information that may be recovered error-free over a Gaussian noise-corrupted, bandwidth-limited channel [36, 70]. *Navigation potential* theory is a new, analogous concept that provides a theoretical performance limit on estimating *navigation* parameters from a received signal. Essentially, navigation potential theory is an information theory-like concept applied to navigation systems. Navigation potential, by itself, is defined as a scalar metric that quantifies the ability to estimate navigation parameters of interest. For example, just as information theory predicts that an arbitrarily large amount of information may be recovered error-free from a noiseless, bandwidth-limited channel, navigation potential predicts that the error in the navigation parameters' estimates using a transmitted signal absent of measurement noise may be arbitrarily small.

This dissertation is dedicated to the development of navigation potential theory. Presented herein is the motivation for navigation potential theory, previous results which provide insight into navigation potential theory, background material necessary for understanding the mathematics of navigation potential theory, the formal derivation of navigation potential theory, and selected applications that demon-

strate navigation potential theory. The remainder of this chapter will motivate and overview this research, state the research contributions, and outline the remainder of this dissertation.

1.1 Research Motivation and Overview

The Global Positioning System (GPS) has revolutionized position determination on Earth. Systems and applications have become dependent upon reliable and accurate position determination. There are many navigation alternatives when GPS navigation solutions are unattainable or degraded. An area of recent interest in the literature [18, 34, 35, 62] is the navigational use of "signals of opportunity," or SOP.[1] SOP are signals that are transmitted for non-navigation purposes, but can be exploited for navigation using various techniques. SOP are convenient sources of navigation, in part, because they are often more numerous, and at a higher signal-to-noise ratio at the receiver, than GPS signals [34].

Given a limited ability as to the number of SOP that may be exploited, SOP navigation entails a process of selecting which SOP to exploit from the numerous possibilities. Since each SOP may possess unique transmitted signal and expected measurement noise characteristics, this research motivates that the proper selection of *which SOP to exploit* should be based, in part,[2] upon the theoretical navigation potential of a given SOP. Prior to the navigation potential theory developed in this research, SOP were chosen based upon their coverage areas and signal structures

[1]Throughout this dissertation, SOP may be used to denote either "signal of opportunity" or "signal*s* of opportunity". The plurality should be apparent from the context.

[2]Coverage area, desired frequency bands, etc. are also factors in selecting SOP.

(from the perspective of preferring either well-understood, simple signals or signals with synchronization pulses). There was no rigorous method to determine the potential navigation performance of a proposed SOP. The navigation potential theory developed in this research enables a designer to compare and select SOP based upon the theoretical performance bounds of the resulting navigation solution.

Navigation potential (*NP*) is developed based upon a stochastic mapping of the transmitted signal and measurement noise into the received signal. This approach enables the designer to select mappings consistent with the received signal's anticipated relationship with the transmitted signal and measurement noise. Then, the *NP* of the *received* signal quantifies the ability to determine the navigation parameters of interest in terms of the transmitted signal and measurement noise. *NP* relates signal characteristics to the ability to navigate through the Fisher Information Matrix (FIM) [43]. The FIM provides performance bounds on parameter estimates from a given signal (through its probability density function). The FIM is well-known for a signal without noise, or a signal in additive, measurement noise, given the signal and noise joint probability density function [28, 43, 82]. *NP* theory benefits from these results when the mappings are chosen such that the received signal is the transmitted signal in additive measurement noise, although the *NP* framework is not limited to these rather simple mappings.

The general approach of *NP* theory may be used to predict navigation performance for a wide variety of received signal models for which no performance metrics were previously available. For example, through the proper selection of a multipath mapping, the *NP* may be found for a received signal consisting of the transmitted

signal, multiple delayed and attenuated replicas of the transmitted signal, and measurement noise. Multipath-based *NP* is considered a better predictor of the actual system performance than that of a metric based upon the transmitted signal in measurement noise alone, since significant multipath is often a factor for navigation [18]. This result, in and of itself, is an innovative development, since multipath is the dominant error source foreseen in SOP-based navigation systems.

While SOP navigation provides a motivation for creating *NP* theory, the general nature of *NP* accommodates its application to signals other than SOP. As an example, *NP* may be used to predict GPS correlation error performance. *NP* provides novel theoretical performance bounds on GPS correlation error for the case in which the stochastic mapping is chosen to be a multipath mapping. Prior to this research, no theoretical performance bounds on GPS correlation error which address multipath were available. When the mapping is chosen to be the transmitted signal in measurement noise alone, *NP* provides additional insight over, yet is consistent with, previously developed GPS correlation error performance bounds.

1.2 Research Contributions

The focus of this research is the development of *NP* theory. In the previous section, specific mappings and signals were referenced to motivate this research; *NP* theory is not confined to, or limited by, these constraints. This section details more clearly (than the previous section) the specific, claimed research contributions of this dissertation.

1.2.1 Navigation Potential (NP) Theory

The primary contribution of this research is *NP* theory, or the concept of characterizing the ability to estimate parameters of interest, given a received signal. This new thought process provides a selection criterion that addresses the needs of the navigation user—namely, it answers the question, "How well may this signal be used for navigation?" *NP* theory enables a wide variety of signals' navigation ability to be predicted and compared.

1.2.2 NP for Signals in Multipath and Noise

NP theory is applied to a received signal modeled as the transmitted signal, attenuated and delayed replicas of the transmitted signal, and measurement noise. Prior to this research, no performance bounds were available that addressed estimating navigation parameters from a received signal with multipath effects. This novel result is a significant contribution to radio-frequency-based navigation, since multipath is a major error source in most radio-frequency-based navigation systems.

1.2.3 Predicting GPS Correlation Error Performance Bounds

This research uses *NP* theory to predict GPS correlation error performance bounds for the case in which the received signal contains multipath signals. Prior to this research, no theoretical performance bounds were available that address this issue. Since multipath is the dominant error source for code-tracking GPS, this contribution provides significant and much needed insight into GPS correlation error performance. When multipath is absent, *NP* provides insight over, yet is consistent with, previously published performance bounds.

1.2.4 SOP Navigation Process

This research presents a systematic process for using SOP-based time difference of arrival (TDOA) measurements for navigation. This new process may be applied over a wide range of SOP, thereby introducing a more universal SOP navigation approach than previous SOP navigation methods. Signal selection is addressed appropriately with the newly-found *NP*. Furthermore, the navigation solution is a novel approach that permits SOP-based TDOA measurements to be used in well-understood GPS algorithms.

1.3 Dissertation Outline

Chapter 2 motivates using time difference of arrival (TDOA) measurements obtained from signals of opportunity (SOP) as an alternative to GPS navigation and provides the background upon which this research is based. Chapter 3 presents a systematic SOP navigation approach to standardize SOP navigation, to apply SOP-based TDOA measurements to a well-known navigation algorithm, and to motivate the development of the navigation potential (*NP*).

Chapter 4 presents the concept of *NP*. A multipath model and the resulting *NP* are developed. Furthermore, the *NP* is found for the case in which the received signal may be appropriately modeled as a Gaussian process.

Chapter 5 validates and demonstrates *NP* theory with several examples. First, it is shown that previous performance metrics are special cases of *NP*. Second, it is shown that GPS correlation error performance can be predicted using *NP* theory for the case in which the received signal is the transmitted signal in measurement noise.

Finally, GPS correlation error performance is developed using *NP* theory for the case in which the received signal is modeled as the transmitted signal with multipath and noise. Chapter 6 provides a research summary and an outline for future research.

Several appendices provide supporting details to the developments in the main document. Appendix A reviews common analog modulation techniques frequently used in SOP. Appendix B presents SOP examples that may be used for navigation. Appendix C lists several probability density identities used in the development of navigation potential. Appendix D outlines stochastic Fourier analysis. Appendix E develops the autocorrelation kernel for a stochastic process formed as the Fourier transform of a finite time-length observation of a stochastic process.

Chapter 2 - Signals of Opportunity Background

2.1 Introduction

This chapter introduces navigation alternatives to the Global Positioning System (GPS), summarizes previous exploitations of signals of opportunity (SOP) for navigation, and describes traditional time difference of arrival (TDOA) navigation. SOP are transmitted for a primary application other than navigation, yet with clever techniques, they can also be used for navigation. One motivation for navigation potential theory, developed later in this dissertation, is to provide a selection criterion for SOP based upon how well a SOP may be used for navigation. This chapter motivates that the exploitation of SOP for navigation is a promising navigation method.

Section 2.2 compares traditional navigation methods, exploiting SOP for navigation, and other navigation methods. Section 2.2 also motivates using TDOA measurements obtained from signals of opportunity (SOP) rather than other SOP exploitation techniques.

The remainder of this chapter provides the background necessary to become familiar with SOP and TDOA measurements, to prepare the reader for the new developments that follow in subsequent chapters. Section 2.3 provides a summary of the research conducted with SOP. Section 2.4 presents the current formation and application of TDOA measurements. Finally, Section 2.5 provides a summary.

2.2 Alternatives to GPS Navigation

The Global Positioning System (GPS) provides an accurate position determination in a variety of environments. It is not surprising that the demand for such

information is growing beyond the capability that GPS can provide. GPS is a line-of-sight (LOS) system—that is, the satellites must be in "view" of the receiver antenna to receive the signal. Efforts are made to reduce this limitation, most notably in urban areas and indoors. Urban areas are characterized by tall buildings, which block satellites from view and create multipath signals. Antennas indoors are not generally in view of the satellites; although in the 1-2 GHz region, the signals are present but greatly attenuated.

Several methods to aid in GPS navigation, or to navigate without GPS, are presented in this section. The objective of this section is to familiarize the reader with these methods and motivate that navigation using signals of opportunity (SOP) is the most promising alternative to GPS navigation. Similar to GPS, each method discussed is self-solving and passive. With *self-solving navigation*, the user's position is determined by the user. For example, a satellite image used to locate the user is not considered a self-solving technique. With *passive navigation*, the user at the location to be determined does not transmit anything, and this provides the benefits of reduced power consumption, maintaining covert operations, allowing unlimited users, etc.

Besides self-solving and passive, each method discussed also falls into one of two solution categories—absolute or incremental. *Absolute navigation* determines the user's position without prior knowledge of the user's position. *Incremental navigation* determines the change in the user's position from one time to another. When combined with knowledge of the user's starting position, incremental position can be used to determine the user's position (e.g., inertial navigation systems). Absolute positioning does not require knowledge of a prior position, allowing the user the ability

to regain a position solution after losing track. The remainder of this section details possible self-solving, passive navigation techniques that can be used as an alternative to GPS positioning or to improve upon GPS positioning in urban areas or indoors.

2.2.1 Traditional Navigation

Traditional navigation techniques are forerunners to current GPS methods and generally provide poorer accuracy than GPS; however, each alternative method may aid navigation in urban areas or indoor environments. This non-exhaustive navigation list includes celestial navigation, long-range navigation, and an inertial navigation system.

2.2.1.1 Celestial Navigation. A user's absolute position can be derived by observing distant stars with a sextant, star charts, and a chronometer. Precise setup, precise star charts, and a timing accuracy on the order of 1 msec are required for celestial navigation to approach GPS-like accuracy [12]. The United States Naval Observatory (USNO) maintains precise star charts and has implemented such a scheme [12]. Another celestial navigation method is incremental navigation using time difference of arrival (TDOA) measurements from x-ray pulsars. [17, 69, 74]

2.2.1.2 Long-Range Navigation (LORAN). LORAN is a federally provided navigation system for civil marine use in all of the coastal and inland navigable waters and FAA-approved for use in the U.S. airspace. Loran-C, the system in use today, covers much of the northern hemisphere and performs hyperbolic positioning through the time-difference of arrival (TDOA) of *synchronized* pulse signals from a "chain" of towers [53]. A typical chain consists of a master and 2-3 secondary tow-

ers separated by approximately 1000 km. Each tower transmits high-power (1 MW peak), synchronized pulses in the 90 to 110 kHz region. Loran-C provides a horizontal position accuracy of approximately 250 m and is expected to be operation until 2008. [53]

2.2.1.3 Inertial Navigation System (INS).

An INS is fundamentally different from GPS in many ways. INS does not require receipt of any signal; consequently, performance is independent of location (whether in urban areas or indoor environments). INS is an incremental navigation technique; its solution is based upon incremental position changes from a *given* initial position. The INS position solution cannot be more accurate than the initial position accuracy [76]. Furthermore, the error in each increment accumulates over time, and INS is characterized by an RMS position error that increases over time (called INS drift). Consequently, the initial position accuracy, drift rate, and elapsed time since the initial position affect the accuracy of the current INS-computed position estimate.

2.2.2 Signals of Opportunity (SOP)

SOP are signals from land-based or space-based transmitters that are transmitted for a purpose other than navigation; however, they can be used also for navigation through proper exploitation. (Refer to Appendix B for several examples.) Their exploitation is challenging, because the signal transmissions are generally unsynchronized, the transmit time is unknown, and signal is not maintained by the navigational user. In urban areas, SOP can provide many measurements which may potentially be used to overcome blocked signals and identify multipath signals through a Receiver

Autonomous Integrity Monitoring (RAIM) technique [57]. Signals of opportunity have a much higher received signal power, possibly allowing the signals to be received and exploited indoors. The following list is based upon the *exploitation method* used with signals of opportunity:

2.2.2.1 Angle of Arrival (AOA). AOA measurements can be made using an antenna triad by comparing the received signal into each of the three antennas. A triad with 1m spacing between antennas may provide an absolute position with an accuracy on the order of tens of meters using satellites in the K-band [12].

2.2.2.2 Time of Arrival (TOA). If signals of opportunity that transmit precise time information and ephemeris data exist, TOA measurements can be used for absolute navigation via trilateration. If the user has precise *a priori* knowledge of the transmit time or transmitter location, that information need not be transmitted. This closely resembles the GPS system.

2.2.2.3 Time Difference of Arrival (TDOA). If the location of a signal transmitter is known (or transmitted), TDOA measurements can be used for absolute navigation via hyperbolic positioning [53]. TDOA measurements are formed by differencing the arrival time of two signals by a single receiver, or by differencing the arrival time of a single signal at two separate receivers. Both formulations are useful when the actual transmit time of the signal is not known. The former case, discussed in more detail in Section 2.4.1, is useful when the relative difference in transmission time between the two signals is known (requiring synchronized transmissions). The

latter case, discussed in more detail in Section 3.2, is useful when the bias in the measured received time at the two receivers is known or remains constant over some interval.

2.2.3 Other GPS Alternatives

2.2.3.1 Object Tracking. Algorithms which track objects within successive images may be used to determine the user's change in position for incremental navigation [79]. This method's appeal is that it does not require object identification (that is, a physical description of the object) or object location This method does, however, require object detection within each image and the ability to track objects within successive images.

2.2.3.2 Satellite Tracking. Similar to that which is done with celestial bodies, satellites can be tracked using a telescope for absolute navigation [12]. This method relies upon the ability to locate the satellite *optically*, and does not require a satellite transmission. Since satellites are at a lower altitude than celestial bodies, a satellite-derived position solution can be more accurate than a celestial-body-derived position solution, assuming the same angular precision is obtained in both cases.

Alternatively, for a given position accuracy requirement, the angular measurement precision requirements for satellite tracking is less stringent than for celestial tracking. Consequently, the equipment setup precision requirements for satellite angular tracking may be more feasible in the field than those of celestial tracking [12]. As with celestial tracking, satellite tracking requires precise knowledge of the satellite location.

2.2.3.3 Gravimetry.

High-precision gravimetric instruments can be used to measure the local gravity. When these measurements are combined with a database of highly accurate gravitation corrections, an absolute position may be obtained with an accuracy on the order of 10-15m (at mid-latitude) [12]. A notable disadvantage of this method compared to GPS is that high-precision gravimetric instruments are not as easily transported as GPS receivers [12].

2.2.4 Comparison of Navigation Alternatives to GPS

Of the techniques listed, SOP are convenient sources of navigation for the following reasons:

1. SOP are abundant. (To demonstrate this claim, selected SOP examples are given in Appendix B.) This characteristic is useful for reducing the position error and ensuring that sufficient signals are available for position determination.

2. The signal-to-noise ratio is often higher than for signals such as GPS [34].

3. SOP provide the potential for accuracy similar to that of GPS [34].

4. There are no deployment costs or operating expenses related to the signal for the navigational user. Of course, there would be costs associated with the equipment used for navigation (such as receivers).

Additionally, using SOP to form TDOA measurements using two separate receivers (coined "SOP-based TDOA navigation") is the most appealing alternate to GPS navigation for the following reasons:

1. SOP-based TDOA navigation is an absolute navigation technique (as are all of the techniques except for INS navigation and object tracking).

2. SOP-based TDOA navigation may allow physically smaller user equipment relative to celestial, object tracking, satellite tracking, gravimetry and SOP using AOA techniques [12].

3. Forming TDOA measurements may be less complicated than object tracking.

4. SOP-based TDOA navigation does not require knowledge of the transmit time, unlike exploitation of SOP using TOA measurements.

5. SOP-based TDOA measurements may be formed via the two-receiver method discussed in Section 2.2.2.3 without requiring synchronized transmitters.

2.3 Previous Exploitations of Signals of Opportunity

This section outlines the most relevant research efforts in exploiting signals of opportunity (SOP) for navigation. Extensive research is being conducted in the use of cellular phones for navigation [26]. These efforts are not discussed here, since all current methods require the receiver to transmit [26] which violates the passive navigation constraint presented in Section 2.2 (and in Section B.1 of Appendix B). Standard broadcasting, analog television, and digital television are the only SOP currently being investigated, and they are discussed in Sections 2.3.1, 2.3.2, and 2.3.3, respectively. Finally, passive coherent location (PCL), a related application of SOP, is introduced in Section 2.3.4 and compared to navigation with SOP.

2.3.1 Standard Broadcasting

Hall, Counselman, and Misra [34] explored the use of standard broadcasting signals (discussed in Section B.2.1 of Appendix B on page 174) for a variety of venues: outdoors in the clear, in woods, and in an urban area (Boston, MA); and inside a wood-frame house. World-wide availability, long wavelengths suitable for indoor and underwater navigation, and a simple receiver design were reasons for choosing standard broadcasting. The authors point out the following characterizations of AM signals (compared to GPS signals): nearby, ground-based, stationary transmitters; high SNR; broad frequency range (3:1); long wavelengths; unsynchronized transmitter oscillators; poor transmitter frequency accuracy and stability; and modulation not designed for navigating.

The navigation scheme applied was similar to a differential carrier phase GPS application. The base station was at a known location, while the rover was to be determined. The amplitude, frequency, and phase of each AM signal at each station was recorded. Since the phase observable is ambiguous, preliminary studies were conducted without resolving the ambiguities. In these preliminary studies, the rover started at a *known location* and phase increments at each epoch were constructed. An epoch, or update period, of 5 seconds was chosen based upon the rover dynamics and oscillator stability. Double-difference phase increments were used in a least-squares algorithm to solve for the *incremental* position corrections at each epoch. [34, 35]

Realizing the limitations of a system that needs an accurate initial position and that must maintain lock, an ambiguity resolution approach, called the Ambiguity Function Method [13, 14, 35], was incorporated. Position space ambiguity resolution

was accomplished by *maximizing* a cost function at each epoch (independent of the solutions at other epochs). Unlike GPS ambiguities, AM signals' double-difference measurement space ambiguities are not integer-valued in general. Because the carriers of AM broadcast stations are spaced 10 kHz apart (see Figure 19 on page 175), the ambiguity function used is periodic with a period $T = \frac{1}{10 \text{ kHz}} = 100$ μsec [34, 35]. To avoid this ambiguity, the receiver clock offset was required to be known *a priori* within 100 μsec. This was accomplished by transmitting a synchronization pulse at the start of the experiment. The clock drift was tracked by comparing the relative received signal frequencies at the base and mobile receivers. The authors mention a more clever approach might be to cross-correlate the received signals at the base and mobile receivers. The offset where the peak correlation occurs can be used to obtain the clock bias. The clock bias was searched within a 100 μsec window of the estimate with step sizes equivalent to ten percent of the shortest wavelength in the AM band. A brief calculation estimates this value to be 0.6 nsec, resulting in 166,000 increments in the t direction.

It was demonstrated that the AM-only system has meter-level accuracy outdoors for baselines up to two kilometers, and its accuracy is only slightly degraded for baselines up to 35 kilometers. The authors cite that the chief, and practically the only significant, cause of error for the AM-only system is close proximity to extended electrical conductors, such as power transmission lines and conductors underground, in nearby buildings and inside a wood-frame house. Foliage, as in woods, had no significant effect on the AM system. When an AM navigation receiver and a stand-alone GPS receiver were driven under foliage, the following results were observed: (1) the

AM system performance was not degraded, (2) the GPS performance under foliage was poorer than that of unimpeded GPS performance, and (3) the GPS performance under foliage was poorer than that of the AM system under foliage.

2.3.2 NTSC Television

Eggert and Raquet [18, 19] evaluated the navigation potential of the National Television System Committee (NTSC), analog television broadcast signal using TDOA measurements obtained from NTSC broadcast signals collected in low and high multipath environments. (Analog television signals are discussed in Section B.2.3 of Appendix B on page 179.) These measurements were then used to evaluate the severity and dynamic effects of NTSC broadcast multipath signals. Three data reduction algorithms were developed—one that modifies the classical cross-correlation TDOA approach, and two that difference the signals' arrival time at each receiver. Multipath was shown to be the dominant error source; however, errors due to the particular hardware configuration were also significant.

Simulations were performed using eight television station locations near Dayton, Ohio. Typical results for overall position error and TDOA measurement error were found to be 40 meters and 10-40 meters, respectively. Extreme measurement errors from high multipath areas reduced the overall position accuracy to 100 meters. Additionally, using the same transmitter geometry, simulation results showed that a TDOA measurement error in the range of 5 to 10 meters was required to provide position estimates with 10 meter accuracy—the accuracy of readily available single frequency GPS receivers.

2.3.3 Digital Television

With a focus on Enhanced 911 [26], Rosum Corporation has been exploring the exploitation of digital television (DTV) transmissions and cellular communications for cellular phone location services. It was proposed that the synchronization sequence $\{-1, +1, +1, -1\}$ from a local DTV station could be "tracked" using either software or hardware correlation techniques. (DTV is discussed in Section B.2.4 of Appendix B on page 185.) Rosum [62, 63] conducted preliminary dilution of precision (DOP) calculations for current transmitter locations and analyzed tracking the DTV signal and analyzed the feasibility of navigating with DTV. The authors cite that the DTV signal can accommodate robust indoor positioning where GPS tends to fail, since the synchronization signals typically have a power advantage over GPS of more than 40dB. In addition, the effects of multipath are substantially mitigated since the signals have a bandwidth of roughly 6 MHz, and considerably superior position geometry over that which GPS can provide.

2.3.4 Passive Coherent Location

RAdio Detection and Ranging (RADAR) is used to locate a user by energizing the user with a radio frequency transmitter and analyzing the return emissions received by a receiver. In monostatic radar, the transmitter and receiver are collocated; whereas in bistatic radar, the transmitter and receiver are not collocated [33, 81]. Passive coherent location (PCL) is a form of bistatic radar for which the transmitted signal is a signal of opportunity. Lockheed Martin developed the *Silent Sentry*® system to use everyday broadcast signals, such as those for television and radio, to illuminate, detect and track targets [3,33]. Thus, the system is passive, since the receiver does not

transmit (and the transmitter is considered to be part of the everyday environment). It does not provide a self-solving navigation solution; however, its use of signals of opportunity merits discussion.

The effects of various signals of opportunity on PCL have been explored [61]. For example, wideband systems should provide greater accuracy over narrowband systems [71]. Most PCL literature is based on FM broadcasts and analog TV signals [10, 32, 33, 39, 40, 65]. Guner [33] compares the use of different signals of opportunity. If an AM broadcast carrier, or the audio or video carrier of an analog TV signal is used, then a narrowband PCL system uses Doppler analysis and Angle of Arrival (AOA) measurements to estimate the range, position and velocity of a target. Using FM broadcast signals, time difference of arrival (TDOA) measurements obtained through matched filtering can achieve a range resolution of 2.0 km [65]. Silent Sentry®, the first off-the-shelf, commercially available PCL product, uses FM broadcasts as the SOP [3, 33].

2.3.5 Summary

In this section, previous SOP exploitations have been summarized. AM broadcast exploitation, analog and digital TV exploitation, and passive coherent location (PCL) were detailed. AM and analog TV research efforts were direct applications of passive, self-solving navigation using SOP. (Digital TV and PCL are not passive, self-solving navigation schemes; however, their use of SOP merited their inclusion.) Two themes emerge from the SOP navigation efforts:

1. Each exploitation technique is an innovative method to navigate with a specific

SOP (or specific set of SOP), and

2. The exploited SOP were chosen based upon their coverage areas and signal structures (from the perspective of preferring either well-understood, simple signals or signals with synchronization pulses), not the anticipated performance of the resulting navigation solution.

The first issue will be addressed in Chapter 3 by introducing a navigation process applicable to a wide range of SOP. The second issue will be detailed more completely in Chapter 3 and finally resolved with navigation potential theory in Chapter 4. The following section discusses time difference of arrival measurements to complete the background needed to use signals of opportunity to form time difference of arrival measurements (and to use these measurements for navigation).

2.4 Traditional Time Difference of Arrival

This section presents the traditional method used to form time difference of arrival (TDOA) measurements. Navigation using signals of opportunity (SOP)-based TDOA measurements will be formalized in the next chapter. While the TDOA measurements used in subsequent chapters are *not* found using the traditional form described herein, this section presents traditional TDOA in Section 2.4.1 to provide background for the two-receiver method proposed later (in Section 3.2). Section 2.4.2 discusses specific applications of traditional TDOA. Finally, Section 2.4.3 summarizes the insights that will be useful when the TDOA formulation is altered in Section 3.2 to accommodate SOP.

2.4.1 Traditional Time Difference of Arrival Development

The traditional time difference of arrival (TDOA) measurement situation is shown in Figure 1. Shown is exactly one transmitter with N receivers. Each receiver location is known, while the transmitter location will be determined through the measurements. The signal $s(t)$ is transmitted at time t_t by the transmitter and is received by the i^{th} receiver at time t_i.

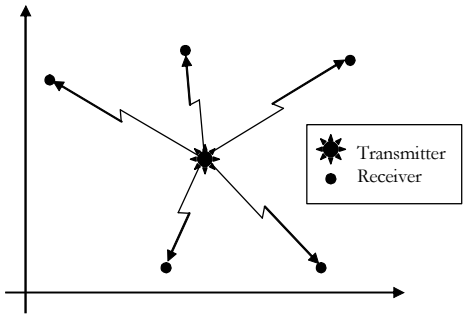

Figure 1. Traditional TDOA

The time difference of arrival measurement in seconds, δ_{ij}, is the time difference of arrival of the signal to the i^{th} receiver compared to the j^{th} receiver, or

$$\delta_{ij} = t_i - t_j \tag{2.1}$$

Converting times into distances by multiplying by the speed of the signal (assumed to be the speed of light, c), Equation (2.1) becomes

$$c\delta_{ij} \triangleq \Delta_{ij} = ct_i - ct_j \tag{2.2}$$

$$= (ct_i - ct_t) - (ct_j - ct_t) \tag{2.3}$$

$$\Delta_{ij} = d_i - d_j \tag{2.4}$$

where t_t is the unknown time of transmission and d_i is the distance from the transmitter to the i^{th} tower. Equation (2.4) relates the TDOA measurement in meters to the distances from the transmitter to the i^{th} and j^{th} towers; some authors appropriately refer to this as the range-difference measurement [72].

The extension for multiple, synchronized receivers has also been made. For convenience, let an arbitrary receiver be the *reference receiver*, denoted with $i = 0$, and label the remaining receivers $i = 1, \cdots, N-1$. Define a local coordinate system in Earth-centered, Earth-fixed (ECEF) coordinates such that the reference receiver is located at the origin, $\mathbf{x}_0$, the remaining receivers are located at $\mathbf{x}_i$, and the transmitter is located at $\mathbf{x}_t$, i.e.,

$$\mathbf{x}_0 = \mathbf{0} \qquad \mathbf{x}_i = \begin{bmatrix} x_i \\ y_i \\ z_i \end{bmatrix} \qquad \mathbf{x}_t = \begin{bmatrix} x_t \\ y_t \\ z_t \end{bmatrix} \tag{2.5}$$

The relative distances from the reference receiver to the i^{th} receiver and from the transmitter to the i^{th} receiver, denoted with d_0^i and d_t^i, respectively, may be written as

$$d_0^i = \|\mathbf{x}_i - \mathbf{x}_0\| = \|\mathbf{x}_i\| = \sqrt{x_i^2 + y_i^2 + z_i^2} \tag{2.6}$$

and

$$d_t^i = \|\mathbf{x}_i - \mathbf{x}_t\| = \sqrt{(x_i - x_t)^2 + (y_i - y_t)^2 + (z_i - z_t)^2} \tag{2.7}$$

$$= \sqrt{x_i^2 + y_i^2 + z_i^2 - 2(x_i x_t + y_i y_t + z_i z_t) + x_t^2 + y_t^2 + z_t^2} \tag{2.8}$$

$$= \sqrt{\|\mathbf{x}_i\|^2 - 2\mathbf{x}_i^T \mathbf{x}_t + \|\mathbf{x}_t\|^2} \tag{2.9}$$

A TDOA system is comprised of the measurements given in Equation (2.4) for all of the receivers; that is, for N receivers one can form $N-1$ measurements. Without loss of generality, assume each TDOA measurement is formed using the reference receiver, i.e., $j = 0$ in Equation (2.4). Using the relationships in Equations (2.6) and (2.9), Equation (2.4) becomes

$$\Delta_i = d_t^i - d_0^i \tag{2.10}$$

$$= \sqrt{\|\mathbf{x}_i\|^2 - 2\mathbf{x}_i^T \mathbf{x}_t + \|\mathbf{x}_t\|^2} - \|\mathbf{x}_i\| \tag{2.11}$$

for $i = 1, \cdots, N-1$. Notice that each Δ_i is measured (with noise), $\mathbf{x}_i$ is known *a priori*, and $\mathbf{x}_t$ is the desired unknown – resulting in a system of $N-1$ equations with three unknowns (each element in $\mathbf{x}_t$). Several exact solutions to this non-linear system of equations have been presented [4, 5, 11, 49, 50, 72] in addition to linearized iterative techniques [27, 77], non-iterative approximations [11], and search algorithms [1].

2.4.2 Applications of Traditional TDOA

Traditional TDOA has been used extensively to locate a transmitter through TDOA measurements from receivers at known locations. Clearly, locating the *transmitter* is not a passive navigation technique! Nonetheless, the following examples serve to clarify how traditional TDOA is used.

2.4.2.1 *Search and Rescue Satellites (SARSAT).*

Search and Rescue Satellites (SARSAT) employ a TDOA system to locate the distress signal of a ship or other vehicle equipped with the appropriate transmitter [67]. In an emergency, a vessel transmits a sinusoidal wave at a known frequency. Satellites receive the signal and transmit the received time to a ground station. The ground station calculates the position of the satellites (the receivers in this case) using ephemeris data. Finally, an algorithm such as one discussed previously in Section 2.4.1 is used to locate the vessel, or transmitter. Several algorithms have been developed specifically for the "stranded ship" application by including the additional constraint that the transmitter is on the surface of the Earth (or mean sea level), modelling the surface of the Earth as a sphere [37] or an ellipsoid [38]. This additional constraint allows the minimum number of satellites in view to be reduced from four to three. Other algorithms have included the use of the Doppler shift of the received signal in a Frequency Difference of Arrival (FDOA) algorithm. [38]

2.4.2.2 *Global Positioning System (GPS) Jammer Location.*

Mellen introduced a method to determine the location of a GPS jammer using a time difference of arrival (TDOA) technique with multiple GPS receivers at known locations [49, 50]. The transmitter and receivers are all synchronized (except for local oscillator phase) to GPS-like accuracies. The transmitted signal is colored Gaussian noise. The TDOA measurements are obtained by cross-correlating the received signal with a reference signal. The transmitter location is then estimated based on

the range difference measurements and known sensor locations using a "closed-form signal source location algorithm".

2.4.2.3 LORAN. LORAN, previously discussed in Section 2.2.1.2, uses synchronized transmitters to allow a receiver to determine its location. Because the receivers are synchronized, the navigation problem and solution are the dual of traditional TDOA presented in Section 2.4.1. (Note that duality does not hold for unsynchronized transmitters. The unsynchronized case is discussed in Section 3.2.)

2.4.3 Remarks on Traditional TDOA

With the development of traditional TDOA in place and examples supporting its use, several observations can be made with the anticipation of applying these measurements to existing signals.

1. Since t_t cancelled when deriving Equation (2.4), the transmit time need not be known. Furthermore, the transmitter clock does not affect the TDOA measurement other than for signal integrity. Thus, precise clocks may not be necessary.

2. Essential to traditional TDOA (so much so, that in most papers its fact is omitted! [11, 20, 37, 38]) is that all the receivers' clocks *must* be synchronized. This requirement (of synchronized receivers) is not overly restrictive when *designing* a TDOA location system; however, as will be shown in Section 3.2, this constraint must be lifted to apply TDOA measurements to *existing* non-synchronized systems.

3. It is acknowledged that synchronization is not perfect, and the synchronization error is generally accepted as the error in the TDOA measurement [4].

4. A TDOA measurement may be obtained by cross-correlating the signals received at two receivers.

2.5 Conclusion

This chapter motivated and provided the background for using SOP-derived TDOA measurements for navigation. Section 2.2 motivated using SOP-derived TDOA measurements over the other alternate methods presented. Section 2.3 presented three current research efforts using SOP for navigation: AM broadcast exploitation, digital television exploitation, and passive coherent location. Finally, Section 2.4 presented traditional TDOA with its development and application.

With the insight gained from previous SOP exploitations and traditional TDOA, the next chapter presents a systematic approach to SOP navigation using TDOA measurements. Furthermore, this systematic approach may provide the foundations for expressing the navigation potential of a SOP.

Chapter 3 - Navigation Using Signals of Opportunity

3.1 Introduction

This chapter presents the exploitation of signals of opportunity (SOP) for navigation through the three-step process depicted graphically in Figure 2—signal selection, measurement formation, and measurement application—where a time difference of arrival (TDOA) measurement is motivated as an appropriate measurement that can be derived from many SOP. As will be shown, this structured approach provides (1) portable technology that can be applied to many SOP, (2) performance bounds that may be used as selection criteria for SOP, and (3) navigation solutions that embrace well-known techniques.

Each step shown in Figure 2 is detailed in this chapter. Section 3.2 describes SOP-based TDOA measurements in detail and provides an optimal method (under certain conditions) for calculating the TDOA measurement. Section 3.3 derives a novel adaptation of current Global Positioning System (GPS) position algorithms which will allow the use of TDOA measurements to determine a position solution. Section 3.4 applies the results from the previous sections to aid in signal selection. Finally, Section 3.5 provides a summary.

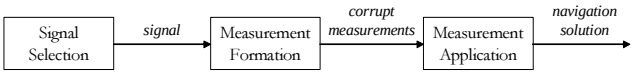

Figure 2. SOP Navigation Process

3.2 Measurement Formation

During *measurement formation*, measurements are formed from the chosen signals of opportunity (SOP). In this section, time difference of arrival (TDOA) measurements are motivated as an appropriate measurement choice for many applications. Then, the measurement scenario and governing equations are developed. Third, the generalized cross correlation method is introduced and applied to SOP-based TDOA measurements. Finally, a summary is provided.

3.2.1 TDOA Measurement Motivation

SOP-based TDOA measurements found using two receivers to determine the signal's TDOA between the two receivers are beneficial for the following reasons. More explicit justification will be presented throughout this chapter when these topics arise.

1. SOP-based TDOA navigation applies to a wide range of signals, because, in general, the *a priori* knowledge of the signal and noise is not overly restrictive. Each transmitter location, the reference receiver location, the transmitted signal power spectral densities, and the noise power spectral densities at each of the two receivers are required.

2. The SOP transmit time does not need to be known (or determined) to obtain a navigation solution. This timing leniency enables SOP-based navigation, since a SOP is transmitted for purposes other than navigation and is normally controlled by some entity other than the navigation user.

3. TDOA formation does not require synchronous transmitters. This is essential,

since, in general, each SOP transmitter is not synchronized to any of the other transmitters. For example, a local radio station's broadcast is not generally synchronized to other radio stations.

4. The formation does not require synchronous receivers. While this allows inexpensive, imprecise receiver clocks, the resulting TDOA measurements are biased due to unsynchronized receiver clocks. The bias represents an additional unknown parameter that is found during the measurement application.

5. The navigation solution using SOP-based TDOA measurements is found readily with current GPS algorithms; consequently, many aspects of SOP-based navigation (such as dilution of precision) may already be in place.

3.2.2 TDOA Measurement Development

TDOA measurements are now developed to gain a physical interpretation of the measurement and to derive a measurement equation. Figure 3 shows a SOP "travelling" to two, separate receivers. One receiver, called the base station, is a

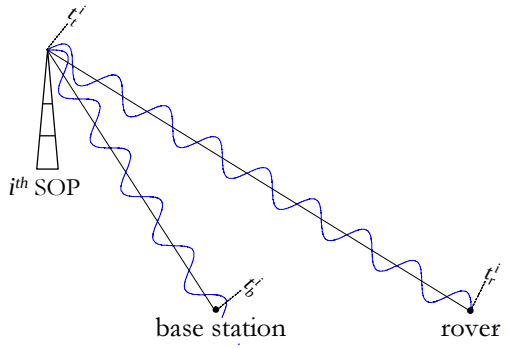

Figure 3. TDOA Measurement of i^{th} SOP

reference receiver at a known location while the other receiver, called the rover, is at an unknown location. The SOP transmitter location is assumed to be known. Fixed SOP transmitter locations (such as fixed towers) can be determined a priori through surveying. The location of moving SOP transmitters can be found using "orbital prediction" for space-based, orbiting transmitters, or determined with additional base stations in a separate, simultaneous algorithm [50].

The *true TDOA*, $\delta^i_{br}\big|_{true}$, is defined as the difference in received time of the i^{th} SOP at the base station, denoted by t^i_b, compared to the received time of the i^{th} SOP at the rover, denoted by t^i_r, i.e.,

$$\delta^i_{br}\big|_{true} \triangleq t^i_b - t^i_r \tag{3.1}$$

The *TDOA measurement*, $\hat{\delta}^i_{br}$, is an estimate of the difference in the received time of i^{th} SOP at the base station according to the base station clock compared to the received time of i^{th} SOP at therover according to the rover clock. In other words, $\hat{\delta}^i_{br}$ is an estimate of δ^i_{br}, and

$$\delta^i_{br} = t^i_b\big|_b - t^i_r\big|_r \tag{3.2}$$

where $t^i_b|_b$ is the received time of the i^{th} SOP at the base station according to the base station clock and $t^i_r|_r$ is the received time of the i^{th} SOP at the rover according to the rover clock. The $|_b$ and $|_r$ denote that the time is measured by the base station and rover, respectively, and allow for imperfect and unsynchronized base station and rover clocks. The received time of the i^{th} signal at the base station according to the base station clock, $t^i_b|_b$, is related to the true received time of the i^{th} signal at the

base station, t_b^i, by

$$t_b^i\big|_b = t_b^i + \epsilon_b\left(t_b^i\right) \tag{3.3}$$

where $\epsilon_b\left(t_b^i\right)$ is defined as the base station clock error at the true received time. Likewise, the received time of the i^{th} signal at the rover according to the rover clock, $t_r^i|_r$, is related to the true received time of the i^{th} signal at the rover, t_r^i, by

$$t_r^i\big|_r = t_r^i + \epsilon_r\left(t_r^i\right) \tag{3.4}$$

where $\epsilon_r\left(t_r^i\right)$ is defined as the rover clock error at the true received time. Substituting Equations (3.3) and (3.4) into Equation (3.2), the TDOA measurement provides an estimate of

$$\delta_{br}^i = t_b^i + \epsilon_b\left(t_b^i\right) - \left[t_r^i + \epsilon_r\left(t_r^i\right)\right] \tag{3.5}$$

$$\delta_{br}^i = t_b^i - t_r^i + \epsilon_b\left(t_b^i\right) - \epsilon_r\left(t_r^i\right) \tag{3.6}$$

Indentifying $\epsilon_b\left(t_b^i\right) - \epsilon_r\left(t_r^i\right)$ as the *difference in the clock errors* of the base station and rover, denoted by ϵ_{br}^i, and using the definition of $\delta_{br}^i\big|_{true}$ in Equation (3.1), Equation (3.6) becomes

$$\delta_{br}^i = \delta_{br}^i\big|_{true} + \epsilon_{br}^i \tag{3.7}$$

The TDOA measurement, $\hat{\delta}_{br}^i$, provides an estimate of the true TDOA plus the difference in clock errors. The following subsection details estimating δ_{br}^i given in Equation (3.7). Section 3.3 will apply TDOA measurements to solve for the position of the rover (assuming the base station and SOP transmitter locations are known).

3.2.3 TDOA Measurement Estimation

There are several methods for estimating δ_{br}^{i} given in Equation (3.7). One way to form a TDOA measurement is to time-tag a specific portion of the incoming signal at each location and determine the difference in the received times [18]. The ability to time-tag the same portion of the signal at each receiver precisely may require SOP that possess distinct time domain features. Another method that can be used for nearly any SOP is cross-correlating a portion of the incoming signal at each receiver. In both cases, either a datalink between the rover and reference receivers must be in place for near-real time operation, or data must be stored for subsequent post processing.

This section presents an existing, maximum likelihood approach to estimate δ_{br}^{i}, termed the generalized cross correlation (GCC) [44]. The GCC method filters two incoming signals followed by computing the cross correlation of the filtered signals [44]. This method is appealing, because it (1) achieves the Cramer Rao Lower Bound (CRLB) and (2) may be applied to a wide range of signals.

The GCC method may be applied when the incoming signals are a signal in noise and the same signal with a time delay in noise. When the received signals are modeled with the specific form given in Equations (3.8) and (3.9) and the prefilters are chosen properly, the time delay estimate that maximizes the GCC is the maximum likelihood estimate of the time delay [44]. The maximum likelihood estimate is appealing because it achieves the Cramer Rao Lower Bound (CRLB) [78] and is the optimal estimate in terms of minimizing the mean-squared error of the estimate relative to the true value.

As shown in Figure 4, assume the i^{th} signal received at the base station, $x_b^i(t)$, and the i^{th} signal received at the rover, $x_r^i(t)$, are

$$x_b^i(t) = s_i(t) + n_b(t) \tag{3.8}$$

$$x_r^i(t) = s_i\left(t + \delta_{br}^i\right) + n_r(t) \tag{3.9}$$

where δ_{br}^i is the time difference of arrival of the i^{th} signal at the rover compared to the base station, $s_i(t)$ is the i^{th} signal, and $n_b(t)$ and $n_r(t)$ are the receiver noise at the base station and rover, respectively. Furthermore, $s_i(t)$, $n_b(t)$, and $n_r(t)$ are modeled as real-valued, pairwise jointly stationary, pairwise jointly wide-sense ergodic, independent Gaussian stochastic processes, and $n_b(t)$ and $n_r(t)$ are zero-mean. Stationarity and ergodicity of stochastic processes are reasonable assumptions that are required to consider the spectral properties of a stochastic process. Assume that the following power spectral densities exist and are known *a priori*:

$$G_{s_i s_i}(f), G_{n_b n_b}(f), G_{n_r n_r}(f) \tag{3.10}$$

(Stochastic processes, stationarity, ergodicity, and the power spectral density functions of stochastic processes are covered in more detail in Appendix D.)

The GCC method prefilters the signals and cross correlates the filtered signals. In the frequency domain, consider the Fourier transform, denoted by $\mathcal{F}$, of $x_b^i(t)$ and $x_r^i(t)$ (where $\tilde{}$ denotes that a quantity is complex-valued):

$$\tilde{x}_b^i(f) = \mathcal{F}\left\{x_b^i(t)\right\} \tag{3.11}$$

$$\tilde{x}_r^i(f) = \mathcal{F}\left\{x_r^i(t)\right\} \tag{3.12}$$

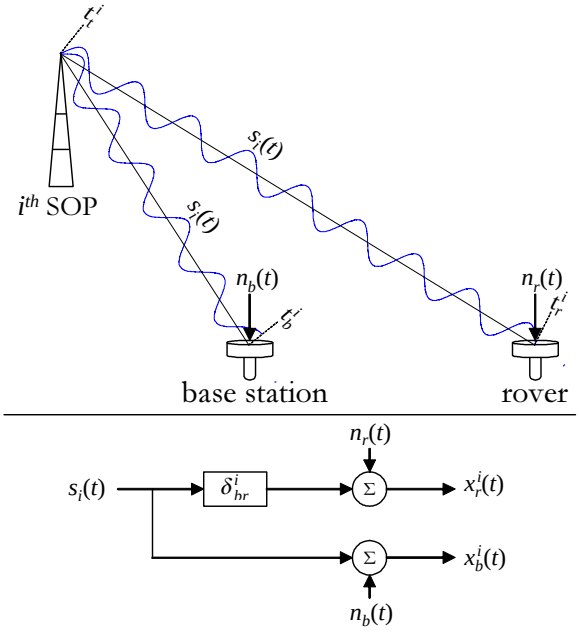

Figure 4. TDOA Measurement Depiction with Block Diagram

Given the prefilters $\tilde{H}_r^i(f)$ and $\tilde{H}_b^i(f)$, the filtered signals can be denoted as

$$\tilde{y}_r(f) = \tilde{H}_r^i(f)\,\tilde{x}_r^i(f) \tag{3.13}$$

$$\tilde{y}_b(f) = \tilde{H}_b^i(f)\,\tilde{x}_b^i(f) \tag{3.14}$$

The cross power spectral density of the filter outputs can be written as

$$\tilde{G}_{y_r y_b}^i(f) = \tilde{y}_r(f)\,\tilde{y}_b^*(f) \tag{3.15}$$

$$= \tilde{H}_r^i(f)\left[\tilde{H}_b^i(f)\right]^* \tilde{x}_r^i(f)\left[\tilde{x}_b^i(f)\right]^* \tag{3.16}$$

$$= \tilde{H}_r^i(f)\left[\tilde{H}_b^i(f)\right]^* \tilde{G}_{x_r x_b}^i(f) \tag{3.17}$$

where $*$ denotes the complex conjugate and $\tilde{G}_{x_r x_b}^i(f) = \tilde{x}_r^i(f)\left[\tilde{x}_b^i(f)\right]^*$. The GCC of $x_r^i(t)$ and $x_b^i(t)$ is the inverse Fourier transform, denoted by $\mathcal{F}^{-1}$, of $\tilde{G}_{y_r y_b}^i(f)$:

$$R_{y_r y_b}^i(\tau) = \mathcal{F}^{-1}\left\{\tilde{G}_{y_r y_b}^i(f)\right\} \tag{3.18}$$

Notice when $\tilde{H}_r^i(f) = \tilde{H}_b^i(f) = 1$, the GCC reduces to the normal definition of cross correlation. Knapp and Carter [44] provide a summary of common prefilter choices.

The maximum likelihood estimate (MLE) of δ_{br}^i, denoted $\hat{\delta}_{br}^i$, was found by Knapp and Carter [44]. The following steps produce the same result as finding the MLE value of δ_{br}^i:

1. Choose prefilters that satisfy

$$\psi(f) \triangleq \tilde{H}_r^i(f)\left[\tilde{H}_b^i(f)\right]^* \tag{3.19}$$

$$= \frac{1}{\left|\tilde{G}_{x_b^i x_r^i}(f)\right|}\left(\frac{\left|\tilde{\gamma}_{x_b^i x_r^i}(f)\right|^2}{1-\left|\tilde{\gamma}_{x_b^i x_r^i}(f)\right|^2}\right) \tag{3.20}$$

where $|\cdot|$ denotes the absolute value or modulus, $\left|\tilde{\gamma}_{x_b^i x_r^i}(f)\right|^2$ is the coherence magnitude squared of x_b^i and x_r^i defined as

$$\left|\tilde{\gamma}_{x_b^i x_r^i}(f)\right|^2 \triangleq \frac{\left|\tilde{G}_{x_b^i x_r^i}(f)\right|^2}{\left|\tilde{G}_{x_b^i x_b^i}(f)\,\tilde{G}_{x_r^i x_r^i}(f)\right|} \tag{3.21}$$

and assuming

$$\left|\tilde{\gamma}_{x_b^i x_r^i}(f)\right|^2 \neq 1 \tag{3.22}$$

2. The TDOA MLE, $\hat{\tilde{\delta}}_{br}^i$, is equivalent to the delay value that maximizes the GCC given in Equation (3.18), or

$$\hat{\tilde{\delta}}_{br}^i = \arg\left\{\max_{\tau\in\mathbb{R}}\left[R_{y_r y_b}^i(\tau)\right]\right\} \tag{3.23}$$

Essentially, when the prefilters satisfy Equation (3.20), $\hat{\tilde{\delta}}_{br}^i$ is given by Equation (3.23). Filtering in Step 1 prepares the input signal for cross correlation in Step 2 by "prewhitening" the signal and placing a weight at each frequency as a function of $\left|\tilde{\gamma}_{x_b^i x_r^i}(f)\right|^2$. This weighting may be interpreted loosely as accentuating frequencies at which the signal power is higher than the noise power.

The assumption in Equation (3.22) merits some discussion. In general, the term $\left|\tilde{\gamma}_{x_b^i x_r^i}(f)\right|^2$ can take on values

$$0 \leq \left|\tilde{\gamma}_{x_b^i x_r^i}(f)\right|^2 \leq 1 \tag{3.24}$$

The spectral densities in Equation (3.21) can be related to the known spectra given in Equation (3.10) using Equations (3.8) and (3.9):

$$\tilde{G}_{x_b^i x_r^i}(f) = G_{s_i s_i}(f)\, e^{-j2\pi f \delta_{br}^i} \tag{3.25}$$

$$G_{x_b^i x_b^i}(f) = G_{s_i s_i}(f) + G_{n_b n_b}(f) \tag{3.26}$$

$$G_{x_r^i x_r^i}(f) = G_{s_i s_i}(f) + G_{n_r n_r}(f) \tag{3.27}$$

Now, the numerator of Equation (3.21) can be written as

$$\left|\tilde{G}_{x_b^i x_r^i}(f)\right|^2 = \left|G_{s_i s_i}(f)\right|^2 \tag{3.28}$$

and the denominator of Equation (3.21) can be written (with dependence upon f not shown) as

$$\left|G_{x_b^i x_b^i} G_{x_r^i x_r^i}\right| = \left|(G_{s_i s_i})^2 + G_{n_b n_b} G_{n_r n_r} + G_{s_i s_i}\left(G_{n_b n_b} + G_{n_r n_r}\right)\right| \tag{3.29}$$

revealing that $\left|\tilde{\gamma}_{x_b^i x_r^i}(f)\right|^2 \neq 1$ holds for all f that satisfy

$$G_{s_i s_i}(f) \neq 0 \quad \text{and} \quad G_{n_b n_b}(f) \neq 0 \tag{3.30}$$

or

$$G_{s_i s_i}(f) \neq 0 \quad \text{and} \quad G_{n_r n_r}(f) \neq 0 \tag{3.31}$$

or

$$G_{n_b n_b}(f) \neq 0 \quad \text{and} \quad G_{n_r n_r}(f) \neq 0 \tag{3.32}$$

Therefore, if noise is present at all frequencies, then the assumption in Equation (3.22) is satisfied.

When the terms in Equation (3.10) are known, the filters in Step 1 can be determined. If the terms in Equation (3.10) are not known completely, $\left|\tilde{\gamma}_{x_b^i x_r^i}(f)\right|^2$ and $\left|\tilde{G}_{x_b^i x_r^i}(f)\right|$ can be estimated using spectral analysis techniques [8,9,44,59]. Filters resulting from estimates of $\left|\tilde{\gamma}_{x_b^i x_r^i}(f)\right|^2$ and $\left|\tilde{G}_{x_b^i x_r^i}(f)\right|$ will be approximations to the optimal filters; therefore, an efficient estimate of δ_{br}^i cannot be guaranteed under those conditions.

3.2.4 Summary

In this section, TDOA measurements were motivated as a suitable choice for SOP, and their formation was detailed. The TDOA estimate, $\hat{\delta}_{br}^i$, was defined as an estimate of δ_{br}^i, where δ_{br}^i was found in Equation (3.6) as

$$\delta_{br}^i = t_b^i - t_r^i + \epsilon_b\left(t_b^i\right) - \epsilon_r\left(t_r^i\right) \tag{3.33}$$

Furthermore, the GCC method for TDOA was introduced, and the MLE of δ_{br}^i was given in Equation (3.23) as

$$\hat{\delta}_{br}^i = \arg\left\{\max_{\tau}\left[R_{y_r y_b}^i(\tau)\right]\right\} \tag{3.34}$$

The procedure can be summarized as follows: Known characteristics of the selected SOP and the receiver noises are used to form the prefilters $\tilde{H}_r^i(f)$ and $\tilde{H}_b^i(f)$. The GCC is found using filtered versions of the input signals. Finally, the delay value that maximizes the GCC is the TDOA MLE. The following section will now apply these results to determine the location of the unknown receiver.

3.3 Measurement Application

This section introduces a novel approach to apply existing Global Positioning System (GPS) algorithms to SOP-based TDOA measurements to determine an unknown receiver's position. The SOP-based TDOA measurements may be found through the results of the previous section or using some other method. The SOP navigation scenario is described detailing appropriate assumptions followed by the transformation of the SOP-based TDOA measurements into "GPS-like" pseudorange measurements.

Figure 5 shows the scenario considered (for which each tower transmission is shown in Figure 3). Assume the location of the i^{th} SOP transmitter for $i = 1, 2, \cdots, N$ at time t is known and defined as $\mathbf{x}_i(t)$. The equipment needed consists of two stationary or moving receivers: a base station at a known location, $\mathbf{x}_b(t)$, and a rover unit at the location to be determined, $\mathbf{x}_r(t)$. The known locations $\mathbf{x}_i(t)$ and $\mathbf{x}_b(t)$ may be at a fixed, surveyed site or determined using an available navigation system such as GPS.

The TDOA estimate of the i^{th} signal to the base station relative to the receiver, $\hat{\delta}^i_{br}$, was defined as an estimate of δ^i_{br}, where δ^i_{br} was given in Equation (3.6). Recall that no clock synchronization assumptions are made. A situation may nevertheless occur in which transmitters *are* synchronized; however, in order to encompass a wider range of SOP, this scenario does not take advantage of this additional constraint. Converting travel times into distances by multiplying by the signal's propagation

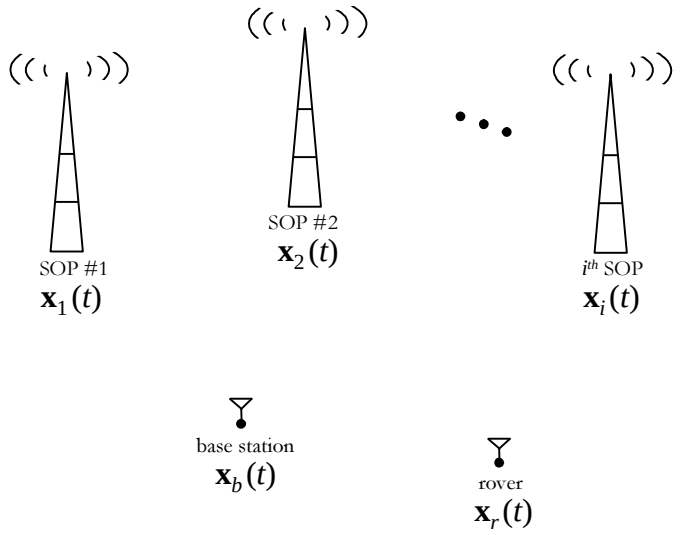

Figure 5. TDOA Transmitter and Receiver Scenario

speed, c, Equation (3.6) becomes

$$\begin{aligned}\Delta_{br}^{i} &\triangleq c\delta_{br}^{i} = ct_{b}^{i} - ct_{r}^{i} + c\epsilon_{b}\left(t_{b}^{i}\right) - c\epsilon_{r}\left(t_{r}^{i}\right) \\ &= \left(ct_{b}^{i} - ct_{t}^{i}\right) - \left(ct_{r}^{i} - ct_{t}^{i}\right) + \left[c\epsilon_{b}\left(t_{b}^{i}\right) - c\epsilon_{r}\left(t_{r}^{i}\right)\right] \\ &= d_{b}^{i} - d_{r}^{i} + \left[c\epsilon_{b}\left(t_{b}^{i}\right) - c\epsilon_{r}\left(t_{r}^{i}\right)\right] \end{aligned} \tag{3.35}$$

where t_{t}^{i} is the unknown transmit time of the i^{th} SOP, $c\delta_{br}^{i} \triangleq \Delta_{br}^{i}$, and d_{b}^{i} and d_{r}^{i} are the distances from the i^{th} SOP transmitter to the base station and rover, respectively. Figure 6 shows the relationship of and d_{b}^{i}, d_{r}^{i} and Δ_{br}^{i}. Using this insight, Equation (3.35) is rearranged as

$$d_{r}^{i} - \left[c\epsilon_{b}\left(t_{b}^{i}\right) - c\epsilon_{r}\left(t_{r}^{i}\right)\right] = d_{b}^{i} - \Delta_{br}^{i} \tag{3.36}$$

Equation (3.36) closely resembles the form of a *GPS pseudorange equation* [53], in which

1. $d_{b}^{i} - \Delta_{br}^{i}$ resembles GPS pseudorange to be estimated (in distance),
2. $[c\epsilon_{b}\left(t_{b}^{i}\right) - c\epsilon_{r}\left(t_{r}^{i}\right)]$ resembles an unknown clock bias (although it is actually the unknown difference in the clock errors expressed in units of distance of the base station and the rover), and
3. d_{r}^{i} is true range from the rover to the i^{th} SOP.

If the difference in the clock errors could be formed such that they do not vary over the measurements taken, then GPS algorithms may be employed to determine $\mathbf{x}_{r}\left(t\right)$ (and the difference in clock errors of the base station and rover) from estimates of

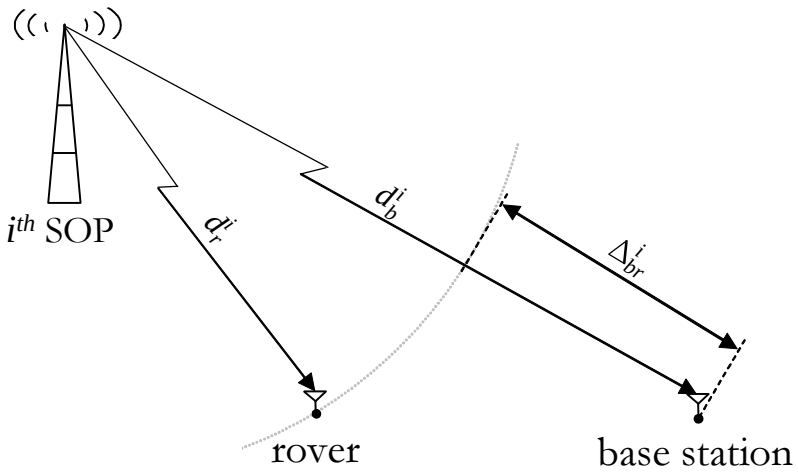

Figure 6. Geometric Interpretation of TDOA

$[d_b^i - \Delta_{br}^i]$. (In the TDOA case, Δ_{br}^i is actually estimated as $c\hat{\delta}_{br}^i$. An estimate of $[d_b^i - \Delta_{br}^i]$ may be formed as $\left[d_b^i - c\hat{\delta}_{br}^i\right]$.)

The conditions which permit the difference in clock errors to be constant over the measurements taken are now considered. Using N SOP transmitters, N measurements can be taken. For three dimensional positioning, $N \geq 4$ is required. In general, each of the terms in Equation (3.36) with the superscript i vary as the SOP transmitter varies. Since TDOA is formed as the difference in received times at two receivers, without loss of generality, the user may *select* the time that the i^{th} SOP is received at the rover, t_r^i, be constant over i. This may be accomplished using multiple channels, in which each of the N SOP are received simultaneously at the time, t_r, i.e.,

$$t_r \triangleq t_r^1 = t_r^2 = \cdots = t_r^N$$

It follows that the rover clock error remains the same for each SOP and can be denoted as $\delta_r(t_r)$.

The time at which the i^{th} SOP is received at the base station, t_b^i, may take on values between $t_r - \frac{B}{c}$ and $t_r + \frac{B}{c}$, or

$$t_b^i \in \left[t_r - \frac{B}{c}, t_r + \frac{B}{c}\right]$$

where B is the distance between the base station and the rover and c is the speed of propagation. If B is constrained such that the base station clock drift is sufficiently small over the possible range of base station received times, then

$$\delta_b(t) \approx k \qquad \forall t \in \left[t_r - \frac{B}{c}, t_r + \frac{B}{c}\right] \tag{3.37}$$

where k is a constant. Furthermore, Equation (3.37) holds for each SOP, so that

$$\delta_b\left(t_b^1\right) \approx \delta_b\left(t_b^2\right) \approx \cdots \approx \delta_b\left(t_b^N\right) \triangleq \delta_b\left(t_b\right)$$

Finally, replacing $\delta_r\left(t_r^i\right)$ with $\delta_r\left(t_r\right)$ and $\delta_b\left(t_b^i\right)$ with $\delta_b\left(t_b\right)$, Equation (3.36) becomes

$$d_r^i - \left[c\delta_b\left(t_b\right) - c\delta_r\left(t_r\right)\right] = d_b^i - \Delta_{br}^i \tag{3.38}$$

Equation (3.38) parallels the GPS pseudorange equation, in which $d_b^i - \Delta_{br}^i$ is the i^{th} pseudorange measurement, d_r^i is range from the rover to the i^{th} GPS transmitter (or satellite), and $\left[c\delta_b\left(t_b\right) - c\delta_r\left(t_r\right)\right]$ is a bias term constant over all N measurements. The difference is that, in conventional GPS, the bias term represents the user clock error, whereas for SOP TDOA measurements, the bias term represents the *difference* in the clock errors of the base station and rover. Standard GPS algorithms, such as one presented by Misra and Enge [53], or closed-form solutions such as in [54], can be used to solve for the rover position and the difference in clock errors of the base station clock and rover clock. Note that the algorithm using SOP TDOA measurements cannot be used to estimate true time, since the bias found represents a difference in clock errors and not a single clock error compared to the true time. This new approach allows SOP-based navigation dilution of precision considerations to be addressed in a manner consistent with GPS techniques such as those found in [53, 58].

3.4 Signal Selection

Signal selection is deciding which signals of opportunity (SOP) to use for navigation. From a Bayesian viewpoint, the best performance is achieved when all SOP

are used. Naturally, signal selection assumes there are more SOP available than the user has resources to exploit. Considering radio, television, cellular phone, and other telecommunication signals emitted both terrestially and celestially, signal selection is confronted quickly! (See Appendix B for specific examples.) Furthermore, this task is critical, because the chosen SOP's characteristics will affect navigation performance. Current SOP exploitations such as AM radio have been chosen, in part, because of their large coverage areas and well-understood signal structures [34]. A more appropriate decision tool may be the ability to determine navigation parameters of interest using a given signal, called the *navigation potential* of a signal.

In Section 3.2 and *under restricted received signal models*, the maximum likelihood estimate for a SOP-based time difference of arrival (TDOA) measurement was found. In Section 3.3, a navigation algorithm employed SOP-based TDOA measurements to determine the unknown, rover position. The quality of the TDOA estimates may be quantified based upon the lowest variance achievable by any unbiased estimator, or the Cramer Rao Lower Bound (CRLB). Knapp and Carter show that the variance of $\hat{\delta}^i_{br}$, denoted with $var\left\{\hat{\delta}^i_{br}\right\}$, must satisfy [44]

$$var\left\{\hat{\delta}^i_{br}\right\} \geq \left\{ T \int_{-\infty}^{\infty} (2\pi f)^2 \frac{\left|\tilde{\gamma}_{x^i_b x^i_r}(f)\right|^2}{1-\left|\tilde{\gamma}_{x^i_b x^i_r}(f)\right|^2} df \right\}^{-1} \tag{3.39}$$

where T is the finite-timelength observation interval of $x^i_b(t)$ and $x^i_r(t)$ used to compute the Fourier transform of $x^i_b(t)$ and $x^i_r(t)$. This expression assumes that the observation interval, T, is large compared to the delay δ^i_{br} plus the correlation time of the signal [44].

Equation (3.39) is insightful; for example, as the observation time (T) increases or as the coherence magnitude squared approaches unity, the CRLB decreases. Furthermore, when navigation is accomplished consistent with the preceding sections, the TDOA estimate given in Equation (3.23) is efficient [44]. That is, the variance of the estimate *achieves* the CRLB.

The CRLB given in Equation (3.39) is applicable only when the signals are appropriately represented by the models given in Equations (3.8) and (3.9). For example, a major source of error for SOP is multipath [18, 19]; Equations (3.8) and (3.9) do not account for multipath.

With the insight gained through this systematic navigation process, Chapter 4 will develop navigation potential theory. Navigation potential theory covers a large class of problems, one of which is the simplified model presented here.

3.5 Summary

The SOP-based TDOA navigation process shown in Figure 2 is summarized as:

1. *Signal Selection* – Characterize each candidate SOP's spectra defined in Equation (3.10) and its transmitter location (or location path). Assuming the signals are appropriately modeled by Equations (3.8) and (3.9), calculate (using Equation (3.39)) the minimum variance achievable by any unbiased TDOA estimate. Select SOP based upon this performance bound and geometry effects. Recall, well-known GPS techniques such as those described in [53] can be used to characterize the geometry effects.

2. *Measurement Formation* – Compute (or approximate) optimal filters that

satisfy Equation (3.20). Use the Generalized Cross Correlation method given in Equation (3.23) to compute $\hat{\delta}_{br}^{i}$.

3. *Measurement Application* – Use the measurement $\Delta_{br}^{i} = c\hat{\delta}_{br}^{i}$ in Equation (3.38) to form a GPS-like pseudorange measurement. Combine each measurement at a given time to compute the location of an unknown receiver using well-known GPS algorithms [53, 54, 58].

This systematic navigation method is an alternative, and/or augmentation, to current navigation methods such as GPS and applies to nearly all SOP using time difference of arrival (TDOA) measurements obtained from a generalized cross correlation. This approach enables positioning systems in which none of the transmitters or receivers require precise clocks, nor do they need to be synchronized. Only the SOP and noise spectra, SOP transmitters' location, and base station location is needed. Furthermore, a decision tool for proper selection of SOP may be the CRLB. Finally, SOP TDOA measurements can be processed with existing GPS algorithms to solve for user positions and the rover clock error relative to the base station clock error.

This navigation process may suffice in many cases. Methods other than GCC may be used to form the TDOA estimate. The GPS-like navigation algorithm given in this chapter applies regardless of which SOP is selected or how the TDOA measurement is obtained, although a more clever technique may be appropriate for a particular class of SOP. The process presented here provides insight into the navigation potential theory developed in the following chapter.

Chapter 4 - Navigation Potential

4.1 Introduction

In this chapter, the concept of *navigation potential* (*NP*) is presented. The overall approach in developing the navigation potential of a signal is to describe the received signal's relationship to the navigation parameter(s) of interest, followed by quantifying the ability to estimate the navigation parameter(s) based upon the received signal. As motivated in Chapter 3, time difference of arrival (TDOA) measurements are useful particularly when the received signal is based upon a signal of opportunity (SOP), since the transmit time is not needed to determine a position solution. It is shown that the ability to determine the TDOA of a SOP received at two receivers may be characterized through the inverse of the TDOA estimate's Cramer Rao Lower Bound given the received signals. Assumptions about the received signals and their relationship to the TDOA measurement are made in succession to simplify the analysis and afford more practical *NP* forms.

To aid in following the *NP* development, Figure 7(b) provides the "Table of Contents" for this chapter while (a) depicts graphically how the assumptions made therein fit together. The outermost gray area, "Box I", corresponds to the measurement model and *NP* described in Section 4.2 and is the most general measurement form considered in this document. The received signals, x_i, are assumed to be the result of a *stochastic* mapping, $g_i\left(t, \varpi; s, n_i, \tau_i\right)$. The first two arguments capture the stochastic nature of g_i, while the remaining arguments indicate that g_i is parameterized by the transmitted signal, s, noise, n_i, and time delay, τ_i. The general nature of

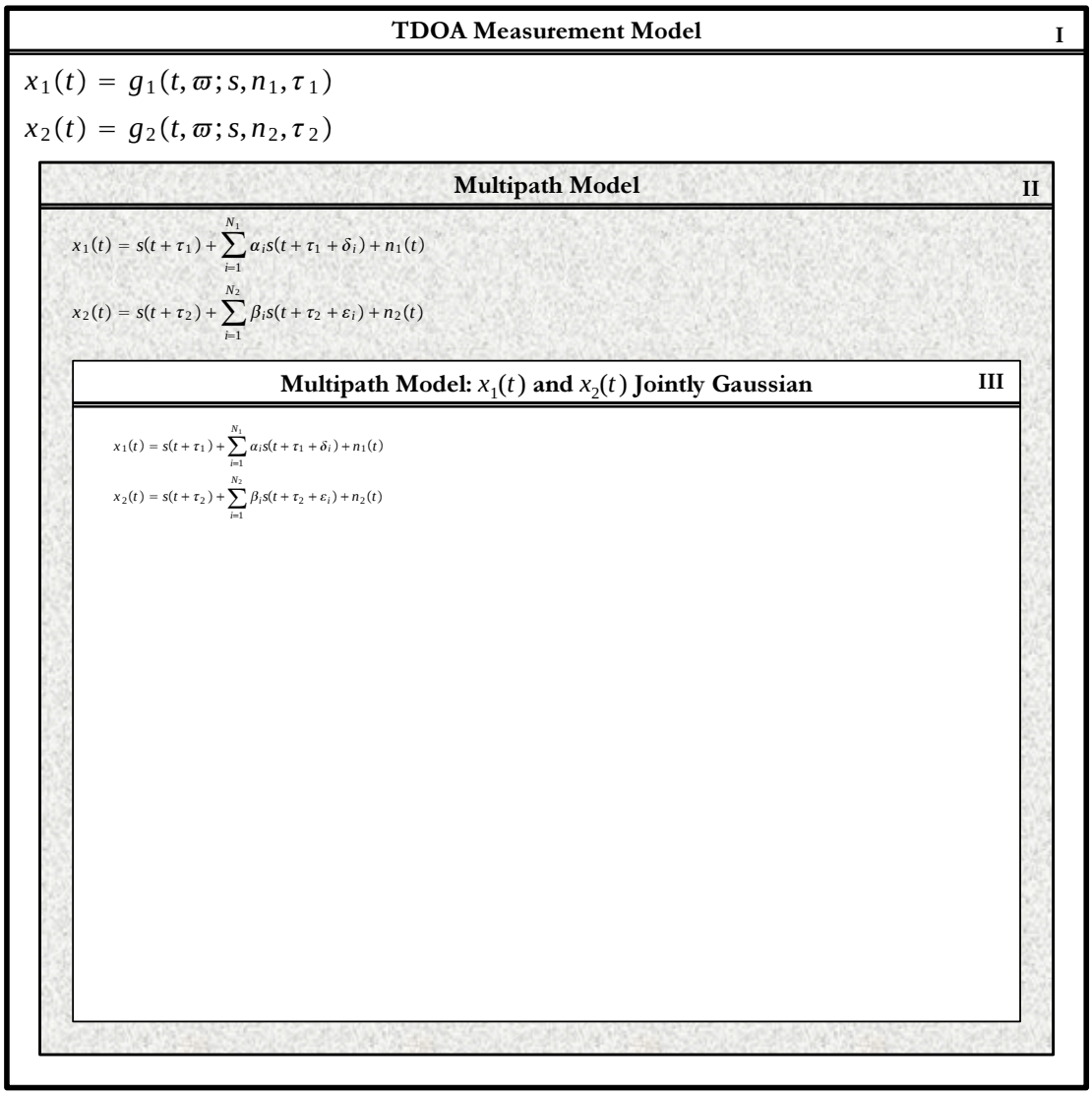

(a) Navigation Potential Diagram

(b) Chapter 4 "Table of Contents"

Figure 7. Chapter 4 Overview Diagram and Table of Contents

this model encompasses a wide range of problems; however, considerably more insight into *NP* is gained when the model is constrained. Section 4.3 (Box II) presents a multipath model by constraining g_i, s, and n_i; briefly, g_i maps the transmitted signal and noise into the received signal as the direct signal in noise in addition to multiple delayed and attenuated versions of the direct signal. Section 4.4 (Box III) constrains the multipath model such that the transmitted signal, measurement noise, and received signals are jointly Gaussian. (Figure 7 contains considerable "blank space." Figure 9 in Chapter 5 fills this space with diagrams representing example problems. The spacing is maintained in Figures 7 and 9 for a consistent appearance.)

4.2 TDOA Navigation Potential

This section details navigation potential (*NP*) as it applies to the very general problem of determining the time difference of arrival (TDOA) of a signal received at two separate locations. Measurements constructed from a single signal received at two separate locations covers a wide range of navigation problems. As stated in Chapter 3, this form is appealing for signals of opportunity, because it eliminates the need to know the transmit time of the signal. Furthermore, Chapter 5 shows that this form can be equated to receiving the signal at a single receiver and using a receiver-generated replica signal as the second received signal. The remainder of this section presents *NP* in its most general form by describing the received signals, the navigation parameters of interest, and the ability to determine the navigation parameters from the received signals.

4.2.1 Signal Model

The most general form of the signal received at the i^{th} receiver, $x_i(\cdot,\cdot)$, is the stochastic process defined as

$$x_i(\cdot,\cdot) \triangleq g_i[\cdot,\cdot; s(\cdot,\cdot), n_i(\cdot,\cdot), \tau_i(\cdot)] \quad \text{for} \quad i = 1,2 \tag{4.1}$$

where $x_i(\cdot,\cdot)$, $s(\cdot,\cdot)$, and $n_i(\cdot,\cdot)$ are scalar-valued stochastic processes representing the received signal at the i^{th} receiver, the transmitted SOP, the noise at the i^{th} receiver, respectively. Each of these stochastic processes is defined on $\mathbb{R}^1 \times \Xi$, where the first argument denotes "time" with $t \in \mathbb{R}^1$ and the second argument denotes samples from a sample space[3] with $\xi \in \Xi$. The single argument on $\tau_i(\cdot)$ denotes time with $t \in \mathbb{R}^1$. The range of $x_i(\cdot,\cdot)$, $s(\cdot,\cdot)$, and $n_i(\cdot,\cdot)$ is $\mathbb{X}_{x_i} \subseteq \mathbb{R}^1$, $\mathbb{X}_s \subseteq \mathbb{R}^1$, and $\mathbb{X}_{n_i} \subseteq \mathbb{R}^1$, respectively. As an example[4], consider $s(\cdot,\cdot)$ when confined in its arguments:

- For some fixed t, $s(t,\cdot)$ is a random variable (and is a function of ξ).
- For some fixed ξ, each $s(\cdot,\xi)$ is a *sample* from the stochastic process and is a function of t.
- For some fixed t and ξ, each $s(t,\xi)$ is a point in $\mathbb{X}_s \subseteq \mathbb{R}^1$; it can be viewed as a *realization* of the *random variable* $s(t,\cdot)$ or the *specific value* of the *sample* $s(\cdot,\xi)$ at a specific time t.

[3]Some authors use $\omega \in \Omega$ rather than $\xi \in \Xi$; however, the latter notation avoids confusion with $\omega \triangleq 2\pi f$ used in Fourier analysis.

[4]Section D.2 in Appendix D provides a more complete description of stochastic processes and their characteristics.

The time delay incurred by the transmitted SOP to travel to the i^{th} receiver, $\tau_i(\cdot)$, is a function of time, t, with $t \in \mathbb{R}^1$. Finally, the mapping, g_i, is itself a mapping of $\mathbb{R}^1 \times \Xi$ into $\mathbb{X}_{x_i} \subseteq \mathbb{R}^1$ (parameterized by $s(\cdot,\cdot)$, $n_i(\cdot,\cdot)$, and $\tau_i(\cdot)$).

The aim of *NP* theory is to quantify the ability to estimate the navigation parameters of interest given the received signal $\mathbf{x}(\cdot,\cdot)$ defined as

$$\mathbf{x}(\cdot,\cdot) \triangleq \begin{bmatrix} x_1(\cdot,\cdot) \\ x_2(\cdot,\cdot) \end{bmatrix} = \begin{bmatrix} g_1[\cdot,\cdot; s(\cdot,\cdot), n_1(\cdot,\cdot), \tau_1(\cdot)] \\ g_2[\cdot,\cdot; s(\cdot,\cdot), n_2(\cdot,\cdot), \tau_2(\cdot)] \end{bmatrix} \tag{4.2}$$

The following discussion clarifies which parameters are "of interest".

4.2.2 Parameters of Interest

The *true TDOA* of the signal at the first receiver relative to the second receiver, or $\tau_\Delta(t)$, is defined as

$$\tau_\Delta(t) \triangleq \tau_1(t) - \tau_2(t) \tag{4.3}$$

where $\tau_1(t)$ and $\tau_2(t)$ are the arrival times (at time t) of the signal at the first and second receiver, respectively. An estimate of the true TDOA, $\hat{\tau}_\Delta(t)$, called the *TDOA estimate*, may be used to solve for an unknown receiver position as detailed in Chapter 3. Ideally, the true TDOA is the navigation parameter of interest for which an estimate is sought, because this parameter is used in the TDOA navigation scheme detailed in Chapter 3. (Other parameters of interest may be considered. An example parameter of interest *not* used here is the received signal's amplitude.) When the parameter is confined to TDOA, the expressions for *NP* characterize the ability to estimate the TDOA given $\mathbf{x}(\cdot,\cdot)$.

In general, $\tau_\Delta(t)$ cannot be estimated directly, so both $\tau_1(t)$ and $\tau_2(t)$ must be estimated. This can be represented as estimating the vector

$$\boldsymbol{\theta}(t) \triangleq \begin{bmatrix} \tau_1(t) \\ \tau_2(t) \end{bmatrix} \tag{4.4}$$

Once an estimate of $\boldsymbol{\theta}(t)$ is found, denoted as $\hat{\boldsymbol{\theta}}(t)$, $\hat{\tau}_\Delta(t)$ may be found as

$$\hat{\tau}_\Delta(t) = \begin{bmatrix} 1 & -1 \end{bmatrix} \begin{bmatrix} \hat{\tau}_1(t) \\ \hat{\tau}_2(t) \end{bmatrix} \tag{4.5}$$

$$\triangleq \mathbf{h}\left[\hat{\boldsymbol{\theta}}(t)\right] \tag{4.6}$$

where $\mathbf{h}$ is the transformation (which is linear and time-invariant here) used to go from $\hat{\boldsymbol{\theta}}(t)$ to $\hat{\tau}_\Delta(t)$.

Thus, while $\tau_\Delta(t)$ is the navigation parameter of interest, the need may arise to estimate a vector of parameters, $\boldsymbol{\theta}(t)$, where there exists some transformation, $\mathbf{h}$, such that $\mathbf{h}$ maps $\hat{\boldsymbol{\theta}}(t)$ to $\hat{\tau}_\Delta(t)$. An expression for *NP* should permit this subtle distinction. The following section introduces performance bounds for the estimates of $\tau_\Delta(t)$ and $\boldsymbol{\theta}(t)$ as the precursor to a formal definition for *NP*.

4.2.3 Cramer Rao Lower Bound

It is desired to quantify the performance of $\hat{\tau}_\Delta(t)$. One commonly used indicator of an estimator's performance is the mean-squared error (MSE) [15, 43, 68, 78], or

$$E\left\{\left[\tau_\Delta - \mathcal{E}(\tau_\Delta)\right]^2\right\}$$

where $\mathcal{E}(\cdot)$ is an estimator and time dependence is not shown. The $\mathcal{E}(\cdot)$ operator may depend upon a time history of measurements. One might consider quantifying

NP through the inverse of the minimum MSE achievable by *any* estimator of τ_Δ:

$$NP(\mathbf{x}) \triangleq \left[\min_{\mathcal{E}} \left(E\left\{\left[\tau_\Delta - \mathcal{E}(\tau_\Delta)\right]^2\right\}\right)\right]^{-1} \tag{4.7}$$

where the expectation is taken over the probability density function of $\mathbf{x}$ and the *minimum is taken over all estimators*, $\{\mathcal{E}(\cdot)\}$. The optimal estimator (in terms of minimizing the MSE), defined as $\mathcal{E}_{MMSE}(\cdot)$, follows for τ_Δ as

$$\mathcal{E}_{MMSE}(\tau_\Delta) = \arg\left\{\min_{\mathcal{E}} \left(E\left\{\left[\tau_\Delta - \mathcal{E}(\tau_\Delta)\right]^2\right\}\right)\right\} \tag{4.8}$$

In fact, it can be shown that $\mathcal{E}_{MMSE}(\cdot)$ is, in general, the conditional expectation of the quantity of interest, conditioned on the measurements that have been observed.

Defining

$$\hat{\tau}_\Delta \triangleq \mathcal{E}(\tau_\Delta) \tag{4.9}$$

$$\mu_{\hat{\tau}_\Delta} \triangleq E\{\hat{\tau}_\Delta\} \tag{4.10}$$

it follows that

$$E\left\{\left[\tau_\Delta - \mathcal{E}(\tau_\Delta)\right]^2\right\} = E\left\{\left[\left(\tau_\Delta - \mu_{\hat{\tau}_\Delta}\right) + \left(\mu_{\hat{\tau}_\Delta} - \hat{\tau}_\Delta\right)\right]^2\right\} \tag{4.11}$$

and, upon expanding,

$$\begin{aligned} E\left\{\left[\tau_\Delta - \mathcal{E}(\tau_\Delta)\right]^2\right\} &= E\left\{\left(\tau_\Delta - \mu_{\hat{\tau}_\Delta}\right)^2\right\} + E\left\{\left(\mu_{\hat{\tau}_\Delta} - \hat{\tau}_\Delta\right)^2\right\} + \\ &\quad + 2E\left\{\left(\tau_\Delta - \mu_{\hat{\tau}_\Delta}\right)\left(\mu_{\hat{\tau}_\Delta} - \hat{\tau}_\Delta\right)\right\} \end{aligned} \tag{4.12}$$

Defining

$$E\left\{\left(\mu_{\hat{\tau}_\Delta} - \hat{\tau}_\Delta\right)^2\right\} \triangleq \left(\sigma_{\hat{\tau}_\Delta}\right)^2 \tag{4.13}$$

and noting that τ_Δ and $\mu_{\hat{\tau}_\Delta}$ are not random, Equation (4.12) becomes

$$E\left\{\left[\tau_\Delta - \mathcal{E}\left(\tau_\Delta\right)\right]^2\right\} = \left(\tau_\Delta - \mu_{\hat{\tau}_\Delta}\right)^2 + \left(\sigma_{\hat{\tau}_\Delta}\right)^2 + \left[2\left(\tau_\Delta - \mu_{\hat{\tau}_\Delta}\right)\left(\mu_{\hat{\tau}_\Delta} - E\left\{\hat{\tau}_\Delta\right\}\right)\right] \quad (4.14)$$

But, from Equation (4.10),

$$\mu_{\hat{\tau}_\Delta} - E\left\{\hat{\tau}_\Delta\right\} = 0 \quad (4.15)$$

so

$$E\left\{\left[\tau_\Delta - \mathcal{E}\left(\tau_\Delta\right)\right]^2\right\} = \left(\tau_\Delta - \mu_{\hat{\tau}_\Delta}\right)^2 + \left(\sigma_{\hat{\tau}_\Delta}\right)^2 \quad (4.16)$$

When $\mu_{\hat{\tau}_\Delta} = \tau_\Delta$, the MSE becomes

$$E\left\{\left[\tau_\Delta - \mathcal{E}\left(\tau_\Delta\right)\right]^2\right\} = \left(\sigma_{\hat{\tau}_\Delta}\right)^2 \quad (4.17)$$

An estimator of τ_Δ, denoted by $\mathcal{E}\left(\tau_\Delta\right) = \hat{\tau}_\Delta$, such that $E\left\{\hat{\tau}_\Delta\right\} = \tau_\Delta$ is termed an *unbiased* estimator [43, 78], and the MSE of such an estimator is the variance of the estimator itself, or $\left(\sigma_{\hat{\tau}_\Delta}\right)^2$. The Cramer Rao Lower Bound places a lower limit on the variance of any unbiased estimator of τ_Δ as defined in the following theorem.

Theorem 1 (Cramer Rao Lower Bound (CRLB)) *[43]*

Let the measurements $\mathbf{x}$ *be given, where the probability density function of* $\mathbf{x}$, $f\left(\mathbf{x};\boldsymbol{\theta}\right)$, *is known and is a function of the parameter vector to be estimated,* $\boldsymbol{\theta}$. *Furthermore, it is assumed* $f\left(\mathbf{x};\boldsymbol{\theta}\right)$ *satisfies the regularity condition*

$$E\left\{\frac{\partial \ln\left[f\left(\mathbf{x};\boldsymbol{\theta}\right)\right]}{\partial \boldsymbol{\theta}}\right\} = \mathbf{0}^T \quad (4.18)$$

Then, the variance of any unbiased estimate of θ_i, defined as $C_{\hat{\theta}_i}$, must satisfy the CRLB given as

$$C_{\hat{\theta}_i} \geq \left[\mathbf{I}^{-1}(\boldsymbol{\theta})\right]_{ii} \tag{4.19}$$

or, in matrix form,

$$\mathbf{C}_{\hat{\boldsymbol{\theta}}} - \mathbf{I}^{-1}(\boldsymbol{\theta}) \geq \mathbf{0} \tag{4.20}$$

where $\geq \mathbf{0}$ is interpreted as meaning the matrix must be positive semidefinite and $\mathbf{I}(\boldsymbol{\theta})$ is the Fisher Information Matrix (FIM) defined component-wise as

$$\left[\mathbf{I}(\boldsymbol{\theta})\right]_{ij} \triangleq E\left\{\frac{\partial \ln\left[f(\mathbf{x};\boldsymbol{\theta})\right]}{\partial\theta_i}\frac{\partial \ln\left[f(\mathbf{x};\boldsymbol{\theta})\right]}{\partial\theta_j}\right\} \tag{4.21}$$

Furthermore, it can be shown that [46]

$$\left[\mathbf{I}(\boldsymbol{\theta})\right]_{ij} = -E\left\{\frac{\partial^2 \ln\left[f(\mathbf{x};\boldsymbol{\theta})\right]}{\partial\theta_i\partial\theta_j}\right\} \tag{4.22}$$

Proof: *See [43].* ■

Finally, consider the case in which τ_Δ cannot be estimated directly; rather, $\boldsymbol{\theta}$ is estimated where $\tau_\Delta = \mathbf{h}(\boldsymbol{\theta})$ for some given mapping $\mathbf{h}$. The following corollary describes the FIM for transformations of variables.

Corollary 2 (CRLB for Transformations of Variables) *[43]*

The variance of any unbiased estimator of $\boldsymbol{\alpha} = \mathbf{h}(\boldsymbol{\theta})$, defined as $\mathbf{C}_{\hat{\boldsymbol{\alpha}}}$, must satisfy

$$\mathbf{C}_{\hat{\boldsymbol{\alpha}}} - \frac{\partial \mathbf{h}(\boldsymbol{\theta})}{\partial \boldsymbol{\theta}}\mathbf{I}^{-1}(\boldsymbol{\theta})\left[\frac{\partial \mathbf{h}(\boldsymbol{\theta})}{\partial \boldsymbol{\theta}}\right]^T \geq \mathbf{0} \tag{4.23}$$

where $\frac{\partial \mathbf{h}(\boldsymbol{\theta})}{\partial \boldsymbol{\theta}}$ *is the Jacobian matrix defined component-wise as*

$$\left[\frac{\partial \mathbf{h}\left(\boldsymbol{\theta}\right)}{\partial \boldsymbol{\theta}}\right]_{ij} = \frac{\partial \left[\mathbf{h}\left(\boldsymbol{\theta}\right)\right]_i}{\partial \theta_j} \tag{4.24}$$

Proof: *See [43].* ■

4.2.4 NP Definition

Using the notation from the previous subsection, *NP* is defined formally as

$$\boxed{NP\left(\mathbf{x}\right) \triangleq \left(\frac{\partial \mathbf{h}(\boldsymbol{\theta})}{\partial \boldsymbol{\theta}} \mathbf{I}^{-1}\left(\boldsymbol{\theta}\right) \left[\frac{\partial \mathbf{h}(\boldsymbol{\theta})}{\partial \boldsymbol{\theta}}\right]^T\right)^{-1}} \tag{4.25}$$

where $\boldsymbol{\theta}$ is the vector of parameters estimated, $\mathbf{I}\left(\boldsymbol{\theta}\right)$ is the FIM of $\boldsymbol{\theta}$, and $\mathbf{h}$ maps $\boldsymbol{\theta}$ to τ_Δ. Notice that $NP\left(\mathbf{x}\right)$ is a scalar-valued function and accommodates estimating a vector of parameters for which there exists a mapping of the estimated parameters to the TDOA. Furthermore, Equation (4.25) may be written as

$$NP\left(\mathbf{x}\right) \triangleq \left(C_{\hat{\tau}_\Delta}\right)^{-1} \tag{4.26}$$

where $C_{\hat{\tau}_\Delta}$ is the CRLB on any unbiased estimate of τ_Δ. *NP* is the *inverse* of the CRLB for $\hat{\tau}_\Delta$, so that the navigation potential increases as the expected variance on an unbiased estimate of τ_Δ decreases.

The CRLB is a suitable foundation for defining *NP*, since it represents the minimum MSE achievable by any unbiased estimator of the navigation parameters of interest given the probability density function of the received signal. Since this bound holds for any unbiased estimator, $NP\left(\mathbf{x}\right)$ does not depend upon the estimator that will be used to estimate τ_Δ. Rather, the second partial in Equation (4.22) captures the *curvature* of the natural logarithm of the probability density function of $\mathbf{x}$ with

respect to the navigation parameters. Thus, the intrinsic ability to navigate from a received signal lies in the received signal's susceptibility to change in the navigation parameters. Strong curvature of the density function as a function of τ_Δ provides more *navigation potential*, or provides the potential for better estimation of τ_Δ, than does a density function that is flatter as a function of τ_Δ. For example, suppose the receiver moves in position (and, hence, the navigation parameters have changed). *NP* addresses the question, "How does the received signal change when the navigation parameter changes?" Heuristically, a signal with relatively small changes due to this position change would have less *NP* than signals which exhibit large changes due to the same position change.

Equation (4.25) defines the *NP* of $\mathbf{x}$ in terms the element of the inverse of the FIM that corresponds to τ_Δ. When τ_Δ alone is estimated, Equation (4.25) becomes

$$NP(\mathbf{x}) = I(\hat{\tau}_\Delta) \tag{4.27}$$

which is just the inverse of the CRLB for any unbiased estimate of τ_Δ. When two parameters are estimated, the inverse of the FIM for $\boldsymbol{\theta}_{2\times 1}$ is

$$\mathbf{I}^{-1}(\boldsymbol{\theta}) = \frac{1}{|\mathbf{I}(\boldsymbol{\theta})|}\begin{bmatrix} [\mathbf{I}(\boldsymbol{\theta})]_{22} & -[\mathbf{I}(\boldsymbol{\theta})]_{12} \\ -[\mathbf{I}(\boldsymbol{\theta})]_{12} & [\mathbf{I}(\boldsymbol{\theta})]_{11} \end{bmatrix} \tag{4.28}$$

where

$$|\mathbf{I}(\boldsymbol{\theta})| = [\mathbf{I}(\boldsymbol{\theta})]_{11}[\mathbf{I}(\boldsymbol{\theta})]_{22} - ([\mathbf{I}(\boldsymbol{\theta})]_{12})^2 \tag{4.29}$$

and the subscript $[\ ]_{ij}$ denotes "the i-j component of" the matrix. (Note that the symmetry of the FIM has been exploited.)

When τ_Δ is estimated simultaneously with another parameter, e.g.,

$$\boldsymbol{\theta} \triangleq \begin{bmatrix} \tau_\Delta \\ \nu \end{bmatrix} \tag{4.30}$$

the TDOA estimate is given through

$$\hat{\tau}_\Delta = \begin{bmatrix} 1 & 0 \end{bmatrix} \hat{\boldsymbol{\theta}} \tag{4.31}$$

so that

$$\frac{\partial \mathbf{h}(\boldsymbol{\theta})}{\partial \boldsymbol{\theta}} = \begin{bmatrix} 1 & 0 \end{bmatrix} \tag{4.32}$$

Substituting Equations (4.28), (4.29), and (4.32) into Equation (4.25), the NP of $\mathbf{x}$ when another parameter, ν, is estimated in addition to τ_Δ is

$$NP(\mathbf{x}) = [\mathbf{I}(\boldsymbol{\theta})]_{\tau_\Delta \tau_\Delta} - \frac{\left([\mathbf{I}(\boldsymbol{\theta})]_{\tau_\Delta \nu}\right)^2}{[\mathbf{I}(\boldsymbol{\theta})]_{\nu\nu}} \tag{4.33}$$

Notice that estimating another parameter reduces the NP when the likelihood function is not separable with respect to the two parameters (indicated by $\mathbf{I}(\boldsymbol{\theta})_{\tau_\Delta \nu} \neq 0$) and the nuisance parameter is not completely unknown (indicated by $\mathbf{I}(\boldsymbol{\theta})_{\nu\nu} \neq 0$).

When τ_1 and τ_2 are estimated, e.g.,

$$\boldsymbol{\theta} \triangleq \begin{bmatrix} \tau_1 \\ \tau_2 \end{bmatrix} \tag{4.34}$$

the TDOA estimate is found as

$$\hat{\tau}_\Delta \triangleq \hat{\tau}_1 - \hat{\tau}_2 = \begin{bmatrix} 1 & -1 \end{bmatrix} \hat{\boldsymbol{\theta}} \tag{4.35}$$

and

$$\frac{\partial \mathbf{h}(\boldsymbol{\theta})}{\partial \boldsymbol{\theta}} = \begin{bmatrix} 1 & -1 \end{bmatrix} \tag{4.36}$$

Substituting Equations (4.28), (4.29), and (4.36) into Equation (4.25), the NP of $\mathbf{x}$ when τ_1 and τ_2 are estimated is

$$NP(\mathbf{x}) = (C_{\tau_\Delta})^{-1} = \frac{[\mathbf{I}(\boldsymbol{\theta})]_{\tau_1\tau_1}[\mathbf{I}(\boldsymbol{\theta})]_{\tau_2\tau_2} - \left([\mathbf{I}(\boldsymbol{\theta})]_{\tau_1\tau_2}\right)^2}{[\mathbf{I}(\boldsymbol{\theta})]_{\tau_1\tau_1} + [\mathbf{I}(\boldsymbol{\theta})]_{\tau_2\tau_2} + 2[\mathbf{I}(\boldsymbol{\theta})]_{\tau_1\tau_2}} \tag{4.37}$$

Notice that $NP(\mathbf{x})$ decreases as the "cross information" of τ_1 and τ_2 represented in $\mathbf{I}(\boldsymbol{\theta})_{\tau_1\tau_2}$ increases.

4.2.5 NP Usefulness

The CRLB-based definition of $NP(\mathbf{x})$ given in Equation (4.25) is most appropriate when there exists an unbiased estimator that achieves this bound. Such an estimator is termed *efficient*; its existence is outlined in the following corollary.

Corollary 3 (Existence of an Efficient Estimate) *[43]*

An unbiased, efficient estimator of $\boldsymbol{\theta}$ *exists if and only if there exists a function* $\mathbf{g}$ *such that*

$$\frac{\partial}{\partial \boldsymbol{\theta}} \ln f(\mathbf{x};\boldsymbol{\theta}) = \mathbf{I}(\boldsymbol{\theta})[\mathbf{g}(\mathbf{x}) - \boldsymbol{\theta}] \tag{4.38}$$

If it exists, $\hat{\boldsymbol{\theta}} = \mathbf{g}(\mathbf{x})$ *is an unbiased, efficient estimator of* $\boldsymbol{\theta}$ *and its covariance is* $\mathbf{I}^{-1}(\boldsymbol{\theta})$.

Proof: *See [43].* ■

A common parameter estimation technique is the maximum likelihood estimate (MLE) approach. (Maybeck [48] provides a good discussion of the MLE approach.) The MLE is the value of $\boldsymbol{\theta}$ that maximizes $f(\mathbf{x};\boldsymbol{\theta})$ for $\mathbf{x}$ fixed; it is found as $\hat{\boldsymbol{\theta}}$ such

that [43]

$$\frac{\partial}{\partial \boldsymbol{\theta}} \ln f\left(\mathbf{x};\boldsymbol{\theta}\right)|_{\boldsymbol{\theta}=\hat{\boldsymbol{\theta}}} = \mathbf{0}^T \qquad \text{and} \qquad \frac{\partial^2}{\left(\partial \boldsymbol{\theta}\right)^2} \ln f\left(\mathbf{x};\boldsymbol{\theta}\right)|_{\boldsymbol{\theta}=\hat{\boldsymbol{\theta}}} \leq \mathbf{0} \tag{4.39}$$

If an efficient estimate exists, then the maximum likelihood estimate (MLE) approach will produce it [43].

When the signal model in Equation (4.2) provides a good indication of the real-world received model and an efficient estimate exists, the expression for $NP\left(\mathbf{x}\right)$ given in Equation (4.25) provides a good indication of navigation performance achievable with $\mathbf{x}$. In other words, *NP* is a useful indicator of *realizable* performance.

When an efficient estimator does not exist, $NP\left(\mathbf{x}\right)$ may be an overly optimistic indicator of *NP*; that is, the realizable performance may be worse than what is predicted from $NP\left(\mathbf{x}\right)$. Realizable lower bounds (higher than the CRLB) may be useful in defining $NP\left(\mathbf{x}\right)$ when an efficient estimate does not exist; however, many of these bounds are specific to particular classes of signals or require low signal-to-noise ratios [80,83,84]. The CRLB definition of $NP\left(\mathbf{x}\right)$ will be used in this research, because it applies for any $\mathbf{x}$ (even though it may be optimistic in some cases).

4.2.6 Evaluating $NP\left(\mathbf{x}\right)$ in General

Evaluating the expression for NP given in Equation (4.25) requires knowledge of $f\left(\mathbf{x};\boldsymbol{\theta}\right)$ to evaluate the terms of the FIM given in Equation (4.22). If $f\left(\mathbf{x};\boldsymbol{\theta}\right)$ is known or can be found, then $NP\left(\mathbf{x}\right)$ is completely defined.

In some cases, $f\left(\mathbf{x};\boldsymbol{\theta}\right)$ may be found experimentally without knowledge of the underlying mappings g_1 and g_2. For example, assuming $\mathbf{x}\left(\cdot,\cdot\right)$ is ergodic, one approach may be to find the mean and moments of $\mathbf{x}\left(\cdot,\cdot\right)$ using a time history of mea-

surements. Under the assumption of ergodicity, the mean of $\mathbf{x}(\cdot,\cdot)$, denoted by $\mu_{\mathbf{x}}$, is constant over t and given by

$$\mu_{\mathbf{x}} = E\{\mathbf{x}(t,\cdot)\}$$

While this method may be suitable for specific cases, it would be difficult to extend this to a general class of problems.

Section 4.3 will make reasonable assumptions about the mappings g_1 and g_2 to write $f(\mathbf{x};\boldsymbol{\theta})$ in terms of the mapping, signal, and noise probability density functions. The resulting *NP* expressions are found in more physically motivated terms than that which uses characteristics of the received signal directly. (Figure 7 in Section 4.1, page 50, shows graphically the model assumptions in this section and the sections that follow.)

4.3 Multipath Form of g_1 and g_2

In this section, a multipath model for g_1 and g_2 that captures a wide range of received signals is motivated. Without modeling g_1 and g_2, the designer may determine $f_{\mathbf{x}}(\cdot)$ experimentally (as discussed previously) or model it directly. This section confines the mappings g_1 and g_2 to specific forms, allowing $f_{\mathbf{x}}(\cdot)$ to be expressed in terms of physically meaningful probability density functions. Modeling $f_{\mathbf{x}}(\cdot)$ in terms of these density functions may be more readily accomplished than modeling $f_{\mathbf{x}}(\cdot)$ directly.

Prior to this research, only relatively simple models (such as modeling the received signal as the transmitted signal in noise) have been used to characterize navigation potential (*NP*). Furthermore, multipath models have been proposed in order

to reduce the effects of multipath upon the navigation solution (termed multipath mitigation) [2,58]. This research does not present a multipath mitigation technique; rather, it quantifies the ability to estimate the parameters of interest when the received signal includes the direct signal and multipath signals in noise. Furthermore, the form of the resulting $NP(\mathbf{x})$ may give insight into design considerations, multipath effects, or SOP selection.

To accomplish this task, Section 4.3.1 develops the multipath model. Section 4.3.2 translates the problem into the frequency domain. Section 4.3.3 relates $f_{\mathbf{x}}(\cdot)$ to the transmitted signal and noise when a multipath model is used. Finally, Section 4.3.4 derives an expression for $NP(\mathbf{x})$ under the multipath model constraint. (Figure 7 on page 50 shows graphically the model assumptions in this section as Box II.) Appendix D provides a more complete discussion on stochastic processes and their Fourier transforms.

4.3.1 Signal Model for $\mathbf{x}_{mp}$

The general form of the measurement random process, $\mathbf{x}(\cdot,\cdot)$, was given in Equation (4.2) and is restated here as

$$\mathbf{x}(\cdot,\cdot) \triangleq \begin{bmatrix} x_1(\cdot,\cdot) \\ x_2(\cdot,\cdot) \end{bmatrix} = \begin{bmatrix} g_1[\cdot,\cdot; s(\cdot,\cdot), n_1(\cdot,\cdot), \tau_1(\cdot)] \\ g_2[\cdot,\cdot; s(\cdot,\cdot), n_2(\cdot,\cdot), \tau_2(\cdot)] \end{bmatrix} \tag{4.2}$$

where the arguments $(\cdot,\cdot)$ denote time, t, where $t \in \mathbb{R}^1$, and some point in the sample space, ξ, where $\xi \in \Xi$, respectively; the argument $(\cdot)$ denotes time, t, where $t \in \mathbb{R}^1$. Furthermore, s models the received signal, n_i models the noise at the i^{th} receiver, τ_i is the time delay incurred by the transmitted signal to travel to the i^{th} receiver, and g_i is a mapping for the received signal at the i^{th} receiver.

The remainder of this subsection will introduce specific mappings, g_1 and g_2, that represent a received signal with multipath effects. The assumptions upon and the relationships between the transmitted signal, measurement noise, time delays, and mappings will be presented. Refer to Section D.2 in Appendix D for a more complete discussion on stochastic processes.

Consider when s, n_1, n_2, τ_1 and τ_2 are mapped into x_1 and x_2 for all t as [58]

$$\begin{aligned} x_{1_{mp}}(t,\cdot) &= s(t-\tau_1(t),\cdot) + n_1(t,\cdot) + \\ &\quad + \sum_{l=1}^{N_1} \alpha_l(t,\cdot)\, s[t-\tau_1(t)-\delta_l(t,\cdot),\cdot] \end{aligned} \tag{4.40}$$

$$\begin{aligned} x_{2_{mp}}(t,\cdot) &= s(t-\tau_2(t),\cdot) + n_2(t,\cdot) + \\ &\quad + \sum_{l=1}^{N_2} \beta_l(t,\cdot)\, s[t-\tau_2(t)-\varepsilon_l(t,\cdot),\cdot] \end{aligned} \tag{4.41}$$

This mapping represents the received signal as the transmitted signal in noise plus multiple delayed and attenuated replicas of the transmitted signal.

The received signals, $x_{1_{mp}}(\cdot,\cdot)$ and $x_{2_{mp}}(\cdot,\cdot)$, are stochastic processes with a probability density function at time t denoted by $f_{x_{1_{mp}}(t,\cdot)}(\xi)$ and $f_{x_{2_{mp}}(t,\cdot)}(\xi)$, respectively. The signal, $s(\cdot,\cdot)$, is modeled as a zero-mean, ergodic, wide-sense stationary, stochastic process. The joint probability density function, $f_{s(t_1,\cdot),\ldots,s(t_N,\cdot)}(\xi_1,\ldots,\xi_N)$, is assumed to exist and be known for all time sequences $\{t_1,\ldots,t_N\}$. The noise stochastic processes, $n_1(\cdot,\cdot)$ and $n_2(\cdot,\cdot)$, represent additive noise and have probability density functions at time t denoted by $f_{n_1(t,\cdot)}(\xi)$ and $f_{n_2(t,\cdot)}(\xi)$, respectively. $\tau_1(t)$ and $\tau_2(t)$ represent the delay at time t incurred by the transmitted signal resulting from traveling from the transmitter to the receivers. In general, this is a function

of the distance between the transmitter and receiver at time t. Given the signal propagation speed c, the i^{th} delay is

$$\tau_i(t) = \frac{d_i(t)}{c}$$

where $d_i(t)$ is the distance from the transmitter to the i^{th} receiver at time t.

Within the summation, each term represents a delayed and attenuated replica of the transmitted signal, and the number of replica signals, N_1 and N_2, are assumed to be known integers. The attenuation stochastic processes, $\alpha_l(\cdot,\cdot)$ and $\beta_m(\cdot,\cdot)$, represent the scaling incurred by the l^{th} replica of the s in x_1 and the m^{th} replica of s in x_2, respectively. The joint probability density functions, $f_{\alpha_l(t_1,\cdot),\ldots,\alpha_l(t_N,\cdot)}(\xi_1,\ldots,\xi_N)$ and $f_{\beta_m(t_1,\cdot),\ldots,\beta_m(t_N,\cdot)}(\xi_1,\ldots,\xi_N)$, are assumed to exist and be known for all time sequences $\{t_1,\ldots,t_N\}$, for all $l \in \{1,2,\cdots,N_1\}$, and for all $m \in \{1,2,\cdots,N_2\}$. The delay stochastic processes, $\delta_l(\cdot,\cdot)$ and $\varepsilon_m(\cdot,\cdot)$, represent the delay, *in addition to* τ_1, incurred by the l^{th} replica of the s in x_1 and the delay, *in addition to* τ_2, incurred by the m^{th} replica of s in x_2, respectively. The joint probability density functions, $f_{\delta_l(t_1,\cdot),\ldots,\delta_l(t_N,\cdot)}(\xi_1,\ldots,\xi_N)$ and $f_{\varepsilon_m(t_1,\cdot),\ldots,\varepsilon_m(t_N,\cdot)}(\xi_1,\ldots,\xi_N)$, are assumed to exist and be known for all time sequences $\{t_1,\ldots,t_N\}$, for all $l \in \{1,2,\cdots,N_1\}$, and for all $m \in \{1,2,\cdots,N_2\}$.

The relationships of the stochastic process in Equations (4.40) and (4.41) are shown in Table 1. A 0 denotes the processes are independent for all time; otherwise, the joint probability density function that describes the relationship is shown. These dependencies are physically motivated as follows.

Table 1. Relationship of Stochastic Processes in Eqs. (4.40) and (4.41)

	s	n_1	n_2	α_l	δ_l	β_p	ε_p	$\alpha_{m\neq l}$	$\delta_{m\neq l}$	$\beta_{q\neq p}$	$\varepsilon_{q\neq p}$
s	$\cdot$	0	0	0	0	0	0	0	0	0	0
n_1	0	$\cdot$	0	0	0	0	0	0	0	0	0
n_2	0	0	$\cdot$	0	0	0	0	0	0	0	0
α_l	0	0	0	$\cdot$	f_{α_l,δ_l}	0	0	0	0	0	0
δ_l	0	0	0	f_{α_l,δ_l}	$\cdot$	0	0	0	0	0	0
β_p	0	0	0	0	0	$\cdot$	$f_{\beta_p,\varepsilon_p}$	0	0	0	0
ε_p	0	0	0	0	0	$f_{\beta_p,\varepsilon_p}$	$\cdot$	0	0	0	0
$\forall l, m \in \{1, 2, \cdots, N_1\}$ $\quad$ $\forall p, q \in \{1, 2, \cdots, N_2\}$											

0 denotes independence; otherwise, f_{α_l,δ_l} and $f_{\beta_p,\varepsilon_p}$ are shorthand notations defined $\forall l \in \{1, 2, \cdots, N_1\}$, $\forall p \in \{1, 2, \cdots, N_2\}$, and for all time sequences $\{t_1, \ldots, t_N\}$ and $\{t_1, \ldots, t_M\}$ as

$$f_{\alpha_l,\delta_l} \triangleq f_{\alpha_l(t_1,\cdot),\ldots,\alpha_l(t_N,\cdot),\delta_l(t_1,\cdot),\ldots,\delta_l(t_M,\cdot)}\left(\xi_1, \ldots, \xi_N, \rho_1, \ldots, \rho_M\right)$$
$$f_{\beta_p,\varepsilon_p} \triangleq f_{\beta_m(t_1,\cdot),\ldots,\beta_m(t_N,\cdot),\varepsilon_m(t_1,\cdot),\ldots,\varepsilon_m(t_M,\cdot)}\left(\xi_1, \ldots, \xi_N, \rho_1, \ldots, \rho_M\right)$$

The noise terms are assumed to be receiver measurement noise and independent of each other and the signals (whether direct or replicated). Each replica signal has an associated attenuation and delay variable, perhaps resulting from the transmitted signal being reflected off an object before receipt. It is assumed that the receivers are spaced sufficiently far apart such that the local environments affecting each replica's attenuation and delay are independent of each other. Thus, the attenuation and delay variables associated with any replica at one receiver are independent of all attenuation and delay variables at the other receiver. Furthermore, each replica is assumed to result from a unique object or phenomenon. Consequently, the attenuation and delay variables are independent of all the remaining replicas' attenuation and delay variables. As shown in Table 1, the only related variables are the attenuation and delay of a given replica. Attenuation is due, in part, to a longer travel path length, absorbent reflective surfaces, scattering upon reflection, etc. The delay variable is a time representation of the additional travel path length. Thus, the attenuation and delay variables for a given replica are related through the joint probability density functions given in Table 1. Note that a phase shift of the replica signal compared to the direct transmitted signal may be represented in the attenuation or delay variable and does not impact the results in this section.

4.3.2 Spectral Representation of $\mathbf{x}_{mp}(\cdot,\cdot)$

In this subsection, Fourier analysis is used to translate the problem at hand into the frequency domain. The motivation for doing so is that (1) spectral properties may sometimes be more readily assumed or found experimentally than time domain properties, and (2) the frequency domain representation may be more mathemati-

cally tractable than a time domain representation. The result of this subsection is an equivalent expression of Equations (4.40) and (4.41) in the frequency domain. Appendix D provides much of the background theory for this section.

Typically, practical systems employ a finite-timelength observation of $\mathbf{x}_{mp}(\cdot,\cdot)$ for estimation of the navigation parameters (as opposed to considering $\mathbf{x}_{mp}(\cdot,\cdot)$ for all time). In this subsection, the Fourier transform of $\mathbf{x}_{mp}(\cdot,\cdot)$ is limited to a finite-timelength observation of $\mathbf{x}_{mp}(\cdot,\cdot)$. This formulation accounts for the observation length of $\mathbf{x}_{mp}(\cdot,\cdot)$ (allowing the effects of the observation length upon *NP* to be analyzed), while also permitting a somewhat less cumbersome spectral analysis than one which considers all time. The remainder of this subsection develops the spectral representation for a finite-timelength observation of $\mathbf{x}_{mp}(\cdot,\cdot)$ and relates this representation to the transmitted signal, the measurement noises, and the multipath mapping effects.

Consider a time segment of $\mathbf{x}_{mp}(\cdot,\cdot)$ centered at t_i consisting of all $\mathbf{x}_{mp}(t,\cdot)$ over the region $t \in \left[t_i - \frac{T}{2}, t_i + \frac{T}{2}\right]$, written as

$$\mathbf{x}_{mp,\Pi}(t,\cdot) \triangleq \frac{1}{T}\prod\left(\frac{t-t_i}{T}\right)\mathbf{x}_{mp}(t,\cdot) \quad \forall t \in \mathbb{R}^1 \tag{4.42}$$

where the *pulse function* is defined as

$$\prod(x) \triangleq \begin{cases} 1 & x \in \left[-\frac{1}{2}, +\frac{1}{2}\right] \\ 0 & \text{otherwise} \end{cases} \tag{4.43}$$

and Π in the subscript denotes the signal is "time-gated". The inclusion of the $\frac{1}{T}$ factor in Equation (4.42) makes the results consistent with results from a formulation which constrains $\mathbf{x}_{mp}(t,\cdot)$ to be periodic and measures one period [44, 45].

Since $\mathbf{x}_{mp,\Pi}(\cdot,\cdot)$ is nonzero over a measurable segment of t [59], the ordinary Fourier transform of $\mathbf{x}_{mp,\Pi}(t,\cdot)$ given in Equation (4.42) defined over all t, denoted by $\tilde{\mathbf{x}}_{mp,\Pi}(\cdot,\cdot)$, is given for all f as

$$\tilde{\mathbf{x}}_{mp,\Pi}(f,\cdot) \triangleq \mathcal{F}\{\mathbf{x}_{mp,\Pi}(t,\cdot)\} \tag{4.44}$$

$$= \mathcal{F}\left\{\frac{1}{T}\prod\left(\frac{t-t_i}{T}\right)\mathbf{x}_{mp}(t,\cdot)\right\} \tag{4.45}$$

where $\mathcal{F}$ denotes the Fourier transform. (Notice that the Fourier transform is written in terms of f rather than ω. This convention avoids scaling factors of 2π that result from $\omega = 2\pi f$.) Writing $\mathbf{x}_{mp}(t,\cdot)$ in terms of its components, Equation (4.45) becomes

$$\tilde{\mathbf{x}}_{mp,\Pi}(\cdot,\cdot) = \mathcal{F}\left\{\frac{1}{T}\prod\left(\frac{t-t_i}{T}\right)\begin{bmatrix} x_{1_{mp}}(t,\cdot) \\ x_{2_{mp}}(t,\cdot) \end{bmatrix}\right\} \quad \forall t \tag{4.46}$$

Notice that $\tilde{\mathbf{x}}_{mp,\Pi}(\cdot,\cdot)$ is a stochastic process. Each realization of $\mathbf{x}_{mp}(\cdot,\cdot)$ can be used to generate a realization of $\tilde{\mathbf{x}}_{mp,\Pi}(\cdot,\cdot)$. At each f, $\tilde{\mathbf{x}}_{mp,\Pi}(f,\cdot)$ is a random variable.

Consider writing $\tilde{\mathbf{x}}_{mp,\Pi}(\cdot,\cdot)$ in terms of the transmitted signal, the measurement noises, and the multipath mapping effects. Assuming the time delays and attenuations are constant over the interval $\left[t_i - \frac{T}{2}, t_i + \frac{T}{2}\right]$ and recalling $x_{1_{mp}}(\cdot,\cdot)$ and $x_{2_{mp}}(\cdot,\cdot)$ were defined in Equations (4.40) and (4.41), respectively, Equation (4.46)

may be written for all t as

$$\tilde{\mathbf{x}}_{mp,\Pi}(\cdot,\cdot) = \mathcal{F}\left\{ \frac{1}{T}\prod\left(\frac{t-t_i}{T}\right) \left[\begin{array}{l} s\left(t-\tau_1\left(t_i\right),\cdot\right)+n_1\left(t,\cdot\right) \\ \quad +\sum_{l=1}^{N_1}\alpha_l\left(t_i,\cdot\right)s\left[t-\tau_1\left(t_i\right)-\delta_l\left(t_i,\cdot\right),\cdot\right] \\ \\ s\left(t-\tau_2\left(t_i\right),\cdot\right)+n_2\left(t,\cdot\right) \\ \quad +\sum_{l=1}^{N_2}\beta_l\left(t_i,\cdot\right)s\left[t-\tau_2\left(t_i\right)-\varepsilon_l\left(t_i,\cdot\right),\cdot\right] \end{array} \right] \right\} \tag{4.47}$$

Finally, $\tilde{\mathbf{x}}_{mp,\Pi}(\cdot,\cdot)$ may be written for all f as

$$\tilde{\mathbf{x}}_{mp,\Pi}(f,\cdot) = \left[\begin{array}{l} \tilde{s}_\Pi(f,\cdot)\,e^{-j2\pi f\tau_1(t_i)}\left(1+\sum_{l=1}^{N_1}\alpha_l\left(t_i,\cdot\right)e^{-j2\pi f\delta_l(t_i,\cdot)}\right) \\ \\ \tilde{s}_\Pi(f,\cdot)\,e^{-j2\pi f\tau_2(t_i)}\left(1+\sum_{l=1}^{N_2}\beta_l\left(t_i,\cdot\right)e^{-j2\pi f\varepsilon_l(t_i,\cdot)}\right) \end{array} \right] + \tilde{\mathbf{n}}_\Pi(f,\cdot) \tag{4.48}$$

where

$$\tilde{s}_\Pi(f,\cdot) \triangleq \mathcal{F}\left\{\frac{1}{T}\prod\left(\frac{t-t_i}{T}\right)s(t,\cdot)\right\} \tag{4.49}$$

and

$$\tilde{\mathbf{n}}_\Pi(f,\cdot) \triangleq \mathcal{F}\left\{\frac{1}{T}\prod\left(\frac{t-t_i}{T}\right)\mathbf{n}(t,\cdot)\right\} \tag{4.50}$$

4.3.3 Characterization of $\tilde{\mathbf{x}}_{mp,\Pi}(\cdot,\cdot)$

This subsection characterizes the stochastic nature of $\tilde{\mathbf{x}}_{mp,\Pi}(\cdot,\cdot)$, defined as the Fourier transform of a finite-timelength observation of $\mathbf{x}_{mp}(\cdot,\cdot)$. If it exists, $\tilde{\mathbf{x}}_{mp,\Pi}(\cdot,\cdot)$ is completely characterized through the joint probability density function

$$f_{\tilde{\mathbf{x}}_{mp,\Pi}(f_1,\cdot),\ldots,\tilde{\mathbf{x}}_{mp,\Pi}(f_N,\cdot)}\left(\boldsymbol{\xi}_1,\ldots,\boldsymbol{\xi}_N\right) \tag{4.51}$$

for all sequences $\{f_1, \ldots, f_N\}$. Using the frequency-domain model for $\mathbf{x}_{mp}(\cdot,\cdot)$ developed in Subsection 4.3.1, $\tilde{\mathbf{x}}_{mp,\Pi}(\cdot,\cdot)$ and, consequently, the *NP* of $\tilde{\mathbf{x}}_{mp,\Pi}(\cdot,\cdot)$, may be characterized through the stochastic nature of the transmitted signal, the measurement noises, and the multipath model effects. The impact of this formulation is that the *NP* may be expressed in terms that are meaningful to the designer.

The relationship of $\tilde{\mathbf{x}}_{mp,\Pi}(\cdot,\cdot)$ to

$$\tilde{s}_{\Pi}(\cdot,\cdot),\ \tilde{\mathbf{n}}_{\Pi}(\cdot,\cdot),\ \alpha(t_i,\cdot),\ \beta(t_i,\cdot),\ \delta(t_i,\cdot),\ \text{and}\ \varepsilon(t_i,\cdot)$$

is given in Equation (4.48). The following development considers the probability density function of $\tilde{\mathbf{x}}_{mp,\Pi}(\cdot,\cdot)$ *for a single* f. An extension to the single-f case presented here could be found by augmenting the random variables over each frequency to accommodate an arbitrary sequence $\{f_1, \ldots, f_N\}$.

The aim of this subsection is to find the probability density function of $\tilde{\mathbf{x}}_{mp,\Pi}(f)$ *for a single* f, denoted as $f_{\tilde{\mathbf{x}}_{mp,\Pi}(f,\cdot)}(\boldsymbol{\xi})$, in terms of the joint probability density function

$$f_{\tilde{s}_{\Pi}(f,\cdot)\tilde{\mathbf{n}}_{\Pi}(f,\cdot),\boldsymbol{\alpha}(t_i,\cdot),\boldsymbol{\beta}(t_i,\cdot),\boldsymbol{\delta}(t_i,\cdot),\boldsymbol{\varepsilon}(t_i,\cdot)}(\cdot,\cdot,\cdot,\cdot,\cdot,\cdot) \tag{4.52}$$

where

$$\boldsymbol{\alpha}(t_i,\cdot) \triangleq \left[\ \alpha_1(t_i,\cdot) \quad \cdots \quad \alpha_{N_1}(t_i,\cdot)\ \right]^T \tag{4.53}$$

$$\boldsymbol{\beta}(t_i,\cdot) \triangleq \left[\ \beta_1(t_i,\cdot) \quad \cdots \quad \beta_{N_2}(t_i,\cdot)\ \right]^T \tag{4.54}$$

$$\boldsymbol{\delta}(t_i,\cdot) \triangleq \left[\ \delta_1(t_i,\cdot) \quad \cdots \quad \delta_{N_2}(t_i,\cdot)\ \right]^T \tag{4.55}$$

$$\boldsymbol{\varepsilon}(t_i,\cdot) \triangleq \left[\ \varepsilon_1(t_i,\cdot) \quad \cdots \quad \varepsilon_{N_2}(t_i,\cdot)\ \right]^T \tag{4.56}$$

Note that the following also hold:

$$f_{\boldsymbol{\alpha}(t_i,\cdot)} \triangleq f_{\alpha_1(t_i,\cdot),\ldots,\alpha_{N_1}(t_i,\cdot)} \tag{4.57}$$

$$f_{\boldsymbol{\beta}(t_i,\cdot)} \triangleq f_{\beta_1(t_i,\cdot),\ldots,\beta_{N_2}(t_i,\cdot)} \tag{4.58}$$

$$f_{\boldsymbol{\delta}(t_i,\cdot)} \triangleq f_{\delta_1(t_i,\cdot),\ldots,\delta_{N_2}(t_i,\cdot)} \tag{4.59}$$

$$f_{\boldsymbol{\varepsilon}(t_i,\cdot)} \triangleq f_{\varepsilon_1(t_i,\cdot),\ldots,\varepsilon_{N_2}(t_i,\cdot)} \tag{4.60}$$

Recall from Table 1 on page 67 that

1. s, n_1, and n_2 are pairwise independent.
2. α_l and δ_m are pairwise independent of s, n_1, and n_2 for all $l, m \in [1, N_1]$.
3. α_l and δ_m are pairwise independent of each other for all $l \neq m$.
4. β_p and ε_q are pairwise independent of s, n_1, and n_2 for all $p, q \in [1, N_2]$.
5. β_p and ε_q are pairwise independent of each other for all $p \neq q$.

Therefore, the joint probability density function in Equation (4.52) is equivalent to

$$\begin{aligned} &f_{\tilde{s}_\Pi(f,\cdot)\tilde{\mathbf{n}}_\Pi(f,\cdot),\boldsymbol{\alpha}(t_i,\cdot),\boldsymbol{\beta}(t_i,\cdot),\boldsymbol{\delta}(t_i,\cdot),\boldsymbol{\varepsilon}(t_i,\cdot)}(\cdot,\cdot,\cdot,\cdot,\cdot,\cdot,\cdot) = \\ &\quad f_{\tilde{s}_\Pi(f,\cdot)}(\cdot)\, f_{\tilde{n}_{\Pi_1}(f,\cdot)}(\cdot)\, f_{\tilde{n}_{\Pi_2}(f,\cdot)}(\cdot)\, f_{\alpha_1(t_i,\cdot),\delta_1(t_i,\cdot)}(\cdot,\cdot) \\ &\quad \cdots f_{\alpha_{N_1}(t_i,\cdot),\delta_{N_1}(t_i,\cdot)}(\cdot,\cdot)\, f_{\beta_1(t_i,\cdot),\varepsilon_1(t_i,\cdot)}(\cdot,\cdot) \cdots f_{\beta_{N_2}(t_i,\cdot),\varepsilon_{N_2}(t_i,\cdot)}(\cdot,\cdot) \end{aligned} \tag{4.61}$$

Sequential "change of variables" on the probability density functions (as dictated by the underlying processes' relationships in Equation (4.48)) will result in an expression for $f_{\tilde{\mathbf{x}}_{mp,\Pi}(f,\cdot)}(\boldsymbol{\xi})$ in terms of $f_{\tilde{s}_\Pi(f,\cdot)}(\cdot)$, $f_{\tilde{n}_{\Pi_1}(f,\cdot)}(\cdot)$, $f_{\tilde{n}_{\Pi_2}(f,\cdot)}(\cdot)$, $f_{\alpha_l(t_i,\cdot),\delta_l(t_i,\cdot)}(\cdot,\cdot)$, and

$f_{\beta_p(t_i,\cdot),\varepsilon_p(t_i,\cdot)}(\cdot,\cdot)$ for all $l \in \{1,2,\cdots,N_1\}$ and for all $p \in \{1,2,\cdots,N_2\}$. It is assumed that each probability density function in Equation (4.61) is known.

Since this development becomes quite nested, Figure 8 provides a graphical depiction of the development flow and the intermediate random variable definitions for evaluating Equation (4.48). As shown therein, the following development will progress by defining the intermediate random variables δ_{e_l}, γ_{1_l}, γ_{1_Σ}, γ_{1_Σ}, γ'_{1_Σ}, γ''_{1_Σ}, γ''_{2_Σ}, $\boldsymbol{\gamma}''_\Sigma$, $\mathbf{y}$, and finally ending with $\tilde{\mathbf{x}}_{mp,\Pi}$. At each step, the appropriate probability density function will be given. Furthermore, all of the theorems referenced during the remainder of this subsection may be found in Appendix C. Note that each stochastic process has been evaluated to a random variable. Specifically, the stochastic processes in this development, i.e.,

$$\begin{gathered}\tilde{s}_\Pi(\cdot,\cdot),\, \tilde{n}_{\Pi_1}(\cdot,\cdot),\, \tilde{n}_{\Pi_2}(\cdot,\cdot),\, \alpha_l(\cdot,\cdot),\, \delta_l(\cdot,\cdot),\, \beta_p(\cdot,\cdot),\, \varepsilon_p(\cdot,\cdot) \\ \forall l \in \{1,2,\cdots,N_1\}, p \in \{1,2,\cdots,N_2\}\end{gathered} \tag{4.62}$$

have been evaluated to yield random variables, i.e.,

$$\begin{gathered}\tilde{s}_\Pi(f,\cdot),\, \tilde{n}_{\Pi_1}(f,\cdot),\, \tilde{n}_{\Pi_2}(f,\cdot),\, \alpha_l(t_i,\cdot),\, \delta_l(t_i,\cdot),\, \beta_p(t_i,\cdot),\, \varepsilon_p(t_i,\cdot) \\ \forall l \in \{1,2,\cdots,N_1\}, p \in \{1,2,\cdots,N_2\}\end{gathered} \tag{4.63}$$

To find expression for $f_{\tilde{\mathbf{x}}_{mp,\Pi}(f,\cdot)}(\boldsymbol{\xi})$ in terms of each probability density function in Equation (4.61), begin with the innermost definition in Figure 8. Define, for the l^{th} delay stochastic process at the first receiver,

$$\delta_{e_l}\left(t_i,\xi_{\delta_l}\right) \triangleq e^{-j2\pi f\delta_l\left(t_i,\xi_{\delta_l}\right)} \tag{4.64}$$

and the transformations θ_{α_l} and θ_{δ_l} for each l such that

$$\begin{bmatrix} \alpha_l(t_i,\cdot) \\ \delta_{e_l}(t_i,\cdot) \end{bmatrix} = \begin{bmatrix} \theta_{\alpha_l}[\alpha_l(t_i,\cdot)] \\ \theta_{\delta_l}[\delta_l(t_i,\cdot)] \end{bmatrix} = \begin{bmatrix} \alpha_l(t_i,\cdot) \\ e^{-j2\pi f\delta_l(t_i,\cdot)} \end{bmatrix} \tag{4.65}$$

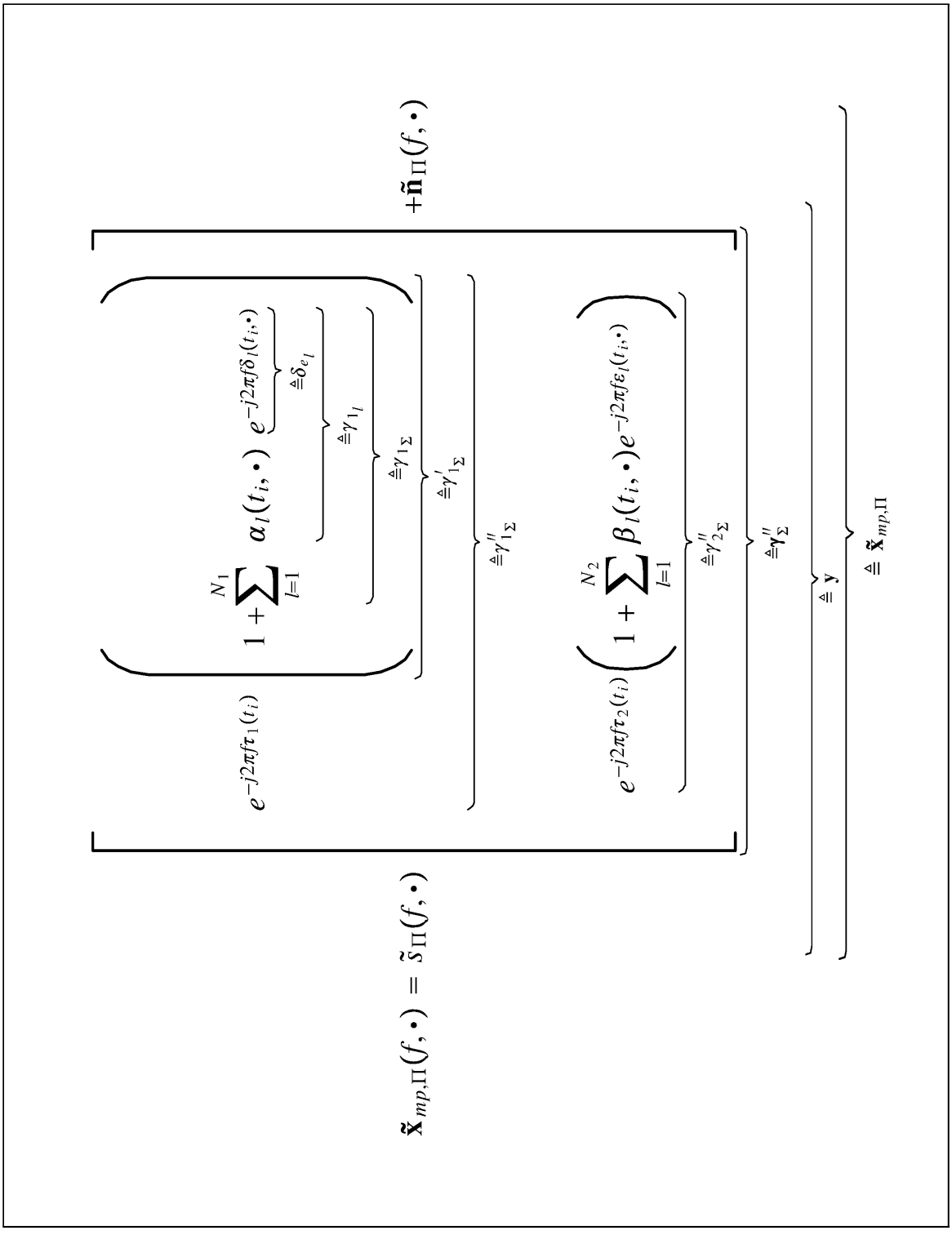

Figure 8. Development Flow and Intermediate Random Variable Definitions for Evaluating Equation (4.48).

Using Theorem 4 on page 195 with

$$(\theta_{\alpha_l})^{-1}\,\alpha_l\,(t_i,\cdot) \;=\; \alpha_l\,(t_i,\cdot) \tag{4.66}$$

$$(\theta_{\delta_l})^{-1}\,\delta_{e_l}\,(t_i,\cdot) \;=\; \frac{\ln\left[\delta_{e_l}\,(t_i,\cdot)\right]}{-j2\pi f} \tag{4.67}$$

and

$$\begin{aligned}
\left\|\frac{\partial\left[(\theta_{\alpha_l})^{-1}\left(\xi_{\alpha_l}\right),(\theta_{\delta_l})^{-1}\left(\xi_{\delta_{e_l}}\right)\right]}{\partial\left(\xi_{\alpha_l},\xi_{\delta_{e_l}}\right)}\right\| &= \left\| \begin{array}{cc} \frac{\partial}{\partial\xi_{\alpha_l}}(\theta_{\alpha_l})^{-1}\left(\xi_{\alpha_l}\right) & \frac{\partial}{\partial\xi_{\delta_{e_l}}}(\theta_{\alpha_l})^{-1}\left(\xi_{\alpha_l}\right) \\ \frac{\partial}{\partial\xi_{\alpha_l}}(\theta_{\delta_l})^{-1}\left(\xi_{\delta_{e_l}}\right) & \frac{\partial}{\partial\xi_{\delta_{e_l}}}(\theta_{\delta_l})^{-1}\left(\xi_{\delta_{e_l}}\right) \end{array} \right\| \\
&= \left\| \begin{array}{cc} \frac{\partial}{\partial\xi_{\alpha_l}}\left(\xi_{\alpha_l}\right) & \frac{\partial}{\partial\xi_{\delta_{e_l}}}\left(\xi_{\alpha_l}\right) \\ \frac{\partial}{\partial\xi_{\alpha_l}}\frac{\ln\left(\xi_{\delta_{e_l}}\right)}{-j2\pi f} & \frac{\partial}{\partial\xi_{\delta_{e_l}}}\frac{\ln\left(\xi_{\delta_{e_l}}\right)}{-j2\pi f} \end{array} \right\| \\
&= \left\| \begin{array}{cc} 1 & 0 \\ 0 & \frac{1}{-j2\pi f\xi_{\delta_{e_l}}} \end{array} \right\| \\
&= \frac{1}{2\pi\,|f|}
\end{aligned}$$

Thus, each $f_{\alpha_l(t_i,\cdot),\delta_{e_l}(t_i,\cdot)}\left(\xi_{\alpha_l},\xi_{\delta_{e_l}}\right)$ can be expressed in terms of $f_{\alpha_l(t_i,\cdot),\delta_l(t_i,\cdot)}\left(\xi_{\alpha_l},\xi_{\delta_l}\right)$ as

$$f_{\alpha_l(t_i,\cdot),\delta_{e_l}(t_i,\cdot)}\left(\xi_{\alpha_l},\xi_{\delta_{e_l}}\right) = \frac{1}{2\pi\,|f|} f_{\alpha_l(t_i,\cdot),\delta_l(t_i,\cdot)}\left(\xi_{\alpha_l},\frac{\ln\left(\xi_{\delta_{e_l}}\right)}{-j2\pi f}\right) \tag{4.68}$$

Next, define

$$\gamma_{1_l}\,(t_i,\cdot) \triangleq \alpha_l\,(t_i,\cdot)\,\delta_{e_l}\,(t_i,\cdot) \tag{4.69}$$

which represents

$$\gamma_{1_l}\,(t_i,\cdot) = \alpha_l\,(t_i,\cdot)\,e^{-j2\pi f\delta_l(t_i,\cdot)} \tag{4.70}$$

At this point, $\gamma_{1_\Sigma}(t_i,\cdot)$ is a random variable representing the summation within the first receiver's received signal. The probability density function of $\gamma_{1_\Sigma}(t_i,\cdot)$, or $f_{\gamma_{1_\Sigma}(t_i,\cdot)}\left(\xi_{\gamma_{1_\Sigma}}\right)$, is given by Equation (4.77). Each probability density function on the right-hand side of Equation (4.77) may be found in terms of $f_{\alpha_l(t_i,\cdot),\delta_{e_l}(t_i,\cdot)}(\cdot,\cdot)$ using Equation (4.71). Finally, each probability density function of $f_{\alpha_l(t_i,\cdot),\delta_{e_l}(t_i,\cdot)}(\cdot,\cdot)$ may be found in terms of $f_{\alpha_l(t_i,\cdot),\delta_l(t_i,\cdot)}(\cdot,\cdot)$ using Equation (4.68), in which, each $f_{\alpha_l(t_i,\cdot),\delta_l(t_i,\cdot)}(\cdot,\cdot)$ is assumed to be known. Thus, $\gamma_{1_\Sigma}(t_i,\cdot)$ may be used to represent the multipath effects within the first received signal.

Continuing through Figure 8, let

$$\gamma'_{1_\Sigma}(t_i,\cdot) \triangleq 1+\gamma_{1_\Sigma}(t_i,\cdot) \tag{4.78}$$

Using Theorem 7 on page 196, the probability density function of $\gamma'_{1_\Sigma}(t_i,\cdot)$ in terms of $f_{\gamma_{1_\Sigma}(t_i,\cdot)}\left(\xi_{\gamma_{1_\Sigma}}\right)$ is

$$f_{\gamma'_{1_\Sigma}(t_i,\cdot)}\left(\xi_{\gamma'_{1_\Sigma}}\right) = f_{\gamma_{1_\Sigma}(t_i,\cdot)}\left(\xi_{\gamma'_{1_\Sigma}}-1\right) \tag{4.79}$$

Defining

$$\begin{aligned}\gamma''_{1_\Sigma}(t_i,\cdot) &\triangleq e^{-j2\pi f\tau_1(t_i)}\gamma'_{1_\Sigma}(t_i,\cdot) &(4.80)\\ &= e^{-j2\pi f\tau_1(t_i)}\left(1+\sum_{l=1}^{N_1}\alpha_l(t_i,\cdot)\,e^{-j2\pi f\delta_l(t_i,\cdot)}\right) &(4.81)\end{aligned}$$

and noting

$$\left\|e^{j2\pi f\tau_1(t_i)}\right\| = 1 \tag{4.82}$$

application of Theorem 7 results in

$$f_{\gamma''_{1_\Sigma}(t_i,\cdot)}\left(\xi_{\gamma''_{1_\Sigma}};\tau_1(t_i)\right) = f_{\gamma'_{1_\Sigma}(t_i,\cdot)}\left(\xi_{\gamma''_{1_\Sigma}} e^{j2\pi f\tau_1(t_i)}\right) \tag{4.83}$$

As indicated in Figure 8, the same procedure as was accomplished for $\gamma''_{1_\Sigma}(t_i,\cdot)$ could be conducted for

$$\gamma''_{2_\Sigma}(t_i,\cdot) \triangleq e^{-j2\pi f\tau_2(t_i)}\left(1+\sum_{l=1}^{N_1}\beta_l(t_i,\cdot)\,e^{-j2\pi f\varepsilon_l(t_i,\cdot)}\right) \tag{4.84}$$

to find $f_{\gamma''_{2_\Sigma}(t_i,\cdot)}\left(\xi_{\gamma''_{2_\Sigma}};\tau_2(t_i)\right)$ in terms of each $f_{\beta_l(t_i,\cdot),\varepsilon_l(t_i,\cdot)}(\cdot,\cdot)$. Furthermore, $\gamma''_{1_\Sigma}(t_i,\cdot)$ and $\gamma''_{2_\Sigma}(t_i,\cdot)$ are independent, since all $\gamma''_{1_l}(t_i,\cdot)$ and $\gamma''_{2_m}(t_i,\cdot)$ are mutually independent $\forall l \in \{1,2,\cdots,N_1\}$ and $\forall m \in \{1,2,\cdots,N_2\}$. Thus,

$$\begin{aligned} &f_{\gamma''_{1_\Sigma}(t_i,\cdot),\gamma''_{2_\Sigma}(t_i,\cdot)}\left(\xi_{\gamma''_{1_\Sigma}},\xi_{\gamma''_{2_\Sigma}};\tau_1(t_i),\tau_2(t_i)\right) \\ &\quad = f_{\gamma''_{1_\Sigma}(t_i,\cdot)}\left(\xi_{\gamma''_{1_\Sigma}};\tau_1(t_i)\right) f_{\gamma''_{2_\Sigma}(t_i,\cdot)}\left(\xi_{\gamma''_{2_\Sigma}};\tau_2(t_i)\right) \end{aligned} \tag{4.85}$$

This can be written as

$$f_{\boldsymbol{\gamma}''_\Sigma(t_i,\cdot)}\left(\boldsymbol{\xi}_{\gamma''_\Sigma};\tau_1(t_i),\tau_2(t_i)\right) \triangleq f_{\gamma''_{1_\Sigma}(t_i,\cdot),\gamma''_{2_\Sigma}(t_i,\cdot)}\left(\xi_{\gamma''_{1_\Sigma}},\xi_{\gamma''_{2_\Sigma}};\tau_1(t_i),\tau_2(t_i)\right) \tag{4.86}$$

where

$$\boldsymbol{\gamma}''_\Sigma(t_i,\cdot) \triangleq \begin{bmatrix} \gamma''_{1_\Sigma}(t_i,\cdot) \\ \gamma''_{2_\Sigma}(t_i,\cdot) \end{bmatrix} \tag{4.87}$$

For clarity, it is remarked that substitutions in Figure 8 have been used to reduce Equation (4.48) to

$$\tilde{\mathbf{x}}_{mp,\Pi}(f,\cdot) = \tilde{s}_\Pi(f,\cdot)\,\boldsymbol{\gamma}''_\Sigma(t_i,\cdot) + \tilde{\mathbf{n}}_\Pi(f,\cdot) \tag{4.88}$$

for which the probability density functions of $s(t,\cdot)$, $\boldsymbol{\gamma}''_\Sigma(t,\cdot)$, and $\mathbf{n}(t,\cdot)$ are all known and pairwise independent.

Continuing with Figure 8, define the intermediate term

$$\mathbf{y}\left(f,\cdot\right)=\tilde{s}_{\Pi}\left(f,\cdot\right)\boldsymbol{\gamma}''_{\Sigma}\left(t_i,\cdot\right) \tag{4.89}$$

Using Theorem 8 on page 196,

$$f_{\mathbf{y}(f,\cdot)}\left(\boldsymbol{\xi}_y\right)=\int_{-\infty}^{+\infty}\frac{1}{\left(\xi_s\right)^2}f_{\tilde{s}_{\Pi}(f,\cdot)}\left(\xi_s\right)f_{\gamma''_{1_{\Sigma}}(t_i,\cdot)}\left(\frac{\xi_{y_1}}{\xi_s}\right)f_{\gamma''_{2_{\Sigma}}(t_i,\cdot)}\left(\frac{\xi_{y_2}}{\xi_s}\right)d\xi_s \tag{4.90}$$

Finally,

$$\tilde{\mathbf{x}}_{mp,\Pi}\left(f,\cdot\right)=\mathbf{y}\left(f,\cdot\right)+\tilde{\mathbf{n}}_{\Pi}\left(f,\cdot\right) \tag{4.91}$$

is found using Theorem 9 as

$$f_{\mathbf{x}_{mp,\Pi}(f,\cdot)}\left(\boldsymbol{\xi}_x\right)=\int_{-\infty}^{+\infty}\int_{-\infty}^{+\infty}f_{\mathbf{y}(f,\cdot),\tilde{\mathbf{n}}_{\Pi}(f,\cdot)}\left(\boldsymbol{\xi}_y,\boldsymbol{\xi}_x-\boldsymbol{\xi}_y\right)d\xi_{y_1}d\xi_{y_2} \tag{4.92}$$

Since $\mathbf{z}$ and $\mathbf{n}$ are independent,

$$f_{\mathbf{x}_{mp,\Pi}(f,\cdot)}\left(\boldsymbol{\xi}_x\right)=\int_{-\infty}^{+\infty}\int_{-\infty}^{+\infty}f_{\mathbf{y}(f,\cdot)}\left(\boldsymbol{\xi}_y\right)f_{\tilde{\mathbf{n}}_{\Pi}(f,\cdot)}\left(\boldsymbol{\xi}_x-\boldsymbol{\xi}_y\right)d\xi_{y_1}d\xi_{y_2} \tag{4.93}$$

Note that $f_{\mathbf{x}_{mp,\Pi}(f,\cdot)}\left(\boldsymbol{\xi}_x\right)$ may be defined in terms of the know probability density functions, since $f_{\tilde{\mathbf{n}}_{\Pi}(f,\cdot)}\left(\boldsymbol{\xi}_n\right)$ is known and $f_{\mathbf{y}(f,\cdot)}\left(\boldsymbol{\xi}_y\right)$ can be related known probability density functions.

These results may be combined to find $f_{\mathbf{x}_{mp,\Pi}(f,\cdot)}\left(\boldsymbol{\xi}_x\right)$ in terms of the known probability density functions in Equation (4.61). Recall the previous results:

$$f_{\mathbf{y}(f,\cdot)}\left(\boldsymbol{\xi}_y\right)=\int_{-\infty}^{+\infty}\frac{1}{\left(\xi_s\right)^2}f_{\tilde{s}_{\Pi}(f,\cdot)}\left(\xi_s\right)f_{\gamma''_{1_{\Sigma}}(t_i,\cdot)}\left(\frac{\xi_{y_1}}{\xi_s}\right)f_{\gamma''_{2_{\Sigma}}(t_i,\cdot)}\left(\frac{\xi_{y_2}}{\xi_s}\right)d\xi_s \tag{4.90}$$

$$f_{\gamma''_{1_{\Sigma}}(t_i,\cdot)}\left(\xi_{\gamma''_{1_{\Sigma}}};\tau_1\left(t_i\right)\right)=f_{\gamma'_{1_{\Sigma}}(t_i,\cdot)}\left(\xi_{\gamma''_{1_{\Sigma}}}e^{j2\pi f\tau_1(t_i)}\right) \tag{4.83}$$

$$f_{\gamma'_{1_\Sigma}(t_i,\cdot)}\left(\xi_{\gamma'_{1_\Sigma}}\right) = f_{\gamma_{1_\Sigma}(t_i,\cdot)}\left(\xi_{\gamma'_{1_\Sigma}} - 1\right) \tag{4.79}$$

$$\begin{aligned} f_{\gamma_{1_\Sigma}(t_i,\cdot)}\left(\xi_{\gamma_{1_\Sigma}}\right) &= \int_{-\infty}^{+\infty}\int_{-\infty}^{+\infty}\cdots\int_{-\infty}^{+\infty} f_{\gamma_{1_1}(t_i,\cdot)}\left(\xi_{\gamma_{1_\Sigma}} - \xi_{\gamma_{1_2}} - \xi_{\gamma_{1_3}}\cdots - \xi_{\gamma_{1_{N_1}}}\right)\bullet \\ &\quad f_{\gamma_{1_2}(t_i,\cdot)}\left(\xi_{\gamma_{1_2}}\right) f_{\gamma_{1_3}(t_i,\cdot)}\left(\xi_{\gamma_{1_3}}\right)\cdots f_{\gamma_{1_{N_1}}(t_i,\cdot)}\left(\xi_{\gamma_{1_{N_1}}}\right)\bullet \\ &\quad d\xi_{\gamma_{1_2}} d\xi_{\gamma_{1_3}}\cdots d\xi_{\gamma_{1_{N_1}}} \end{aligned} \tag{4.77}$$

$$f_{\gamma_{1_l}(t_i,\cdot)}\left(\xi_{\gamma_{1_l}}\right) = \int_{-\infty}^{+\infty}\frac{1}{\left|\xi_{\alpha_l}\right|} f_{\alpha_l(t_i,\cdot),\delta_{e_l}(t_i,\cdot)}\left(\xi_{\alpha_l}, \frac{\xi_{\gamma_l}}{\xi_{\alpha_l}}\right) d\xi_{\alpha_l} \tag{4.71}$$

$$f_{\alpha_l(t_i,\cdot),\delta_{e_l}(t_i,\cdot)}\left(\xi_{\alpha_l}, \xi_{\delta_{e_l}}\right) = \frac{1}{2\pi\left|f\right|} f_{\alpha_l(t_i,\cdot),\delta_l(t_i,\cdot)}\left(\xi_{\alpha_l}, \frac{\ln\left(\xi_{\delta_{e_l}}\right)}{-j2\pi f}\right) \tag{4.68}$$

Substituting Equation (4.90) into Equation (4.93), the probability density function of $\tilde{\mathbf{x}}_{mp,\Pi}(f,\cdot)$ is

$$f_{\tilde{\mathbf{x}}_{mp,\Pi}(f,\cdot)}\left(\boldsymbol{\xi}_x\right) = \int_{-\infty}^{+\infty}\int_{-\infty}^{+\infty} f_{\mathbf{y}(f,\cdot)}\left(\boldsymbol{\xi}_y\right) f_{\tilde{\mathbf{n}}_\Pi(f,\cdot)}\left(\boldsymbol{\xi}_x - \boldsymbol{\xi}_y\right) d\xi_{y_1} d\xi_{y_2} \tag{4.94}$$

$$\begin{aligned} &= \int_{-\infty}^{+\infty}\int_{-\infty}^{+\infty}\left[\int_{-\infty}^{+\infty}\frac{1}{\left(\xi_s\right)^2} f_{\tilde{s}_\Pi(f,\cdot)}\left(\xi_s\right)\bullet\right. \\ &\qquad \left. f_{\gamma''_{1_\Sigma}(t_i,\cdot)}\left(\frac{\xi_{y_1}}{\xi_s}\right) f_{\gamma''_{2_\Sigma}(t_i,\cdot)}\left(\frac{\xi_{y_2}}{\xi_s}\right) d\xi_s\right]\bullet \\ &\qquad f_{\tilde{\mathbf{n}}_\Pi}\left(f,\cdot\right)\left(\boldsymbol{\xi}_x - \boldsymbol{\xi}_z\right) d\xi_{y_1} d\xi_{y_2} \end{aligned} \tag{4.95}$$

$$\begin{aligned} &= \int_{\mathbb{R}^3}\frac{1}{\left(\xi_s\right)^2} f_{\tilde{s}_\Pi(f,\cdot)}\left(\xi_s\right) f_{\boldsymbol{\gamma}''_\Sigma(t_i,\cdot)}\left(\frac{\boldsymbol{\xi}_y}{\xi_s}\right)\bullet \\ &\qquad f_{\tilde{\mathbf{n}}_\Pi(f,\cdot)}\left(\boldsymbol{\xi}_x - \boldsymbol{\xi}_y\right) d\xi_s d\boldsymbol{\xi}_y \end{aligned} \tag{4.96}$$

Using Equation (4.83) and the dual of Equation (4.83) for $\gamma'_{2_\Sigma}(t_i,\cdot)$,

$$\begin{aligned} f_{\tilde{\mathbf{x}}_{mp,\Pi(f,\cdot)}}(\boldsymbol{\xi}_x) &= \int_{\mathbb{R}^3}\left[\frac{1}{(\xi_s)^2} f_{\tilde{s}_{\Pi(f,\cdot)}}(\xi_s)\, f_{\gamma'_{1_\Sigma}(t_i,\cdot)}\left(\frac{\xi_{y_1}}{\xi_s}e^{j2\pi f\tau_1(t_i)}\right)\bullet\right. \\ &\quad \left. f_{\gamma'_{2_\Sigma}(t_i,\cdot)}\left(\frac{\xi_{y_2}}{\xi_s}e^{j2\pi f\tau_2(t_i)}\right) f_{\tilde{\mathbf{n}}_{\Pi(f,\cdot)}}\left(\boldsymbol{\xi}_x-\boldsymbol{\xi}_y\right)\right] d\xi_s d\boldsymbol{\xi}_y \end{aligned} \tag{4.97}$$

Using Equation (4.79) and the dual of Equation (4.83) for $\gamma_{2_\Sigma}(t_i,\cdot)$,

$$\begin{aligned} f_{\tilde{\mathbf{x}}_{mp(f,\cdot)}}(\boldsymbol{\xi}_x) &= \int_{\mathbb{R}^3}\left[\frac{1}{(\xi_s)^2} f_{\tilde{s}_{\Pi(f,\cdot)}}(\xi_s)\, f_{\gamma_{1_\Sigma}(t_i,\cdot)}\left(\frac{\xi_{y_1}}{\xi_s}e^{j2\pi f\tau_1(t_i)}-1\right)\bullet\right. \\ &\quad \left. f_{\gamma_{2_\Sigma}(t_i,\cdot)}\left(\frac{\xi_{y_2}}{\xi_s}e^{j2\pi f\tau_2(t_i)}-1\right) f_{\tilde{\mathbf{n}}_{\Pi(f,\cdot)}}\left(\boldsymbol{\xi}_x-\boldsymbol{\xi}_y\right)\right] d\xi_s d\boldsymbol{\xi}_y \end{aligned} \tag{4.98}$$

Now, in the general case, Equation (4.77) is used to write $\gamma_{1_\Sigma}(t_i,\cdot)$ as the convolution of N_1 terms. The results for an arbitrary $N_1 \geq 0$ have been provided, but *for space considerations*, consider when $N_1 = 1$ (and, likewise, $N_2 = 1$):

$$\begin{aligned} f_{\tilde{\mathbf{x}}_{mp(f,\cdot)}}(\boldsymbol{\xi}_x) &= \int_{\mathbb{R}^3}\left[\frac{1}{(\xi_s)^2} f_{\tilde{s}_{\Pi(f,\cdot)}}(\xi_s)\, f_{\gamma_{1_l}(t_i,\cdot)}\left(\frac{\xi_{y_1}}{\xi_s}e^{j2\pi f\tau_1(t_i)}-1\right)\bullet\right. \\ &\quad \left. f_{\gamma_{2_m}(t_i,\cdot)}\left(\frac{\xi_{y_2}}{\xi_s}e^{j2\pi f\tau_2(t_i)}-1\right) f_{\tilde{\mathbf{n}}_{\Pi(f,\cdot)}}\left(\boldsymbol{\xi}_x-\boldsymbol{\xi}_y\right)\right] d\xi_s d\boldsymbol{\xi}_y \end{aligned} \tag{4.99}$$

where only the l^{th} and m^{th} multipath terms in $x_{1_{mp}}(\cdot,\cdot)$ and $x_{1_{mp}}(\cdot,\cdot)$, respectively, have been retained. Using Equation (4.71) and the dual of Equation (4.71) for $\gamma_{2_m}(t_i,\cdot)$,

$$\begin{aligned} f_{\tilde{\mathbf{x}}_{mp,\Pi(f,\cdot)}}(\boldsymbol{\xi}_x) &= \int_{\mathbb{R}^3}\frac{1}{(\xi_s)^2} f_{\tilde{s}_{\Pi(f,\cdot)}}(\xi_s)\bullet \\ &\quad \int_{-\infty}^{+\infty}\frac{1}{|\xi_{\alpha_l}|} f_{\alpha_l(t_i,\cdot),\delta_{e_l}(t_i,\cdot)}\left\{\xi_{\alpha_l},\frac{1}{\xi_{\alpha_l}}\left[\frac{\xi_{y_1}}{\xi_s}e^{j2\pi f\tau_1(t_i)}-1\right]\right\} d\xi_{\alpha_l}\bullet \\ &\quad \int_{-\infty}^{+\infty}\frac{1}{|\xi_{\beta_m}|} f_{\beta_m(t_i,\cdot),\varepsilon_{e_m}(t_i,\cdot)}\left\{\xi_{\beta_m},\frac{1}{\xi_{\beta_m}}\left[\frac{\xi_{y_2}}{\xi_s}e^{j2\pi f\tau_2(t_i)}-1\right]\right\} d\xi_{\beta_m}\bullet \\ &\quad f_{\tilde{\mathbf{n}}_{\Pi(f,\cdot)}}\left(\boldsymbol{\xi}_x-\boldsymbol{\xi}_y\right) d\xi_s d\boldsymbol{\xi}_y \end{aligned} \tag{4.100}$$

Rearranging,

$$
\begin{aligned}
f_{\tilde{\mathbf{x}}_{mp,\Pi}(f,\cdot)}\left(\boldsymbol{\xi}_x\right) &= \int_{\mathbb{R}^5} \frac{1}{\left(\xi_s\right)^2} f_{\tilde{s}_\Pi(f,\cdot)}\left(\xi_s\right) f_{\tilde{\mathbf{n}}_\Pi(f,\cdot)}\left(\boldsymbol{\xi}_x - \boldsymbol{\xi}_y\right) \cdot \\
&\quad \frac{1}{\left|\xi_{\alpha_l}\right|} f_{\alpha_l(t_i,\cdot),\delta_{e_l}(t_i,\cdot)}\left\{\xi_{\alpha_l}, \frac{1}{\xi_{\alpha_l}}\left[\frac{\xi_{y_1}}{\xi_s} e^{j2\pi f \tau_1(t_i)} - 1\right]\right\} \cdot \\
&\quad \frac{1}{\left|\xi_{\beta_m}\right|} f_{\beta_m(t_i,\cdot),\varepsilon_{e_m}(t_i,\cdot)}\left\{\xi_{\beta_m}, \frac{1}{\xi_{\beta_m}}\left[\frac{\xi_{y_2}}{\xi_s} e^{j2\pi f \tau_2(t_i)} - 1\right]\right\} \cdot \\
&\quad d\xi_{\alpha_l} d\xi_{\beta_m} d\xi_s d\boldsymbol{\xi}_y
\end{aligned} \tag{4.101}
$$

Using Equation (4.68) and the dual of Equation (4.68) for $\beta_m\left(t_i,\cdot\right)$ and $\varepsilon_{e_m}\left(t_i,\cdot\right)$,

$$
\begin{aligned}
f_{\tilde{\mathbf{x}}_{mp,\Pi}(f,\cdot)}\left(\boldsymbol{\xi}_x\right) &= \frac{1}{\left(2\pi\left|f\right|\right)^2} \int_{\mathbb{R}^5} \frac{1}{\left(\xi_s\right)^2} f_{\tilde{s}_\Pi(f,\cdot)}\left(\xi_s\right) f_{\tilde{\mathbf{n}}_\Pi(f,\cdot)}\left(\boldsymbol{\xi}_x - \boldsymbol{\xi}_y\right) \cdot \\
&\quad \frac{1}{\left|\xi_{\alpha_l}\right|} f_{\alpha_l(t_i,\cdot),\delta_l(t_i,\cdot)}\left(\xi_{\alpha_l}, \frac{1}{-j2\pi f} \ln\left\{\frac{1}{\xi_{\alpha_l}}\left[\frac{\xi_{y_1}}{\xi_s} e^{j2\pi f \tau_1(t_i)} - 1\right]\right\}\right) \cdot \\
&\quad \frac{1}{\left|\xi_{\beta_m}\right|} f_{\beta_m(t_i,\cdot),\varepsilon_m(t_i,\cdot)}\left(\xi_{\beta_m}, \frac{1}{-j2\pi f} \ln\left\{\frac{1}{\xi_{\beta_m}}\left[\frac{\xi_{y_2}}{\xi_s} e^{j2\pi f \tau_2(t_i)} - 1\right]\right\}\right) \cdot \\
&\quad d\xi_{\alpha_l} d\xi_{\beta_m} d\xi_s d\boldsymbol{\xi}_y
\end{aligned} \tag{4.102}
$$

Equation (4.102) expresses $f_{\tilde{\mathbf{x}}_{mp,\Pi}(f,\cdot)}\left(\cdot\right)$ at a given frequency, f, in terms of the following known probability density functions:

$$
f_{\tilde{s}_\Pi(f,\cdot)}\left(\cdot\right),\ f_{\tilde{\mathbf{n}}_\Pi(f,\cdot)}\left(\cdot\right),\ f_{\alpha_l(t_i,\cdot),\delta_l(t_i,\cdot)}\left(\cdot\right),\ f_{\beta_m(t_i,\cdot),\varepsilon_m(t_i,\cdot)}\left(\cdot\right)
$$

This is the desired result—the stochastic nature of the received signal is written in terms of the transmitted signal, the measurement noises, and the multipath model effects. Recall, a complete characterization of $\tilde{\mathbf{x}}_{mp,\Pi}\left(f,\cdot\right)$ requires finding the joint probability density function given in Equation (4.51), repeated here as

$$
f_{\tilde{\mathbf{x}}_{mp,\Pi}(f_1,\cdot),\ldots,\tilde{\mathbf{x}}_{mp,\Pi}(f_N,\cdot)}\left(\boldsymbol{\xi}_1,\ldots,\boldsymbol{\xi}_N\right) \tag{4.51}
$$

for all sequences $\{f_1, \ldots, f_N\}$. A procedure similar to the one presented here could be used to find an expression for $f_{\tilde{\mathbf{x}}_{mp,\Pi}(f_1,\cdot),\ldots,\tilde{\mathbf{x}}_{mp,\Pi}(f_N,\cdot)}$. Furthermore, each $\tilde{\mathbf{x}}_{mp,\Pi}(f_i,\cdot)$ is orthogonal to $\tilde{\mathbf{x}}_{mp,\Pi}(f_j,\cdot)$ for all $f_j \neq f_i$. If only the characteristics up to second order of the joint probability density function in Equation (4.51) were used in an analysis, the orthogonality of $\tilde{\mathbf{x}}_{mp,\Pi}(f_i,\cdot)$ could be exploited to simplify the process to go from Equation (4.102) to Equation (4.51). Section 4.4 considers one example for which this is a reasonable analysis – jointly Gaussian processes – since characteristics up to second order for a Gaussian probability density function completely characterize the probability density function. Without employing the up-to-second-order-simplification, the next section continues a general approach to the *NP* of $\tilde{\mathbf{x}}_{mp,\Pi}$ using the joint density of $f_{\tilde{\mathbf{x}}_{mp,\Pi}}$ in Equation (4.51).

4.3.4 Finding $NP(\tilde{\mathbf{x}}_{mp,\Pi})$

The *NP* of $\tilde{\mathbf{x}}_{mp,\Pi}(\cdot,\cdot)$ can be found in terms of the joint probability density function (jpdf) given in Equation (4.51). The jpdf of $\tilde{\mathbf{x}}_{mp,\Pi}(f_1,\cdot),\ldots,\tilde{\mathbf{x}}_{mp,\Pi}(f_N,\cdot)$ for an arbitrary sequence $\{f_1,\ldots,f_N\}$ is in general a function of τ_1 and τ_2 (and not the difference $\tau_1 - \tau_2$). Thus, Equation (4.22) can be used to find the FIM of

$$\boldsymbol{\theta} \triangleq \begin{bmatrix} \tau_1 & \tau_2 \end{bmatrix}^T \tag{4.103}$$

given the random variable, $\tilde{\mathbf{x}}_{mp,\Pi}(\cdot)$, defined as

$$\tilde{\mathbf{x}}_{mp,\Pi}(\cdot) \triangleq \begin{bmatrix} \tilde{\mathbf{x}}_{mp,\Pi}(f_1,\cdot)^T & \cdots & \tilde{\mathbf{x}}_{mp,\Pi}(f_N,\cdot)^T \end{bmatrix}^T \tag{4.104}$$

for some arbitrary sequence $\{f_1, \ldots, f_N\}$. The result is

$$\mathbf{I}(\boldsymbol{\theta}) = \begin{bmatrix} -E\left\{\frac{\partial^2 \ln\left[f\left(\tilde{\mathbf{x}}_{mp,\Pi}(\cdot);\tau_1,\tau_2\right)\right]}{(\partial\tau_1)^2}\right\} & -E\left\{\frac{\partial^2 \ln\left[f\left(\tilde{\mathbf{x}}_{mp,\Pi}(\cdot);\tau_1,\tau_2\right)\right]}{\partial\tau_1\partial\tau_2}\right\} \\ -E\left\{\frac{\partial^2 \ln\left[f\left(\tilde{\mathbf{x}}_{mp,\Pi}(\cdot);\tau_1,\tau_2\right)\right]}{\partial\tau_2\partial\tau_1}\right\} & -E\left\{\frac{\partial^2 \ln\left[f\left(\tilde{\mathbf{x}}_{mp,\Pi}(\cdot);\tau_1,\tau_2\right)\right]}{(\partial\tau_2)^2}\right\} \end{bmatrix} \tag{4.105}$$

Finally, using Equation (4.105) in Equation (4.37),

$$NP\left\{\tilde{\mathbf{x}}_{mp,\Pi}(\cdot)\right\} = -\frac{E\left\{\frac{\partial^2 \ln\left[f\left(\tilde{\mathbf{x}}_{mp,\Pi}(\cdot);\tau_1,\tau_2\right)\right]}{(\partial\tau_1)^2}\right\} E\left\{\frac{\partial^2 \ln\left[f\left(\tilde{\mathbf{x}}_{mp,\Pi}(\cdot);\tau_1,\tau_2\right)\right]}{(\partial\tau_2)^2}\right\} - E\left\{\frac{\partial^2 \ln\left[f\left(\tilde{\mathbf{x}}_{mp,\Pi}(\cdot);\tau_1,\tau_2\right)\right]}{\partial\tau_1\partial\tau_2}\right\}^2}{E\left\{\frac{\partial^2 \ln\left[f\left(\tilde{\mathbf{x}}_{mp,\Pi}(\cdot);\tau_1,\tau_2\right)\right]}{(\partial\tau_1)^2}\right\} + E\left\{\frac{\partial^2 \ln\left[f\left(\tilde{\mathbf{x}}_{mp,\Pi}(\cdot);\tau_1,\tau_2\right)\right]}{(\partial\tau_2)^2}\right\} + 2E\left\{\frac{\partial^2 \ln\left[f\left(\tilde{\mathbf{x}}_{mp,\Pi}(\cdot);\tau_1,\tau_2\right)\right]}{\partial\tau_1\partial\tau_2}\right\}} \tag{4.106}$$

The general nature of this formulation results in an expression for $NP\left\{\tilde{\mathbf{x}}_{mp,\Pi}(\cdot)\right\}$ that is not readily interpreted. However, given the densities of the signal, noise, and multipath characteristics, the results found here can be used to find $NP\left\{\tilde{\mathbf{x}}_{mp,\Pi}(\cdot)\right\}$. Due to the lax constraints, many problems of practical interest may be solved using this new result. Chapter 5 will specify some typical densities to show how this may be used in practice. The next section finds the *NP* when the received signal is assumed to be Gaussian. This greatly simplifies the expression for the *NP*, since the probability density function of the received signal may be characterized completely through the first and second order moments.

4.4 Multipath Model: Gaussian Received Signal

The *NP* for a received signal with multipath effects has been presented in very general terms. An interesting subclass of problems results when $\tilde{\mathbf{x}}_{mp,\Pi}(\cdot,\cdot)$ is modeled as a Gaussian stochastic process, denoted as $\tilde{\mathbf{x}}_{gmp,\Pi}(\cdot,\cdot)$ to indicate explicitly that it is assumed Gaussian. This section introduces this restriction to yield a more tractable form for the navigation potential (*NP*). (This assumption's relationship with other assumptions within this chapter is shown as Box III in Figure 7 on page 50.)

In the previous section, multipath mappings were given in the time domain in Equations (4.40) and (4.41) and the frequency domain in Equation (4.48). Modifying the subscript to indicate a multipath model with Gaussian assumptions, the *time-domain signal model* is

$$\mathbf{x}_{gmp}(\cdot,\cdot) = \begin{bmatrix} x_{1_{gmp}}(\cdot,\cdot) \\ x_{2_{gmp}}(\cdot,\cdot) \end{bmatrix} \tag{4.107}$$

where $x_{1_{gmp}}$ is, for all admissible t,

$$\begin{aligned} x_{1_{gmp}}(t,\cdot) &= s(t-\tau_1(t),\cdot) + n_1(t,\cdot) \\ &\quad + \sum_{l=1}^{N_1} \alpha_l(t,\cdot)\, s[t-\tau_1(t)-\delta_l(t,\cdot),\cdot] \end{aligned} \tag{4.108}$$

and $x_{2_{gmp}}$ is, for all admissible t,

$$\begin{aligned} x_{2_{gmp}}(t,\cdot) &= s(t-\tau_2(t),\cdot) + n_2(t,\cdot) \\ &\quad + \sum_{l=1}^{N_2} \beta_l(t,\cdot)\, s[t-\tau_2(t)-\varepsilon_l(t,\cdot),\cdot] \end{aligned} \tag{4.109}$$

Similarly, the *frequency-domain signal model* may be written for Gaussian assumptions as

$$\tilde{\mathbf{x}}_{gmp,\Pi}(f,\cdot) = \begin{bmatrix} \tilde{s}_{\Pi}(f,\cdot)\, e^{-j2\pi f\tau_1(t_i)} \left(1 + \sum_{l=1}^{N_1} \alpha_l(t_i,\cdot)\, e^{-j2\pi f\delta_l(t_i,\cdot)}\right) \\ \tilde{s}_{\Pi}(f,\cdot)\, e^{-j2\pi f\tau_2(t_i)} \left(1 + \sum_{l=1}^{N_2} \beta_l(t_i,\cdot)\, e^{-j2\pi f\varepsilon_l(t_i,\cdot)}\right) \end{bmatrix} + \tilde{\mathbf{n}}_{\Pi}(f,\cdot) \tag{4.110}$$

Many of the stochastic process in Equations (4.108) and (4.109) will be modeled as Gaussian stochastic processes. Briefly, a Gaussian stochastic process, $\mathbf{y}(\cdot,\cdot)$, is defined as a stochastic process for which the joint probability density function

$$f_{\mathbf{y}(t_1,\cdot),\ldots,\mathbf{y}(t_N,\cdot)}(\boldsymbol{\xi}_1,\ldots,\boldsymbol{\xi}_N)$$

is Gaussian for all time sequences $\{t_1,\ldots,t_N\}$ if it exists. A Gaussian probability density function for an arbitrary, real-valued, m-dimensional random variable $\mathbf{y}(\cdot)$ is given by

$$f_{\mathbf{y}(\cdot)}(\boldsymbol{\xi}) = \frac{1}{(2\pi)^{\frac{m}{2}} |\mathbf{C}|^{\frac{1}{2}}} e^{\left[-\frac{1}{2}(\boldsymbol{\xi}-\boldsymbol{\mu})^T \mathbf{C}^{-1}(\boldsymbol{\xi}-\boldsymbol{\mu})\right]} \tag{4.111}$$

where $\boldsymbol{\xi}$ is the realization of $\mathbf{y}$, $\boldsymbol{\mu} \triangleq E\{\mathbf{y}(\cdot)\}$, and $\mathbf{C} \triangleq E\left\{[\mathbf{y}(\cdot)-\boldsymbol{\mu}][\mathbf{y}(\cdot)-\boldsymbol{\mu}]^T\right\}$. The following list motivates the assumptions for each term in $\mathbf{x}_{gmp}(\cdot,\cdot)$.

1. $s(\cdot,\cdot)$ represents the received signal stochastic process. Many signals of interest may be approximated a zero-mean, ergodic, wide-sense stationary, stochastically continuous, Gaussian stochastic process. For the i^{th} receiver, each $s(t-\tau_i(t),\cdot)$ for all admissible t is a zero-mean, ergodic, wide-sense

stationary, stochastically continuous, Gaussian stochastic process with the known power spectral density, $G_{ss}(f)$. The probability density function at some time, $f_{s(t,\cdot)}(\xi)$, is known, where the form of $f_{s(t,\cdot)}(\xi)$ is given in Equation (4.111) with $m_s = 1$, $\mu_s = 0$, and $C_s = \sigma_s^2$, or

$$f_{s(t,\cdot)}(\xi) = \frac{1}{\sqrt{2\pi}\sigma_s} e^{\left(-\frac{\xi^2}{2\sigma_s^2}\right)} \tag{4.112}$$

2. $n_i(\cdot,\cdot)$ represents the i^{th} receiver's measurement noise stochastic process and is assumed to be a zero-mean, ergodic, strict sense stationary, Gaussian stochastic process. Letting

$$\mathbf{n}(\cdot,\cdot) \triangleq \begin{bmatrix} n_1(\cdot,\cdot) \\ \\ n_2(\cdot,\cdot) \end{bmatrix} \tag{4.113}$$

$\mathbf{n}(\cdot,\cdot)$ is a zero-mean, ergodic, strict sense stationary, Gaussian stochastic process with the known power spectral densities $G_{n_1n_1}(f)$ and $G_{n_2n_2}(f)$ and the known cross-spectral density $G_{n_1n_2}(f)$. For each t, the probability density function, $f_{\mathbf{n}(t,\cdot)}(\boldsymbol{\xi})$, is known, with the form given in Equation (4.111) with $m_{\mathbf{n}} = 2$, $\boldsymbol{\mu}_{\mathbf{n}} = \mathbf{0}$, and

$$\mathbf{C}_{\mathbf{n}} = \begin{bmatrix} \sigma_{n_1}^2 & 0 \\ \\ 0 & \sigma_{n_2}^2 \end{bmatrix} \tag{4.114}$$

3. Since $\mathcal{F}\{\cdot\}$ is a linear transformation, $\tilde{s}_{\Pi}(\cdot,\cdot)$, $\tilde{n}_{\Pi_1}(\cdot,\cdot)$, and $\tilde{n}_{\Pi_2}(\cdot,\cdot)$ are zero-mean, Gaussian stochastic processes. Furthermore, from the results in

Appendix E, the autocorrelation kernels of $\tilde{s}_{\Pi}(\cdot,\cdot)$, $\tilde{n}_{\Pi_1}(\cdot,\cdot)$, and $\tilde{n}_{\Pi_2}(\cdot,\cdot)$ are

$$E\left\{\tilde{s}_{\Pi}(f,\cdot)\left[\tilde{s}_{\Pi}(f-\epsilon,\cdot)\right]^*\right\} \approx \frac{1}{T}G_{ss}(f)\,\delta_{\kappa}(\epsilon) \tag{4.115}$$

$$E\left\{\tilde{n}_{\Pi_1}(f,\cdot)\left[\tilde{n}_{\Pi_1}(f-\epsilon,\cdot)\right]^*\right\} \approx \frac{1}{T}G_{n_1n_1}(f)\,\delta_{\kappa}(\epsilon) \tag{4.116}$$

$$E\left\{\tilde{n}_{\Pi_2}(f,\cdot)\left[\tilde{n}_{\Pi_2}(f-\epsilon,\cdot)\right]^*\right\} \approx \frac{1}{T}G_{n_2n_2}(f)\,\delta_{\kappa}(\epsilon) \tag{4.117}$$

where $\delta_{\kappa}(\cdot)$ is the modified Kronecker delta function with a continuous argument, i.e., $\delta_{\kappa}(\epsilon)$ is defined for all $\epsilon \in \mathbb{R}^1$ through

$$\delta_{\kappa}(\epsilon) \triangleq \begin{cases} 1 & \epsilon = 0 \\ 0 & \text{otherwise} \end{cases} \tag{4.118}$$

This list represents the assumptions that will be used for the remainder of this section. For clarity, $(\cdot)_{gmp}$ indicates the identical multipath model as $(\cdot)_{mp}$ under the additional constraint that these Gaussian assumptions hold.

The aim of this section is to find the *NP* of the received signal when it is appropriately modeled with jointly Gaussian stochastic processes. To accomplish this task, the remainder of the this section will (1) develop the Gaussian received signal model, and (2) find an expression for *NP*.

4.4.1 Gaussian $\tilde{\mathbf{x}}_{gmp,\Pi}(\cdot,\cdot)$

Consider when the received signal is modeled as a Gaussian stochastic process. Referring to Equation (4.110), this condition may be established when

$$\tilde{s}_{\Pi}(f,\cdot)\,e^{-j2\pi f\tau_1(t_i)}\left(1+\sum_{l=1}^{N_1}\alpha_l(t_i,\cdot)\,e^{-j2\pi f\delta_l(t_i,\cdot)}\right) \tag{4.119}$$

over all admissible f is a Gaussian stochastic process. Notice that $\tilde{\mathbf{n}}_{\Pi}(\cdot,\cdot)$ is not included in the above expression. Recall that the linear combination of two inde-

pendent Gaussian random variables is Gaussian. Since each $\tilde{n}_i(f,\cdot)$ is a Gaussian random variable independent of each of the remaining random variables in Equation (4.110) (which are stochastic processes evaluated for some f), the expression in Equation (4.119) being jointly Gaussian for all sequences $\{f_1,\ldots,f_N\}$ is sufficient for $\tilde{\mathbf{x}}_{gmp,\Pi}(\cdot,\cdot)$ to be Gaussian.

Gaussian assumptions may be considered as an approximation to the true joint probability density function. Typical Gaussian justifications reason that Gaussian density functions capture the overall distribution in many instances [47]. Gaussian approximations are suitable for *NP* applications when the *curvature* of $\tilde{\mathbf{x}}_{mp,\Pi}(\cdot,\cdot)$ about the *true value* for $\boldsymbol{\theta}$, i.e.,

$$\ln f_{\tilde{\mathbf{x}}_{mp,\Pi}(f_1,\cdot),\ldots,\tilde{\mathbf{x}}_{mp,\Pi}(f_N,\cdot)}(\boldsymbol{\xi};\boldsymbol{\theta}) \tag{4.120}$$

(where $f_{\tilde{\mathbf{x}}_{mp,\Pi}(f_1,\cdot),\ldots,\tilde{\mathbf{x}}_{mp,\Pi}(f_N,\cdot)}(\boldsymbol{\xi};\boldsymbol{\theta})$ is *not* necessarily Gaussian) is well-represented by the *curvature* of $\tilde{\mathbf{x}}_{gmp,\Pi}(\cdot,\cdot)$ about the true value for $\boldsymbol{\theta}$, i.e.,

$$\ln f_{\tilde{\mathbf{x}}_{gmp,\Pi}(f_1,\cdot),\ldots,\tilde{\mathbf{x}}_{gmp,\Pi}(f_N,\cdot)}(\boldsymbol{\xi};\boldsymbol{\theta}) \tag{4.121}$$

(where $f_{\tilde{\mathbf{x}}_{gmp,\Pi}(f_1,\cdot),\ldots,\tilde{\mathbf{x}}_{gmp,\Pi}(f_N,\cdot)}(\boldsymbol{\xi};\boldsymbol{\theta})$ *is* Gaussian). That $f_{\tilde{\mathbf{x}}_{mp,\Pi}(f_1,\cdot),\ldots,\tilde{\mathbf{x}}_{mp,\Pi}(f_N,\cdot)}(\boldsymbol{\xi};\boldsymbol{\theta})$ may be well-represented as Gaussian in $\boldsymbol{\xi}$ is not the issue for *NP* considerations (even though it is often the case that this assumption is valid for real systems [47]). Furthermore, no claim is made that $f_{\tilde{\mathbf{x}}_{mp,\Pi}(f_1,\cdot),\ldots,\tilde{\mathbf{x}}_{mp,\Pi}(f_N,\cdot)}(\boldsymbol{\xi};\boldsymbol{\theta})$ is Gaussian in $\boldsymbol{\theta}$; rather, $f_{\tilde{\mathbf{x}}_{mp,\Pi}(f_1,\cdot),\ldots,\tilde{\mathbf{x}}_{mp,\Pi}(f_N,\cdot)}(\boldsymbol{\xi};\boldsymbol{\theta})$ is *parameterized* by $\boldsymbol{\theta}$. *The validity of a Gaussian assumption as it pertains to NP is that the curvature of the original density function is well represented by the curvature of a Gaussian approximation to the original density*

function. This slight distinction should be considered when making approximations for *NP* calculations.

Assuming $\tilde{\mathbf{x}}_{gmp,\Pi}(\cdot,\cdot)$ is a complex-valued, Gaussian stochastic process, the joint probability density function for any sequence $\{f_1,\ldots,f_N\}$ may be characterized through the mean and autocorrelation matrix of the vector formed by

$$\left[\begin{array}{ccc} \tilde{\mathbf{x}}_{gmp,\Pi}(f_1,\cdot)^T & \cdots & \tilde{\mathbf{x}}_{gmp,\Pi}(f_N,\cdot)^T \end{array}\right]^T$$

Furthermore, the process mean and autocorrelation kernel may be used to describe a Gaussian stochastic process. (It will be shown that $\tilde{\mathbf{x}}_{gmp,\Pi}(\cdot,\cdot)$ is also orthogonal; therefore, the process mean and autocorrelation matrix provide a complete description of $f_{\tilde{\mathbf{x}}_{gmp,\Pi}(f,\cdot)}$ for any admissible f.) The remainder of this section finds the process mean for all admissible f, denoted by $\boldsymbol{\mu}_{\tilde{x}_{gmp,\Pi}(\cdot,\cdot)}(f)$, and the autocorrelation kernel for all admissible f_1 and f_2, denoted by $\mathbf{C}_{\tilde{x}_{gmp,\Pi}(\cdot,\cdot)}(f_1,f_2)$.

4.4.1.1 Mean of $\tilde{\mathbf{x}}_{gmp,\Pi}(\cdot,\cdot)$. The *process mean* of $\tilde{\mathbf{x}}_{gmp,\Pi}(\cdot,\cdot)$ for all admissible f is defined as

$$\boldsymbol{\mu}_{\tilde{x}_{gmp,\Pi}(\cdot,\cdot)}(f) \triangleq E\left\{\tilde{\mathbf{x}}_{gmp,\Pi}(f,\cdot)\right\} \tag{4.122}$$

Since $\tilde{s}_{\Pi}(f,\cdot)$ and $\tilde{\mathbf{n}}_{\Pi}(f,\cdot)$ are zero-mean and independent of the terms in $\tilde{\mathbf{x}}_{gmp,\Pi}(f,\cdot)$ given in Equation (4.110), the process mean of $\tilde{\mathbf{x}}_{gmp,\Pi}(\cdot,\cdot)$ for all admissible f is

$$\boldsymbol{\mu}_{\tilde{x}_{gmp,\Pi}(\cdot,\cdot)}(f) = \mathbf{0} \tag{4.123}$$

4.4.1.2 Autocorrelation Kernel of $\tilde{\mathbf{x}}_{gmp,\Pi}(\cdot,\cdot)$.

The *autocorrelation kernel* of $\tilde{\mathbf{x}}_{gmp,\Pi}(\cdot,\cdot)$ for all admissible f,$f-\epsilon$ is defined as

$$\tilde{\mathbf{C}}_{\tilde{x}_{gmp,\Pi}(\cdot,\cdot)}(f,f-\epsilon) \triangleq E\left\{\tilde{\mathbf{x}}_{gmp,\Pi}(f,\cdot)\left[\tilde{\mathbf{x}}_{gmp,\Pi}(f-\epsilon,\cdot)\right]^{H}\right\} \tag{4.124}$$

where ^{H} denotes the conjugate transpose ("H" for "Hermitian"). Using the received signal model given in Equation (4.110), the remainder of this subsection finds the autocorrelation kernel of $\tilde{\mathbf{x}}_{gmp,\Pi}(\cdot,\cdot)$ in terms of the transmitted signal, the measurement noises, and the multipath model effects.

Let $\tilde{\mathbf{x}}_{gmp,\Pi}(\cdot,\cdot)$ given in Equation (4.110) for all admissible f be represented by

$$\tilde{\mathbf{x}}_{gmp,\Pi}(f,\cdot) = \tilde{s}_{\Pi}(f,\cdot)\,\mathbb{E}(f)\,\tilde{\boldsymbol{\lambda}}(f,\cdot) + \tilde{\mathbf{n}}_{\Pi}(f,\cdot) \tag{4.125}$$

where

$$\mathbb{E}(f) \triangleq \begin{bmatrix} e^{-j2\pi f\tau_1(t_i)} & 0 \\ 0 & e^{-j2\pi f\tau_2(t_i)} \end{bmatrix} \tag{4.126}$$

and

$$\tilde{\boldsymbol{\lambda}}(f,\cdot) \triangleq \begin{bmatrix} 1+\sum_{l=1}^{N_1}\alpha_l(t_i,\cdot)\,e^{-j2\pi f\delta_l(t_i,\cdot)} \\ \\ 1+\sum_{l=1}^{N_2}\beta_l(t_i,\cdot)\,e^{-j2\pi f\varepsilon_l(t_i,\cdot)} \end{bmatrix} \tag{4.127}$$

Now, Equation (4.124) becomes

$$\tilde{\mathbf{C}}_{\tilde{x}_{gmp,\Pi}(\cdot,\cdot)}(f,f-\epsilon) = E\left\{\tilde{\mathbf{x}}_{gmp,\Pi}(f,\cdot)\left[\tilde{\mathbf{x}}_{gmp,\Pi}(f-\epsilon,\cdot)\right]^{H}\right\} \tag{4.128}$$

$$= E\left\{\begin{bmatrix} \tilde{s}_{\Pi}(f,\cdot)\,\mathbb{E}(f)\,\tilde{\boldsymbol{\lambda}}(f,\cdot) + \\ +\tilde{\mathbf{n}}_{\Pi}(f,\cdot) \end{bmatrix} \cdot \begin{bmatrix} \tilde{s}_{\Pi}(f-\epsilon,\cdot)\,\mathbb{E}(f-\epsilon)\,\tilde{\boldsymbol{\lambda}}(f-\epsilon,\cdot) + \\ +\tilde{\mathbf{n}}_{\Pi}(f-\epsilon,\cdot) \end{bmatrix}^{H}\right\} \tag{4.129}$$

Noting that $\mathbb{E}(f)$ is deterministic for all admissible f, and $\tilde{s}_{\Pi}(f,\cdot)$, $\tilde{\boldsymbol{\lambda}}(f,\cdot)$, and $\tilde{\mathbf{n}}_{\Pi}(f,\cdot)$ are all zero-mean and pairwise independent for all admissible f, Equation (**??**) becomes

$$\begin{aligned}\tilde{\mathbf{C}}_{\tilde{x}_{gmp,\Pi}(\cdot,\cdot)}(f,f-\epsilon) &= \Bigg(E\left\{\tilde{s}_{\Pi}(f,\cdot)\left[\tilde{s}_{\Pi}(f-\epsilon,\cdot)\right]^{*}\right\}\mathbb{E}(f)\bullet \\ &\quad E\left\{\tilde{\boldsymbol{\lambda}}(f,\cdot)\left[\tilde{\boldsymbol{\lambda}}(f-\epsilon,\cdot)\right]^{H}\right\}\left[\mathbb{E}(f-\epsilon)\right]^{*}\Bigg)+ \\ &\quad +E\left\{\tilde{\mathbf{n}}_{\Pi}(f,\cdot)\left[\tilde{\mathbf{n}}_{\Pi}(f-\epsilon,\cdot)\right]^{H}\right\} \qquad (4.130)\end{aligned}$$

Using the results from Appendix E with $\tilde{\mathbf{z}}(f,\cdot) \triangleq \tilde{s}_{\Pi}(f,\cdot)$, the autocorrelation kernel of $\tilde{s}_{\Pi}(\cdot,\cdot)$ is given in Equation (4.115) and repeated here as

$$E\left\{\tilde{s}_{\Pi}(f,\cdot)\left[\tilde{s}_{\Pi}(f-\epsilon,\cdot)\right]^{*}\right\} \approx \frac{1}{T}G_{ss}(f)\,\delta_{\kappa}(\epsilon) \qquad (4.115)$$

in which $\delta_{\kappa}(\cdot)$ is the Kronecker delta function given in Equation (4.118) and repeated here as

$$\delta_{\kappa}(\epsilon) \triangleq \begin{cases} 1 & \epsilon = 0 \\ 0 & \text{otherwise} \end{cases} \qquad (4.118)$$

The Kronecker delta function arises because the spectral representation of $s(\cdot,\cdot)$ is orthogonal, i.e., for all admissible $f_1 \neq f_2$,

$$E\left\{\tilde{s}_{\Pi}(f_1,\cdot)\left[\tilde{s}_{\Pi}(f_2,\cdot)\right]^{*}\right\} = 0 \qquad (4.131)$$

Likewise, the results from Appendix E may be used to obtain the autocorrelation kernels of $\tilde{n}_{\Pi_1}(f_1,\cdot)$ and $\tilde{n}_{\Pi_2}(f_2,\cdot)$ given in Equations (4.116) and (4.117), respectively. Recalling $\tilde{n}_{\Pi_1}(f_1,\cdot)$ and $\tilde{n}_{\Pi_2}(f_2,\cdot)$ are pairwise independent for all f_1 and f_2,

$$E\left\{\tilde{\mathbf{n}}_{\Pi}(f,\cdot)\left[\tilde{\mathbf{n}}_{\Pi}(f-\epsilon,\cdot)\right]^{H}\right\} \approx \frac{1}{T}\mathbf{G}_{nn}(f)\,\delta_{\kappa}(\epsilon) \qquad (4.132)$$

where

$$\mathbf{G}_{nn}(f) = \begin{bmatrix} G_{n_1 n_1}(f) & 0 \\ 0 & G_{n_2 n_2}(f) \end{bmatrix} \tag{4.133}$$

Substituting Equations (4.115) and (4.132) in Equation (4.130),

$$\begin{aligned} \tilde{\mathbf{C}}_{\tilde{x}_{gmp,\Pi}(\cdot,\cdot)}(f, f-\epsilon) &\approx \frac{1}{T} G_{ss}(f)\,\delta(\epsilon)\,\mathbb{E}(f)\,E\left\{\tilde{\boldsymbol{\lambda}}(f,\cdot)\left[\tilde{\boldsymbol{\lambda}}(f-\epsilon,\cdot)\right]^H\right\}[\mathbb{E}(f-\epsilon)]^* \\ &\quad + \frac{1}{T}\mathbf{G}_{nn}(f)\,\delta_\kappa(\epsilon) \end{aligned} \tag{4.134}$$

Due to the effects of $\delta_\kappa(\epsilon)$, Equation (4.134) may be written as

$$\begin{aligned} \tilde{\mathbf{C}}_{\tilde{x}_{gmp,\Pi}(\cdot,\cdot)}(f, f-\epsilon) &\approx \left(\frac{1}{T} G_{ss}(f)\,\mathbb{E}(f)\,E\left\{\tilde{\boldsymbol{\lambda}}(f,\cdot)\left[\tilde{\boldsymbol{\lambda}}(f,\cdot)\right]^H\right\}[\mathbb{E}(f)]^* + \right. \\ &\quad \left. + \frac{1}{T}\mathbf{G}_{nn}(f)\right)\delta_\kappa(\epsilon) \end{aligned} \tag{4.135}$$

Using the definitions for $\tilde{\boldsymbol{\lambda}}(f,\cdot)$ and $\mathbb{E}(f)$, Equation (4.135) may be exploited further. First, $E\left\{\tilde{\boldsymbol{\lambda}}(f,\cdot)\left[\tilde{\boldsymbol{\lambda}}(f,\cdot)\right]^H\right\}$ may be defined as

$$\tilde{\mathbf{C}}_{\tilde{\lambda}}(f) \triangleq E\left\{\tilde{\boldsymbol{\lambda}}(f,\cdot)\left[\tilde{\boldsymbol{\lambda}}(f,\cdot)\right]^H\right\} = \begin{bmatrix} C_{\tilde{\lambda}_{11}}(f) & \tilde{C}_{\tilde{\lambda}_{12}}(f) \\ \tilde{C}_{\tilde{\lambda}_{12}}(f)^* & C_{\tilde{\lambda}_{22}}(f) \end{bmatrix} \tag{4.136}$$

Using the definition of $\boldsymbol{\gamma}(f,\cdot)$ in Equation (4.127) and the relationship of each attenuation and delay term (given in Table 1 on page 67), the first diagonal term in Equation (4.136) may be found as

$$C_{\tilde{\lambda}_{11}}(f) \triangleq E\left\{\tilde{\lambda}_1(f,\cdot)\left[\tilde{\lambda}_1(f,\cdot)\right]^*\right\} \tag{4.137}$$

$$\begin{aligned} &= E\left\{\left[1 + \sum_{l=1}^{N_1} \alpha_l(t_i,\cdot)\, e^{-j2\pi f \delta_l(t_i,\cdot)}\right] \cdot \right. \\ &\quad \left. \left[1 + \sum_{m=1}^{N_1} \alpha_m(t_i,\cdot)\, e^{-j2\pi f \delta_m(t_i,\cdot)}\right]^*\right\} \end{aligned} \tag{4.138}$$

$$C_{\tilde{\lambda}_{11}}(f) = 1 + E\left\{\sum_{l=1}^{N_1}\alpha_l(t_i,\cdot)\,e^{-j2\pi f\delta_l(t_i,\cdot)} + \sum_{m=1}^{N_1}\alpha_m(t_i,\cdot)\,e^{+j2\pi f\delta_m(t_i,\cdot)}\right\} + \\ + E\left\{\left[\sum_{l=1}^{N_1}\alpha_l(t_i,\cdot)\,e^{-j2\pi f\delta_l(t_i,\cdot)}\right]\left[\sum_{m=1}^{N_1}\alpha_m(t_i,\cdot)\,e^{+j2\pi(f-\epsilon)\delta_m(t_i,\cdot)}\right]\right\} \tag{4.139}$$

Again, using the relationship of each attenuation and delay term given in Table 1 and noting that for any complex valued $\tilde{a}$ that

$$\tilde{a} + (\tilde{a})^* = 2\,\mathrm{Re}(\tilde{a}) \tag{4.140}$$

$$\tilde{a}\,(\tilde{a})^* = |\tilde{a}|^2 \tag{4.141}$$

Equation (4.139) becomes

$$C_{\tilde{\lambda}_{11}}(f) = 1 + \sum_{l=1}^{N_1}\left(2E\left\{\mathrm{Re}\left[\alpha_l(t_i,\cdot)\,e^{-j2\pi f\delta_l(t_i,\cdot)}\right]\right\} + E\left\{\left[\alpha_l(t_i,\cdot)\right]^2\right\}\right) + \\ + \sum_{l=1}^{N_1}\sum_{m=l+1}^{N_1} E\left\{2\,\mathrm{Re}\left[\alpha_l(t_i,\cdot)\,\alpha_m(t_i,\cdot)\,e^{-j2\pi f[\delta_l(t_i,\cdot)-\delta_m(t_i,\cdot)]}\right]\right\} \tag{4.142}$$

In a similar manner, the second diagonal term in Equation (4.136), defined as

$$C_{\tilde{\lambda}_{22}}(f) \triangleq E\left\{\tilde{\lambda}_2(f,\cdot)\left[\tilde{\lambda}_2(f,\cdot)\right]^*\right\} \tag{4.143}$$

may be found as

$$C_{\tilde{\lambda}_{22}}(f) = 1 + \sum_{p=1}^{N_2}\left(2E\left\{\mathrm{Re}\left[\beta_p(t_i,\cdot)\,e^{-j2\pi f\varepsilon_p(t_i,\cdot)}\right]\right\} + E\left\{\left[\beta_p(t_i,\cdot)\right]^2\right\}\right) + \\ + \sum_{p=1}^{N_2}\sum_{q=p+1}^{N_2} E\left\{2\,\mathrm{Re}\left[\beta_p(t_i,\cdot)\,\beta_q(t_i,\cdot)\,e^{-j2\pi f[\varepsilon_p(t_i,\cdot)-\varepsilon_q(t_i,\cdot)]}\right]\right\} \tag{4.144}$$

The off-diagonal terms do not reduce much; however, for completeness, $\tilde{C}_{\tilde{\lambda}_{12}}(f)$ defined as

$$\tilde{C}_{\tilde{\lambda}_{12}}(f) \triangleq E\left\{\tilde{\lambda}_1(f,\cdot)\left[\tilde{\lambda}_2(f,\cdot)\right]^*\right\} \tag{4.145}$$

may be written as

$$\begin{aligned}\tilde{C}_{\tilde{\lambda}_{12}}(f) &= 1+E\left\{\sum_{l=1}^{N_1}\alpha_l(t_i,\cdot)\,e^{-j2\pi f\delta_l(t_i,\cdot)}+\sum_{p=1}^{N_2}\beta_p(t_i,\cdot)\,e^{+j2\pi f\varepsilon_p(t_i,\cdot)}\right\}+\\ &\quad +E\left\{\left[\sum_{l=1}^{N_1}\alpha_l(t_i,\cdot)\,e^{-j2\pi f\delta_l(t_i,\cdot)}\right]\left[\sum_{p=1}^{N_2}\beta_p(t_i,\cdot)\,e^{+j2\pi(f-\epsilon)\varepsilon_p(t_i,\cdot)}\right]\right\}\end{aligned} \tag{4.146}$$

Using the relationship of each attenuation and delay term given in Table 1,

$$\begin{aligned}\tilde{C}_{\tilde{\lambda}_{12}}(f) &= 1+\sum_{l=1}^{N_1}E\left\{\alpha_l(t_i,\cdot)\,e^{-j2\pi f\delta_l(t_i,\cdot)}\right\}+\sum_{p=1}^{N_2}E\left\{\beta_p(t_i,\cdot)\,e^{+j2\pi f\varepsilon_p(t_i,\cdot)}\right\}+\\ &\quad +\sum_{l=1}^{N_1}E\left\{\alpha_l(t_i,\cdot)\,e^{-j2\pi f\delta_l(t_i,\cdot)}\right\}\sum_{p=1}^{N_2}E\left\{\beta_p(t_i,\cdot)\,e^{+j2\pi(f-\epsilon)\varepsilon_p(t_i,\cdot)}\right\}\end{aligned} \tag{4.147}$$

Unlike $C_{\tilde{\lambda}_{11}}(f)$ and $C_{\tilde{\lambda}_{22}}(f)$, $\tilde{C}_{\tilde{\lambda}_{12}}(f)$ is in general complex-valued (and annotated with $\tilde{}$).

From the definition of $\mathbb{E}(f)$ in Equation (4.126) and using $\tilde{\mathbf{C}}_{\tilde{\lambda}}(f)$ in Equation (4.136), let $\tilde{\Upsilon}(f;\tau_\Delta)$ be defined as

$$\tilde{\Upsilon}(f;\tau_\Delta) \triangleq \mathbb{E}(f)\,\tilde{\mathbf{C}}_{\tilde{\lambda}}(f)\,[\mathbb{E}(f)]^* \tag{4.148}$$

$$= \begin{bmatrix} C_{\tilde{\lambda}_{11}}(f) & \tilde{C}_{\lambda_{12}}(f)\,e^{-j2\pi f[\tau_1(t_i)-\tau_2(t_i)]} \\ \tilde{C}_{\lambda_{12}}(f)^*\,e^{+j2\pi f[\tau_1(t_i)-\tau_2(t_i)]} & C_{\tilde{\lambda}_{22}}(f) \end{bmatrix} \tag{4.149}$$

Notice that $\tilde{\Upsilon}(f;\tau_\Delta)$ is only parameterized by the difference

$$\tau_\Delta(t_i) \triangleq \tau_1(t_i) - \tau_2(t_i) \tag{4.150}$$

(and so annotated with "$;\tau_\Delta$"). Since $\tilde{\Upsilon}(f;\tau_\Delta)$ is the only term in

$$\tilde{\mathbf{C}}_{\tilde{x}_{gmp,\Pi}(\cdot,\cdot)}(f, f-\epsilon)$$

that depends upon $\tau_1(t_i)$ or $\tau_2(t_i)$, the stochastic nature of $\tilde{\mathbf{x}}_{gmp,\Pi}(f,\cdot)$ is parameterized by $\tau_\Delta(t_i)$ only.

Using these relationships for $\boldsymbol{\lambda}(f,\cdot)$ and $\mathbb{E}(f)$, Equation (4.135) may be written as

$$\tilde{\mathbf{C}}_{\tilde{x}_{gmp,\Pi}(\cdot,\cdot)}(f, f-\epsilon;\tau_\Delta) \approx \frac{1}{T}\left[G_{ss}(f)\,\tilde{\Upsilon}(f;\tau_\Delta) + \mathbf{G}_{nn}(f)\right]\delta_\kappa(\epsilon) \tag{4.151}$$

where the dependence upon the parameter τ_Δ is shown explicitly. When $\epsilon = 0$, the autocorrelation kernel reduces to the autocorrelation matrix, $\tilde{\mathbf{C}}_{\tilde{x}_{gmp,\Pi}(\cdot,\cdot)}(f;\tau_\Delta)$, given by

$$\tilde{\mathbf{C}}_{\tilde{x}_{gmp,\Pi}(f,\cdot)}(f;\tau_\Delta) \approx \frac{1}{T}\left[G_{ss}(f)\,\tilde{\Upsilon}(f;\tau_\Delta) + \mathbf{G}_{nn}(f)\right] \tag{4.152}$$

Using $\mathbf{G}_{nn}(f)$ and $\tilde{\Upsilon}(f;\tau_\Delta)$ given in Equations (4.133) and (4.149), respectively, Equation (4.152) becomes

$$\tilde{\mathbf{C}}(f;\tau_\Delta) = \frac{1}{T}\begin{bmatrix} G_{ss}(f)\,C_{\tilde{\lambda}_{11}}(f) + G_{n_1n_1}(f) & G_{ss}(f)\,\tilde{C}_{\tilde{\lambda}_{12}}(f)\,e^{-j2\pi f\tau_\Delta(t_i)} \\ G_{ss}(f)\,\tilde{C}_{\tilde{\lambda}_{12}}(f)^*\,e^{+j2\pi f\tau_\Delta(t_i)} & G_{ss}(f)\,C_{\tilde{\lambda}_{22}}(f) + G_{n_2n_2}(f) \end{bmatrix} \tag{4.153}$$

Thus, Equation (4.110) was used to characterize $\tilde{\mathbf{x}}_{gmp,\Pi}(\cdot,\cdot)$ in terms of the transmitted signal, the measurement noises, and the multipath model effects. In fact, since

$\tilde{\mathbf{x}}_{gmp,\Pi}(\cdot,\cdot)$ is an *orthogonal*, Gaussian stochastic process, $f_{\tilde{\mathbf{x}}_{gmp,\Pi}(\cdot,\cdot;\tau_\Delta)}$ is completely characterized for all admissible f through the mean and autocorrelation kernel given in Equations (4.123) and (4.151), respectively, and repeated here as

$$\boldsymbol{\mu}_{\tilde{x}_{gmp,\Pi}}(f) = \mathbf{0} \tag{4.123}$$

$$\tilde{\mathbf{C}}_{\tilde{x}_{gmp,\Pi}(\cdot,\cdot)}(f, f-\epsilon;\tau_\Delta) \approx \frac{1}{T}\left[G_{ss}(f)\,\tilde{\Upsilon}(f;\tau_\Delta) + \mathbf{G}_{nn}(f)\right]\delta_\kappa(\epsilon) \tag{4.151}$$

Note that $\Upsilon(f;\tau_\Delta)$ is given in Equation (4.149). Alternatively, the autocorrelation kernel may be expanded using Equation (4.153) in Equation (4.151) to yield

$$\begin{aligned}&\tilde{\mathbf{C}}_{\tilde{x}_{gmp,\Pi}(\cdot,\cdot)}(f, f-\epsilon;\tau_\Delta)\\ &\quad\approx \tfrac{1}{T}\begin{bmatrix} G_{ss}(f)\,C_{\tilde{\lambda}_{11}}(f) + G_{n_1n_1}(f) & G_{ss}(f)\,\tilde{C}_{\tilde{\lambda}_{12}}(f)\,e^{-j2\pi f\tau_\Delta(t_i)} \\ G_{ss}(f)\,\tilde{C}_{\tilde{\lambda}_{12}}(f)^*\,e^{+j2\pi f\tau_\Delta(t_i)} & G_{ss}(f)\,C_{\tilde{\lambda}_{22}}(f) + G_{n_2n_2}(f)\end{bmatrix}\delta_\kappa(\epsilon)\end{aligned} \tag{4.154}$$

Next, the relationships developed in this subsection will be used to find the *NP* for $\tilde{\mathbf{x}}_{gmp,\Pi}(\cdot,\cdot)$.

4.4.2 Finding the NP for a Gaussian $\tilde{\mathbf{x}}_{gmp,\Pi}(\cdot,\cdot)$

In this subsection, the *NP* for a Gaussian $\tilde{\mathbf{x}}_{gmp,\Pi}(\cdot,\cdot)$ is found in terms of the transmitted signal, the measurement noises, and the multipath model effects. This section combines the characterization of $\tilde{\mathbf{x}}_{gmp,\Pi}(\cdot,\cdot)$ found in the previous subsection with *NP* theory developed in Section 4.2. (This assumption's relationship with other assumptions within this chapter is shown as Box III in Figure 7 on page 50.)

Let $\tilde{\mathbf{x}}_{gmp,\Pi}(\cdot,\cdot)$ be a zero-mean, ergodic, wide-sense stationary, Gaussian stochastic process with an autocorrelation kernel given by Equation (4.151). Using

Equation (4.27), the *NP* of $\tilde{\mathbf{x}}_{gmp,\Pi}(\cdot,\cdot)$ quantifies the ability to estimate

$$\tau_\Delta \triangleq \tau_1 - \tau_2$$

given the stochastic process $\tilde{\mathbf{x}}_{gmp,\Pi}(\cdot,\cdot)$ through

$$NP\left(\tilde{\mathbf{x}}_{gmp,\Pi}\right) = I_{\tilde{\mathbf{x}}_{gmp,\Pi}}\left(\hat{\tau}_\Delta\right) \tag{4.155}$$

where $I_{\tilde{\mathbf{x}}_{gmp,\Pi}}(\hat{\tau}_\Delta)$ is the scalar case for the Fisher information matrix (FIM) given in Equation (4.22). Since $\tilde{\mathbf{x}}_{gmp,\Pi}(\cdot,\cdot)$ is also an orthogonal process, $I_{\tilde{\mathbf{x}}_{gmp,\Pi}}(\hat{\tau}_\Delta)$ may be found through

$$I_{\tilde{\mathbf{x}}_{gmp,\Pi}}\left(\hat{\tau}_\Delta\right) = \int_{-\infty}^{+\infty} I_{\tilde{\mathbf{x}}_{gmp,\Pi}(f,\cdot)}\left(f;\hat{\tau}_\Delta\right) df \tag{4.156}$$

where $I_{\tilde{\mathbf{x}}_{gmp,\Pi}(f,\cdot)}(f;\hat{\tau}_\Delta)$ is the information about τ_Δ contained in $\tilde{\mathbf{x}}_{gmp,\Pi}(\cdot,\cdot)$ at the frequency f and is given by

$$I_{\tilde{\mathbf{x}}_{gmp,\Pi}(f,\cdot)}\left(f;\tau_\Delta\right) = -E\left\{\frac{\partial^2}{\left(\partial\tau_\Delta\right)^2}\ln\left[f_{\tilde{\mathbf{x}}_{gmp,\Pi}(f,\cdot)}\left(\tilde{\boldsymbol{\xi}};\tau_\Delta\right)\right]\right\} \tag{4.157}$$

The probability density function for an arbitrary, *complex*-valued, m-dimensional Gaussian random variable $\tilde{\mathbf{y}}(\cdot)$ is given by

$$f_{\tilde{\mathbf{y}}(\cdot)}\left(\boldsymbol{\xi}\right) = \frac{1}{\pi^m\left|\tilde{\mathbf{C}}\right|}e^{\left[-\frac{1}{2}\left(\tilde{\boldsymbol{\xi}}-\tilde{\boldsymbol{\mu}}\right)^H\tilde{\mathbf{C}}^{-1}\left(\tilde{\boldsymbol{\xi}}-\tilde{\boldsymbol{\mu}}\right)\right]} \tag{4.158}$$

where $\tilde{\boldsymbol{\xi}}$ is the realization of $\tilde{\mathbf{y}}$, $\tilde{\boldsymbol{\mu}} \triangleq E\left\{\tilde{\mathbf{y}}(\cdot)\right\}$, $\tilde{\mathbf{C}} \triangleq E\left\{\left[\tilde{\mathbf{y}}(\cdot)-\tilde{\boldsymbol{\mu}}\right]\left[\tilde{\mathbf{y}}(\cdot)-\tilde{\boldsymbol{\mu}}\right]^H\right\}$, and ^{H} denotes the conjugate transpose. Thus, for some f, the probability density function of the zero-mean (from Equation (4.123)), complex-valued, Gaussian random variable

$\tilde{\mathbf{x}}_{gmp,\Pi}(f,\cdot)$ is given by

$$f_{\tilde{\mathbf{x}}_{gmp,\Pi}(f,\cdot)}\left(\tilde{\boldsymbol{\xi}};\tau_\Delta\right)=\frac{1}{\pi^2\left|\tilde{\mathbf{C}}_{\tilde{\mathbf{x}}_{gmp,\Pi}(f,\cdot)}(f;\tau_\Delta)\right|}e^{\left\{-\frac{1}{2}\tilde{\boldsymbol{\xi}}^H\left[\tilde{\mathbf{C}}_{\tilde{\mathbf{x}}_{gmp,\Pi}(f,\cdot)}(f;\tau_\Delta)\right]^{-1}\tilde{\boldsymbol{\xi}}\right\}} \tag{4.159}$$

where $\tilde{\mathbf{C}}_{\tilde{\mathbf{x}}_{gmp,\Pi}(f,\cdot)}(f;\tau_\Delta)$, given through Equation (4.153), is the autocorrelation matrix of $\tilde{\mathbf{x}}_{gmp,\Pi}(f,\cdot)$ parameterized by τ_Δ.

Evaluating $I(f;\tau_\Delta)$ given in Equation (4.157) (and dropping the subscripts on $\tilde{\mathbf{C}}_{\tilde{\mathbf{x}}_{gmp,\Pi}(f,\cdot)}(f;\tau_\Delta)$ and $I_{\tilde{\mathbf{x}}_{gmp,\Pi}(f,\cdot)}(f;\tau_\Delta)$),

$$\begin{aligned} I(f;\tau_\Delta) &= -E\left\{\frac{\partial^2}{(\partial\tau_\Delta)^2}\ln\left[f_{\tilde{\mathbf{x}}_{gmp,\Pi}(f,\cdot;\tau_\Delta)}\left(\tilde{\boldsymbol{\xi}};\tau_\Delta\right)\right]\right\} && (4.160)\\ &= E\left\{\frac{\partial^2}{(\partial\tau_\Delta)^2}\left[2\ln\pi+\ln\left|\tilde{\mathbf{C}}(f;\tau_\Delta)\right|+\frac{1}{2}\tilde{\boldsymbol{\xi}}^H\left[\tilde{\mathbf{C}}(f;\tau_\Delta)\right]^{-1}\tilde{\boldsymbol{\xi}}\right]\right\} && (4.161)\end{aligned}$$

From $\tilde{\mathbf{C}}(f;\tau_\Delta)$ given in Equation (4.153), it can be shown that $\left|\tilde{\mathbf{C}}(f;\tau_\Delta)\right|$ is independent of τ_Δ. Consequently, only the last term in Equation (4.161) is a function of τ_Δ:

$$\begin{aligned} I(f;\tau_\Delta) &= E\left\{\frac{1}{2}\tilde{\boldsymbol{\xi}}^H\frac{\partial^2\left[\tilde{\mathbf{C}}(f;\tau_\Delta)\right]^{-1}}{(\partial\tau_\Delta)^2}\tilde{\boldsymbol{\xi}}\right\} && (4.162)\\ &= E\left\{\frac{1}{2}\tilde{\boldsymbol{\xi}}^H\frac{\partial^2}{(\partial\tau_\Delta)^2}\left(\frac{adj\left\{\tilde{\mathbf{C}}(f;\tau_\Delta)\right\}}{\left|\tilde{\mathbf{C}}(f;\tau_\Delta)\right|}\right)\tilde{\boldsymbol{\xi}}\right\} && (4.163)\end{aligned}$$

Since $\tilde{\mathbf{C}}(f;\tau_\Delta)$ is Hermitian (and notating the $i-j$ element of $\tilde{\mathbf{C}}(f;\tau_\Delta)$ by $\tilde{C}_{ij}(f;\tau_\Delta)$), the adjoint of $\tilde{\mathbf{C}}(f;\tau_\Delta)$, denoted by $adj\left[\tilde{\mathbf{C}}(f;\tau_\Delta)\right]$, is

$$adj\left\{\tilde{\mathbf{C}}(f;\tau_\Delta)\right\}=\begin{bmatrix}\tilde{C}_{22}(f;\tau_\Delta) & -\tilde{C}_{12}(f;\tau_\Delta)\\ -\left[\tilde{C}_{12}(f;\tau_\Delta)\right]^* & \tilde{C}_{11}(f;\tau_\Delta)\end{bmatrix} \tag{4.164}$$

and $\left|\tilde{\mathbf{C}}\left(f;\tau_\Delta\right)\right|$ is

$$\left|\tilde{\mathbf{C}}\left(f;\tau_\Delta\right)\right| = \tilde{C}_{11}\left(f;\tau_\Delta\right)\tilde{C}_{22}\left(f;\tau_\Delta\right) - \left|\tilde{C}_{12}\left(f;\tau_\Delta\right)\right|^2 \tag{4.165}$$

Now, noting from Equation (4.153) that $\tilde{C}_{11}\left(f;\tau_\Delta\right), \tilde{C}_{22}\left(f;\tau_\Delta\right)$, and $\left|\tilde{\mathbf{C}}\left(f;\tau_\Delta\right)\right|$ are *not* functions of τ_Δ, Equation (4.163) becomes

$$\begin{aligned}
I\left(f;\tau_\Delta\right) &= E\left\{\frac{1}{2}\tilde{\boldsymbol{\xi}}^H\left[\left(\frac{T}{\left|\tilde{\mathbf{C}}\left(f;\tau_\Delta\right)\right|}\right)\cdot\right.\right. \\
&\qquad \left.\left.\frac{\partial^2}{\left(\partial\tau_\Delta\right)^2}\left(\begin{bmatrix} \tilde{C}_{22}\left(f;\tau_\Delta\right) & -\tilde{C}_{12}\left(f;\tau_\Delta\right) \\ -\left[\tilde{C}_{12}\left(f;\tau_\Delta\right)\right]^* & \tilde{C}_{11}\left(f;\tau_\Delta\right) \end{bmatrix}\right)\right]\tilde{\boldsymbol{\xi}}\right\} \qquad (4.166) \\
&= \frac{T}{2\left|\tilde{\mathbf{C}}\left(f;\tau_\Delta\right)\right|}E\left\{\begin{bmatrix} \tilde{\xi}_1^* \\ \tilde{\xi}_2^* \end{bmatrix}^T\left(\begin{bmatrix} 0 & -\frac{\partial^2\tilde{C}_{12}\left(f;\tau_\Delta\right)}{\left(\partial\tau_\Delta\right)^2} \\ -\frac{\partial^2\left[\tilde{C}_{12}\left(f;\tau_\Delta\right)^*\right]}{\left(\partial\tau_\Delta\right)^2} & 0 \end{bmatrix}\right)\begin{bmatrix} \tilde{\xi}_1 \\ \tilde{\xi}_2 \end{bmatrix}\right\} \qquad (4.167) \\
&= -\frac{T}{2\left|\tilde{\mathbf{C}}\left(f;\tau_\Delta\right)\right|}E\left\{\left(\tilde{\xi}_2^*\frac{\partial^2\left[\tilde{C}_{12}\left(f;\tau_\Delta\right)\right]^*}{\left(\partial\tau_\Delta\right)^2}\tilde{\xi}_1 + \tilde{\xi}_1^*\frac{\partial^2\tilde{C}_{12}\left(f;\tau_\Delta\right)}{\left(\partial\tau_\Delta\right)^2}\tilde{\xi}_2\right)\right\} \qquad (4.168) \\
&= -\frac{T}{2\left|\tilde{\mathbf{C}}\left(f;\tau_\Delta\right)\right|}\left(\frac{\partial^2\left[\tilde{C}_{12}\left(f;\tau_\Delta\right)\right]^*}{\left(\partial\tau_\Delta\right)^2}E\left\{\tilde{\xi}_1\tilde{\xi}_2^*\right\} + \frac{\partial^2\tilde{C}_{12}\left(f;\tau_\Delta\right)}{\left(\partial\tau_\Delta\right)^2}E\left\{\tilde{\xi}_1^*\tilde{\xi}_2\right\}\right) \qquad (4.169) \\
&= -\frac{T}{2\left|\tilde{\mathbf{C}}\left(f;\tau_\Delta\right)\right|}\left(\frac{\partial^2\left[\tilde{C}_{12}\left(f;\tau_\Delta\right)\right]^*}{\left(\partial\tau_\Delta\right)^2}\tilde{C}_{12}\left(f;\tau_\Delta\right) + \right. \\
&\qquad \left. + \frac{\partial^2\tilde{C}_{12}\left(f;\tau_\Delta\right)}{\left(\partial\tau_\Delta\right)^2}\left[\tilde{C}_{12}\left(f;\tau_\Delta\right)\right]^*\right) \qquad (4.170) \\
&= -\frac{T}{\left|\tilde{\mathbf{C}}\left(f;\tau_\Delta\right)\right|}\mathrm{Re}\left(\frac{\partial^2\tilde{C}_{12}\left(f;\tau_\Delta\right)}{\left(\partial\tau_\Delta\right)^2}\left[\tilde{C}_{12}\left(f;\tau_\Delta\right)\right]^*\right) \qquad (4.171)
\end{aligned}$$

Notice that $I(f;\tau_\Delta)$ is real-valued. Using the property [43]

$$I(f;\tau_\Delta) \geq 0 \tag{4.172}$$

and noting that $C_{12}(f) \geq 0$, the curvature of $\tilde{G}_{\tilde{x}_{1,gmp}\tilde{x}_{2,gmp}}(f)$ near the true delay will be negative (concave down). Furthermore, $\tilde{C}_{12}(f;\tau_\Delta)$ is the only factor in $I(f;\tau_\Delta)$ that depends upon τ_Δ. Intuitively, the steepness of $\tilde{C}_{12}(f;\tau_\Delta)$ dictates the information about τ_Δ contained in $\tilde{\mathbf{x}}_{gmp,\Pi}(\cdot,\cdot)$ at f.

Since $\tilde{\mathbf{x}}_{gmp,\Pi}(\cdot,\cdot)$ is an orthogonal process, $I_{\tilde{\mathbf{x}}_{gmp,\Pi}}(\hat{\tau}_\Delta)$ may be found using Equation (4.156):

$$I_{\tilde{\mathbf{x}}_{gmp,\Pi}}(\hat{\tau}_\Delta) = T\int_{-\infty}^{+\infty} \frac{-\operatorname{Re}\left(\frac{\partial^2 \tilde{C}_{12}(f;\tau_\Delta)}{(\partial\tau_\Delta)^2}\left[\tilde{C}_{12}(f;\tau_\Delta)\right]^*\right)}{\left|\tilde{\mathbf{C}}(f;\tau_\Delta)\right|} df \tag{4.173}$$

It is noted when T is not sufficiently large, $\tilde{\mathbf{x}}_{gmp,\Pi}(f)$ may be correlated over f, resulting in the degraded information $I_D(\tau_\Delta) \leq I(\tau_\Delta)$. Furthermore, $I_{\tilde{\mathbf{x}}_{gmp,\Pi}}(\hat{\tau}_\Delta)$ is linear in T. (A necessary condition for $I_{\tilde{\mathbf{x}}_{gmp,\Pi}}(\hat{\tau}_\Delta)$ to be linear in T is that the time delays and attenuations are constant over the interval $\left[t_i - \frac{T}{2}, t_i + \frac{T}{2}\right]$. See page 70.) From Equation (4.27), Equation (4.173) is also $NP(\tilde{\mathbf{x}}_{gmp,\Pi})$.

Using Equation (4.153), the following identities hold:

$$\tilde{C}_{12}(f;\tau_\Delta) = G_{ss}(f)\,\tilde{C}_{\tilde{\lambda}_{12}}(f)\,e^{-j2\pi f\tau_\Delta(t_i)} \tag{4.174}$$

$$\left|\tilde{\mathbf{C}}(f;\tau_\Delta)\right| = \tilde{C}_{11}(f;\tau_\Delta)\,\tilde{C}_{22}(f;\tau_\Delta) - \left|\tilde{C}_{12}(f;\tau_\Delta)\right|^2 \tag{4.175}$$

$$= \left[G_{ss}(f)\,C_{\tilde{\lambda}_{11}}(f) + G_{n_1n_1}(f)\right]\left[G_{ss}(f)\,C_{\tilde{\lambda}_{22}}(f) + G_{n_2n_2}(f)\right] - \left|G_{ss}(f)\,\tilde{C}_{\tilde{\lambda}_{12}}(f)\,e^{-j2\pi f\tau_\Delta(t_i)}\right|^2 \tag{4.176}$$

$$\begin{aligned}\left|\tilde{\mathbf{C}}\left(f;\tau_{\Delta}\right)\right| &= G_{ss}\left(f\right)^{2}\left[C_{\tilde{\lambda}_{11}}\left(f\right)C_{\tilde{\lambda}_{22}}\left(f\right)-\left|\tilde{C}_{\tilde{\lambda}_{12}}\left(f\right)\right|^{2}\right] \\ &\quad +G_{ss}\left(f\right)\left[G_{n_1n_1}\left(f\right)C_{\tilde{\lambda}_{22}}\left(f\right)+G_{n_2n_2}\left(f\right)C_{\tilde{\lambda}_{11}}\left(f\right)\right] \\ &\quad +G_{n_1n_1}\left(f\right)G_{n_2n_2}\left(f\right) \end{aligned} \tag{4.177}$$

Thus, the *NP* of $\tilde{\mathbf{x}}_{gmp,\Pi}\left(\cdot,\cdot\right)$ is

$$NP\left(\tilde{\mathbf{x}}_{gmp,\Pi}\right)=T\int_{-\infty}^{+\infty}\frac{\begin{array}{c}-G_{ss}\left(f\right)^{2}\left|\tilde{C}_{\tilde{\lambda}_{12}}\left(f\right)\right|^{2}\bullet \\ \mathrm{Re}\left(\frac{\partial^{2}}{\left(\partial\tau_{\Delta}\right)^{2}}\left[e^{-j2\pi f\tau_{\Delta}(t_i)}\right]\left[e^{-j2\pi f\tau_{\Delta}(t_i)}\right]^{*}\right)\end{array}}{\left(\begin{array}{c}G_{ss}\left(f\right)^{2}\left[C_{\tilde{\lambda}_{11}}\left(f\right)C_{\tilde{\lambda}_{22}}\left(f\right)-\left|\tilde{C}_{\tilde{\lambda}_{12}}\left(f\right)\right|^{2}\right] \\ +G_{ss}\left(f\right)\left[G_{n_1n_1}\left(f\right)C_{\tilde{\lambda}_{22}}\left(f\right)+G_{n_2n_2}\left(f\right)C_{\tilde{\lambda}_{11}}\left(f\right)\right] \\ +G_{n_1n_1}\left(f\right)G_{n_2n_2}\left(f\right)\end{array}\right)}df \tag{4.178}$$

and then, finally:

$$NP\left(\tilde{\mathbf{x}}_{gmp,\Pi}\right)=T\int_{-\infty}^{+\infty}\frac{\left(2\pi f\right)^{2}G_{ss}\left(f\right)^{2}\left|\tilde{C}_{\tilde{\lambda}_{12}}\left(f\right)\right|^{2}}{\left(\begin{array}{c}G_{ss}\left(f\right)^{2}\left[C_{\tilde{\lambda}_{11}}\left(f\right)C_{\tilde{\lambda}_{22}}\left(f\right)-\left|\tilde{C}_{\tilde{\lambda}_{12}}\left(f\right)\right|^{2}\right] \\ +G_{ss}\left(f\right)\left[G_{n_1n_1}\left(f\right)C_{\tilde{\lambda}_{22}}\left(f\right)+G_{n_2n_2}\left(f\right)C_{\tilde{\lambda}_{11}}\left(f\right)\right] \\ +G_{n_1n_1}\left(f\right)G_{n_2n_2}\left(f\right)\end{array}\right)}df \tag{4.179}$$

Equation (4.179) is the *NP* of $\tilde{\mathbf{x}}_{gmp,\Pi}\left(\cdot,\cdot\right)$ in terms of the transmitted signal, the measurement noises, and the multipath model effects. Chapter 5 develops trends using this result. The assumptions that led to the result in Equation (4.179) can be summarized as follows. First, the received signal was modeled by a Gaussian transmitted signal with multiple, delayed and attenuated signals in additive, Gaussian noise observed for T seconds. Then, the stochastic nature of the received signal was modeled through its spectral representation. This allowed the *NP* to be found in the compact notation given in Equation (4.179). These results do not apply when a

Gaussian probability density function is a poor approximation to $f_{\mathbf{x}_{gmp,\Pi(f,\cdot)}}$; rather, Equation (4.106) should be used under those conditions.

4.5 Summary

This chapter presented navigation potential (*NP*) using a very general stochastic model whereby the transmitted signal is mapped into the received signal using Equation (4.2), repeated here as

$$\mathbf{x}(\cdot,\cdot) \triangleq \begin{bmatrix} x_1(\cdot,\cdot) \\ x_2(\cdot,\cdot) \end{bmatrix} = \begin{bmatrix} g_1[\cdot,\cdot;s(\cdot,\cdot),n_1(\cdot,\cdot),\tau_1(\cdot)] \\ g_2[\cdot,\cdot;s(\cdot,\cdot),n_2(\cdot,\cdot),\tau_2(\cdot)] \end{bmatrix} \tag{4.2}$$

The *NP* of a received signal was related to the Fisher Information Matrix in Equation (4.25), i.e.,

$$\boxed{NP(\mathbf{x}) \triangleq \left(\frac{\partial \mathbf{h}(\boldsymbol{\theta})}{\partial \boldsymbol{\theta}} \mathbf{I}^{-1}(\boldsymbol{\theta}) \left[\frac{\partial \mathbf{h}(\boldsymbol{\theta})}{\partial \boldsymbol{\theta}} \right]^T \right)^{-1}} \tag{4.25}$$

without limiting the mapping used. This novel outlook permits the designer to build a model and have the tools for finding the *NP* of the received signal. (Graphically, the signal model and navigation potential for Figure 7(a) −Box I from page 50 are given by Equations (4.2) and (4.25), respectively.)

A multipath mapping whereby the received signal was modeled as the transmitted signal, measurement noise, and multiple delayed and attenuated replicas of the transmitted signal was introduced in Equations (4.40) and (4.41), repeated here for all admissible t as

$$\begin{aligned} x_{1_{mp}}(t,\cdot) &= s(t-\tau_1(t),\cdot) + n_1(t,\cdot) + \\ &\quad + \sum_{l=1}^{N_1} \alpha_l(t,\cdot)\, s[t-\tau_1(t)-\delta_l(t,\cdot),\cdot] \end{aligned} \tag{4.40}$$

$$x_{2_{mp}}(t,\cdot) = s(t-\tau_2(t),\cdot) + n_2(t,\cdot) + \\ + \sum_{l=1}^{N_2} \beta_l(t,\cdot)\, s[t-\tau_2(t)-\varepsilon_l(t,\cdot),\cdot] \tag{4.41}$$

The spectral representation for a finite-timelength observation of the multipath model was found in Equation (4.48), repeated here for all admissible f as

$$\tilde{\mathbf{x}}_{mp,\Pi}(f,\cdot) = \begin{bmatrix} \tilde{s}_\Pi(f,\cdot)\, e^{-j2\pi f\tau_1(t_i)} \left(1 + \sum_{l=1}^{N_1} \alpha_l(t_i,\cdot)\, e^{-j2\pi f\delta_l(t_i,\cdot)}\right) \\ \\ \tilde{s}_\Pi(f,\cdot)\, e^{-j2\pi f\tau_2(t_i)} \left(1 + \sum_{l=1}^{N_2} \beta_l(t_i,\cdot)\, e^{-j2\pi f\varepsilon_l(t_i,\cdot)}\right) \end{bmatrix} + \tilde{\mathbf{n}}_\Pi(f,\cdot) \tag{4.48}$$

This multipath representation enabled the NP to be expressed in the form given by Equation (4.106), i.e.,

$$NP\{\tilde{\mathbf{x}}_{mp,\Pi}(\cdot)\} = -\frac{E\left\{\frac{\partial^2 \ln\left[f\left(\tilde{\mathbf{x}}_{mp,\Pi}(\cdot);\tau_1,\tau_2\right)\right]}{(\partial\tau_1)^2}\right\} E\left\{\frac{\partial^2 \ln\left[f\left(\tilde{\mathbf{x}}_{mp,\Pi}(\cdot);\tau_1,\tau_2\right)\right]}{(\partial\tau_2)^2}\right\} - E\left\{\frac{\partial^2 \ln\left[f\left(\tilde{\mathbf{x}}_{mp,\Pi}(\cdot);\tau_1,\tau_2\right)\right]}{\partial\tau_1\partial\tau_2}\right\}^2}{E\left\{\frac{\partial^2 \ln\left[f\left(\tilde{\mathbf{x}}_{mp,\Pi}(\cdot);\tau_1,\tau_2\right)\right]}{(\partial\tau_1)^2}\right\} + E\left\{\frac{\partial^2 \ln\left[f\left(\tilde{\mathbf{x}}_{mp,\Pi}(\cdot);\tau_1,\tau_2\right)\right]}{(\partial\tau_2)^2}\right\} + 2E\left\{\frac{\partial^2 \ln\left[f\left(\tilde{\mathbf{x}}_{mp,\Pi}(\cdot);\tau_1,\tau_2\right)\right]}{\partial\tau_1\partial\tau_2}\right\}} \tag{4.106}$$

which is more explicit than the general case yet encompasses a wide range of problems. This new result provided theory to quantify the ability to estimate a time difference of arrival estimate in terms of the transmitted signal, the measurement noises, and the multipath effects. (The signal model given by Equations (4.40) and (4.41), and navigation potential given by Equation (4.106), are represented graphically by Figure 7(a) −Box II.)

Finally, the received signal was modeled as Gaussian in Equations (4.108) and (4.109) by applying the assumptions given in the list on page 87. Equations (4.108) and (4.109) are repeated here for all admissible t:

$$\begin{aligned} x_{1_{gmp}}(t,\cdot) &= s(t-\tau_1(t),\cdot)+n_1(t,\cdot) \\ &\quad +\sum_{l=1}^{N_1}\alpha_l(t,\cdot)\,s[t-\tau_1(t)-\delta_l(t,\cdot),\cdot] \end{aligned} \tag{4.108}$$

$$\begin{aligned} x_{2_{gmp}}(t,\cdot) &= s(t-\tau_2(t),\cdot)+n_2(t,\cdot) \\ &\quad +\sum_{l=1}^{N_2}\beta_l(t,\cdot)\,s[t-\tau_2(t)-\varepsilon_l(t,\cdot),\cdot] \end{aligned} \tag{4.109}$$

The spectral representation for a finite-timelength observation of the Gaussian received signal, $\tilde{\mathbf{x}}_{gmp,\Pi}(\cdot,\cdot)$, was found in Equation (4.110) and repeated here for all admissible f as

$$\tilde{\mathbf{x}}_{gmp,\Pi}(f,\cdot)=\begin{bmatrix} \tilde{s}_\Pi(f,\cdot)\,e^{-j2\pi f\tau_1(t_i)}\left(1+\sum_{l=1}^{N_1}\alpha_l(t_i,\cdot)\,e^{-j2\pi f\delta_l(t_i,\cdot)}\right) \\ \\ \tilde{s}_\Pi(f,\cdot)\,e^{-j2\pi f\tau_2(t_i)}\left(1+\sum_{l=1}^{N_2}\beta_l(t_i,\cdot)\,e^{-j2\pi f\varepsilon_l(t_i,\cdot)}\right) \end{bmatrix}+\tilde{\mathbf{n}}_\Pi(f,\cdot) \tag{4.110}$$

The NP of $\tilde{\mathbf{x}}_{gmp,\Pi}(\cdot,\cdot)$ was expressed in Equation (4.179) in terms explicitly associated with the transmitted signal, the measurement noises, and the multipath effects; Equation (4.179) is repeated here as

$$NP(\tilde{\mathbf{x}}_{gmp,\Pi})=T\int_{-\infty}^{+\infty}\frac{(2\pi f)^2\,G_{ss}(f)^2\left|\tilde{C}_{\tilde{\lambda}_{12}}(f)\right|^2}{\left(\begin{array}{c} G_{ss}(f)^2\left[C_{\tilde{\lambda}_{11}}(f)\,C_{\tilde{\lambda}_{22}}(f)-\left|\tilde{C}_{\tilde{\lambda}_{12}}(f)\right|^2\right] \\ +G_{ss}(f)\left[G_{n_1n_1}(f)\,C_{\tilde{\lambda}_{22}}(f)+G_{n_2n_2}(f)\,C_{\tilde{\lambda}_{11}}(f)\right] \\ +G_{n_1n_1}(f)\,G_{n_2n_2}(f) \end{array}\right)}df \tag{4.179}$$

(The signal model given by Equations (4.108) and (4.109) (or, equivalently, Equation (4.110)) and the *NP* given by Equation (4.179) are represented graphically by Figure 7(a) −Box III.)

These new tools were intentionally not demonstrated in this chapter to stress the general nature of the problem formulation used herein. This generalization permits *NP* to apply to a wide class of problems. Chapter 5 will explore specific details and trends that can be drawn from the developments in this chapter, and *NP* theory will be used to evaluate specific problems.

Chapter 5 - Predicting Performance Bounds with Navigation Potential

5.1 Introduction

In this chapter, navigation potential (*NP*) theory developed in Chapter 4 is used to predict the theoretical navigation performance bounds of several example signals. These examples demonstrate that (1) current performance bounds are a special case of the new *NP* theory, (2) *NP* may provide additional insight over other performance bounds, and (3) the general nature of *NP* theory encompasses received signal models for which no performance bounds were previously available.

Section 5.2 treats the case of a simplified signal model with no multipath (used to introduce SOP in Chapter 3) as a special case of *NP* theory, and shows that the theory is consistent with previously derived results for this special case. Figure 9 represents this example with Box "A" to show its relationship to the assumptions and other examples. (Figure 9 is derived from Figure 7, given in Chapter 4 on page 50.) Using this graphical aid, problems framed within Box "A" assume a TDOA measurement model with the transmitted signal, measurement noise, and received signal all being Gaussian, and no multipath present (i.e., $N_1 = N_2 = 0$).

The remaining sections apply *NP* theory to predict the theoretical GPS correlation error performance bounds under more general conditions than used to generate present performance bounds. In a typical GPS receiver [58], the time delay of the incoming GPS signal incurred to travel from the transmitter to the receiver, denoted by τ_Δ, is compared to the time delay of the internally generated signal, denoted by

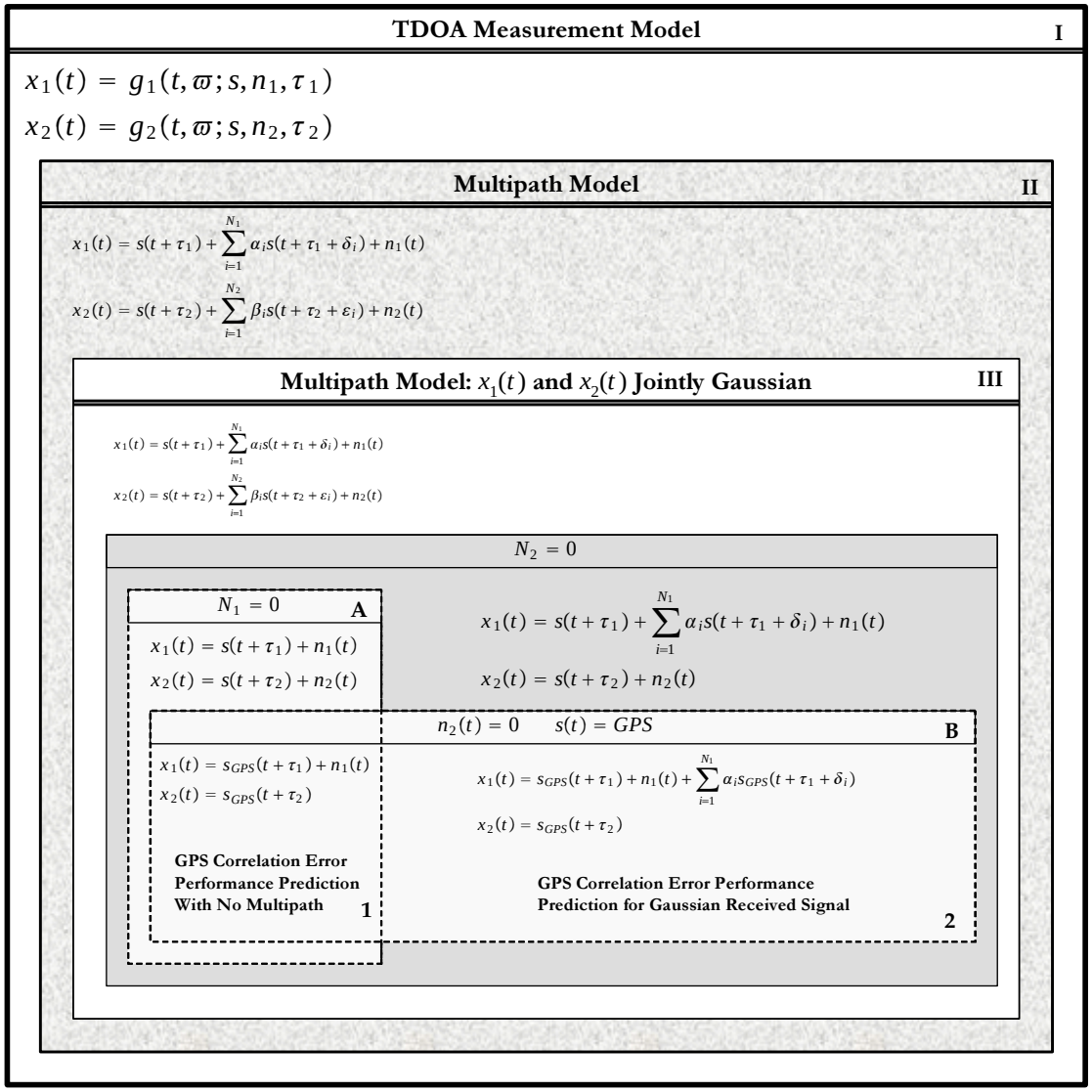

Figure 9. Relationship of Navigation Potential Assumptions and Examples

$\tau_\Delta|_{track}$. A GPS receiver uses a correlator to estimate the tracking error, $\tau_\Delta - \tau_\Delta|_{track}$, (which may be treated as a TDOA measurement) to track the incoming signal.

GPS correlation error performance bounds may be found using the *NP*-based models shown graphically as Box "B" in Figure 9. As indicated by the location of Box "B" in Figure 9, all examples within this class assume a TDOA measurement, a multipath model, and a Gaussian transmitted signal in Gaussian noise. Furthermore, the second "received" signal (actually, the signal internally generated by the second receiver tracking purposes) exhibits no multipath or noise.

Two GPS correlation error performance bound prediction examples are discussed, each with a different model of the received signal; namely, Section 5.3 assumes no multipath is present in the received signals (Box "B1"), while Section 5.4 assumes Gaussian received signals are composed of the transmitted signal, multipath, and noise (Box "B2"). When appropriate, the *NP* results will be compared to previously developed performance bounds.

While all of these examples are confined to a Gaussian transmitted signal in Gaussian noise, *NP* theory is not limited to these types of signals and noise. Non-Gaussian signals are included within the theory; however, the computational complexity increases with non-Gaussian signals for which moments higher than second order are considered. (See Section 4.3.) The presented examples represent a small subset of the signals that may be analyzed with *NP* theory.

5.2 Navigation Potential for SOP-Based TDOA without Multipath

In this section, *NP* theory is used to evaluate SOP-based TDOA without multipath (a special case of the general results) in order to demonstrate that *NP* expressions are consistent with previous performance bounds when properly constrained. In particular, SOP-based TDOA navigation (as presented in detail in Chapter 3) estimates the difference in arrival times of the i^{th} SOP at two receivers. A navigation solution (as detailed in Section 3.3 in Chapter 3) may be obtained using N TDOA estimates from N SOP using the same two receivers for each of the $i = 1, 2, \cdots, N$ measurements. Figure 5 in Chapter 3 (page 41) presents the overall navigation system, while Figure 6 in Chapter 3 (page 43) shows a geometric interpretation for a single SOP-based TDOA measurement.

The remainder of this section presents (1) a time-domain model, and an equivalent frequency-domain model, for SOP-Based TDOA without multipath, (2) the *NP* of SOP-Based TDOA without multipath, and (3) a comparison of *NP* to previous performance bounds.

5.2.1 Signal Model

NP theory may be applied to SOP-based TDOA without multipath through the following *time-domain model* for all t (which is equivalent to Equations (3.8) and (3.9) in Chapter 3 without notation to indicate the i^{th} SOP):

$$\mathbf{x}(t,\cdot) = \begin{bmatrix} s(t,\cdot) \\ s[t+\delta_{br}(t,\cdot),\cdot] \end{bmatrix} + \mathbf{n}(t,\cdot) \tag{5.1}$$

or

$$\begin{bmatrix} x_b(t,\cdot) \\ x_r(t,\cdot) \end{bmatrix} = \begin{bmatrix} s(t,\cdot) \\ s[t+\delta_{br}(t),\cdot] \end{bmatrix} + \begin{bmatrix} n_b(t,\cdot) \\ n_r(t,\cdot) \end{bmatrix} \tag{5.2}$$

The signal, $s(\cdot,\cdot)$, the measurement noise at the base station, $n_b(\cdot,\cdot)$, and the measurement noise at the rover, $n_r(\cdot,\cdot)$, are mutually independent, zero-mean, ergodic, wide-sense stationary, Gaussian stochastic processes with known power spectral densities:

$$G_{ss}(f), G_{n_b n_b}(f), G_{n_r n_r}(f)$$

Furthermore, $\delta_{br}(\cdot)$ is the time difference of arrival of the signal at the base station relative to the rover (modeled as constant over a finite-timelength observation interval, $\left[t_i - \frac{T}{2}, t_i + \frac{T}{2}\right] \subset \mathbb{R}^1$).

A *frequency-domain model* may be found, as in Equation (4.125), for all admissible f as

$$\tilde{\mathbf{x}}_\Pi(f,\cdot) = \tilde{s}_\Pi(f,\cdot)\,\mathbb{E}(f)\,\tilde{\boldsymbol{\lambda}}(f,\cdot) + \tilde{\mathbf{n}}_\Pi(f,\cdot) \tag{5.3}$$

where $\tilde{s}_\Pi(\cdot,\cdot)$ is the spectral representation of $s(\cdot,\cdot)$ defined, as in Equation (4.49), for all admissible f as

$$\tilde{s}_\Pi(f,\cdot) \triangleq \mathcal{F}\left\{\frac{1}{T}\prod\left(\frac{t-t_i}{T}\right) s(t,\cdot)\right\} \tag{5.4}$$

and $\tilde{\mathbf{n}}_\Pi(f,\cdot)$ is the spectral representation of $\mathbf{n}(\cdot,\cdot)$ defined, as in Equation (4.50), for all admissible f as

$$\tilde{\mathbf{n}}_\Pi(f,\cdot) \triangleq \mathcal{F}\left\{\frac{1}{T}\prod\left(\frac{t-t_i}{T}\right) \mathbf{n}(t,\cdot)\right\} \tag{5.5}$$

Furthermore, the matrix which contains the delays incurred by the signal to travel to each receiver, $\mathbb{E}(f)$, is defined for all admissible f as

$$\mathbb{E}(f) \triangleq \begin{bmatrix} 1 & 0 \\ 0 & e^{-j2\pi f \delta_{br}(t_i)} \end{bmatrix} \tag{5.6}$$

An analogous result using Equation (4.126) may be found using

$$\tau_1(t_i) \triangleq 0 \tag{5.7}$$

$$\tau_2(t_i) \triangleq -\delta_{br}(t_i) \tag{5.8}$$

and, consequently, the statistics of $\tilde{\mathbf{x}}_{\Pi}(\cdot,\cdot)$ are a function of the time difference $\tau_1(t_i) - \tau_2(t_i) = \delta_{br}(t_i)$ only. The final segment of the frequency-domain model is the multipath effect matrix, $\tilde{\boldsymbol{\lambda}}(f,\cdot)$, defined for all admissible f as (see also Equation (4.127))

$$\tilde{\boldsymbol{\lambda}}(f,\cdot) \triangleq \begin{bmatrix} 1 \\ 1 \end{bmatrix} \tag{5.9}$$

In this case, the autocorrelation matrix for $\tilde{\boldsymbol{\lambda}}(f,\cdot)$ is (see also Equation (4.136))

$$\tilde{\mathbf{C}}_{\tilde{\lambda}}(f) \triangleq E\left\{\tilde{\boldsymbol{\lambda}}(f,\cdot)\left[\tilde{\boldsymbol{\lambda}}(f,\cdot)\right]^H\right\} \tag{5.10}$$

$$= \begin{bmatrix} 1 & 1 \\ 1 & 1 \end{bmatrix} \tag{5.11}$$

5.2.2 Navigation Potential

In general, the *NP* of $\tilde{\mathbf{x}}(\cdot,\cdot)$ for a Gaussian received signal modeled with a multipath mapping is given through Equation (4.179) and repeated here as

$$NP\left(\tilde{\mathbf{x}}_{gmp,\Pi}\right) = T\int_{-\infty}^{+\infty} \frac{(2\pi f)^2 G_{ss}(f)^2 \left|\tilde{C}_{\tilde{\lambda}_{12}}(f)\right|^2}{\left(\begin{array}{c} G_{ss}(f)^2\left[C_{\tilde{\lambda}_{11}}(f) C_{\tilde{\lambda}_{22}}(f) - \left|\tilde{C}_{\tilde{\lambda}_{12}}(f)\right|^2\right] \\ +G_{ss}(f)\left[G_{n_1n_1}(f) C_{\tilde{\lambda}_{22}}(f) + G_{n_2n_2}(f) C_{\tilde{\lambda}_{11}}(f)\right] \\ +G_{n_1n_1}(f) G_{n_2n_2}(f) \end{array}\right)} df \tag{4.179}$$

SOP-based TDOA *NP* for the "no multipath" case (as represented by Box "A" of Figure 9) may be found using Equation (4.179) with the frequency-domain model given in the previous subsection:

$$NP(\mathbf{x}) = T\int_{-\infty}^{+\infty} \frac{(2\pi f)^2 G_{ss}(f)^2 (1)}{\left(\begin{array}{c} G_{ss}(f)^2 (0) \\ +G_{ss}(f)\left[(1) G_{n_bn_b}(f) + (1) G_{n_rn_r}(f)\right] \\ +G_{n_bn_b}(f) G_{n_rn_r}(f) \end{array}\right)} df \tag{5.12}$$

Simplifying,

$$NP(\mathbf{x}) = T\int_{-\infty}^{+\infty} \frac{(2\pi f)^2 G_{ss}(f)^2}{G_{ss}(f)\left[G_{n_bn_b}(f) + G_{n_rn_r}(f)\right] + G_{n_bn_b}(f) G_{n_rn_r}(f)} df \tag{5.13}$$

5.2.3 NP Comparison with Other Performance Bounds

NP is shown to be consistent with previous performance bounds for this case. Under the scalar case (with respect to the parameters being estimated), the *NP* is related to the Cramer Rao lower bound (CRLB) of any unbiased estimate of δ_{br}, denoted by $C_{\hat{\delta}_{br}}$, through Equation (4.26):

$$NP(\mathbf{x}) \triangleq \left(C_{\hat{\delta}_{br}}\right)^{-1} \tag{5.14}$$

Thus, $C_{\hat{\delta}_{br}}$ for SOP-based TDOA measurements (using the $NP(\mathbf{x})$ found in Equation (5.13)) is given by

$$C_{\hat{\delta}_{br}} = \left(T \int_{-\infty}^{+\infty} \frac{(2\pi f)^2 G_{ss}(f)^2}{G_{ss}(f)\left[G_{n_b n_b}(f) + G_{n_r n_r}(f)\right] + G_{n_b n_b}(f) G_{n_r n_r}(f)} df \right)^{-1} \tag{5.15}$$

Using a model with the same restrictions, the CRLB for SOP-based TDOA measurements may be found through Equation (3.39) as

$$C_{\hat{\delta}_{br}}\big|_p = \left(T \int_{-\infty}^{\infty} \frac{(2\pi f)^2 \left|\tilde{\gamma}_{x_b^i x_r^i}(f)\right|^2}{1 - \left|\tilde{\gamma}_{x_b^i x_r^i}(f)\right|^2} df \right)^{-1} \tag{5.16}$$

where $|_p$ indicates "previous" results (see [44]) and the coherence magnitude squared, $\left|\tilde{\gamma}_{x_b x_r}(f)\right|^2$, was defined in Equation (3.21) and repeated here as

$$\left|\tilde{\gamma}_{x_b^i x_r^i}(f)\right|^2 \triangleq \frac{\left|\tilde{G}_{x_b^i x_r^i}(f)\right|^2}{\left|\tilde{G}_{x_b^i x_b^i}(f)\,\tilde{G}_{x_r^i x_r^i}(f)\right|} \tag{3.21}$$

Note that

$$\tilde{G}_{x_b x_r}(f) = G_{ss}(f)\, e^{-j2\pi f \delta_{br}} \tag{3.25}$$

$$G_{x_b x_b}(f) = G_{ss}(f) + G_{n_b n_b}(f) \tag{3.26}$$

$$G_{x_r x_r}(f) = G_{ss}(f) + G_{n_r n_r}(f) \tag{3.27}$$

(Since $s(t)$ and $n(t)$ are real-valued, $G_{ss}(f)$ and $G_{nn}(f)$ are real-valued functions [68]). Now, $C_{\hat{\delta}_{br}}\big|_p$ given by Equation (5.16) may be written as

$$C_{\hat{\delta}_{br}}\big|_p = \left(T \int_{-\infty}^{\infty} \frac{(2\pi f)^2 \left|\tilde{\gamma}_{x_b^i x_r^i}(f)\right|^2}{1 - \left|\tilde{\gamma}_{x_b^i x_r^i}(f)\right|^2} df \right)^{-1} \tag{5.17}$$

$$= \left(T \int_{-\infty}^{\infty} \frac{(2\pi f)^2 \left|\tilde{G}_{x_b x_r}(f)\right|^2}{\left|\tilde{G}_{x_b x_b}(f)\,\tilde{G}_{x_r x_r}(f)\right| - \left|\tilde{G}_{x_b x_r}(f)\right|^2} df \right)^{-1} \tag{5.18}$$

$$= \left(T \int_{-\infty}^{\infty} \frac{(2\pi f)^2 G_{ss}(f)^2}{[G_{ss}(f) + G_{n_b n_b}(f)][G_{ss}(f) + G_{n_r n_r}(f)] - G_{ss}(f)^2} df \right)^{-1} \tag{5.19}$$

$$= \left(T \int_{-\infty}^{\infty} \frac{(2\pi f)^2 G_{ss}(f)^2}{G_{ss}(f)[G_{n_b n_b}(f) + G_{n_r n_r}(f)] + G_{n_b n_b}(f) G_{n_r n_r}(f)} df \right)^{-1} \tag{5.20}$$

This matches the CRLB predicted through *NP* theory, i.e.,

$$C_{\hat{\delta}_{br}}\big|_p = C_{\hat{\delta}_{br}} \tag{5.21}$$

in which $C_{\hat{\delta}_{br}}\big|_p$ is the CRLB given by previous results and $C_{\hat{\delta}_{br}}$ is the CRLB found in Equation (5.15) by restricting *NP* theory to the simplified SOP-based TDOA, no multipath case (represented in Figure 9 with Box "A").

5.3 Predicting GPS Correlation Error Performance Bounds with Navigation Potential

The theoretical navigation potential (*NP*) developed in Chapter 4 may be applied to many different kinds of signals. This section applies *NP* theory to the Global Positioning System (GPS) signal with no multipath present. In this respect, *NP*

will be used to describe the ability to determine the pseudorange of a GPS signal by predicting GPS correlation error performance bounds. The overall GPS problem set is represented in Figure 9 with Box "B". This section addresses problems for which the assumptions represented by Box "B1" in Figure 9 apply.

Section 5.3.1 presents the GPS signal model used in this derivation. Then, Section 5.3.2 develops the theoretical *NP* for GPS as a new way to characterize GPS correlation error performance bounds. Finally, Section 5.3.3 compares this new characterization to performance bounds developed previously.

5.3.1 GPS Signal Structure

This section overviews the GPS signal structure used in subsequent analyses. The signal received at the transmitter is modeled as

$$x(t) = s(t) + n(t) \tag{5.22}$$

where $s(t)$ is the received GPS signal and $n(t)$ represents additive, white, Gaussian noise. The noise is assumed ergodic and independent of $s(t)$ with the noise strength, N_o, given as [53]

$$N_o = -201 \quad \frac{\text{dBW}}{\text{Hz}} \tag{5.23}$$

The power spectral density of the noise is constant over all frequencies, with value

$$G_{nn}(f) = \frac{N_o}{2} \tag{5.24}$$

Assuming the Doppler frequency shift is removed by a separate carrier tracking algorithm, the coarse acquisition (C/A) part of the GPS signal is [58]

$$s(t) = \sqrt{2P_{ave}}\, d(t)\, c(t) \cos(2\pi f_o t) \tag{5.25}$$

where

$$\begin{aligned} P_{ave} &\triangleq \text{average received signal power at the antenna} && (5.26)\\ &\geq -160 \quad \text{dBW} \quad \text{(specified)} && (5.27)\\ &\approx -157 \quad \text{dBW} \quad \text{(typical)} && (5.28)\\ f_o &\triangleq \text{carrier frequency} && (5.29)\\ &= 1575.42 \quad \text{MHz} \quad \text{(L1 band)} && (5.30) \end{aligned}$$

and $d(t)$ and $c(t)$ are pseudo-random binary waveforms (PRBW) with the following data (R_d) and code (R_c) rates:

$$R_d = 50 \quad \frac{\text{bits}}{\text{sec}} \triangleq \frac{1}{T_d} \tag{5.31}$$

$$R_c = 1.023 \quad \frac{\text{Mbits}}{\text{sec}} \triangleq \frac{1}{T_c} \tag{5.32}$$

Since $R_c = NR_d$ where $N \in Integers$ and $d(t)$ and $c(t)$ are chip-synchronous, a new PRBW, $g(t)$, may be defined as

$$g(t) \triangleq d(t)\, c(t) \tag{5.33}$$

with a data rate

$$R_g = R_c = \frac{1}{T_c} \tag{5.34}$$

Using $g(t)$, the coarse acquisition (C/A) part of the GPS signal is

$$s(t) = \sqrt{2P_{ave}}\, g(t) \cos(2\pi f_o t) \tag{5.35}$$

The envelope of the power spectral density of $s(t)$ given in Equation (5.35) can be found in a straightforward manner as [58]

$$G_{ss}(f) = \frac{P_{ave}T_c}{2}\left\{sinc^2\left[(f-f_o)T_c\right] + sinc^2\left[(f+f_o)T_c\right]\right\} \tag{5.36}$$

Equations (5.24) and (5.36) represent the noise and signal power spectral densities and are defined over all frequencies. Typically, the incoming signal and noise are bandlimited with a bandwidth B centered about the carrier frequency f_o. In this case, the signal and noise power spectral densities can be represented as

$$\begin{aligned} G_{ss}(f) = \tfrac{P_{ave}T_c}{2}\left\{sinc^2\left[(f-f_o)T_c\right] + sinc^2\left[(f+f_o)T_c\right]\right\} \\ \forall\, |f| \in \left[f_o - \tfrac{B}{2}, f_o + \tfrac{B}{2}\right] \end{aligned} \tag{5.37}$$

and

$$G_{nn}(f) = \frac{N_o}{2} \quad \forall\, |f| \in \left[f_o - \frac{B}{2}, f_o + \frac{B}{2}\right] \tag{5.38}$$

A more accurate (and more complex) bandlimited signal model might represent the bandlimited signal as the original signal affected by attenuation, frequency rolloff, harmonics, etc. Also, $s(t)$ is actually periodic, not random. (However, its mean and autocorrelation function exhibit properties that permit it to be treated as random — termed pseudo-random.) The periodic nature of $s(t)$ results in $G_{ss}(f)$ being composed of spectral lines. The spectral lines are spaced at the code repeat rate and follow the envelope given in Equation (5.36).

5.3.2 Theoretical GPS NP

This subsection applies *NP* theory to the GPS signal. First, GPS receiver architecture is fit into the mappings used to developed *NP* theory. Second, the *NP* for GPS signals is found using the GPS signal structure presented in the previous subsection.

5.3.2.1 Applying GPS to an NP Theory Mapping Model. The theoretical *NP* is related to the theoretical minimum mean squared error of a TDOA estimate of two received signals. In a typical GPS receiver, the time delay of the received signal as compared to an internally generated signal is found through cross correlation within a delay lock loop [58]. The delay lock loop process may be modeled by choosing x_1 as a delayed received signal defined in Equation (5.22) and x_2 as an internally generated signal, written as

$$x_1(t) = s(t - \tau_\Delta) + n(t) \tag{5.39}$$

$$x_2(t) = s(t - \tau_\Delta|_{track}) \tag{5.40}$$

where $s(t)$ represents the GPS signal, $n(t)$ represents the measurement noise, τ_Δ represents the time delay of the received GPS signal incurred to travel from the transmitter to the receiver, and $\tau_\Delta|_{track}$ is the time delay of the internally generated signal. A GPS receiver uses an estimate of the tracking error, $[\tau_\Delta - \tau_\Delta|_{track}]$, to track the incoming signal. Analogously, this tracking error may be treated as a TDOA measurement. Furthermore, it is assumed that noise on the internally generated signal can be neglected, and that the internally generated signal is identical in structure to

the transmitted signal. The overall navigation performance of the GPS depends, in part, upon system geometry, the satellite signals' synchronization accuracy, and the ability to track (i.e., the ability to estimate the tracking error of) each incoming signal. System geometry and satellite synchronization are factors that affect the overall navigation solution, while the underlying navigation potential of a single GPS signal rests upon how well the tracking error can be estimated. Thus, the *NP* of estimating $[\tau_\Delta - \tau_\Delta|_{track}]$ given x_1 and x_2 may well characterize the GPS correlation error performance.

The time delay estimate in GPS is found by comparing the received signal to an internally generated signal; this same approach can be fit into the *NP* theory derived in Chapter 4. In doing this, GPS correlation error performance bounds may be described through the scalar-case *NP* found in Equation (4.27), and repeated here as

$$NP(\mathbf{x}) = I(\hat{\tau}_e) \tag{4.27}$$

where

$$\mathbf{x} = \begin{bmatrix} x_1 \\ x_2 \end{bmatrix} \tag{5.41}$$

is composed of the received signal, x_1, and the internally generated signal, x_2, and $\hat{\tau}_e$ is an unbiased estimate of

$$\tau_e \triangleq \tau_\Delta - \tau_\Delta|_{track} \tag{5.42}$$

Let x_1 and x_2 be modeled through Equations (5.39) and (5.40) with the following known power spectral densities: $G_{ss}(f)$ as given by Equation (5.37), $G_{n_b n_b}(f) \triangleq$

$G_{nn}(f)$ as given by Equation (5.38), and $G_{n_r n_r}(f) = 0$. Now, the *NP* is given through Equation (5.13) as

$$NP(\mathbf{x}) = T\int_{-\infty}^{+\infty}(2\pi f)^2 \frac{G_{ss}(f)^2}{G_{ss}(f)\left[G_{nn}(f)\right]}df \tag{5.43}$$

$$= T\int_{-\infty}^{+\infty}(2\pi f)^2 \frac{G_{ss}(f)}{G_{nn}(f)}df \tag{5.44}$$

where T, the finite-timelength observation duration, may be equated to the process integration time for a GPS correlator [60]. Consistent with the derivation of Equation (5.13), Equation (5.44) also assumes $G_{nn}(f) \neq 0$ is satisfied. This condition is satisfied if noise is present at all frequencies *over which the integral is taken*. The remainder of this subsection uses $G_{ss}(f)$ and $G_{nn}(f)$ to solve for an explicit expression for GPS *NP*.

5.3.2.2 Explicit Expression for GPS NP. The bandlimited power spectral densities given in Equations (5.37) and (5.38) may be used in Equation (5.44) to solve for an explicit expression for GPS *NP*. In the bandlimited case, the limits of integration in Equation (5.44) become

$$NP(\mathbf{x}) = T\left[\int_{-f_o-\frac{B}{2}}^{-f_o+\frac{B}{2}}(2\pi f)^2 \frac{G_{ss}(f)}{G_{nn}(f)}df + \int_{f_o-\frac{B}{2}}^{f_o+\frac{B}{2}}(2\pi f)^2 \frac{G_{ss}(f)}{G_{nn}(f)}df\right] \tag{5.45}$$

Since $G_{nn}(f) = \frac{N_o}{2} \triangleq G_{nn}$ is independent of f, Equation (5.45) may be written as

$$NP(\mathbf{x}) = \frac{T}{G_{nn}}\left[\int_{-f_o-\frac{B}{2}}^{-f_o+\frac{B}{2}}(2\pi f)^2 G_{ss}(f)\,df + \int_{f_o-\frac{B}{2}}^{f_o+\frac{B}{2}}(2\pi f)^2 G_{ss}(f)\,df\right] \tag{5.46}$$

Furthermore, since $G_{ss}(f)$ is even symmetric in f, $(2\pi f)^2 G_{ss}(f)$ is also even symmetric in f. Using the identity

$$\int_{-f_o-\frac{B}{2}}^{-f_o+\frac{B}{2}} (2\pi f)^2 G_{ss}(f)\, df = \int_{f_o-\frac{B}{2}}^{f_o+\frac{B}{2}} (2\pi f)^2 G_{ss}(f)\, df \tag{5.47}$$

Equation (5.46) may be rewritten as

$$NP(\mathbf{x}) = \frac{2T}{G_{nn}} \int_{f_o-\frac{B}{2}}^{f_o+\frac{B}{2}} (2\pi f)^2 G_{ss}(f)\, df \tag{5.48}$$

Substituting the bandlimited power spectral densities given in Equations (5.38) and (5.37) into Equation (5.48),

$$NP(\mathbf{x}) = \frac{2T}{\frac{N_o}{2}} \int_{f_o-\frac{B}{2}}^{f_o+\frac{B}{2}} (2\pi f)^2 \left(\frac{P_{ave}T_c}{2}\right) \left\{sinc^2\left[(f-f_o)T_c\right] + sinc^2\left[(f+f_o)T_c\right]\right\} df \tag{5.49}$$

$$NP(\mathbf{x}) = \frac{2P_{ave}T_cT}{N_o} \int_{f_o-\frac{B}{2}}^{f_o+\frac{B}{2}} (2\pi f)^2 \left\{sinc^2\left[(f-f_o)T_c\right] + sinc^2\left[(f+f_o)T_c\right]\right\} df \tag{5.50}$$

Given the f_o and T_c for GPS and the limits of integration in Equation (5.50),

$$sinc^2\left[(f-f_o)T_c\right] \gg sinc^2\left[(f+f_o)T_c\right] \tag{5.51}$$

Thus, Equation (5.50) can be approximated as

$$NP(\mathbf{x}) \approx \frac{2P_{ave}T_cT}{N_o} \int_{f_o-\frac{B}{2}}^{f_o+\frac{B}{2}} (2\pi f)^2 sinc^2\left[(f-f_o)T_c\right] df \tag{5.52}$$

Changing the variable of integration, let $g \triangleq f - f_o$ so that $f = g + f_o$ and $dg = df$.

The limits of integration become

$$f = f_o - \frac{B}{2} \quad \Rightarrow \quad g = -\frac{B}{2} \tag{5.53}$$

$$f = f_o + \frac{B}{2} \quad \Rightarrow \quad g = +\frac{B}{2} \tag{5.54}$$

Now, Equation (5.52) becomes

$$NP(\mathbf{x}) \approx \frac{2P_{ave}T_cT}{N_o} \int_{-\frac{B}{2}}^{+\frac{B}{2}} [2\pi(g + f_o)]^2 \, sinc^2(T_c g)\, dg \tag{5.55}$$

$$\approx \frac{8P_{ave}T_cT}{N_o} \int_{-\frac{B}{2}}^{+\frac{B}{2}} \pi^2 \left(g^2 + 2gf_o + f_o^2\right) sinc^2(T_c g)\, dg \tag{5.56}$$

$$\approx \frac{8P_{ave}T_cT}{N_o} \left(\underbrace{\frac{1}{T_c^2} \int_{-\frac{B}{2}}^{+\frac{B}{2}} sin^2(\pi T_c g)\, dg}_{\mathbb{A}} + \underbrace{+2\pi^2 f_o \int_{-\frac{B}{2}}^{+\frac{B}{2}} g \cdot sinc^2(T_c g)\, dg}_{\mathbb{B}} + \underbrace{+\pi^2 f_o^2 \int_{-\frac{B}{2}}^{+\frac{B}{2}} sinc^2(T_c g)\, dg}_{\mathbb{C}} \right) \tag{5.57}$$

As an aid, three terms in Equation (5.57) are specified as $\mathbb{A}$, $\mathbb{B}$, and $\mathbb{C}$.

First, consider $\mathbb{A}$. Note that $sin^2\alpha = \frac{1-cos(2\alpha)}{2}$, $sin(-\alpha) = -sin(\alpha)$.

$$\mathbb{A} = \frac{1}{T_c^2} \int_{-\frac{B}{2}}^{+\frac{B}{2}} sin^2(\pi T_c g)\, dg = \frac{1}{T_c^2} \int_{-\frac{B}{2}}^{+\frac{B}{2}} \left[\frac{1}{2} - \frac{cos(2\pi T_c g)}{2}\right] dg \tag{5.58}$$

$$= \frac{1}{T_c^2} \left[\frac{B}{2} - \int_{-\frac{B}{2}}^{+\frac{B}{2}} \frac{cos(2\pi T_c g)}{2} dg\right] = \frac{1}{T_c^2} \left[\frac{B}{2} - \frac{1}{4\pi T_c} sin(2\pi T_c g)\Big|_{-\frac{B}{2}}^{+\frac{B}{2}}\right] \tag{5.59}$$

$$= \frac{1}{T_c^2} \left[\frac{B}{2} - \frac{1}{2\pi T_c} sin(\pi T_c B)\right] \tag{5.60}$$

Notice that, if $BT_c = k$, where $k \in Integers$, then $\mathbb{A} = \frac{k}{2T_c^3}$. (This constraint is not made at this point in the development.)

Consider $\mathbb{B}$. Note that $\int_{-\beta}^{+\beta} x \cdot sinc^2(\alpha x)\, dx = 0$, since x is an odd function, $sinc^2(\cdot)$ is an even function, and the limits of integration are equidistant from zero. Thus,

$$\mathbb{B} = 2\pi^2 f_o \int_{-\frac{B}{2}}^{+\frac{B}{2}} g \cdot sinc^2(T_c g)\, dg \tag{5.61}$$

$$= 0 \tag{5.62}$$

Consider $\mathbb{C}$.

$$\mathbb{C} = \pi^2 f_o^2 \int_{-\frac{B}{2}}^{+\frac{B}{2}} sinc^2(T_c g)\, dg = \frac{\pi^2 f_o^2}{T_c} \left[T_c \int_{-\frac{B}{2}}^{+\frac{B}{2}} sinc^2(T_c g)\, dg \right] \tag{5.63}$$

$$= \frac{\pi^2 f_o^2}{T_c} A_{sinc^2}(B) \tag{5.64}$$

where $A_{sinc^2}(B)$ is the area under a $sinc^2(\cdot)$ function defined as

$$A_{sinc^2}(B) \triangleq T_c \int_{-\frac{B}{2}}^{+\frac{B}{2}} sinc^2(T_c x)\, dx \tag{5.65}$$

Furthermore, the dependence upon the bandwidth B is shown explicitly. In general, T_c is fixed for the C/A code of GPS (and given through Equation (5.32)), while B may vary, depending upon the receiver. Given B (or B as a function of T_c), the area can be determined; e.g.,

$$A_{sinc^2}\left(\frac{0.85}{T_c}\right) \approx 0.900 \tag{5.66}$$

$$A_{sinc^2}\left(\frac{1}{T_c}\right) \approx 0.902 \tag{5.67}$$

$$A_{sinc^2}\left(\frac{2}{T_c}\right) \approx 0.949 \tag{5.68}$$

Equation (5.57) can now be written as

$$NP(\mathbf{x}) \approx \frac{8P_{ave}T_cT}{N_o}(\mathbb{A}+\mathbb{B}+\mathbb{C}) \tag{5.69}$$

$$\approx \frac{8P_{ave}T_cT}{N_o}\left(\frac{1}{T_c^2}\left[\frac{B}{2}-\frac{1}{2\pi T_c}sin(\pi T_cB)\right]+\frac{\pi^2 f_o^2}{T_c}A_{sinc^2}(B)\right) \tag{5.70}$$

$$\approx \frac{8P_{ave}T}{N_o}\left[\frac{B}{2T_c}-\frac{1}{2\pi T_c^2}sin(\pi T_cB)+\pi^2 f_o^2 A_{sinc^2}(B)\right] \tag{5.71}$$

Equation (5.71) is the NP for estimating τ_e from a GPS signal (in $\sec^{-2}$). This result, and the procedure used to find it, are novel. In the next subsection, this new result will be analyzed as a design tool.

5.3.3 Analyzing the Theoretical GPS NP

The GPS correlation error performance is given in terms of the NP in Equation (5.71). If the signal-to-noise ratio is assumed to be fixed, the only parameters that an end user may vary are the bandwidth, B, and the process integration time (or observation interval), T. Clearly, $NP(\mathbf{x})$ is linear in T, i.e., $NP(\mathbf{x})$ increases in direct proportion to an increase in the process integration time. A necessary condition for $NP(\mathbf{x})$ to be linear in T is that the time delays are constant over the interval $\left[t_i-\frac{T}{2}, t_i+\frac{T}{2}\right]$. (See page 70.) From a practical standpoint, as T increases, it is more difficult integrate over the period T and more difficult to satisfy the assumption that the time delays are constant over the interval T. Thus, an engineering trade-off of performance versus implementation practicality should be employed when selecting T.

The NP for C/A GPS at L_1 as B varies is shown in Figure 10. This plot was generated using $NP(\mathbf{x})$ given in Equation (5.71) with the following values given in

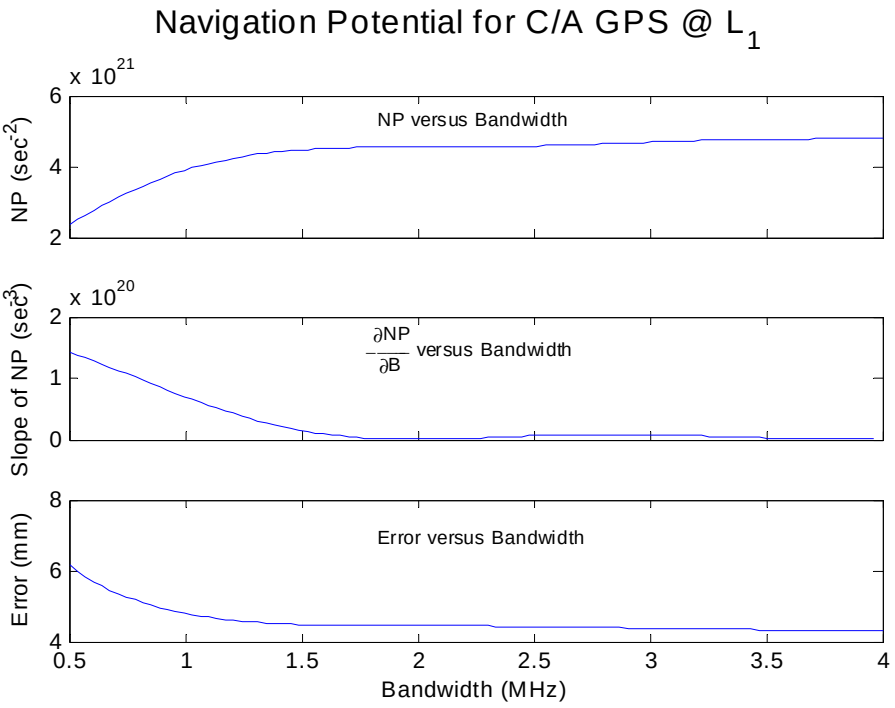

Figure 10. Navigation Potential for C/A GPS @ L_1

Section 5.3.1:

$$P_{ave} = -157 \text{ dB W} \tag{5.72}$$

$$N_o = -201 \frac{\text{dB W}}{\text{Hz}} \tag{5.73}$$

$$T_c = 1.023 \ \mu\text{sec} \tag{5.74}$$

$$f_o = 1575.42 \text{ MHz} \tag{5.75}$$

The process integration time was chosen consistent with typical values as

$$T = 1 \text{ msec} \tag{5.76}$$

The subplots in Figure 10 represent (from top to bottom) the *NP* for GPS, the change in *NP* relative to a change in bandwidth, and the equivalent predicted error in an estimate of τ_e. The error was computed as

$$error \triangleq c\sqrt{\left[NP\left(\mathbf{x}\right)\right]^{-1}} \tag{5.77}$$

where c is the propagation speed of the signal (2.997×10^8 m/sec).

Notice that, for $B \gtrsim 1.7$ MHz, the navigation potential shown in Figure 10 tends to flatten. Thus, choosing $B = 1.7$ MHz would capture much of the navigation potential while freeing resources for other uses or reducing the monetary cost of the receiver over that of a higher bandwidth receiver (assuming monetary cost is proportional to the bandwidth). One caveat to this analysis is that the autocorrelation function is found at *all* time delays. Many practical implementations determine (suboptimally) the autocorrelation at selected time delays (rather than at all time delays) using correlators. It has been demonstrated that, when the autocorrelation

is found for only a selected number of time delays, performance may be substantially improved by using bandwidths much greater than $B = 1.7$ MHz in conjunction with narrowly spaced correlators [60].

Finally, the error shown in Figure 10 represents the theoretically achievable error limits. At $B = 1.7$ MHz, this corresponds to an error of 4.5 mm. If the GPS signal is down-converted for a more practical implementation, the error would increase. (For a particular f_o, Equation (5.71) may be used to determine the $NP(\mathbf{x})$.)

5.3.4 GPS NP Comparison with Other GPS Performance Bounds

While $NP(\mathbf{x})$ given in Equation (5.71) is novel, some analysis exists from which a comparison can be made. Previous work treats the GPS signal in terms of the carrier-only effects and code-only effects. *Carrier-only* analyses neglect the effects of $g(t)$ (i.e., set $g(t) \equiv 1 \ \forall t$) in the GPS signal given by Equation (5.35). *Code-only* analyses neglect the effects of the carrier (i.e., set $f_o \equiv 0$) in the GPS signal given by Equation (5.35).

5.3.4.1 Carrier-Only GPS Correlation Error Performance Bounds.

Spilker [58] found the Cramer Rao Lower Bound (CRLB) of the GPS signal at carrier frequency as

$$(\sigma_\epsilon)^2\big|_{carrier} \approx \frac{1}{SNR}\frac{1}{\Delta\omega^2} \tag{5.78}$$

where $|_{carrier}$ denotes the bound is for the carrier-only portion and $\Delta\omega^2$ is known as the Gabor bandwidth given by [58]

$$\Delta\omega^2 \triangleq \int_{-\infty}^{+\infty} \omega^2 G_{ss}(f)\, df \tag{5.79}$$

While only the effects from the carrier are analyzed, the bandwidth used is as if C/A code were present, i.e.,

$$B = 2.046 \text{ MHz} \tag{5.80}$$

For the bandwidth given in Equation (5.80), the Gabor bandwidth is

$$\Delta\omega^2 = 4\pi^2 f_o^2 \tag{5.81}$$

Therefore, the CRLB for carrier-only GPS is

$$\begin{aligned} \left(\sigma_\epsilon\right)^2\big|_{carrier} &\approx \frac{1}{SNR}\frac{1}{\Delta\omega^2} && (5.82) \\ &\approx \frac{1}{4\pi^2 f_o^2 \cdot SNR} && (5.83) \end{aligned}$$

A similar result can be found using the $NP(\mathbf{x})$ given in Equation (5.71). Rather than re-derive the results with $g(t) \equiv 1 \; \forall t$ in the GPS signal given by Equation (5.35), an equivalent result is to let $T_c \to \infty$ (while maintaining the bandwidth given in Equation (5.80)). Reinserting the definition for $A_{sinc^2}(B)$ in Equation (5.65) into Equation (5.71) while letting $B = 2.046$ MHz and $T_c \to \infty$, the carrier-only NP for GPS is

$$\begin{aligned} NP(\mathbf{x})\big|_{carrier} &= \lim_{T_c\to\infty} \frac{8P_{ave}T}{N_o}\left\{\frac{B}{2T_c} - \frac{1}{2\pi T_c^2} sin\left(\pi T_c B\right) + \right. \\ &\qquad \left. + \pi^2 f_o^2 \left[T_c \int_{-\frac{B}{2}}^{+\frac{B}{2}} sinc^2\left(T_c x\right) dx\right]\right\} \end{aligned} \tag{5.84}$$

The first two terms within the $\{\cdot\}$ go to zero as $T_c \to \infty$, and the factor contributed by $A_{sinc^2}(B)$ goes to unity as $T_c \to \infty$, i.e., (note that B is fixed and finite)

$$\lim_{T_c \to \infty} \frac{B}{2T_c} = 0 \tag{5.85}$$

$$\lim_{T_c \to \infty} \frac{1}{2\pi T_c^2} sin(\pi T_c B) = 0 \tag{5.86}$$

$$\lim_{T_c \to \infty} \left[T_c \int_{-\frac{B}{2}}^{+\frac{B}{2}} sinc^2(T_c x)\, dx \right] = 1 \tag{5.87}$$

Thus, the carrier-only GPS NP is given by

$$NP(\mathbf{x})|_{carrier} = \frac{8P_{ave}T}{N_o}\left(\pi^2 f_o^2\right) \tag{5.88}$$

Using the identity,

$$SNR = \frac{P_{ave}}{\frac{N_o}{2}B_n} \tag{5.89}$$

where B_n is the "equivalent noise bandwidth" approximated as [60]

$$B_n \approx \frac{1}{T} \tag{5.90}$$

it follows that

$$SNR \approx \frac{2P_{ave}T}{N_o} \tag{5.91}$$

Substituting Equation (5.91) into Equation (5.88), the NP for carrier-only GPS may be written as

$$NP(\mathbf{x})|_{carrier} \approx 4\pi^2 f_o^2 \cdot SNR \tag{5.92}$$

Finally, the *NP* is related to the CRLB of any unbiased estimate of $\tau_e|_{carrier}$, denoted by $C_{\hat{\tau}_e}|_{carrier}$, through Equation (4.26):

$$NP\left(\mathbf{x}\right)|_{carrier} \triangleq \left(C_{\hat{\tau}_e}|_{carrier}\right)^{-1} \tag{5.93}$$

Thus, CRLB for carrier-only GPS as computed through *NP* theory is

$$C_{\hat{\tau}_e}|_{carrier} \approx \frac{1}{4\pi^2 f_o^2 \cdot SNR} \tag{5.94}$$

demonstrating that the existing carrier-only bound (given in Equation (5.83)) is a special case of the *NP*.

5.3.4.2 Code-Only GPS Correlation Error Performance Bounds.

Spilker also gives the following performance bound for code-only GPS correlation error performance: [58]

$$\left(\frac{\sigma_\epsilon}{T_c}\right)^2 \approx \frac{N_o B_n}{2P_{ave}} \left(\frac{\delta T}{T_c}\right) \tag{5.95}$$

where the bound is denoted as code-only with $|_{code}$ and a receiver bandwidth, B, given by

$$B \triangleq \frac{2}{T_c} \tag{5.96}$$

is used to derive the result given. Furthermore, the signal's PRBW is modeled as a trapezoidal waveform with the rise time, δT. Practical PRBWs cannot have zero-rise time; a trapezoidal waveform is one method to account for this. The *NP* development modeled practical PRBWs as bandlimited by B. The relationship of rise time to

bandwidth depends upon the definition of each, but a general rule of thumb is [58]

$$\delta T \approx \frac{1}{2B} \tag{5.97}$$

Substituting Equation (5.97) into Equation (5.95) and rearranging terms yields

$$\left(\sigma_\epsilon\right)^2\Big|_{code} \approx \frac{N_o B_n T_c}{4 P_{ave} B} \tag{5.98}$$

NP theory can be constrained to treat code-only GPS which is bandlimited by a specific bandwidth. Code-only effects may be considered by setting $f_o \equiv 0$ in $NP\left(\mathbf{x}\right)$ given in Equation (5.71):

$$NP\left(\mathbf{x}\right)\Big|_{code} \approx \frac{8 P_{ave} T}{N_o}\left[\frac{B}{2T_c} - \frac{1}{2\pi T_c^2} sin\left(\pi T_c B\right)\right] \tag{5.99}$$

Furthermore, using the bandwidth, B, given in Equation (5.96), the sine term in Equation (5.99) becomes

$$sin\left(\pi T_c B\right) = sin\left[\pi T_c\left(\frac{2}{T_c}\right)\right] = 0 \tag{5.100}$$

Therefore, Equation (5.99) may be written as

$$NP\left(\mathbf{x}\right)\Big|_{code} \approx \frac{4 P_{ave} B}{N_o}\frac{T}{T_c} \tag{5.101}$$

Using Equation (5.90), the specific case for code-only GPS is

$$NP\left(\mathbf{x}\right)\Big|_{code} \approx \frac{4 P_{ave} B}{N_o B_n T_c} \tag{5.102}$$

Finally, the *NP* is related to the CRLB through Equation (4.26):

$$NP\left(\mathbf{x}\right)\Big|_{code} \triangleq \left(C_{\hat{\tau}_e}\Big|_{code}\right)^{-1} \tag{5.103}$$

Thus, CRLB for code-only GPS as computed through *NP* theory is

$$C_{\hat{\tau}_e}|_{code} \approx \frac{N_o B_n T_c}{4 P_{ave} B} \tag{5.104}$$

demonstrating that the existing code-only bound (given in Equation (5.98)) is also a special case of the *NP*.

5.3.4.3 NP-Based GPS Correlation Error Performance Bounds.

One distinct advantage in *NP* over other performance bounds is that the relationship of code and carrier performance is more readily available. For this example, using $NP(\mathbf{x})$ given in Equation (5.71) with Equations (5.92) and (5.102) yields

$$NP(\mathbf{x}) \approx NP(\mathbf{x})|_{code} + NP(\mathbf{x})|_{carrier} \tag{5.105}$$

This insight is the result of *NP* theory applied to the specific problem of predicting GPS correlation error performance bounds and cannot be gained through previous performance bounds. (Also, $NP(\mathbf{x})$ given in Equation (5.71) is not limited to specific values for T_c or B.)

Additionally, *NP* is not intrinsically tied to the GPS signal structure. The results from this GPS example may be readily applied to other code-division multiple access (CDMA), spread spectrum signals such as those used in many current cellular phone systems [26].

5.4 Multipath GPS (Gaussian Received Signal)

The navigation potential (*NP*) theory developed in Chapter 4 is not limited to the relatively simplified models in the preceding sections. *NP* theory may also be used to predict Global Positioning System (GPS) correlation error performance

bounds when the received signal contains multipath signals. No performance bound for a correlation process in the presence of multipath is known to exist. This section addresses GPS correlation error performance for the case of the received signal containing multipath signals and being appropriately modeled with a Gaussian received signal. (These assumptions are depicted graphically in Box "B2" of Figure 9.)

First, the GPS signal model with multipath effects is presented. Then, an *NP* expression for this case is found. (Unlike preceding sections, since no comparable bound exists for this problem, a comparison to previous work cannot be made.)

5.4.1 Signal Model

This subsection develops a signal model whereby *NP* theory may be used to predict GPS correlation error performance bounds when the received signal[5] is modeled as a Gaussian stochastic process composed of the transmitted GPS signal, measurement noise, and multipath signals.

The *time-domain* GPS multipath signal is modeled with the received signal, $\mathbf{x}_{mp}(\cdot,\cdot)$, given by

$$\mathbf{x}_{gmp}(\cdot,\cdot) = \begin{bmatrix} x_{gmp_1}(\cdot,\cdot) \\ x_{gmp_2}(\cdot,\cdot) \end{bmatrix} \tag{5.106}$$

where, for all admissible t,

$$\begin{aligned} x_{gmp_1}(t,\cdot) &= s[t-\tau_\Delta(t),\cdot] + n(t,\cdot) \\ &\quad +\alpha(t,\cdot)\, s[t-\tau_\Delta(t)-\delta(t,\cdot),\cdot] \end{aligned} \tag{5.107}$$

$$x_{gmp_2}(t,\cdot) = s[t-\tau_\Delta|_{track}(t),\cdot] \tag{5.108}$$

[5]The GPS signal and noise structures were reviewed in Section 5.3.1, and the justification for using a TDOA-like formulation for GPS was given in Section 5.3.2.

The GPS signal, $s(\cdot,\cdot)$ and the measurement noise, $n(\cdot,\cdot)$, are modeled as independent, zero-mean, ergodic, wide-sense stationary, Gaussian stochastic processes with known power spectral densities, $G_{ss}(f)$ and $G_{nn}(f)$, given in Equations (5.37) and (5.38), respectively. The delay, $\tau_\Delta(\cdot)$, is the delay incurred by the GPS signal to travel from the transmitter to the receiver. The tracking delay, $\tau_\Delta|_{track}(\cdot)$ is varied through the internally generated GPS signal. The desired parameter estimate is

$$\tau_e(\cdot) = \tau_\Delta(\cdot) - \tau_\Delta|_{track}(\cdot) \tag{5.109}$$

A single multipath signal is modeled with an attenuation stochastic process, $\alpha(\cdot,\cdot)$, and delay stochastic process, $\delta(\cdot,\cdot)$. Finally, $\mathbf{x}_{gmp}(\cdot,\cdot)$ is assumed to be appropriately modeled as an ergodic, wide-sense stationary, Gaussian stochastic process.

A *frequency-domain model* may be found, as in Equation (4.125), for all admissible f as

$$\tilde{\mathbf{x}}_{gmp,\Pi}(f,\cdot) = \tilde{s}_\Pi(f,\cdot)\,\mathbb{E}(f)\,\tilde{\boldsymbol{\lambda}}(f,\cdot) + \tilde{\mathbf{n}}_\Pi(f,\cdot) \tag{5.110}$$

where $\tilde{s}_\Pi(\cdot,\cdot)$ is the spectral representation of $s(\cdot,\cdot)$ defined, as in Equation (4.49), for all admissible f as

$$\tilde{s}_\Pi(f,\cdot) \triangleq \mathcal{F}\left\{\frac{1}{T}\prod\left(\frac{t-t_i}{T}\right)s(t,\cdot)\right\} \tag{5.111}$$

and $\tilde{\mathbf{n}}_\Pi(f,\cdot)$ is the spectral representation of $\mathbf{n}(\cdot,\cdot)$ defined, as in Equation (4.50), for all admissible f as

$$\tilde{\mathbf{n}}_\Pi(f,\cdot) \triangleq \begin{bmatrix} \mathcal{F}\left\{\frac{1}{T}\prod\left(\frac{t-t_i}{T}\right)n(t,\cdot)\right\} \\ 0 \end{bmatrix} \tag{5.112}$$

Furthermore, a matrix which contains the "time delays", $\mathbb{E}(f)$, is defined for all admissible f as

$$\mathbb{E}(f) \triangleq \begin{bmatrix} e^{-j2\pi f \tau_{\Delta}(t_i)} & 0 \\ 0 & e^{-j2\pi f \tau_{\Delta}|_{track}(t_i)} \end{bmatrix} \tag{5.113}$$

Finally, the multipath effect matrix, $\tilde{\boldsymbol{\lambda}}(f,\cdot)$, is defined (see also Equation (4.127)) for all admissible f as

$$\tilde{\boldsymbol{\lambda}}(f,\cdot) \triangleq \begin{bmatrix} 1+\alpha(t_i,\cdot)\, e^{-j2\pi f \delta(t_i,\cdot)} \\ 1 \end{bmatrix} \tag{5.114}$$

In this case, the autocorrelation matrix for $\tilde{\boldsymbol{\lambda}}(f,\cdot)$ is (see also Equation (4.136))

$$\tilde{\mathbf{C}}_{\tilde{\lambda}}(f) \triangleq E\left\{\tilde{\boldsymbol{\lambda}}(f,\cdot)\left[\tilde{\boldsymbol{\lambda}}(f,\cdot)\right]^H\right\} \tag{5.115}$$

$$\tag{5.116}$$

$$= \begin{bmatrix} \tilde{C}_{\tilde{\lambda}_{11}}(f) & \tilde{C}_{\tilde{\lambda}_{12}}(f) \\ \tilde{C}_{\tilde{\lambda}_{12}}(f)^* & \tilde{C}_{\tilde{\lambda}_{22}}(f) \end{bmatrix} \tag{5.117}$$

The $1-1$ element of $\tilde{\mathbf{C}}_{\tilde{\lambda}}(f)$ is given by

$$\tilde{C}_{\tilde{\lambda}_{11}}(f) = E\left\{\left[1+\alpha(t_i,\cdot)\, e^{-j2\pi f \delta(t_i,\cdot)}\right]\left[1+\alpha(t_i,\cdot)\, e^{+j2\pi f \delta(t_i,\cdot)}\right]\right\} \tag{5.118}$$

$$= E\left\{1+\alpha(t_i,\cdot)\, e^{-j2\pi f \delta(t_i,\cdot)} + \alpha(t_i,\cdot)\, e^{+j2\pi f \delta(t_i,\cdot)} + \alpha(t_i,\cdot)^2\right\} \tag{5.119}$$

Noting that, for any complex-valued $\tilde{a}$,

$$\tilde{a} + \tilde{a}^* = 2\,\mathrm{Re}\{\tilde{a}\} \tag{5.120}$$

and interchanging $\mathrm{Re}\{\}$ and $E\{\}$,

$$\tilde{C}_{\tilde{\lambda}_{11}}(f) = 1 + 2\,\mathrm{Re}\left\{E\left[\alpha(t_i,\cdot)\, e^{-j2\pi f \delta(t_i,\cdot)}\right]\right\} + E\left[\alpha(t_i,\cdot)^2\right] \tag{5.121}$$

Evaluating the $2-2$ element of $\tilde{\mathbf{C}}_{\tilde{\lambda}}(f)$,

$$\tilde{C}_{\tilde{\lambda}_{22}}(f) = 1 \tag{5.122}$$

Finally, evaluating the $1-2$ element of $\tilde{\mathbf{C}}_{\tilde{\lambda}}(f)$,

$$\begin{aligned} \tilde{C}_{\tilde{\lambda}_{12}}(f) &= E\left\{1+\alpha(t_i,\cdot)\, e^{-j2\pi f\delta(t_i,\cdot)}\right\} && (5.123)\\ &= 1+E\left\{\alpha(t_i,\cdot)\, e^{-j2\pi f\delta(t_i,\cdot)}\right\} && (5.124) \end{aligned}$$

and

$$\begin{aligned} \left|\tilde{C}_{\tilde{\lambda}_{12}}(f)\right|^2 &= 1+2\,\mathrm{Re}\left\{E\left[\alpha(t_i,\cdot)\, e^{-j2\pi f\delta(t_i,\cdot)}\right]\right\}+ \\ &\quad +E\left\{\alpha(t_i,\cdot)\, e^{-j2\pi f\delta(t_i,\cdot)}\right\} E\left\{\alpha(t_i,\cdot)\, e^{-j2\pi f\delta(t_i,\cdot)}\right\}^* \qquad (5.125) \end{aligned}$$

An interesting subclass of problems results when $\alpha(\cdot,\cdot)$ and $\delta(\cdot,\cdot)$ may be assumed independent. One example of this is when the attenuation does not depend upon the additional distance traveled, but is dependent upon the scattering and absorption of the reflecting material. (See the discussion surrounding Table 1 on page 67 for a more complete discussion on the physical interpretation of attenuation and delay processes.)

When $\alpha(\cdot,\cdot)$ and $\delta(\cdot,\cdot)$ may be assumed independent, the multipath effect matrix, $\tilde{\boldsymbol{\lambda}}_I(f,\cdot)$, is denoted with an $_I$ to indicate the independence assumption, and the

autocorrelation matrix for $\tilde{\boldsymbol{\lambda}}_I(f,\cdot)$, is

$$\tilde{\mathbf{C}}_{\tilde{\lambda}_I}(f) \triangleq E\left\{\tilde{\boldsymbol{\lambda}}_I(f,\cdot)\left[\tilde{\boldsymbol{\lambda}}_I(f,\cdot)\right]^H\right\} \tag{5.126}$$

$$= \begin{bmatrix} \tilde{C}_{\tilde{\lambda}_{I,11}}(f) & \tilde{C}_{\tilde{\lambda}_{I,12}}(f) \\ \tilde{C}_{\tilde{\lambda}_{I,12}}(f)^* & \tilde{C}_{\tilde{\lambda}_{I,22}}(f) \end{bmatrix} \tag{5.127}$$

Define the mean, $\mu_{\alpha(\cdot,\cdot)}(\cdot)$, and variance, $\sigma^2_{\alpha(\cdot,\cdot)}(\cdot)$, of $\alpha(\cdot,\cdot)$ for all admissible t as

$$\mu_{\alpha(\cdot,\cdot)}(t) \triangleq E\{\alpha(t,\cdot)\}$$

$$\sigma^2_{\alpha(\cdot,\cdot)}(t) \triangleq E\left\{\left[\alpha(t,\cdot)-\mu_{\alpha(\cdot,\cdot)}(t)\right]^2\right\} \tag{5.128}$$

$$= E\left\{\alpha^2(t,\cdot)\right\} - \mu^2_{\alpha(\cdot,\cdot)}(t) \tag{5.129}$$

Define the mean of $\delta(\cdot,\cdot)$, $\mu_{\delta(\cdot,\cdot)}(\cdot)$, for all admissible t as

$$\mu_{\delta(\cdot,\cdot)}(t) \triangleq E\{\delta(t,\cdot)\}$$

Using Equation (5.121),

$$\tilde{C}_{\tilde{\lambda}_{I,11}}(f) = 1 + 2\,\mathrm{Re}\left\{E\left[\alpha(t_i,\cdot)\,e^{-j2\pi f\delta(t_i,\cdot)}\right]\right\} + E\left[\alpha^2(t_i,\cdot)\right] \tag{5.130}$$

$$= 1 + 2\mu_{\alpha(\cdot,\cdot)}(t_i)\,\mathrm{Re}\left[e^{-j2\pi f\mu_{\delta(\cdot,\cdot)}(t_i)}\right] + \sigma^2_{\alpha(\cdot,\cdot)}(t_i) - \mu^2_{\alpha(\cdot,\cdot)}(t_i) \tag{5.131}$$

$$= 1 + 2\mu_{\alpha(\cdot,\cdot)}(t_i)\cos\left[2\pi f\mu_{\delta(\cdot,\cdot)}(t_i)\right] + \sigma^2_{\alpha(\cdot,\cdot)}(t_i) - \mu^2_{\alpha(\cdot,\cdot)}(t_i) \tag{5.132}$$

Using Equation (5.124),

$$\tilde{C}_{\tilde{\lambda}_{12}}(f) = 1 + E\left\{\alpha(t_i,\cdot)\, e^{-j2\pi f\delta(t_i,\cdot)}\right\} \tag{5.133}$$

$$= 1 + \mu_{\alpha(\cdot,\cdot)}(t_i)\, e^{-j2\pi f\mu_{\delta(\cdot,\cdot)}(t_i)} \tag{5.134}$$

$$= 1 + \mu_{\alpha(\cdot,\cdot)}(t_i)\left\{\cos\left[2\pi f\mu_{\delta(\cdot,\cdot)}(t_i)\right] - j\sin\left[2\pi f\mu_{\delta(\cdot,\cdot)}(t_i)\right]\right\} \tag{5.135}$$

$$= 1 + \mu_{\alpha(\cdot,\cdot)}(t_i)\cos\left[2\pi f\mu_{\delta(\cdot,\cdot)}(t_i)\right] - j\mu_{\alpha(\cdot,\cdot)}(t_i)\sin\left[2\pi f\mu_{\delta(\cdot,\cdot)}(t_i)\right] \tag{5.136}$$

Notice that Equation (5.136) is the form: $\mathrm{Re}\{\}+j\,\mathrm{Im}\{\}$. Rewriting Equation (5.136) in magnitude-phase form,

$$\tilde{C}_{\tilde{\lambda}_{12}}(f) = \mathbb{M}\cdot e^{\left(\tan^{-1}\left\{\frac{\mu_{\alpha(\cdot,\cdot)}(t_i)\sin\left[2\pi f\mu_{\delta(\cdot,\cdot)}(t_i)\right]}{1+\mu_{\alpha(\cdot,\cdot)}(t_i)\cos\left[2\pi f\mu_{\delta(\cdot,\cdot)}(t_i)\right]}\right\}\right)} \tag{5.137}$$

where

$$\mathbb{M} \triangleq \sqrt{\begin{array}{c}\left\{1+\mu_{\alpha(\cdot,\cdot)}(t_i)\cos\left[2\pi f\mu_{\delta(\cdot,\cdot)}(t_i)\right]\right\}^2 \\ +\left\{\mu_{\alpha(\cdot,\cdot)}(t_i)\sin\left[2\pi f\mu_{\delta(\cdot,\cdot)}(t_i)\right]\right\}^2\end{array}} \tag{5.138}$$

Expanding and combining terms, Equation (5.138) becomes

$$\mathbb{M} = \sqrt{\begin{array}{c}1+2\mu_{\alpha(\cdot,\cdot)}(t_i)\cos\left[2\pi f\mu_{\delta(\cdot,\cdot)}(t_i)\right] \\ +\mu_{\alpha(\cdot,\cdot)}(t_i)^2\left\{\begin{array}{c}\cos\left[2\pi f\mu_{\delta(\cdot,\cdot)}(t_i)\right]^2 \\ +\sin\left[2\pi f\mu_{\delta(\cdot,\cdot)}(t_i)\right]^2\end{array}\right\}\end{array}} \tag{5.139}$$

Finally, $\tilde{C}_{\tilde{\lambda}_{12}}(f)$ is expressed as

$$\tilde{C}_{\tilde{\lambda}_{12}}(f) = \left(\sqrt{\begin{array}{c}1+\mu^2_{\alpha(\cdot,\cdot)}(t_i) \\ +2\mu_{\alpha(\cdot,\cdot)}(t_i)\cos\left[2\pi f\mu_{\delta(\cdot,\cdot)}(t_i)\right]\end{array}}\right)\cdot e^{\left(\tan^{-1}\left\{\frac{\mu_{\alpha(\cdot,\cdot)}(t_i)\sin\left[2\pi f\mu_{\delta(\cdot,\cdot)}(t_i)\right]}{1+\mu_{\alpha(\cdot,\cdot)}(t_i)\cos\left[2\pi f\mu_{\delta(\cdot,\cdot)}(t_i)\right]}\right\}\right)} \tag{5.140}$$

From Equation (5.140),

$$\left|\tilde{C}_{\tilde{\lambda}_{12}}(f)\right|^2 = \left\{1 + 2\mu_{\alpha(\cdot,\cdot)}(t_i)\cos\left[2\pi f \mu_{\delta(\cdot,\cdot)}(t_i)\right] + \mu^2_{\alpha(\cdot,\cdot)}(t_i)\right\}^2 \tag{5.141}$$

Now, an *NP*-based model for the GPS signal with multipath, denoted by $\tilde{\mathbf{x}}_{gmp,\Pi}(\cdot,\cdot)$, has been developed. These results will now be used to find the GPS *NP*.

5.4.2 GPS NP

Using the Gaussian received signal modeled with a multipath mapping, the *NP* of $\tilde{\mathbf{x}}_{mp}(\cdot,\cdot)$ is given through Equation (4.179) and repeated here as

$$NP(\tilde{\mathbf{x}}_{gmp,\Pi}) = T\int_{-\infty}^{+\infty} \frac{(2\pi f)^2 G_{ss}(f)^2 \left|\tilde{C}_{\tilde{\lambda}_{12}}(f)\right|^2}{\left(\begin{array}{c} G_{ss}(f)^2\left[C_{\tilde{\lambda}_{11}}(f)C_{\tilde{\lambda}_{22}}(f) - \left|\tilde{C}_{\tilde{\lambda}_{12}}(f)\right|^2\right] \\ +G_{ss}(f)\left[G_{n_1n_1}(f)C_{\tilde{\lambda}_{22}}(f) + G_{n_2n_2}(f)C_{\tilde{\lambda}_{11}}(f)\right] \\ +G_{n_1n_1}(f)G_{n_2n_2}(f)\end{array}\right) df \tag{4.179}$$

The *NP* of a GPS signal under the conditions in the preceding subsection (as represented by Box "B2" of Figure 9) is given by

$$NP(\tilde{\mathbf{x}}_{gmp,\Pi}) = T\int_{-\infty}^{+\infty} \frac{(2\pi f)^2 G_{ss}(f)\left|\tilde{C}_{\tilde{\lambda}_{12}}(f)\right|^2}{\left(\begin{array}{c} G_{ss}(f)\left[C_{\tilde{\lambda}_{11}}(f) - \left|\tilde{C}_{\tilde{\lambda}_{12}}(f)\right|^2\right] \\ +G_{nn}(f)\end{array}\right)} df \tag{5.142}$$

where $G_{ss}(f)$, $G_{nn}(f)$, $C_{\tilde{\lambda}_{11}}(f)$, and $\left|\tilde{C}_{\tilde{\lambda}_{12}}(f)\right|^2$ have all been specified. The only restrictions upon the multipath effects, $\alpha(\cdot,\cdot)$ and $\delta(\cdot,\cdot)$, is that (1) at time t_i, each may be represented as constant over the interval $\left[t_i - \frac{T}{2}, t_i + \frac{T}{2}\right]$, and (2) that the stochastic nature of each permits the received signal to be modeled as a Gaussian

stochastic process. The second constraint may be relaxed if the designer is satisfied with a Gaussian approximation.

Consider imposing the constraint that $\alpha(\cdot,\cdot)$ and $\delta(\cdot,\cdot)$ are independent. Substituting Equations (5.132) and (5.141) into Equation (5.142), the *NP* of $\tilde{\mathbf{x}}_{gmpI,\Pi}(\cdot,\cdot)$ is (where the subscript includes I to denote the independence assumptions)

$$NP\left(\tilde{\mathbf{x}}_{gmpI,\Pi}\right) = T\int_{-\infty}^{+\infty} \frac{(2\pi f)^2 G_{ss}(f)\left\{\begin{array}{c} 1+\mu^2_{\alpha(\cdot,\cdot)}(t_i) \\ +2\mu_{\alpha(\cdot,\cdot)}(t_i)\cos\left[2\pi f \mu_{\delta(\cdot,\cdot)}(t_i)\right]\end{array}\right\}^2}{G_{ss}(f)\,\sigma^2_{\alpha(\cdot,\cdot)}(t_i)+G_{nn}(f)} df \tag{5.143}$$

The *NP* of $\tilde{\mathbf{x}}_{gmpI,\Pi}(\cdot,\cdot)$ given in Equation (5.143) provides much insight into the multipath phenomena. The following list highlights a few observations.

1. For any fixed attenuation mean, $\mu_{\alpha(\cdot,\cdot)}(t)$, an increase in the attenuation variance, $\sigma^2_{\alpha(\cdot,\cdot)}(t)$, decreases the ability to determine the navigation parameters of interest. Intuitively, this makes sense– $\sigma^2_{\alpha(\cdot,\cdot)}(t)$ increases the uncertainty of an estimate of τ_e. For example, in the case that $\sigma^2_{\alpha(\cdot,\cdot)}(t) \equiv 0$ for all t, then the denominator is identical to the denominator for the "no multipath" case given in Equation (5.44) on page 122.

2. The numerator term resulting from $\left|\tilde{C}_{\tilde{\lambda}_{12}}(f)\right|^2$, i.e.,

$$\left\{1+\mu^2_{\alpha(\cdot,\cdot)}(t_i)+2\mu_{\alpha(\cdot,\cdot)}(t_i)\cos\left[2\pi f\mu_{\delta(\cdot,\cdot)}(t_i)\right]\right\}^2 \tag{5.144}$$

   may be interpreted loosely as modeling *multipath interference*. Destructive multipath interference, defined as the condition in which $0 \le \left|\tilde{C}_{\tilde{\lambda}_{12}}(f)\right|^2 < 1$, decreases the *NP* of $\tilde{\mathbf{x}}_{gmpI,\Pi}(\cdot,\cdot)$. Constructive multipath interference, defined

as the condition in which $\left|\tilde{C}_{\tilde{\lambda}_{12}}(f)\right|^2 \geq 1$, *increases* the *NP* of $\tilde{\mathbf{x}}_{gmpI,\Pi}(\cdot,\cdot)$ when $\left|\tilde{C}_{\tilde{\lambda}_{12}}(f)\right|^2 \geq 1$! Thus, $\mu^2_{\alpha(\cdot,\cdot)}(t)$ and $\mu_{\delta(\cdot,\cdot)}(t)$ affect the *NP* of $\tilde{\mathbf{x}}_{gmpI,\Pi}(\cdot,\cdot)$ by characterizing the multipath interference. For example, in the case that $\mu^2_{\alpha(\cdot,\cdot)}(t) \equiv 0$ for all t, then the numerator is identical to the numerator for the "no multipath" case given in Equation (5.44).

3. The variance of the delay has no effect upon the *NP* of $\tilde{\mathbf{x}}_{gmpI,\Pi}(\cdot,\cdot)$.

While a much more extensive analysis regarding the effects of multipath upon the *NP* of $\tilde{\mathbf{x}}_{gmpI,\Pi}(\cdot,\cdot)$ is possible, the emphasis here is to demonstrate the enhanced ability of *NP* theory over any other performance bound — *NP* theory permits a proper treatment of characterizing the ability to determine navigation parameters of interest under a wide range of received signal models.

5.5 Summary

This chapter presented several examples as outlined in Figure 9 on page 109. Signal of opportunity (SOP)-based time difference of arrival (TDOA) navigation was modeled in Equation (5.2), repeated here as

$$\begin{bmatrix} x_b(t,\cdot) \\ x_r(t,\cdot) \end{bmatrix} = \begin{bmatrix} s(t,\cdot) \\ s[t+\delta_{br}(t),\cdot] \end{bmatrix} + \begin{bmatrix} n_b(t,\cdot) \\ n_r(t,\cdot) \end{bmatrix} \tag{5.2}$$

This model represented a Gaussian signal and noise with no multipath. The navigation potential (*NP*) of $\mathbf{x} \triangleq \begin{bmatrix} x_b(\cdot,\cdot) & x_r(\cdot,\cdot) \end{bmatrix}^T$ to estimate $\delta_{br}(\cdot)$ was found in Equation (5.13), repeated here as

$$NP(\mathbf{x}) = T\int_{-\infty}^{+\infty} \frac{(2\pi f)^2 G_{ss}(f)^2}{G_{ss}(f)\left[G_{n_b n_b}(f) + G_{n_r n_r}(f)\right] + G_{n_b n_b}(f) G_{n_r n_r}(f)} df \tag{5.13}$$

Furthermore, *NP* theory was show to be consistent with prior bounds that may be applied to this signal model. These results correspond to Box "A" in Figure 9 on page 109.

NP theory was used to predict GPS correlation error performance bounds. It was justified that, although there is only one receiver in standard GPS techniques, the general nature of *NP* theory permits its application to this case. GPS correlation error performance bounds were predicted without and with multipath effects, in which the received signals for both cases were modeled as Gaussian stochastic processes. Specifically, GPS without multipath was modeled in Equations (5.39) and (5.40), repeated here as

$$x_1(t) = s(t-\tau_\Delta) + n(t) \tag{5.39}$$

$$x_2(t) = s(t-\tau_\Delta|_{track}) \tag{5.40}$$

The *NP* of $\mathbf{x} \triangleq \left[\begin{array}{cc} x_1(\cdot,\cdot) & x_2(\cdot,\cdot) \end{array}\right]^T$ to estimate the tracking error, $[\tau_\Delta - \tau_\Delta|_{track}]$, was found in Equation (5.71), repeated here as

$$NP(\mathbf{x}) \approx \frac{8P_{ave}T}{N_o}\left[\frac{B}{2T_c} - \frac{1}{2\pi T_c^2} sin(\pi T_c B) + \pi^2 f_o^2 A_{sinc^2}(B)\right] \tag{5.71}$$

Other GPS correlation error performance bounds were presented; however, each bound considered only one portion of the GPS signal (either carrier-only or code-only). For example, the *NP* for carrier-only GPS was found in Equation (5.92), repeated here as

$$NP(\mathbf{x})|_{carrier} \approx 4\pi^2 f_o^2 \cdot SNR \tag{5.92}$$

The *NP* for code-only GPS was found in Equation (5.102), repeated here as

$$NP\left(\mathbf{x}\right)\big|_{code} \approx \frac{4P_{ave}B}{N_o B_n T_c} \tag{5.102}$$

NP theory provided *additional insight* into this relationship through Equation (5.105), repeated here as

$$NP\left(\mathbf{x}\right) \approx NP\left(\mathbf{x}\right)\big|_{code} + NP\left(\mathbf{x}\right)\big|_{carrier} \tag{5.105}$$

These results correspond to Box "B1" in Figure 9 on page 109.

Finally, *NP* theory was used to predict GPS correlation error performance bounds when the received signal was modeled as a Gaussian stochastic process which contained multipath effects as given in Equations (5.107) and (5.108), repeated here as

$$x_{gmp_1}\left(t,\cdot\right) = s\left[t-\tau_\Delta\left(t\right),\cdot\right] + \alpha\left(t,\cdot\right)s\left[t-\tau_1\left(t\right)-\delta\left(t,\cdot\right),\cdot\right] + n\left(t,\cdot\right) \tag{5.107}$$

$$x_{gmp_2}\left(t,\cdot\right) = s\left[t-\tau_\Delta\big|_{track}\left(t\right),\cdot\right] \tag{5.108}$$

The *NP* of $\mathbf{x} \triangleq \left[\begin{array}{cc} x_{gmp_1}\left(\cdot,\cdot\right) & x_{gmp_2}\left(\cdot,\cdot\right)\end{array}\right]^T$ to estimate the tracking error

$$\left[\tau_\Delta - \tau_\Delta\big|_{track}\right]$$

was found without constraining the relationships of the multipath effects in Equation (5.142), repeated here as

$$NP\left(\tilde{\mathbf{x}}_{gmp,\Pi}\right) = T\int_{-\infty}^{+\infty} \frac{\left(2\pi f\right)^2 G_{ss}\left(f\right)\left|\tilde{C}_{\tilde{\lambda}_{12}}\left(f\right)\right|^2}{\left(\begin{array}{c} G_{ss}\left(f\right)\left[C_{\tilde{\lambda}_{11}}\left(f\right) - \left|\tilde{C}_{\tilde{\lambda}_{12}}\left(f\right)\right|^2\right] \\ +G_{nn}\left(f\right)\end{array}\right)} df \tag{5.142}$$

A particularly insightful scenario, in which the multipath effects, $\alpha(\cdot,\cdot)$ and $\delta(\cdot,\cdot)$, were considered independent, resulted in the *NP* given in Equation (5.143), repeated here as

$$NP\left(\tilde{\mathbf{x}}_{gmpI,\Pi}\right) = T\int_{-\infty}^{+\infty} \frac{(2\pi f)^2 G_{ss}(f)\left\{\begin{array}{c} 1+\mu^2_{\alpha(\cdot,\cdot)}(t_i) \\ +2\mu_{\alpha(\cdot,\cdot)}(t_i)\cos\left[2\pi f \mu_{\delta(\cdot,\cdot)}(t_i)\right]\end{array}\right\}^2}{G_{ss}(f)\,\sigma_{\alpha(\cdot,\cdot)}(t_i)^2 + G_{nn}(f)} df \tag{5.143}$$

Using this form, *NP* theory revealed insight into the effects of multipath upon the ability to determine the tracking error.

Chapter 6 - Conclusion

6.1 Summary of Results

This research introduced the concept of *navigation potential* (NP) to quantify the ability to estimate parameters of interest from a given received signal. The received signal, $\mathbf{x}(\cdot,\cdot)$, was composed of two signals, each of which was modeled through a mapping parameterized by the transmitted signal, the receiver measurement noise, and the time delay incurred by the transmitted signal to travel to the receiver. This signal model was represented by Equation (4.2), repeated here as

$$\mathbf{x}(\cdot,\cdot) \triangleq \begin{bmatrix} x_1(\cdot,\cdot) \\ x_2(\cdot,\cdot) \end{bmatrix} = \begin{bmatrix} g_1[\cdot,\cdot; s(\cdot,\cdot), n_1(\cdot,\cdot), \tau_1(\cdot)] \\ g_2[\cdot,\cdot; s(\cdot,\cdot), n_2(\cdot,\cdot), \tau_2(\cdot)] \end{bmatrix} \tag{4.2}$$

where $x_i(\cdot,\cdot)$, $s(\cdot,\cdot)$, and $n_i(\cdot,\cdot)$ are scalar, stochastic processes representing the received signal at the i^{th} receiver, the transmitted signal, and the noise at the i^{th} receiver, respectively. Each $\tau_i(\cdot)$ was the time delay incurred by $s(\cdot,\cdot)$ to travel to the i^{th} receiver. The TDOA, $\tau_\Delta(t)$, of the transmitted signal to the first receiver relative to the second receiver was defined in Equation (4.3) and repeated here as

$$\tau_\Delta(t) \triangleq \tau_1(t) - \tau_2(t) \tag{4.3}$$

It was desired to obtain an estimate of the TDOA for use in a navigation scheme. The NP of $\mathbf{x}(\cdot,\cdot)$, denoted by $NP(\mathbf{x})$, was defined as the inverse of the theoretical lower bound on the variance of any unbiased estimator of $\tau_\Delta(t)$. Furthermore, $\tau_\Delta(t)$ may be estimated indirectly through a an estimate of a vector of parameters, or $\boldsymbol{\theta}(t)$, for which there exists some mapping $\mathbf{h}$ such that $\tau_\Delta = \mathbf{h}(\boldsymbol{\theta})$. These developments

resulted in the expression for $NP(\mathbf{x})$ given in Equation (4.25) and repeated here as

$$\boxed{NP(\mathbf{x}) \triangleq \left(\frac{\partial \mathbf{h}(\boldsymbol{\theta})}{\partial \boldsymbol{\theta}} \mathbf{I}^{-1}(\boldsymbol{\theta}) \left[\frac{\partial \mathbf{h}(\boldsymbol{\theta})}{\partial \boldsymbol{\theta}} \right]^T \right)^{-1}} \tag{4.25}$$

where $\mathbf{I}(\boldsymbol{\theta})$ is the Fisher Information Matrix (FIM) defined element-wise in Equation (4.21) and repeated here as

$$[\mathbf{I}(\boldsymbol{\theta})]_{ij} \triangleq E\left\{ \frac{\partial \ln[f(\mathbf{x};\boldsymbol{\theta})]}{\partial \theta_i} \frac{\partial \ln[f(\mathbf{x};\boldsymbol{\theta})]}{\partial \theta_j} \right\} \tag{4.21}$$

A stochastic mapping was introduced in Equations (4.40) and (4.41) to model the received signal, $\mathbf{x}_{mp}(\cdot,\cdot)$, as the transmitted signal, attenuated and delayed replicas of the transmitted signal, and measurement noise. This is a generalization of previous, related work. Equations (4.40) and (4.41) defined the received signal for all admissible t, repeated here as

$$\begin{aligned} x_{1_{mp}}(t,\cdot) &= s[t-\tau_1(t),\cdot] + n_1(t,\cdot) + \\ &\quad + \sum_{l=1}^{N_1} \alpha_l(t,\cdot)\, s[t-\tau_1(t)-\delta_l(t,\cdot),\cdot] \end{aligned} \tag{4.40}$$

$$\begin{aligned} x_{2_{mp}}(t,\cdot) &= s[t-\tau_2(t),\cdot] + n_2(t,\cdot) + \\ &\quad + \sum_{l=1}^{N_2} \beta_l(t,\cdot)\, s[t-\tau_2(t)-\varepsilon_l(t,\cdot),\cdot] \end{aligned} \tag{4.41}$$

where each $\alpha_l(\cdot,\cdot)$ and $\beta_l(\cdot,\cdot)$ are stochastic processes which represent multipath attenuation, and each $\delta_l(\cdot,\cdot)$ and $\varepsilon_l(\cdot,\cdot)$ are stochastic processes which represent the multipath delay. Using a spectral representation for $\mathbf{x}_{mp}(\cdot,\cdot)$, the $NP(\mathbf{x}_{mp})$ was found in Equation (4.106) in general terms. Furthermore, the NP was found when $\mathbf{x}_{mp}(\cdot,\cdot)$ may be modeled as a Gaussian process, denoted by $\mathbf{x}_{gmp}$. Using a spectral

representation of a finite-timelength observation the $\mathbf{x}_{gmp}(\cdot,\cdot)$, denoted by $\tilde{\mathbf{x}}_{gmp,\Pi}(\cdot,\cdot)$, the $NP(\tilde{\mathbf{x}}_{gmp,\Pi})$ was found in Equation (4.179) and repeated here as

$$NP(\tilde{\mathbf{x}}_{gmp,\Pi}) = T\int_{-\infty}^{+\infty} \frac{(2\pi f)^2 G_{ss}(f)^2 \left|\tilde{C}_{\tilde{\lambda}_{12}}(f)\right|^2}{\left(\begin{array}{c} G_{ss}(f)^2\left[C_{\tilde{\lambda}_{11}}(f)C_{\tilde{\lambda}_{22}}(f) - \left|\tilde{C}_{\tilde{\lambda}_{12}}(f)\right|^2\right] \\ +G_{ss}(f)\left[G_{n_1n_1}(f)C_{\tilde{\lambda}_{22}}(f) + G_{n_2n_2}(f)C_{\tilde{\lambda}_{11}}(f)\right] \\ +G_{n_1n_1}(f)G_{n_2n_2}(f) \end{array}\right)} df \tag{4.179}$$

in which $G_{ss}(f)$, $G_{n_1n_1}(f)$, and $G_{n_2n_2}(f)$ are the power spectral densities of $s(\cdot,\cdot)$, $n_1(\cdot,\cdot)$, and $n_2(\cdot,\cdot)$, respectively. Furthermore, $C_{\tilde{\lambda}_{ij}}(f)$ denotes the i-j component of the autocorrelation matrix of $\tilde{\boldsymbol{\lambda}}(f,\cdot)$, defined in Equation (4.127), and repeated here as

$$\tilde{\boldsymbol{\lambda}}(f,\cdot) \triangleq \left[\begin{array}{c} 1+\sum_{l=1}^{N_1}\alpha_l(t_i,\cdot)\,e^{-j2\pi f\delta_l(t_i,\cdot)} \\ \\ 1+\sum_{l=1}^{N_2}\beta_l(t_i,\cdot)\,e^{-j2\pi f\varepsilon_l(t_i,\cdot)} \end{array}\right] \tag{4.127}$$

Several examples were demonstrated using the *NP* result given in Equation (4.179). Signal of opportunity (SOP)-based time difference of arrival (TDOA) navigation was modeled as a Gaussian signal in Gaussian noise with no multipath. This special case of *NP* was found in Equation (5.13) and repeated here as

$$NP(\mathbf{x}) = T\int_{-\infty}^{+\infty} \frac{(2\pi f)^2 G_{ss}(f)^2}{G_{ss}(f)\left[G_{n_bn_b}(f)+G_{n_rn_r}(f)\right]+G_{n_bn_b}(f)G_{n_rn_r}(f)} df \tag{5.13}$$

in which $G_{n_bn_b}(f)$ and $G_{n_rn_r}(f)$ are the power spectral densities of $n_b(\cdot,\cdot)$, and $n_r(\cdot,\cdot)$, respectively. The results obtained were shown to be consistent with prior metrics that may be applied to this signal model.

NP theory was used to predict the theoretical bounds on GPS correlation error performance. It was justified that, although there is only one receiver in standard GPS techniques, the general nature of *NP* theory accommodates predicting the theoretical bounds on estimating the tracking error, $\left[\tau_e \triangleq \tau_\Delta - \tau_\Delta|_{track}\right]$. GPS without multipath was modelled in Equations (5.39) and (5.40), repeated here as

$$x_1(t) = s(t - \tau_\Delta) + n(t) \tag{6.1}$$

$$x_2(t) = s(t - \tau_\Delta|_{track}) \tag{6.2}$$

The *NP* of a GPS signal without multipath to estimate the tracking error was found in Equation (5.71), repeated here as

$$NP(\mathbf{x}) \approx \frac{8P_{ave}T}{N_o}\left[\frac{B}{2T_c} - \frac{1}{2\pi T_c^2} sin(\pi T_c B) + \pi^2 f_o^2 A_{sinc^2}(B)\right] \tag{5.71}$$

The relationship of *NP* to other GPS correlation error performance bounds was presented. Other bounds considered carrier-only GPS or code-only GPS. For example, the *NP* for carrier-only GPS was found in Equation (5.92), repeated here as

$$NP(\mathbf{x})|_{carrier} \approx 4\pi^2 f_o^2 \cdot SNR \tag{5.92}$$

The *NP* for code-only GPS was found in Equation (5.102), repeated here as

$$NP(\mathbf{x})|_{code} \approx \frac{4P_{ave}B}{N_o B_n T_c} \tag{5.102}$$

In contrast, *NP* theory yields results that are a generalized combination of code and carrier results, providing additional insight into this relationship through Equa-

tion (5.105), repeated here as

$$NP(\mathbf{x}) \approx NP(\mathbf{x})|_{code} + NP(\mathbf{x})|_{carrier} \tag{5.105}$$

Finally, since *NP* is not intrinsically tied to the GPS signal structure, these results may be applied to other code-division multiple access (CDMA), spread spectrum signals such as those used in many current cellular phone systems [26].

NP theory was used to predict GPS correlation error performance bounds when the received signal was modeled as a Gaussian stochastic process which contained multipath effects as given in Equations (5.107) and (5.108), repeated here as

$$\begin{aligned} x_{gmp_1}(t,\cdot) &= s[t-\tau_\Delta(t),\cdot] + n(t,\cdot) \\ &\quad +\alpha(t,\cdot)\, s[t-\tau_1(t)-\delta(t,\cdot),\cdot] \end{aligned} \tag{5.107}$$

$$x_{gmp_2}(t,\cdot) = s[t-\tau_\Delta|_{track}(t),\cdot] \tag{5.108}$$

The *NP* of a GPS signal with multipath to estimate the tracking error was found without constraining the relationships of the multipath effects in Equation (5.142), repeated here as

$$NP(\tilde{\mathbf{x}}_{gmp,\Pi}) = T\int_{-\infty}^{+\infty} \frac{(2\pi f)^2 G_{ss}(f)\left|\tilde{C}_{\tilde{\lambda}_{12}}(f)\right|^2}{\left(\begin{array}{c} G_{ss}(f)\left[C_{\tilde{\lambda}_{11}}(f) - \left|\tilde{C}_{\tilde{\lambda}_{12}}(f)\right|^2\right] \\ +G_{nn}(f) \end{array}\right)} df \tag{5.142}$$

A particularly insightful scenario, in which the multipath effects, $\alpha(\cdot,\cdot)$ and $\delta(\cdot,\cdot)$, were considered independent, resulted in the *NP* given in Equation (5.143), repeated

here as

$$NP\left(\tilde{\mathbf{x}}_{gmpI,\Pi}\right) = T\int_{-\infty}^{+\infty} \frac{\left(2\pi f\right)^2 G_{ss}\left(f\right)\left\{\begin{array}{c} 1+\mu_{\alpha(\cdot,\cdot)}\left(t_i\right)^2 \\ +2\mu_{\alpha(\cdot,\cdot)}\left(t_i\right)\cos\left[2\pi f\mu_{\delta(\cdot,\cdot)}\left(t_i\right)\right]\end{array}\right\}^2}{G_{ss}\left(f\right)\sigma_{\alpha(\cdot,\cdot)}\left(t_i\right)^2 + G_{nn}\left(f\right)} df \tag{5.143}$$

In summary, the contributions of this research can be summarized as follows:

1. Navigation potential (*NP*) theory was developed to characterize the ability to estimate parameters of interest from a given signal. The general approach taken enables *NP* theory to encompass a wide range of problems.

2. *NP* theory was evaluated for a received signal modeled as the transmitted signal, measurement noise, and multipath effects. The expressions found provide performance bounds that were previously unknown.

3. *NP* theory was used to find GPS correlation error performance bounds. When the GPS signal was modeled without multipath, the *NP* solutions provided insight over that which may be found in previous bounds. When the GPS signal was modeled with multipath, the *NP* solutions provided new performance bounds that were previously unknown.

4. A systematic approach to navigating with signal of opportunity (SOP)-based time difference of arrival (TDOA) measurements was developed. *NP* provided a SOP selection criterion, and under restricted conditions, SOP-based TDOA *NP* was shown to be equivalent to previous performance bounds. A SOP-based TDOA navigation algorithm was shown to be similar to that of GPS algorithms.

6.2 Recommendations for Future Research

Navigation potential (*NP*) theory opens many research topics. Some potentially promising areas are given in the sections below.

6.2.1 Demonstration of the Three Step Process

In Chapter 3, a method was developed for SOP-based TDOA navigation that may be applied over a wide range of SOP and uses well-known solution algorithms. This tool may be demonstrated with a previously exploited SOP (such as AM radio or analog TV). One future research effort may be to predict performance via *NP*, form TDOA measurements using the generalized cross-correlation (GCC), and determine the navigation solution using GPS algorithms. Then, performance results may be compared to the predicted theoretical results and results from prior research. Questions to answer may be, "How well does the theoretical *NP* predict the actual performance?"; "How does navigation performance of the systematic navigation approach compare to performance using the prior method specific to that SOP?"; "How does uncertainty in the power spectral densities affect navigation performance and the accuracy of the predicted performance?"

6.2.2 Demonstration of NP as a Selection Tool

Appendix B presents many SOP examples. It would be beneficial for future SOP selection to determine and compare the *NP* for each SOP.

6.2.3 Theoretical NP of Signals Modeled with Multipath Effects

Section 4.3 developed the *NP* for received signals modeled as the transmitted signal with multipath effects and noise. In that development, the probability density

function for $\tilde{\mathbf{x}}_{mp}(f,\cdot)$ was given in Equation (4.102), repeated here as

$$\begin{aligned} f_{\tilde{\mathbf{x}}_{mp}(f,\cdot)}(\boldsymbol{\xi}_x) &= \frac{1}{(2\pi|f|)^2}\int_{\mathbb{R}^5}\frac{1}{(\xi_s)^2}f_{\tilde{\mathrm{s}}_\Pi}(\xi_s)\, f_{\tilde{\mathbf{n}}_\Pi}(\boldsymbol{\xi}_x-\boldsymbol{\xi}_y)\cdot \\ &\quad \frac{1}{\left|\xi_{\alpha_l}\right|}f_{\alpha_l,\delta_l}\left(\xi_{\alpha_l},\frac{1}{-j2\pi f}\ln\left\{\frac{1}{\xi_{\alpha_l}}\left[\frac{\xi_{y_1}}{\xi_s}e^{j2\pi f\tau_1(t_i)}-1\right]\right\}\right)\cdot \\ &\quad \frac{1}{\left|\xi_{\beta_m}\right|}f_{\beta_m,\varepsilon_m}\left(\xi_{\beta_m},\frac{1}{-j2\pi f}\ln\left\{\frac{1}{\xi_{\beta_m}}\left[\frac{\xi_{y_2}}{\xi_s}e^{j2\pi f\tau_2(t_i)}-1\right]\right\}\right)\cdot \\ &\quad d\xi_{\alpha_l}d\xi_{\beta_m}d\xi_s d\boldsymbol{\xi}_y \end{aligned} \tag{4.102}$$

Equation (4.102) expresses $f_{\tilde{\mathbf{x}}_{mp}(f,\cdot)}$ at a given f in terms of the following known probability density functions:

$$f_{\tilde{s}_\Pi(f,\cdot)},\ f_{\tilde{\mathbf{n}}_\Pi(f,\cdot)},\ f_{\alpha_l(t_i,\cdot),\delta_l(t_i,\cdot)},\ f_{\beta_m(t_i,\cdot),\varepsilon_m(t_i,\cdot)}$$

The final step in finding the NP was given in Equation (4.106), repeated here as

$$NP\{\tilde{\mathbf{x}}_{mp,\Pi}(\cdot)\} = -\frac{E\left\{\frac{\partial^2\ln\left[f\left(\tilde{\mathbf{x}}_{mp,\Pi}(\cdot);\tau_1,\tau_2\right)\right]}{(\partial\tau_1)^2}\right\}E\left\{\frac{\partial^2\ln\left[f\left(\tilde{\mathbf{x}}_{mp,\Pi}(\cdot);\tau_1,\tau_2\right)\right]}{(\partial\tau_2)^2}\right\} - E\left\{\frac{\partial^2\ln\left[f\left(\tilde{\mathbf{x}}_{mp,\Pi}(\cdot);\tau_1,\tau_2\right)\right]}{\partial\tau_1\partial\tau_2}\right\}^2}{E\left\{\frac{\partial^2\ln\left[f\left(\tilde{\mathbf{x}}_{mp,\Pi}(\cdot);\tau_1,\tau_2\right)\right]}{(\partial\tau_1)^2}\right\}+E\left\{\frac{\partial^2\ln\left[f\left(\tilde{\mathbf{x}}_{mp,\Pi}(\cdot);\tau_1,\tau_2\right)\right]}{(\partial\tau_2)^2}\right\} +2E\left\{\frac{\partial^2\ln\left[f\left(\tilde{\mathbf{x}}_{mp,\Pi}(\cdot);\tau_1,\tau_2\right)\right]}{\partial\tau_1\partial\tau_2}\right\}} \tag{4.106}$$

This form seems somewhat abstract, because few assumptions were imposed upon the stochastic nature of the multipath effects.

Using this theory, an example which models the stochastic nature of the multipath effects without imposing Gaussian assumptions upon the received signal may provide additional insight into NP that is not found in the Gaussian case. Further-

more, this is the place in the research to continue the development for received signals which cannot be well-modeled as Gaussian (and, for which, higher-than-second-order characteristics are desired). These examples may give insight into better understanding the effects of multipath upon the ability to determine navigation parameters of interest.

6.2.4 The Effects of Autocorrelation Sampling Upon the Theoretical GPS NP

The theoretical performance bounds on GPS correlation error performance were found in Section 5.4 in Chapter 5 for a GPS received signal with no multipath and with a single multipath. (A single multipath could be shown to represent the collective effect of many multipath signals. See the discussion surrounding Equation (4.72) on page 77.)

These *NP* results assumed that the entire autocorrelation function is found. Practical implementations do not exhibit this behavior; rather, a finite number of time delays are found. This is roughly equivalent to using *samples of the autocorrelation function rather than the continuous function itself.* The effects of "autocorrelation samples" should be explored in more detail. When the received signal is sampled at (and the internal signal is generated as samples at) the sampling frequency f_s, a Fast Fourier Transform may be used to find autocorrelation samples at a time-delay spacing of $\frac{1}{f_s}$. The effect this has upon *NP* should be explored in more detail. A more extreme case is that of two or three autocorrelation samples being computed about the best estimate for the tracking delay (as is done with early-late correlators). If an expression for *NP* is found that takes into account autocorrelation samples, then

the performance of techniques such as narrowly spaced correlators could be predicted! Furthermore, there may exist a better correlator (in terms of minimizing the mean-square error of the tracking error estimate) that has not been employed.

6.2.5 Simulating the Theoretical GPS NP

A simulation should be conducted to validate the theoretical GPS *NP* results found in Equations (5.71) and (5.143). A Monte Carlo analysis of correlator error performance could be conducted; however, practical implementations would require sampled signals. Once the effects of autocorrelation sampling upon the theoretical GPS *NP* are characterized, a computer-simulated Monte Carlo analysis could be readily accomplished.

6.2.6 GPS NP with Multipath

NP theory was used in Section 5.4 to predict GPS correlation error performance bounds for the case in which the received signal contains multipath effects. The *NP* was found in Equation (5.143), repeated here as

$$NP\left(\tilde{\mathbf{x}}_{gmpI,\Pi}\right) = T\int_{-\infty}^{+\infty} \frac{\left(2\pi f\right)^2 G_{ss}\left(f\right)\left\{\begin{array}{c} 1+\mu^2_{\alpha(\cdot,\cdot)}\left(t_i\right) \\ +2\mu_{\alpha(\cdot,\cdot)}\left(t_i\right)\cos\left[2\pi f\mu_{\delta(\cdot,\cdot)}\left(t_i\right)\right]\end{array}\right\}^2}{G_{ss}\left(f\right)\sigma^2_{\alpha(\cdot,\cdot)}\left(t_i\right)+G_{nn}\left(f\right)}df \tag{5.143}$$

This example was used in this research to demonstrate that the foundations of *NP* theory provide the theoretical basis for new results in many areas. As such, a complete evaluation of Equation (5.143) was not performed in this research.

Additional insight into GPS correlation error performance bounds when multipath is present may be found through further exploitation of Equation (5.143). For

example, one might consider varying $\mu_{\alpha(\cdot,\cdot)}(t)$, $\sigma^2_{\alpha(\cdot,\cdot)}(t)$, and $\mu_{\delta(\cdot,\cdot)}(t)$ over a range of "typical" values to determine more precisely their effect upon the GPS *NP*.

6.2.7 NP Theory Extended to Non-Stationary Processes

Throughout this analysis, wide-sense stationary processes have been assumed. The only attenuation and delay effects that can be considered while maintaining stationarity are those which can be considered constant over the finite-timelength observation interval. As discussed in Section D.3 in Appendix D, this assumption permits "in the mean-square sense" concepts (such as stochastic continuity, the stochastic derivative, and the stochastic integral) to be formally defined.

The *general orthogonal expansion* avoids these expressions while maintaining rigor, resulting in a generalization of the Fourier Stieltjes transform to include processes for which stationarity is not assumed [6]. Thus, a theoretical development for *NP* using this approach would encompass a wider range of mappings than does the approach taken in this research. One obvious mapping that the extended *NP* theory would accommodate is a mapping that models time-varying (over the observation interval) attenuation and delay effects.

Using Theorem 6 on page 196,

$$f_{\gamma_{1_l}(t_i,\cdot)}\left(\xi_{\gamma_{1_l}}\right) = \int_{-\infty}^{+\infty} \frac{1}{\left|\xi_{\alpha_l}\right|} f_{\alpha_l(t_i,\cdot),\delta_{e_l}(t_i,\cdot)}\left(\xi_{\alpha_l}, \frac{\xi_{\gamma_l}}{\xi_{\alpha_l}}\right) d\xi_{\alpha_l} \tag{4.71}$$

Furthermore, all $\gamma_{1_l}(t_i,\cdot)$'s are mutually independent (since $\alpha_l(t_i,\cdot)$ and $\delta_l(t_i,\cdot)$ are independent of all $\alpha_m(t_i,\cdot)$ and $\delta_m(t_i,\cdot)$, $m \neq l$). Using Theorem 5, the probability density function of

$$\gamma_{1_\Sigma}(t_i,\cdot) \triangleq \sum_{l=1}^{N_1} \gamma_{1_l}(t_i,\cdot) \tag{4.72}$$

is the successive convolution of N_1 probability density functions. Omitting the arguments of each $\gamma_{1_l}(t_i,\cdot)$, the convolution result for two terms is

$$f_{\gamma_{1_1}+\gamma_{1_2}}\left(\xi_{\gamma_{1_{12}}}\right) = \int_{-\infty}^{+\infty} f_{\gamma_{1_1}}\left(\xi_{\gamma_{1_{12}}} - \xi_{\gamma_{1_2}}\right) f_{\gamma_{1_2}}\left(\xi_{\gamma_{1_2}}\right) d\xi_{\gamma_{1_2}} \tag{4.73}$$

Continuing with an additional term,

$$\begin{aligned} f_{\gamma_{1_1}+\gamma_{1_2}+\gamma_{1_3}}\left(\xi_{\gamma_{1_{123}}}\right) &= \int_{-\infty}^{+\infty} f_{\gamma_{1_1}+\gamma_{1_2}}\left(\xi_{\gamma_{1_{123}}} - \xi_{\gamma_{1_3}}\right) f_{\gamma_{1_3}}\left(\xi_{\gamma_{1_3}}\right) d\xi_{\gamma_{1_3}} && (4.74) \\ &= \int_{-\infty}^{+\infty} \left[\int_{-\infty}^{+\infty} f_{\gamma_{1_1}}\left(\xi_{\gamma_{1_{123}}} - \xi_{\gamma_{1_2}} - \xi_{\gamma_{1_3}}\right) \cdot \right. \\ &\quad \left. f_{\gamma_{1_2}}\left(\xi_{\gamma_{1_2}}\right) d\xi_{\gamma_{1_2}}\right] f_{\gamma_{1_3}}\left(\xi_{\gamma_{1_3}}\right) d\xi_{\gamma_{1_3}} && (4.75) \\ &= \int_{-\infty}^{+\infty} \int_{-\infty}^{+\infty} f_{\gamma_{1_1}}\left(\xi_{\gamma_{1_{123}}} - \xi_{\gamma_{1_2}} - \xi_{\gamma_{1_3}}\right) \cdot \\ &\quad f_{\gamma_{1_2}}\left(\xi_{\gamma_{1_2}}\right) f_{\gamma_{1_3}}\left(\xi_{\gamma_{1_3}}\right) d\xi_{\gamma_{1_2}} d\xi_{\gamma_{1_3}} && (4.76) \end{aligned}$$

and so on until

$$\begin{aligned} f_{\gamma_{1_\Sigma}(t_i,\cdot)}\left(\xi_{\gamma_{1_\Sigma}}\right) &= \int_{-\infty}^{+\infty} \int_{-\infty}^{+\infty} \cdots \int_{-\infty}^{+\infty} f_{\gamma_{1_1}}\left(\xi_{\gamma_{1_\Sigma}} - \xi_{\gamma_{1_2}} - \xi_{\gamma_{1_3}} \cdots - \xi_{\gamma_{1_{N_1}}}\right) \cdot \\ &\quad f_{\gamma_{1_2}}\left(\xi_{\gamma_{1_2}}\right) f_{\gamma_{1_3}}\left(\xi_{\gamma_{1_3}}\right) \cdots f_{\gamma_{1_{N_1}}}\left(\xi_{\gamma_{1_{N_1}}}\right) d\xi_{\gamma_{1_2}} d\xi_{\gamma_{1_3}} \cdots d\xi_{\gamma_{1_{N_1}}} \end{aligned} \tag{4.77}$$

APPENDIX A - Analog Modulation Review

A.1 Introduction

This appendix reviews common analog modulation techniques that are used in signals of opportunity. The modulation definitions described are often stated by authors without explicitly stating the analytical representation of the modulation. Hence, this appendix serves as a quick reference in interpreting common analog modulation terms.

In radio frequency (RF) communications, the modulated, transmitted carrier, $s(t)$, is of the form

$$s(t) = A[g(t), t] \cos\{\theta[g(t), t]\} \tag{A.1}$$

where $A[g(t), t]$ is the instantaneous amplitude, and $\theta[g(t), t]$ is the instantaneous phase. The information signal, $g(t)$, is a bandlimited signal with the magnitude of its Fourier transform, $|G(f)|$, shown notionally in Figure 11. Equation $(A.1)$ is the most general form; the remaining sections will show how A and θ vary depending upon the modulation scheme. Section A.2 presents *amplitude modulation* (AM),

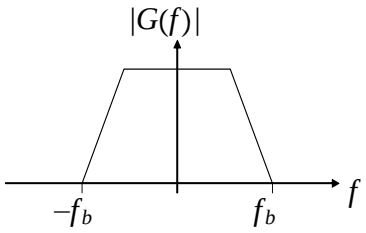

Figure 11. Notional Representation of $|G(f)|$

in which θ is strictly a function of time; Section A.3 presents *frequency modulation* (FM), in which A is strictly a function of time.

A.2 Amplitude Modulation

Amplitude modulation embeds the information in the amplitude of the carrier signal and is the oldest widely-used form of modulation. Through the years, various forms of amplitude modulation have been used. Presented here are: Double Sideband Modulation (DSB) in Section A.2.1, Single Sideband Modulation (SSB) in Section A.2.2, Vestigial Sideband Modulation (VSB) in Section A.2.3, and Double Sideband Full Carrier Amplitude Modulation (AM) in Section A.2.4.

A.2.1 Double Sideband Modulation (DSB)

Double Sideband Modulation (DSB) is a form of AM with a carrier, $c(t)$, given by [31, 55]

$$c(t) \triangleq A_c \cos \omega_c t$$

where A_c is the carrier gain and ω_c is the carrier frequency. In DSB, the information signal, $g(t)$, is considered to have a zero DC component, shown in the time domain in Figure 12(a). When multiplied by the carrier, the DSB signal is given by

$$s_{DSB}(t) = A_c g(t) \cos \omega_c t \tag{A.2}$$

The envelope of $s_{DSB}(t)$, denoted by $g_e(t)$, is shown in Figure 12(b). Recalling $|G(f)|$ shown in Figure 11, the magnitude of the Fourier transform for a DSB signal

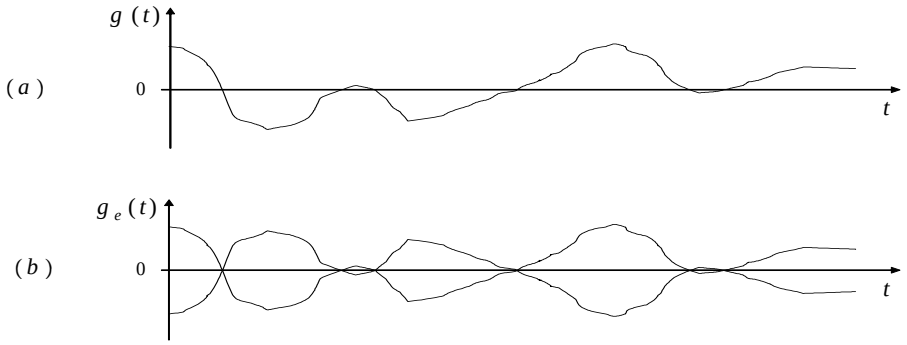

Figure 12. (a) Modulating Signal $g\,(t)$ and (b) Modulation Envelope

is shown in Figure 13 and given as

$$S_{DSB}(f) = \frac{A_c}{2} G(f + f_c) + \frac{A_c}{2} G(f - f_c)$$

where $\omega_c = 2\pi f_c$.

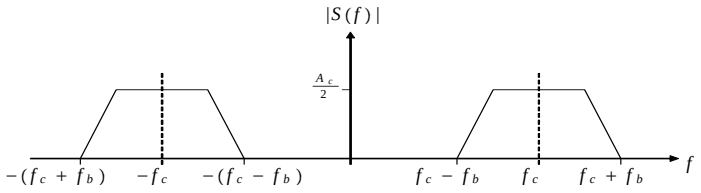

Figure 13. $|S(f)|$ for DSB Modulation

A.2.2 Single Sideband Modulation (SSB)

Since the upper-sideband and lower-side band contain the same information, single sideband modulation (SSB) conserves bandwidth by transmitting exactly one side of the signal. For example, the SSB equivalent for Figure 13 is shown in Figure 14.

A.2.3 Vestigial Sideband Modulation (VSB)

SSB was introduced to conserve bandwidth, but it requires a filter to remove the lower sideband without attenuating or phase shifting the upper sideband. Using real filters in practice, a *vestige* of the lower sideband remains and has led to the name vestigial sideband modulation (VSB) [7]. Figure 15 shows VSB Modulation from a conventional AM scheme. The carrier is passed without attenuation since the spectrum remains unchanged near the carrier frequency. Using VSB from a DSB modulation scheme appears to suppress the carrier, known as Carrier-Suppressed VSB Modulation.

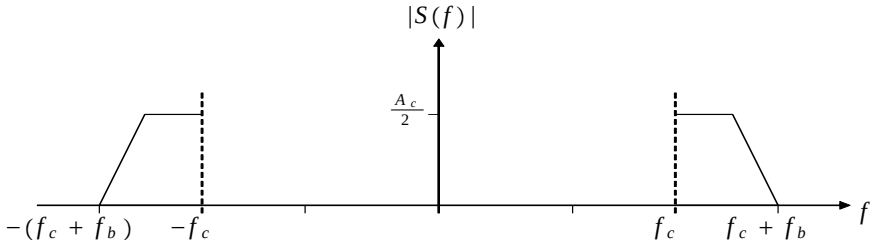

Figure 14. $|S(f)|$ for SSB Modulation

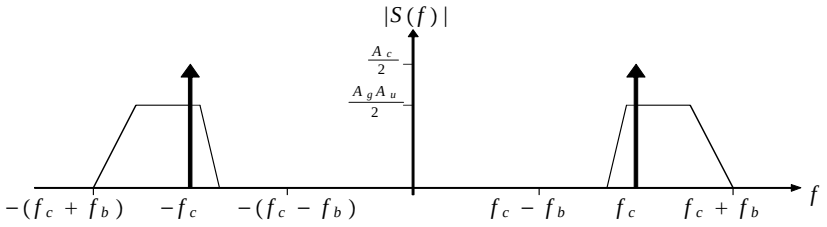

Figure 15. $|S(f)|$ for VSB Modulation

A.2.4 Double Sideband Full Carrier Amplitude Modulation (AM)

In double sideband, full carrier amplitude modulation, commonly called amplitude modulation (AM), a DC component is added to a voltage signal (such as $g(t)$ shown in Figure 12(a)) to elevate the signal above zero [31]. Figure 16 shows the resulting signal in subplot (a) as well as the modulation envelope in subplot (b). Mathematically, given the carrier $c(t) = A_c \cos \omega_c t$, the modulated signal is

$$s_{AM}(t) = A_c g'(t) \cos \omega_c t$$

The modulating signal g' is formed from g by

$$g'(t) = \left(\frac{A_g}{A_c}\right) A_u g(t) + 1$$

where A_u normalizes g to unity, A_g is the modulating signal's peak magnitude, and $+1$ is the DC component used to prevent distortion. The modulation factor, m_{AM}, is defined as

$$m_{AM} \triangleq \frac{A_g}{A_c} \tag{A.3}$$

A_g and A_c must be chosen such that $0 \leq m_{AM} \leq 1$; i.e., A_g must be chosen such that $0 \leq A_g \leq A_c$. Substituting,

$$\begin{aligned} s_{AM}(t) &= A_c \left[\left(\frac{A_g}{A_c}\right) A_u g(t) + 1\right] \cos \omega_c t \\ &= [A_c + A_g A_u g(t)] \cos \omega_c t \end{aligned}$$

Hence, Fourier transform is given in Equation ($A.4$) and shown in Figure 17.

$$S_{AM}(f) = \frac{A_c}{2}\delta(f + f_c) + \frac{A_c}{2}\delta(f - f_c) + \frac{A_g A_u}{2} G(f + f_c) + \frac{A_g A_u}{2} G(f - f_c) \tag{A.4}$$

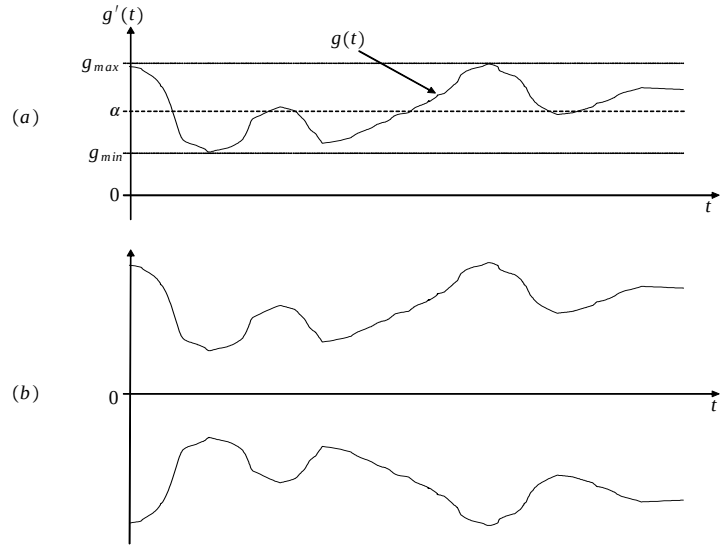

Figure 16. Conventional AM: (a) Modulating Signal and (b) Modulation Envelope

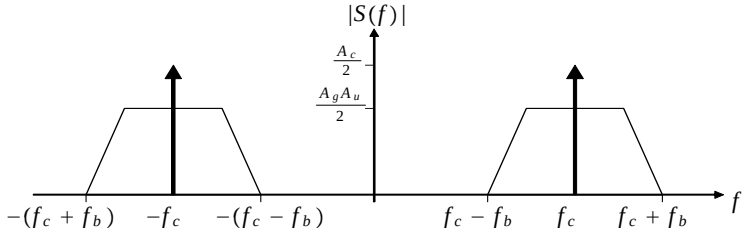

Figure 17. $|S(f)|$ for Conventional Amplitude Modulation

A.3 Frequency Modulation

Frequency modulation embeds the information into the frequency of the waveform rather than the amplitude. The result is reduced transmission noise, since white noise affects the *amplitude*, not the frequency, of the transmitted signal [31]. Section A.3.1 presents frequency modulation (FM), while Section A.3.2 presents phase modulation (PM). Section A.3.3 discusses the sidebands resulting from frequency modulation.

A.3.1 Frequency Modulation (FM)

In frequency modulation (FM), the *instantaneous frequency* of the carrier is varied to embed the information [31]. The carrier, $c(t)$, is defined as

$$c(t) \triangleq A_c \cos(2\pi f_c t + \phi)$$

where A_c is the carrier amplitude, f_c is the carrier frequency, and ϕ is the carrier phase. Frequency modulation is induced by defining the frequency of the transmitted waveform, f_{FM}, as

$$f_{FM} = f_c + (\Delta f)\, g(t) \tag{A.5}$$

where $g(t)$ is the modulating signal and Δf is the *peak frequency deviation*. Following the convention from Equation $(A.1)$ and using the relationship

$$\frac{d\theta_{FM}(g(t), t)}{dt} \triangleq 2\pi f_{FM}$$

Equation $(A.5)$ becomes

$$\frac{d\theta_{FM}(g(t), t)}{dt} = 2\pi f_c + 2\pi(\Delta f)\, g(t) \tag{A.6}$$

where $(\Delta f)\, g(t)$ is called the *frequency deviation*. Integrating Equation $(A.6)$ yields

$$\theta_{FM}(g(t), t) = 2\pi f_c t + 2\pi(\Delta f) \int g(t)\, dt + \theta_0$$

and the final FM signal is

$$s_{FM}(t) = A_c \cos \theta_{FM}(g(t), t) = A_c \cos \left[2\pi f_c t + 2\pi(\Delta f) \int g(t)\, dt + \theta_0 \right] \quad \text{(A.7)}$$

To gain insight into the FM signal, consider the modulating signal, $g(t)$, defined as

$$g(t) \triangleq \cos 2\pi f_g t$$

where f_g is the modulating frequency. Now, Equation $(A.7)$ becomes

$$\begin{aligned} s_{FM}(t) &= A_c \cos \left[2\pi f_c t + 2\pi(\Delta f) \int \cos(2\pi f_g t)\, dt + \theta_0 \right] \\ &= A_c \cos \left[2\pi f_c t + \frac{\Delta f}{f_g} \sin(2\pi f_g t) + \theta_0 \right] \end{aligned} \quad \text{(A.8)}$$

The degree of modulation for FM, m_{FM}, is defined as[6]

$$m_{FM} \triangleq \frac{\Delta f}{f_g} \quad \text{(A.9)}$$

The *amplitude* of the modulating signal determines the frequency deviation, while the *frequency* of the modulating signal, f_g, determines the rate of change of the frequency deviation.

[6]Some authors define the degree of modulation, m, as $m \triangleq \frac{\Delta f}{\max\{\Delta f\}}$, where the numerator is the peak frequency deviation and the denominator can be interpreted as the maximum peak frequency deviation the system is capable of exhibiting. Since Δf is proportional to the amplitude of the modulating signal, m_{FM} defined in Equation $(A.9)$ is more consistent with the definition of m_{AM} in Equation $(A.3)$.

A.3.2 Phase Modulation (PM)

In phase modulation (PM), information is embedded in the phase of the carrier [31]. Using the carrier $c(t) = A_c \cos(2\pi f_c t + \phi)$ and modulating signal $g(t)$, where the amplitude of $g(t)$ varies within ± 1, the phase modulated signal is

$$s_{PM}(t) = A_c \cos\{2\pi f_c t + [\phi_0 + (\Delta\phi)\, g(t)]\} \tag{A.10}$$

where $\Delta\phi$ is the *peak phase deviation* and $(\Delta\phi)\, g(t)$ is the *phase deviation*. The modulation index for PM, m_{PM}, is defined as[7]

$$m_{PM} \triangleq \Delta\phi \tag{A.11}$$

Notice the modulated signals of FM (Equation $(A.7)$) and PM (Equation $(A.10)$) differ in that the FM signal integrates the input signal prior to modulation. This causes causes PM to be more sensitive than FM to the *frequency* of the modulating signal [31]. Most applications of PM counter this effect by integrating the input signal before applying Equation $(A.10)$.

A.3.3 Sidebands of FM

Unlike AM, analyzing the frequency components of FM is much more tedious. It can be shown [31] that Equation $(A.8)$ is equivalent to

$$\begin{aligned} s_{FM}(t) &= A_c \sin\left(2\pi f_c t + \frac{\Delta f}{f_g} \sin 2\pi f_g t + \theta_0'\right) \\ &= A_c \left(\frac{\Delta f}{f_g}\right) \left\{ \begin{array}{c} J_0\left(\frac{\Delta f}{f_g}\right) \sin\left(2\pi f_c t + \theta_0'\right) \\ +J_n\left(\frac{\Delta f}{f_g}\right) \sin\left[2\pi\left(f_c \pm n f_g\right) t + \theta_0'\right] \end{array} \right\} \quad \text{for} \quad n = 1, 2, \cdots \end{aligned}$$

[7] Some authors define the degree of modulation, m, as $m \triangleq \frac{\Delta\phi}{\max\{\Delta\phi\}}$, where the numerator is the peak phase deviation and the denominator can be interpreted as the maximum peak phase deviation the system is capable of exhibiting. Since $\Delta\phi$ is proportional to the amplitude of the modulating signal, m_{PM} defined by Equation $(A.11)$ is more consistent with the definition of m_{AM} in Equation $(A.3)$.

where $J_0(\cdot)$ and $J_n(\cdot)$ are Bessel functions of the first kind of zero order and of the n^{th} order, respectively. The sidebands are *located* at all harmonics of the modulating frequency[8] about the carrier, and their *magnitude* may be found as [52]

$$J_n(m_{FM}) = \frac{m_{FM}}{2} n \left[\frac{1}{n!} - \frac{\left(\frac{m_{FM}}{2}\right)^2}{1!\,(n+1)!} + \frac{\left(\frac{m_{FM}}{2}\right)^4}{2!\,(n+2)!} - \frac{\left(\frac{m_{FM}}{2}\right)^6}{3!\,(n+3)!} + \cdots \right] \qquad \text{for } n \geq 1$$

Analysis of the Bessel functions reveals the following about the power distribution of an FM signal:

1. Low/high modulating frequencies have closely/widely spaced sidelobes.

2. When no modulation is present ($m_{FM} = 0$), all the sidebands are equal to zero.

3. As the frequency modulation is increased, power is shifted away from the carrier towards the sidebands.

4. Power is contained in *all* sidelobes when $m_{FM} \neq 0$ (i.e., the bandwidth is infinite); however, the power in the n^{th} sidelobe reduces as n increases. Thus, the actual FM signal transmitted must be bandlimited by filtering sidelobes beyond an allowable bandwidth prior to transmission.

The effects of $m_{FM} \triangleq \frac{\Delta f}{f_g}$ and f_g on the power distribution of an FM signal are shown in Figure 18. When bandwidth depends upon the power spectral density to fall below some value,[9] the bandwidth increases when either m_{FM} or f_g increases.

---

[8]When more than one modulating frequency is present, the sidebands occur at all sum and difference combinations of the frequencies [31].

[9]For example, one such definition is the 3 dB bandwidth, or half-power bandwidth. The 3 dB bandwidth of a signal is the interval between frequencies at which the signal's power spectral density is lower than one-half the power spectral density peak [70].

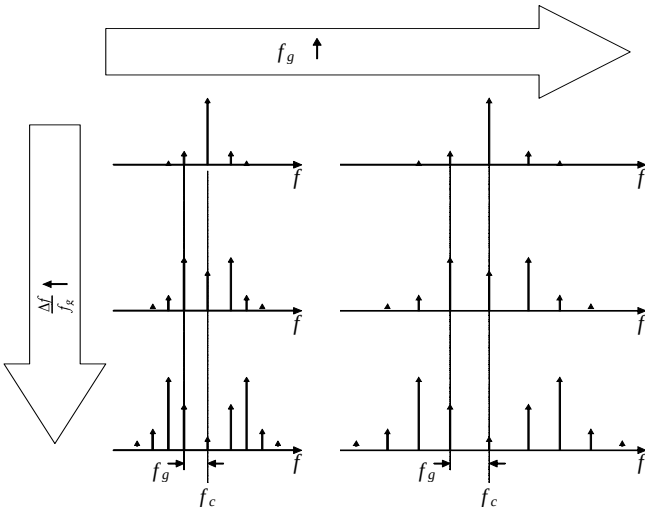

Figure 18. Effects of $\frac{\Delta f}{f_g}$ and f_g on the Location and Magnitude of FM Sidebands

A.4 Summary

In this appendix, common analog modulation schemes were reviewed to understand signals of opportunity better. Information was embedded in the envelope of the carrier using amplitude modulation and the phase of the carrier using frequency modulation. Various forms of amplitude modulation were presented: double sideband modulation (DSB), single sideband modulation (DSB), vestigial sideband modulation (VSB), and double sideband full carrier amplitude modulation (AM). Two frequency modulation techniques were presented: frequency modulation (FM) and phase modulation (PM).

APPENDIX B - Examples of Signals of Opportunity

Navigation using signals of opportunity (SOP) has been motivated as an alternative to GPS navigation. Furthermore, it has been remarked that many SOP are available; this appendix outlines some specific examples of SOP and is not an exhausitive treatment of available SOP. Since SOP are generally not maintained by the navigation user, knowledge of the signal structure may be difficult to obtain. The Federal Communications Commission (FCC) dictates many signals' structure, power level, bandwidth, coverage area, etc. Signals are selected and compared using these data since it is readily available to most designers. Other SOP may be more suitable for particular applications in areas outside the FCC's control.

This appendix outlines specific examples of SOP by limiting the scope of the SOP considered, followed by a presentation of signals grouped as land-based or space-based. Examples are given within each group with consideration given to the signal's structure, coverage area, frequency content, transmitter movement, and passivity. Specifically, Section B.1 outlines the selection criteria and assumptions used to select the examples. SOP examples are presented in Sections B.2 and B.2 with emphasis on their frequency content, signal structure, and coverage. The presentation order is based upon the transmitter location—land-based SOP in Section B.2 and space-based SOP in Section B.3.

B.1 Selection Criteria and Frequency Allocation

Since SOP are abundant, selection criteria are needed when choosing signals of opportunity. For navigation purposes, one might select signals based upon their navigation potential, discussed in more detail in Chapter 4. The following lists the criteria used to select the examples in this appendix.

1. Coverage Area – Ideally, the coverage area of the signals (or system of signals) should be wide enough to be used in most of the world. For example, a signal that exists only near Dayton, Ohio is not of great interest. While any individual signal (such as the Standard Broadcast signal discussed in Section B.2.1) may exist in a limited area, it should be part of a system that transmits similar signals throughout a large cover area.

2. Frequency Range – Naturally, all of these signals are contained in the radio frequency portion of the spectrum, but depending upon the band, there are advantages and disadvantages for use in navigation. For example, high frequency signals may yield more accurate measurements but require greater bandwidth during sampling and processing. Low frequency signals may provide greater penetration indoors or under water. As such, signals are *not* discriminated based upon the band used.

3. Transmitter Movement – The signals discussed have transmitters that are stationary, slowly moving, or rapidly moving. While signals are not excluded based upon this criteria, the transmitter movement of each signal and its effects upon navigation are discussed when each signal is presented.

4. Passivity – The intent is to use these signals in a passive navigation scheme. All land-based cellular networks are excluded since these signals are inherently *not* passive. ("Eavesdropping" on such signals may be passive navigation; their navigation potential can be predicted using the results of Chapter 4 even though they are not detailed in this appendix.)

5. Demodulation – Demodulation is interpreting the modulation of the signal to determine the information conveyed by the signal. For most signals, the demodulation process required to obtain this information is not available to the public. Therefore, it is assumed that demodulating the signal to obtain the information contained therein will not be employed.

Frequencies are allocated through an international treaty with the International Telecommunication Union (ITU), an organ of the United Nations [51]. According to the ITU, the United States lies in Region Two of the three regions of the world. The Federal Communications Commission (FCC) and the National Telecommunications and Information Administration (NITA) govern the frequency allocation and broadcast specifications for the United States through the *Manual of Regulations and Procedures for Federal Radio Frequency Management* [24]. The descriptions of the signals of opportunity in the remainder of this appendix are based upon the FCC mandates for Region 2. Refer to *Reference Data for Engineers* [51] for descriptions of signals of opportunity in other regions.

B.2 Land-Based Signals

Land-based signals are generally transmitted from stationary towers at a fixed elevation. The position of a *stationary* transmitter can be determined precisely,[10] and navigation schemes can take full advantage of this. Furthermore, with sufficient transmitters, the horizontal position can be resolved well from a geometry standpoint, potentially achieving greater accuracy than GPS [34]. Conversely, altitude resolution may be poor, because the geometry associated with using land-based towers has poor sensitivity in the vertical direction (relative to the horizontal directions). Coverage areas are generally small compared to the space-based systems discussed in Section B.3.

Land-based signals are characterized by higher received power than space-based signals and do not have ionospheric and tropospheric propagation delays. Although there is no Doppler effect due to transmitter movement, frequency instabilities in the transmitter may present new problems.

In this section, Standard Broadcasting (commonly known as "AM Radio Stations"), FM Broadcasting (commonly known as "FM Radio Stations"), Television Broadcasting, and Digital Television Broadcasting are discussed.

B.2.1 Standard Broadcasting

Standard broadcasting [21] uses double sideband full carrier amplitude modulation (AM) described in Section A.2.4. A total of 107 carrier frequencies from 540 to 1600 kHz spaced 10 kHz apart occupy the 535 to 1605 kHz band. Each carrier

[10]Station positions can be found from FCC databases, surveying the site, or using multiple receivers to determine the position.

frequency is required to be maintained within ±2 Hz. No additional bandwidth is reserved between channels for interference protection (called a *guard band*), so the bandwidth is generally considered to be 10 kHz. The information content is voice and music in the 50 Hz to 16 kHz range. Figure 19 shows the frequency content in the AM band.

Channels are classified according to the range of coverage (with the number of stations in parentheses): clear (62), regional (41), and local (> 1000) [51]. *Clear channels* service a wide area and are free of interference on the same and adjacent channels. Guidelines are placed on the station's service area, classified as primary and secondary based upon the field intensity. For example, only one clear station is allowed to operate at night within a 750 mile radius, and its maximum transmit power is 50 kW. *Regional channels* service a populated area and the surrounding rural area and are limited to 5 kW. *Local channels* service a city or town and the surrounding rural area and are limited to 1 kW and 250 W during the day and night, respectively.

One limitation of AM broadcasts is that only one channel can be transmitted at a time; thus, stereo effects cannot be achieved. Three methods have been proposed to add stereo (two channels, left and right, denoted by L and R, respectively) to the standard AM broadcast system:

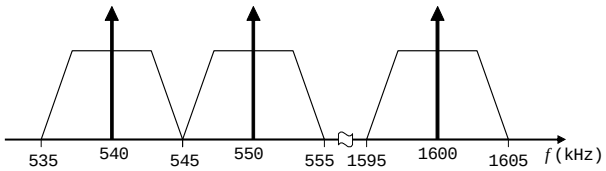

Figure 19. Standard Broadcast Signal Structure

1. Mixed Mode – The carrier is AM with the $(L + R)$ signal and PM/FM with the $(L - R)$ signal.

2. Independent Sideband (Kahn System) – The upper and lower sidebands of the carrier are AM with the L and R signals, respectively.

3. Quadrature (Motorola System) – Two phase-locked carriers are AM and combined at a fixed angle.

A "marketplace approach" has been employed by the FCC, and the Motorola System has been the most widely accepted [51]. Frequncy modulation broadcasting, discussed next, overcomes this limitation as well as reproducing the sound at a higher fidelity and with less noise than AM.

B.2.2 Frequency Modulation Broadcasting

Frequency modulation broadcasting [22] allows for the transmission of voice or music in two channels—left (L) and right (R). FM has improved noise rejection over AM because the information is embedded in the frequency of the carrier, not the amplitude [31]. The FM broadcast uses double sideband suppressed carrier amplitude modulation (AM) described in Section A.2.1 to transmit the $(L - R)$ difference signal and frequency modulation described in Section A.3 to transmit the $(L + R)$ composite signal. Each channel can be reconstructed individually at the receiver, thereby permitting two channels of information.

A total of 101 carrier frequencies from 87.9 to 107.9 MHz spaced 200 kHz apart to occupy the 87.8 to 108 MHz band, denoted Channel 200 through Channel 300. Each carrier frequency is required to be maintained within ± 2 kHz. The maxi-

mum frequency deviation is ±75 kHz; hence, the signal bandwidth is 150 kHz. The allotted channels are 200 kHz, providing 25 kHz guard bands at the upper and lower extremes. Channels 200 (87.9 MHz) through 220 (91.9 MHz) are reserved for noncommercial/educational broadcasts, while channels 221 (92.1 MHz) through 300 (107.9 MHz) are available to commercial and noncommercial/educational broadcasts. Channel 200 (87.9 MHz) is reserved for Class D stations (discussed next) in areas not served by a television broadcast operating on Channel 6 (discussed in Section B.2.3). [51]

Stations are classified into Class A, B, C, or D based upon antenna height and transmitted power. Class A stations service a small city or town and are limited to 3 kW. Class B and C stations serve populated areas and are limited to a 50 kW transmitter up to 500 feet above the surrounding terrain and a 100 kW transmitter up to 2000 feet above the surrounding terrain, respectively. Exceeding height limitation is allowed with a corresponding power reduction. Class D stations are limited to 10 W transmissions. The FCC permits low power (1 W east and 10 W west of the Mississippi River) repeaters to receive a station's broadcast and retransmit (without enhancement) on a different, available channel [51].

Co-channel and adjacent channel interference, population, and land zoning are factors in station operation and separation, but an average separation of 75 miles is maintained. Generally, right-hand circular polarization is used, except Channels 201 (88.1 MHz) through 220 (91.9 MHz) use vertical polarization to minimize interference with a television broadcast operating on Channel 6 (discussed in Section B.2.3).

The frequency spectra of an FM broadcast is shown in Figure 20. At the far left, 0 represents the nominal channel center frequency, and only the upper transmission is shown. Typical modulating signals contain frequencies up to 15 kHz. Thus, the left (L) and right (R) composite signal is FM (see Section A.3) with a bandwidth of 15 kHz residing from 0 to 15 kHz above the channel center frequency. The $(L - R)$ difference signal is double sideband, suppressed carrier (DSBSC) AM with a bandwidth twice the frequency content, or 30 kHz. A carrier with a frequency 38 kHz above the channel center frequency is used, resulting in the DSBSC AM signal to reside from 23 to 53 kHz above the channel center frequency. The lower sideband (LSB) and upper sideband (USB) are shown to emphasize the content of a DSBSC AM signal. A pilot carrier of 19 kHz above the channel center frequency is sent for use in a phase lock loop and for use in demodulating the $(L - R)$ signal. The guard band of 25 kHz is shown from 74 to 99 kHz above the channel center frequency. Finally, an *optional* Subsidiary Communications Authorization (SCA) [23] is shown occupying the upper limits of the channel, including the guard band. This signal is AM and is used to transmit voice or data, related or unrelated to the main transmission.

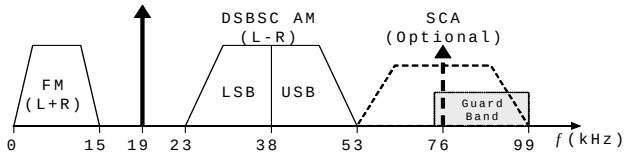

Figure 20. Frequency Modulation Broadcast Signal Structure

B.2.3 Television Broadcasts (TV)

Television broadcasts (TV) [21] provide sound and video service to the general public over the very high frequency (VHF) and ultrahigh frequency (UHF) regions. The VHF/UHF spectrum is broken into 6 MHz, numerically designated, channels as listed in Table 2. Care is taken to separate the transmitter towers to avoid interference based upon effective radiated power, antenna height, and average terrain. Antennas may be directional (with restrictions), typically have horizontal polarization, and are permitted to be right-hand circular polarization. As dictated by the American Television Standard Committee (ATSC), each channel is comprised of a video, audio, and color signal with separate carriers as shown in Figure 21 [51]. The signal components are detailed next.

B.2.3.1 Video Signal The video signal provides the *luminance* of each pixel as well as horizontal and vertical *synchronization* pulses. To understand the information content of the signal, it is important to understand how a television image is refreshed. Television video scanning starts at the upper left of the image (from the viewer's viewpoint) and scans from left to right horizontally across the image. The scanner then returns without scanning to the far left of the screen and is lowered by *twice* the height of one horizontal scan, "skipping" one horizontal

Table 2. TV Channels and Corresponding Frequencies

	Channels	Frequencies (MHz)
VHF	$2-4$	$54-72$
	$5-6$	$76-88$
	$7-13$	$174-216$
UHF	$14-69$	$470-806$

Note: Channels $70-83$ *(*$806-890$ *MHz) are now secondary to land modile applications.*

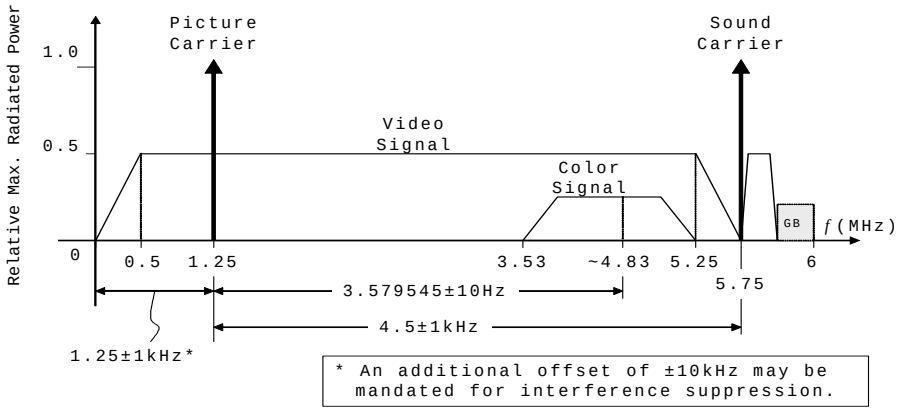

Figure 21. Television Broadcast Signal

line. This scanning process continues to the bottom of the screen, refreshing the odd numbered horizontal lines. The scan then returns near the top of the screen to the horizontal line that was previously "skipped." The scan then continues on these alternate horizontal lines, or even numbered lines, resulting in an interleaved pattern. Each set of alternating lines, called a *field*, is updated at 29.97 Hz. Both fields together, called a *frame*, are updated at 59.94 Hz. Each complete TV screen, or frame, is comprised of 525 horizontal lines updated at 15.734264 kHz. [7, 51, 52] The video signal performs two functions: (1) provides luminance information, and (2) synchronizes the receiver scanner to the source scanner. There are two distinct regions of amplitude to distinguish these tasks. The synchronization pulses have an amplitude within 75 to 100% of the maximum modulation amplitude, while the luminance information amplitude lies from 0 to 75% of the maximum modulation amplitude. This enables the receiver to distinguish the synchronization pulses more readily. [25] During the scan of a line, the amplitude of the signal's modulation corresponds to the luminance (or "brightness") of the image to be reconstructed at that point on the TV screen. The timing of the synchronization pulses synchronizes the horizontal and vertical scan rates of the receiver to the source. Further, to determine the luminance information, the signal's modulation is clipped at 75%, and an amplitude of 75% of the maximum amplitude is considered "black" while 0% of the maximum amplitude is considered "white." Therefore, the synchronization pulses also command no lumination while the scanner returns from right to left after a horizontal line scan or from bottom to top after the completion of a field scan. The

synchronization pulses are band-limited[11] square pulses with well-defined minimum and maximum amplitudes, rise times, and fall times. [25] Just as LORAN uses pulse bursts for navigation (from Section 2.2), the unique sequence of television pulse bursts may also be useful in a navigation scheme. [12]

The frequency content of the video signal is $0 - 4$ MHz, so VSB AM is used (see Section A.2.3) to fit the signal into the allotted space shown in Figure 21. The video signal is centered at 1.25 MHz $\pm$1000 Hz above the lower channel limit, where an additional offset of $\pm$10 kHz may be mandated for interference suppression. Note that the full upper sideband is 4 MHz and the vestige sideband is 750 kHz, each with 500 kHz allotted for trail-off. Due to the horizontal scanning, the video signal's spectra occurs in clusters about the video carrier frequency at each harmonic of the horizontal scanning rate (15.734264 kHz). Although 525 horizontal lines are mandated to be transmitted, approximately 484 lines are used in image reconstruction. Rather than luminance information, the remaining "lines" transmit test signals, control signals, cue signals, text or data transmission such as closed captioning. [7, 25, 51, 52]

B.2.3.2 Color Signal The color signal, which provides the *chrominance* of each pixel, is interleaved between the clusters of the video signal as described previously by selecting a carrier frequency of 3.579545 MHz $\pm$10 Hz above the picture carrier. Chrominance information is separated into in-phase and quadrature components, each of which DSB (suppressed carrier) modulate the color carrier, generating the upper sideband of 500 kHz and a lower sideband of approximately 1.5 MHz as

[11] Part of the video signal, the frequency content of the synchronization pulses must lie within the video signal bandwidth shown in Figure 21.

shown in Figure 21. The in-phase and quadrature color components and the video signal are *added* before transmission. Thus, the magnitude of the signal represents the luminance (or intensity) of the current pixel allowing backwards-compatibility with "black-and-white" receivers, while the instantaneous phase of the signal represents the chrominance (or color) of the current pixel. [7, 52]

B.2.3.3 Audio Signal The audio signal is mandated to have a carrier 4.5 MHz $\pm$1000 Hz above the picture carrier and a maximum bandwidth of 120 kHz. Under the Broadcast Television Sound Committee (BTSC) format, several signals are present as shown in Figure 22. The sound carrier and pilot carrier are transmitted 5.75 MHz and 5.75 MHz +15.75 kHz = 5.76575 MHz above the lower channel limit, respectively. The 15.75 kHz pilot, f_H, is equal to the horizontal scan rate and is used to locate each of the remaining signals within the audio band. The composite of the left (L) and (R) signal is FM (see Section A.3) between $0 \cdot f_H$ and $1 \cdot f_H$, and the $(L - R)$ signal is DSB, suppressed carrier, AM (see Section A.2.1) between $1 \cdot f_H$ and $3 \cdot f_H$. Each is designed to carry up to a 15 kHz signal and enables stereo or mono audio signals corresponding to the video. A separate audio program (SAP) channel is AM about $5 \cdot f_H$, containing related (i.e., similar audio as $(L + R)$ in another language) or unrelated audio up to 12 kHz. A utility audio data channel (PRO channel) with a bandwidth of 3kHz.about $6.5 \cdot f_H$ is designed to carry additional voice or data. [51]

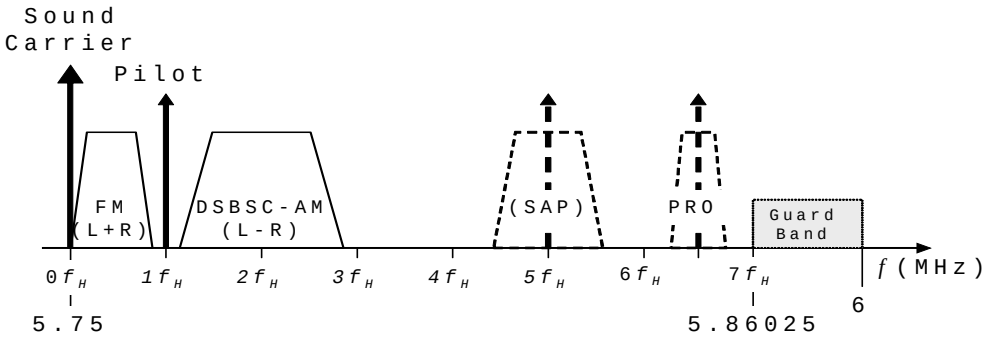

Figure 22. Television Broadcast Audio Signal

B.2.4 Digital Television Broadcasting

Digital Television (DTV) was first introduced in 1998, and by 2001, 1,266 DTV stations received permits from the FCC. According to the FCC, analog TV stations will be phased out, eventually leading to over 1,600 DTV stations. The American Television Standard Committee (ATSC) dictates DTV to use 8-ary VSB (discussed in Section A.2.3) with a symbol rate of $f_{DTV} = 10.762237$ MHz and 2/3 coding.[12] In addition, the carrier is transmitted to aid in coherent demodulation of the signal; and the spectrum (at baseband) is identical to that given in Figure 15 in Section A.2.3. [62]

In analog TV, each screen is comprised of horizontal lines and is refreshed with two interlaced fields. Field 1 contains the odd numbered lines, and field 2 contains the even numbered lines. By varying the amplitude over time, the luminance of each pixel of each line for field 1 and field 2 is transmitted. Various synchronization bursts occur throughout the signal, and the entire screen is refreshed at 60 Hz (and each field at 30 Hz) for black and white.

In DTV, symbols are transmitted (at f_{DTV}) in segments of 832 symbols as shown in Figure 23. As in analog TV, the screen is refreshed with two interlaced fields. The first segment contains field synchronization data, similar to the synchronization bursts at the start of each field in analog TV. The upper right subplot in Figure 23 shows the composition of each field synchronization segment. Subsequently, line data is transmitted as data segments before proceeding to the second field. The lower right subplot in Figure 23 shows the composition of each data segment. The

[12]This means each two-bit data segment is mapped into a three-bit coded data segment for improved error detection or correction. [70]

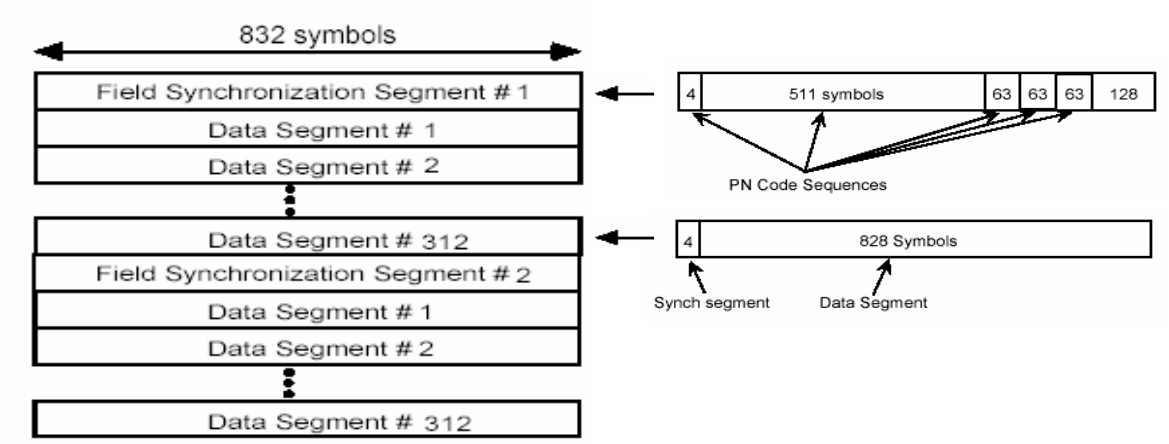

Figure 23. Digital Television (DTV) Frame Structure [62]

synchronization segment, akin to the synchronization bursts at the start of each line in analog TV, are the symbols $\{-1, +1, +1, -1\}$. [62]

B.3 Space-Based Transmitters

Space-based transmitters provide the advantage of global or near-global coverage in many instances. The disadvantage is the transmitters are mobile, so the position must be determined from some other source. This can be done through orbit prediction or ground-network position determination (GPD). In orbit prediction, the orbital parameters as well as the time of transmission are used to estimate the location of the transmitter, while in GPD a network of ground-based receivers at known locations are used to determine the transmitter's location.

The orbit of the transmitter is of critical importance in evaluating its use in position determination; therefore, the remainder of this section discusses satellites based upon the orbital type. Figure 24 shows the relative orbit patterns discussed. *Geostationary* (GEO) satellites lie in the Equatorial plane at an altitude of approximately $35,785$ km above the Earth's surface and provide a 24-hour period and a stationary ground track. The *Molniya* orbit, named after the Russian MOLNIYA series of satellites, orbits the Earth about its poles every 12 hours. The highly elliptical path allows the satellite to hover above the North (or South) pole for approximately 8 hours. Thus, it can be considered as the polar equivalent to a geosynchronous orbit. The remaining non-geosynchronous orbits are Low-earth orbit (LEO), Medium-earth orbit (MEO), and High-earth orbit (HEO), all of which orbit Earth in a non-synchronous

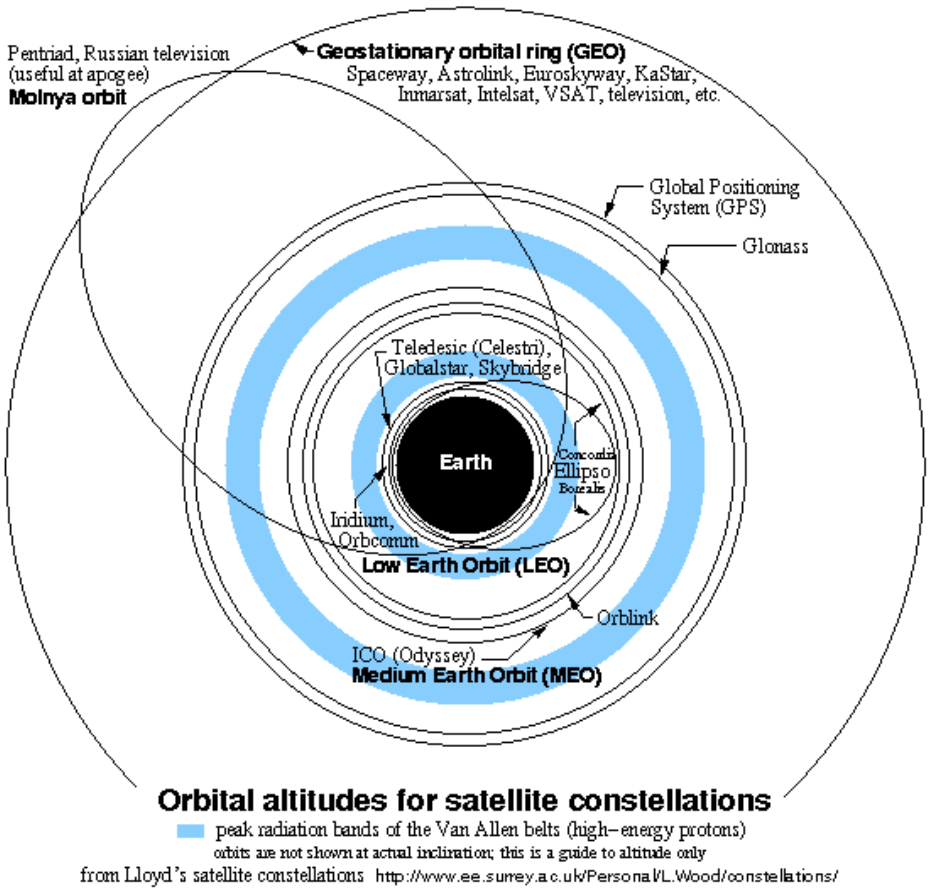

Figure 24. Common Satellite Orbits [29]

manner to provide a more varied ground track than either of the aforementioned orbits.

Remote sensing and observation satellites provide large coverage areas in terms of data collection, but the downlink antennas are focused on a few small ground sites. It may be useful to consider such systems while operating around common ground sites. To take a more general approach, the systems described in this section are primarily communication satellite systems, because the *downlink* provides a large coverage area.

B.3.1 Geostationary (GEO)

Geostationary (GEO) satellites lie overhead the Equator and provide a stationary line-of-sight relative to a fixed point on Earth. The original motivation to place satellites in a GEO orbit was to provide near-global[13] coverage with only 3 satellites. Such coverage is appealling for use in navigation. The position of a GEO satellite relative to a fixed point on Earth is slowly varying due to orbital deviations. The disadvantage in navigating with GEO satellites alone is that the line-of-sight vectors from the user to each satellite may nearly be in the same direction.

The GEO orbit is saturated with satellites. For example, television satellite transponders distribute television networks nationwide (or internationally) using geostationary satellites to receive, amplify, and retransmit the signal. The downlink is $3.7 - 4.2$ GHz, while the uplink is $5.925 - 6.425$ GHz. Frequency-division multiple access (FDMA) and multiple transponders on the same satellite platform provide approximately 100 channels. [51]

[13]Coverage in the polar regions is poor, hence the need for the Russian's Molniya orbit.

B.3.2 Low-Earth Orbit (LEO)

Low-earth orbit (LEO) satellites cost less to deploy than any other orbit; however, more satellites are required for global coverage than any other orbit. LEO constellations have regained interest for "satellite phones", or sat phones, because the mobile unit requires less power to transmit to a LEO satellite than to satellites in higher orbits. Additionally, the relatively low altitude enables short delay times, thereby making near-realtime communication possible [29]. The primary advantage in navigating with LEO satellites is that the solution geometry can be greatly improved over GEO constellations.

Globalstar [30] and Iridium [42] are examples of LEO constellations designed for communications that may also be used for navigation. Their orbits, coverage, data rates, and frequency ranges are discussed next.

B.3.2.1 Globalstar The Globalstar system, developed by Loral Corporation and Qualcomm Inc., provides mobile communications such as voice, data, fax, paging, and position location in areas without terrestrial coverage by allowing a Globalstar mobile unit to transmit to a satellite. The satellite, in turn, downlinks the signal to the nearest terrestrial network to complete the call. Globalstar has 48 satellites (with 4 spares) in 8 LEO orbits at an altitude of 1410 km (orbit period 113.8 minutes) inclined at 52 degrees. [30]

Shown in Figure 25 is Globalstar's coverage, defined as at least four satellites in view to the mobile receiver in addition to a ground site in view to at least one satellite. For comparison, Figure 26 shows the Globalstar system footprint at one

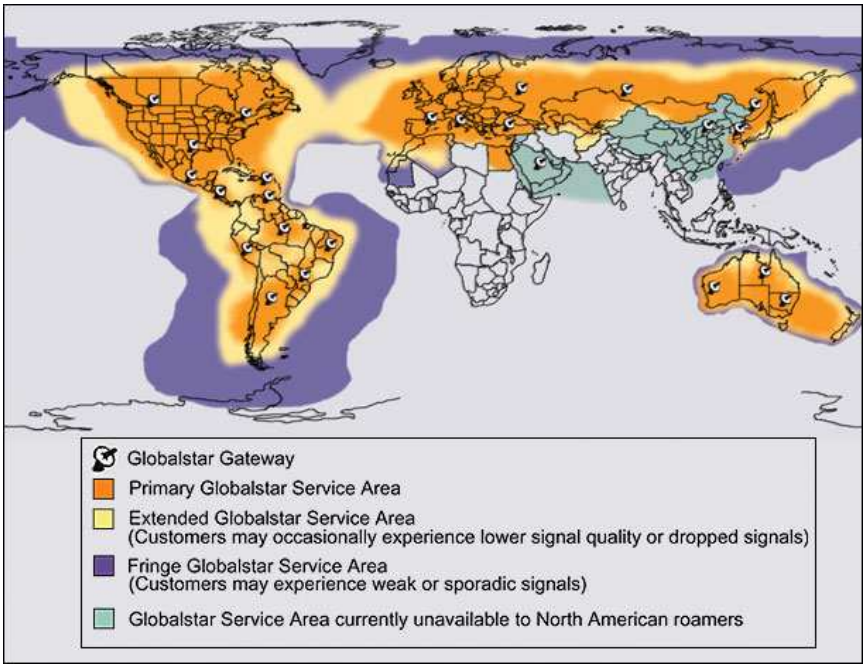

Figure 25. Globalstar Coverage as Reported by Globalstar [30]

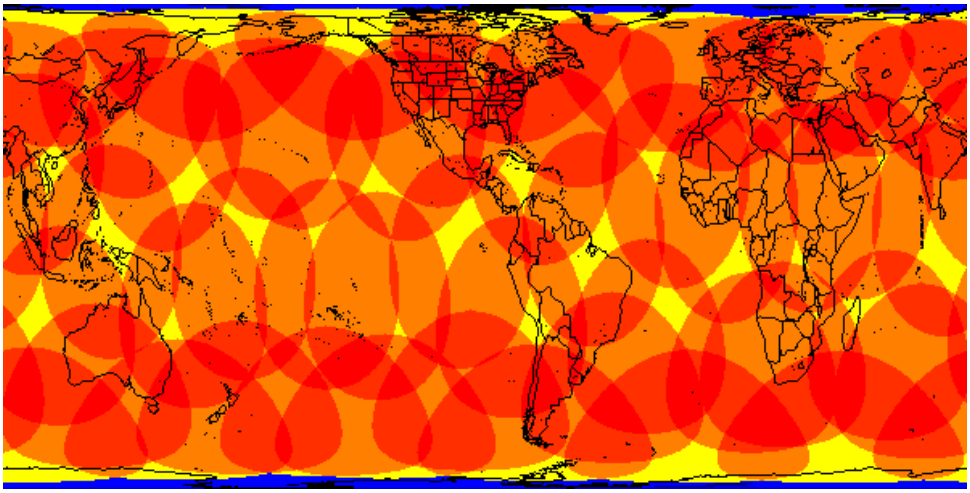

Figure 26. Globalstar Coverage Based Upon [29]

instant in time using Satellite Constellation Visualization. [66]

Globalstar uses code-division multiple access (CDMA) with data rates up to $9,600$ bps, depending on the type of transmission. The system is designed for coverage between $\pm 67^{\circ}$ latitude. The downlink frequencies are $2483.5 - 2500.0$ (MHz), and the uplink frequencies are $1610.0 - 1626.5$ (MHz) [30].

B.3.2.2 Iridium Satellite LLC Iridium Satellite LLC acquired the operating assets of Iridium LLC in December 2000. Based on the GSM cellular standard, Iridium uses time-division multiple access (TDMA) and FDMA techniques with 66 LEO satellites and a ground network connected to the public switched telephone network (PSTN) through gateways to provide world-wide mobile telephone coverage. Since each satellite is connected to its four neighboring satellites through inter-satellite links, the satellite receiving a call need not be in view of a ground station on the ground network. Consequently, fewer satellite footprint overlaps are needed, and land network costs can be reduced by directing the call to the ground station closest to the call destination. The voice and data transmission rates are both 2400 bps. The mobile downlink frequencies are $1610 - 1626.5$ MHz (L-Band), and the mobile uplink frequencies are $1616 - 1626.5$ MHz (L-Band). [42]

B.3.3 Medium-Earth Orbit (MEO)

Medium-earth orbit (MEO) can be considered a compromise between LEO and GEO orbits in regard to cost to orbit (higher than LEO but lower than GEO) and the number of satellites required for global coverage (fewer than LEO but more than GEO). The Doppler shifts (and rates of change) are also a compromise between those

for LEO and GEO orbits, and the navigation solution geometry of MEO constellations is improved over the GEO orbit.

One example of a MEO system that may be of particular interest for navigation is ICO [41]. ICO Global Communications, Uxbridge, England, established in January 1995, is *planning* a family of MEO satellites with a high-bandwidth land network to provide quality voice, wireless Internet and other packet-data services at data rates of up to 144 kbps. ICO's satellite constellation will consist of 10 active MEO satellites at an altitude of $10,390$ km with an orbit period of 361 minutes in two planes inclined at 45 degrees to the equator. Each plane will have five operational satellites plus one spare. ICO's satellites are designed to be transponders between the user equipment and the ground station that is part of the terrestrial infrastructure. The terrestrial infrastructure, rather than satellite-to-satellite communications links, provides the connection to the destination network or end-user. [41]

The intended ICO frequencies are: $1980 - 2010$ MHz (downlink) and $2170 - 2200$ MHz (uplink). TDMA is intended to provide frequency reuse for multiple users. ICO's provision of services will be dependent on a number of regulatory matters, the availability of adequate financing, the successful completion and operation of ICO's technology, and the FCC's approval to re-use ICO's satellite frequencies for terrestrial use. [41]

B.4 Summary

This appendix presented several signals of opportunity (SOP) to provide insight into available SOP. The selection criteria, assumptions, and frequency standards for

considering signals of opportunity were discussed in Section B.1. Land-based SOP were presented in Section B.2; space-based SOP were presented in Section B.3.

APPENDIX C - Probability Density Function Theorems

This appendix provides theorems regarding functions of random variables and the resulting manipulation of the underlying probability density functions (pdf's). Common theorems are cited without proof. Extensions or special cases of existing theorems are provided with justification; however, no claim of originality is made.

For all proofs within this appendix, the following definitions are made:

boldface	$\triangleq$	vector-valued variable
a and b	$\triangleq$	scalar-valued, deterministic
$x(\cdot), y(\cdot)$	$\triangleq$	scalar-valued, random variables with the joint pdf $f_{x,y}(\cdot,\cdot)$
$z(\cdot)$	$\triangleq$	scalar-valued, random variable with the pdf $f_z(\cdot)$
$\mathbf{x}(\cdot), \mathbf{y}(\cdot)$	$\triangleq$	vector-valued, random variables with the joint pdf $f_{\mathbf{x},\mathbf{y}}(\cdot,\cdot)$
$\mathbf{z}(\cdot)$	$\triangleq$	vector-valued, random variable with the pdf $f_{\mathbf{z}}(\cdot)$
$\xi_x, \xi_y, \xi_z, \zeta$	$\triangleq$	scalar-valued "dummy variable", integration variable, or point from an underlying sample space
$\boldsymbol{\xi}_x, \boldsymbol{\xi}_y, \boldsymbol{\xi}_z, \boldsymbol{\zeta}$	$\triangleq$	vector-valued versions of $\xi_x, \xi_y, \xi_z, \zeta$
$\lvert\cdot\rvert$	$\triangleq$	the magnitude of the enclosed scalar quantity
$\lVert\cdot\rVert$	$\triangleq$	the absolute value of the determinate of the enclosed matrix

Note that, for some theorems, additional constraints may be invoked and/or these definitions may be clarified.

Theorem 4 $\quad \mathbf{z} = \boldsymbol{\theta}(\mathbf{x})$

Assume $\boldsymbol{\theta} : \mathbb{R}^n \to \mathbb{R}^n$, $\boldsymbol{\theta}^{-1}$ *exists, and* $\boldsymbol{\theta}$, $\boldsymbol{\theta}^{-1}$ *are continuously differentiable. If* $\mathbf{x}(\cdot)$ *is a random vector with a probability density function* $f_{\mathbf{x}}(\cdot)$ *and* $\mathbf{z}(\cdot) = \boldsymbol{\theta}[\mathbf{x}(\cdot)]$,

then

$$f_{\mathbf{z}}(\boldsymbol{\xi}_z) = f_{\mathbf{x}}\left[\boldsymbol{\theta}^{-1}(\boldsymbol{\xi}_z)\right] \left\| \frac{\partial \boldsymbol{\theta}^{-1}(\boldsymbol{\xi}_z)}{\partial \boldsymbol{\xi}_z} \right\| \tag{C.1}$$

Proof: *See [15].* ■

Theorem 5 $z = x + y$

If $z(\cdot) = x(\cdot) + y(\cdot)$, *then*

$$f_z(\xi_z) = \int_{-\infty}^{+\infty} f_{x,y}(\xi_x, \xi_z - \xi_x)\, d\xi_x \tag{C.2}$$

Proof: *See [15].* ■

Theorem 6 $z = xy$

If $z(\cdot) = x(\cdot)\, y(\cdot)$, *then*

$$f_z(\xi_z) = \int_{-\infty}^{+\infty} \frac{1}{|\xi_x|} f_{x,y}\left(\xi_x, \frac{\xi_z}{\xi_x}\right) d\xi_x \tag{C.3}$$

Proof: *See [15].* ■

Theorem 7 $z = ax + b$

If $z(\cdot) = ax(\cdot) + b$, *then*

$$f_z(\xi_z) = \frac{1}{|a|} f_x\left(\frac{\xi_z - b}{a}\right) \tag{C.4}$$

Proof: *See [15].* ■

Theorem 8 $\mathbf{z} = x\mathbf{y}$ *(Extension to Theorem 6)*

If $\mathbf{z}(\cdot) = x(\cdot)\, \mathbf{y}(\cdot)$, *where*

$$\mathbf{z}(\cdot) \triangleq \begin{bmatrix} z_1(\cdot) \\ z_2(\cdot) \end{bmatrix} \qquad \mathbf{y}(\cdot) = \begin{bmatrix} y_1(\cdot) \\ y_2(\cdot) \end{bmatrix} \tag{C.5}$$

and x, y_1, and y_2 are pairwise independent with known $f_x(\xi_x)$, $f_{y_1}(\xi_{y_1})$, and $f_{y_2}(\xi_{y_2})$, then

$$f_{\mathbf{z}}(\boldsymbol{\zeta}) \triangleq f_{z_1,z_2}(\zeta_1,\zeta_2) = \int_{-\infty}^{+\infty} \frac{1}{(\xi_x)^2} f_x(\xi_x)\, f_{y_1}\left(\frac{\zeta_1}{\xi_x}\right) f_{y_2}\left(\frac{\zeta_2}{\xi_x}\right) d\xi_x \tag{C.6}$$

Proof: *Note the following identity:*

$$f_{\mathbf{z}}(\boldsymbol{\zeta}) = \int_{-\infty}^{+\infty} f_{x,\mathbf{z}}(\xi_x,\boldsymbol{\zeta})\, d\xi_x \tag{C.7}$$

Within the integrand, x takes on values ξ_x, so a change in variables may be accomplished with

$$\mathbf{z}(\cdot) = \theta[\boldsymbol{\gamma}(\cdot)] = \xi_s \boldsymbol{\gamma}(\cdot) \tag{C.8}$$

so that

$$\theta^{-1}[\mathbf{z}(\cdot)] = \frac{1}{\xi_x}\mathbf{z}(\cdot) \tag{C.9}$$

and

$$\left\| \frac{\partial\left[\theta^{-1}(\boldsymbol{\zeta})\right]}{\partial \boldsymbol{\zeta}} \right\| = \left\| \begin{bmatrix} \frac{1}{\xi_x} & 0 \\ 0 & \frac{1}{\xi_x} \end{bmatrix} \right\| = \frac{1}{(\xi_x)^2} \tag{C.10}$$

Then,

$$\begin{aligned} f_{\mathbf{z}}(\boldsymbol{\zeta}) &= \int_{-\infty}^{+\infty} f_{x,\mathbf{z}}(\xi_x,\boldsymbol{\zeta})\, d\xi_x & \text{(C.11)} \\ &= \int_{-\infty}^{+\infty} \frac{1}{(\xi_x)^2} f_{x,\mathbf{y}}\left(\xi_x, \frac{1}{\xi_x}\boldsymbol{\zeta}\right) d\xi_x & \text{(C.12)} \end{aligned}$$

which is the desired result. ■

Theorem 9 $\mathbf{z} = \mathbf{x} + \mathbf{y}$ *(Extension to Theorem 5)*

For the n-dimensional random vectors $\mathbf{z}$, $\mathbf{x}$, *and* $\mathbf{y}$, *let*

$$\mathbf{z}(\cdot) = \mathbf{x}(\cdot) + \mathbf{y}(\cdot) \tag{C.13}$$

and $f_{\mathbf{x},\mathbf{y}}\left(\boldsymbol{\xi}_x, \boldsymbol{\xi}_y\right)$ *be known. Then,*

$$f_{\mathbf{z}}(\boldsymbol{\xi}_z) = \int_{\mathbb{R}^n} f_{\mathbf{x},\mathbf{y}}(\boldsymbol{\xi}_x, \boldsymbol{\xi}_z - \boldsymbol{\xi}_x)\, d\boldsymbol{\xi}_x \tag{C.14}$$

Proof: *To prove this, start with the definition of the distribution function* $F_{\mathbf{z}}(\boldsymbol{\xi}_z)$ *given by*

$$\begin{aligned} F_{\mathbf{z}}(\boldsymbol{\xi}_z) &= P[\mathbf{z} \leq \boldsymbol{\xi}_z] && \text{(C.15)} \\ &= P[\mathbf{x} + \mathbf{y} \leq \boldsymbol{\xi}_z] && \text{(C.16)} \\ &= \int_{\mathbb{R}^n} \int_{\{\boldsymbol{\xi}_y \leq \boldsymbol{\xi}_z - \boldsymbol{\xi}_x\}} f_{\mathbf{x},\mathbf{y}}\left(\boldsymbol{\xi}_x, \boldsymbol{\xi}_y\right) d\boldsymbol{\xi}_y d\boldsymbol{\xi}_x && \text{(C.17)} \end{aligned}$$

The integration is taken over the region $\mathbf{x}+\mathbf{y} \leq \boldsymbol{\xi}_z$ *in* $\mathbb{R}^n \times \mathbb{R}^n$ *space (i.e., in* $\Omega_{\mathbf{x}} \times \Omega_{\mathbf{y}}$ *space). Differentiating,*

$$\begin{aligned} f_{\mathbf{z}}(\boldsymbol{\xi}_z) &= \frac{d^n}{d\xi_{z_1} d\xi_{z_2} \cdots d\xi_{z_n}} F_{\mathbf{z}}(\boldsymbol{\xi}_z) && \text{(C.18)} \\ &= \frac{d^n}{d\xi_{z_1} d\xi_{z_2} \cdots d\xi_{z_n}} \left\{ \int_{\mathbb{R}^n} \int_{\{\boldsymbol{\xi}_y \leq \boldsymbol{\xi}_z - \boldsymbol{\xi}_x\}} f_{\mathbf{x},\mathbf{y}}\left(\boldsymbol{\xi}_x, \boldsymbol{\xi}_y\right) d\boldsymbol{\xi}_y d\boldsymbol{\xi}_x \right\} && \text{(C.19)} \end{aligned}$$

Changing the order of limits,

$$f_{\mathbf{z}}(\boldsymbol{\xi}_z) = \int_{\mathbb{R}^n} \frac{d^n}{d\xi_{z_1} d\xi_{z_2} \cdots d\xi_{z_n}} \left\{ \int_{\{\boldsymbol{\xi}_y \leq \boldsymbol{\xi}_z - \boldsymbol{\xi}_x\}} f_{\mathbf{x},\mathbf{y}}\left(\boldsymbol{\xi}_x, \boldsymbol{\xi}_y\right) d\boldsymbol{\xi}_y \right\} d\boldsymbol{\xi}_x \tag{C.20}$$

Looking at the integrand of $\int_{\mathbb{R}^n}(\cdot)\,d\boldsymbol{\xi}_x$*, defined as* $\mathbb{A}$*,*

$$\mathbb{A} \triangleq \frac{d^n}{d\xi_{z_1}d\xi_{z_2}\cdots d\xi_{z_n}}\int_{-\infty}^{\xi_{z_n}-\xi_{x_n}}\cdots\int_{-\infty}^{\xi_{z_2}-\xi_{x_2}}\int_{-\infty}^{\xi_{z_1}-\xi_{x_1}}\bullet$$
$$f_{\mathbf{x},y_1,y_2,\cdots,y_n}\left(\boldsymbol{\xi}_x,\xi_{y_1},\xi_{y_2},\cdots,\xi_{y_n}\right)d\xi_{y_1}d\xi_{y_2}\cdots d\xi_{y_n} \tag{C.21}$$

Changing the order of limits,

$$\mathbb{A} = \frac{d}{d\xi_{z_n}}\int_{-\infty}^{\xi_{z_n}-\xi_{x_n}}\cdots\frac{d}{d\xi_{z_2}}\int_{-\infty}^{\xi_{z_2}-\xi_{x_2}}\frac{d}{d\xi_{z_1}}\int_{-\infty}^{\xi_{z_1}-\xi_{x_1}}\bullet$$
$$f_{\mathbf{x},y_1,y_2,\cdots,y_n}\left(\boldsymbol{\xi}_x,\xi_{y_1},\xi_{y_2},\cdots,\xi_{y_n}\right)d\xi_{y_1}d\xi_{y_2}\cdots d\xi_{y_n} \tag{C.22}$$

Using Leibnitz' rule, the derivative of the inner-most integral becomes

$$\frac{d}{d\xi_{z_1}}\int_{-\infty}^{\xi_{z_1}-\xi_{x_1}} f_{\mathbf{x},y_1,y_2,\cdots,y_n}\left(\boldsymbol{\xi}_x,\xi_{y_1},\xi_{y_2},\cdots,\xi_{y_n}\right)d\xi_{y_1}$$
$$= f_{\mathbf{x},y_1,y_2,\cdots,y_n}\left(\boldsymbol{\xi}_x,\xi_{z_1}-\xi_{x_1},\xi_{y_2},\xi_{y_3},\cdots,\xi_{y_n}\right) \tag{C.23}$$

Applying Leibnitz' rule for each integral,

$$\mathbb{A} = \frac{d}{d\xi_{z_n}}\int_{-\infty}^{\xi_{z_n}-\xi_{x_n}}\cdots\frac{d}{d\xi_{z_3}}\int_{-\infty}^{\xi_{z_3}-\xi_{x_3}}\frac{d}{d\xi_{z_2}}\int_{-\infty}^{\xi_{z_2}-\xi_{x_2}}\bullet$$
$$f_{\mathbf{x},y_1,y_2,\cdots,y_n}\left(\boldsymbol{\xi}_x,\xi_{z_1}-\xi_{x_1},\xi_{y_2},\xi_{y_3},\cdots,\xi_{y_n}\right)d\xi_{y_2}d\xi_{y_3}\cdots d\xi_{y_n} \tag{C.24}$$
$$= \frac{d}{d\xi_{z_n}}\int_{-\infty}^{\xi_{z_n}-\xi_{x_n}}\cdots\frac{d}{d\xi_{z_3}}\int_{-\infty}^{\xi_{z_3}-\xi_{x_3}}\bullet$$
$$f_{\mathbf{x},y_1,y_2,\cdots,y_n}\left(\boldsymbol{\xi}_x,\xi_{z_1}-\xi_{x_1},\xi_{z_2}-\xi_{x_2},\xi_{y_3},\cdots,\xi_{y_n}\right)d\xi_{y_3}\cdots d\xi_{y_n} \tag{C.25}$$
$$\vdots$$
$$= f_{\mathbf{x},y_1,y_2,\cdots,y_n}\left(\boldsymbol{\xi}_x,\xi_{z_1}-\xi_{x_1},\xi_{z_2}-\xi_{x_2},\cdots,\xi_{z_n}-\xi_{x_n}\right) \tag{C.26}$$

So,

$$f_{\mathbf{z}}(\boldsymbol{\xi}_z) = \int_{\mathbb{R}^n} f_{\mathbf{x},y_1,y_2,\cdots,y_n}\left(\boldsymbol{\xi}_x, \xi_{z_1} - \xi_{x_1}, \xi_{z_2} - \xi_{x_2}, \cdots, \xi_{z_n} - \xi_{x_n}\right) d\boldsymbol{\xi}_x \quad \text{(C.27)}$$

$$= \int_{\mathbb{R}^n} f_{\mathbf{x},\mathbf{y}}\left(\boldsymbol{\xi}_x, \boldsymbol{\xi}_z - \boldsymbol{\xi}_x\right) d\boldsymbol{\xi}_x \quad \text{(C.28)}$$

which is the desired result. ■

APPENDIX D - Stochastic Fourier Analysis

This appendix reviews Fourier analysis with an emphasis on its application to stochastic processes. Fourier analysis is commonly used in engineering applications to express a signal in terms of its spectral properties. Fourier analysis applied to stochastic processes is reviewed here, because the results are used extensively in this research. This appendix is not an exhaustive treatment of the subject; the interested reader is referred to [15, 16, 56, 59] for a more complete discussion. The developments and conventions used in this appendix closely match those found in [59].

Section D.1 introduces Fourier analysis applied to deterministic signals. Emphasis is placed upon the conditions for which a Fourier transform exists for non-periodic functions, because these often overlooked details are critical when forming a rigorous description of the Fourier transform for a stochastic process. Section D.2 describes stochastic processes and their characteristics used in this research. Section D.3 applies Fourier analysis to stochastic processes. Finally, Section D.4 provides a summary.

D.1 The Deterministic Fourier Transform

Fourier analysis is an extensive subject; this subsection focuses on the conditions for which the Fourier transform of a non-periodic function of time exists. This subtopic of Fourier analysis requires special treatment when applying Fourier analysis to stochastic processes. Other topics, such as the existence of the Fourier transform for periodic functions (which is a somewhat trivial consequence of the Fourier

series representation), Parseval's theorem, Fourier transform pairs, etc., are well-documented and are not covered.

Let $x(\cdot)$ be a deterministic, non-periodic[14] function of time. Under certain conditions (discussed in the next paragraph), $x(t)$ may be expressed as

$$x(t) = \int_{-\infty}^{+\infty} \tilde{x}(f)\, e^{+j2\pi ft} df \tag{D.1}$$

where $\tilde{x}(f)$ is the Fourier transform of $x(t)$ defined as

$$\tilde{x}(f) = \int_{-\infty}^{+\infty} x(t)\, e^{-j2\pi ft} dt \tag{D.2}$$

The Fourier operator, $\mathcal{F}$, and inverse Fourier operator, $\mathcal{F}^{-1}$, are defined as

$$\mathcal{F}(\cdot) \triangleq \int_{-\infty}^{+\infty} (\cdot)\, e^{-j2\pi ft} dt \tag{D.3}$$

$$\mathcal{F}^{-1}(\cdot) \triangleq \int_{-\infty}^{+\infty} (\cdot)\, e^{+j2\pi ft} df \tag{D.4}$$

Fourier transforms may be expressed in radians, using $\omega \triangleq 2\pi f$, which results in

$$\mathcal{F}(\cdot) \triangleq a \int_{-\infty}^{+\infty} (\cdot)\, e^{-j\omega t} dt \tag{D.5}$$

$$\mathcal{F}^{-1}(\cdot) \triangleq b \int_{-\infty}^{+\infty} (\cdot)\, e^{+j\omega t} d\omega \tag{D.6}$$

where the product, ab, must be chosen to equal $\frac{1}{2\pi}$.

A sufficient condition on $x(t)$ for $\tilde{x}(f)$ to exist for all $f \in \mathbb{R}^1$ is that $x(t)$ be absolutely integrable over $t \in \mathbb{R}^1$. However, mere existence of $\tilde{x}(f)$ does not guarantee that the right-hand side of Equation $(D.1)$ will equal $x(t)$ for every t. When x is of bounded variation about an interval containing t, then the right-hand

[14] Fourier analysis may be applied to periodic and non-periodic functions. Only non-periodic functions are considered here, since the analysis of non-periodic functions will be of particular interest when stochastic processes are considered.

side of Equation $(D.1)$ converges to $x(t)$ at all continuity points [75]. The above two conditions are presented more concisely in the following definition.

Definition (Fourier Transform Existence Conditions)

The Fourier transform of $x(t)$, denoted by $\tilde{x}(f)$, is said to exist for all $f \in \mathbb{R}^1$ when (1) $x(t)$ is absolutely integrable over $t \in \mathbb{R}^1$, i.e.,

$$\int_{-\infty}^{+\infty} |x(t)|\, dt < \infty \tag{D.7}$$

and (2) $x(t)$ is of bounded variation for all $t \in \mathbb{R}^1$. These two conditions will be jointly referred to in this document as the "Fourier transform existence conditions." When the Fourier transform conditions are met, Equations $(D.1)$ and $(D.2)$ provide a meaningful "Fourier transform pair" denoted by

$$x(t) \overset{\mathcal{F}}{\Longleftrightarrow} \tilde{x}(f) \tag{D.8}$$

The Fourier transform existence conditions provide insight into "typical" functions for which a Fourier transform may exist. The first Fourier transform existence condition (described by Equation $(D.7)$) implies that the limit of $x(t)$ at each "endpoint," *if each exists*, is

$$\lim_{t \to -\infty} x(t) = \lim_{t \to +\infty} x(t) = 0 \tag{D.9}$$

Whether or not the limits above exist, $x(t)$ can be shown to "decay" as $|t|$ becomes large using the following theorem.

Theorem 10

Let $\varepsilon > 0$ and $n \in N$ and define the sets α_n as

$$\alpha_n(\varepsilon) \triangleq \{t : |x(t)| > \varepsilon, n \leq |t| \leq n+1\} \tag{D.10}$$

Then, the measure of $\{\alpha_n\}$ tends to zero as $n \to \infty$.

The second Fourier transform existence condition may be interpreted loosely as $x(t)$ being "well-behaved." Thus, a "typical" function for which a Fourier transform exists may be considered a decaying, well-behaved function of time. This insight will be particularly useful when stochastic processes are considered.

When functions of interest do not satisfy the Fourier transform existence conditions, the Fourier transform is defined in a less rigorous manner. For example, the constant function

$$x(t) = 1 \quad \forall t \in \mathbb{R}^1 \tag{D.11}$$

does not satisfy Equation $(D.7)$; however, a Fourier transform-like expression is often desired. The Fourier transform pair for this case is *defined* using the so-called "Dirac delta function," δ, as

$$\tilde{x}(f) \triangleq \delta(f) \quad \text{for} \quad x(t) = 1 \tag{D.12}$$

where $\delta(f)$ is infinity at $f = 0$ and zero elsewhere with

$$\int_{-\infty}^{+\infty} \delta(f)\, df \triangleq 1 \tag{D.13}$$

D.2 Stochastic Processes

D.2.1 Definition

A *stochastic process*, $\mathbf{x}(\cdot,\cdot)$, is a function defined on $\mathbb{R}^1 \times \Xi$, where the first argument denotes "time" with $t \in \mathbb{R}^1$, and the second argument denotes samples from a sample space with $\xi \in \Xi$. (Some authors use $\omega \in \Omega$ rather than $\xi \in \Xi$; however, the latter notation avoids confusion with $\omega \triangleq 2\pi f$ used in Fourier analysis.) For some fixed t, each $\mathbf{x}(t,\cdot)$ is a *random variable* (and is a function of ξ). For some fixed ξ, each $\mathbf{x}(\cdot,\xi)$ is a *sample* from a stochastic process (and is a function of t). For some fixed t and ξ, each $\mathbf{x}(t,\xi)$ is a point in $\mathbb{R}^n$. An example, scalar (i.e., $n = 1$) stochastic process, $x(\cdot,\cdot)$, is depicted graphically in Figure 27 over the region $t \in [t_i, t_f] \subset \mathbb{R}^1$ and for $\xi \in \{\xi_1, \xi_2, \xi_3, \xi_4\} \subset \Xi$ (i.e., four samples of the process are shown).

A stochastic process at a single time is a random variable which may be characterized through its probability distribution function, or, if it exists, its probability density function. In general, the probabilistic nature of a stochastic process is defined through the infinite-dimensional joint probability distribution function of the random variables generated by the stochastic process at every time instance. Doob [16] provides a theorem which permits a stochastic process to be defined through the joint probability distribution function

$$F_{\mathbf{x}(t_1,\cdot),\ldots,\mathbf{x}(t_N,\cdot)}(\boldsymbol{\xi}_1,\ldots,\boldsymbol{\xi}_N) \tag{D.14}$$

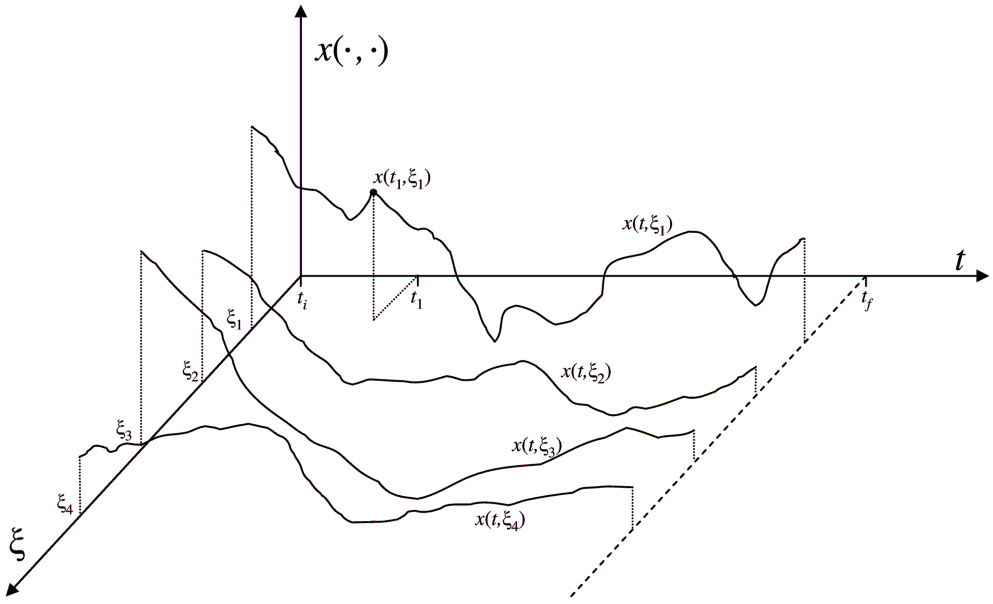

Figure 27. Stochastic Process Example

for all time sequences $\{t_1, \ldots, t_N\}$. If it exists, an equally informative characterization may be found through the joint probability density function

$$f_{\mathbf{x}(t_1,\cdot),\ldots,\mathbf{x}(t_N,\cdot)}\left(\boldsymbol{\xi}_1, \ldots, \boldsymbol{\xi}_N\right) \tag{D.15}$$

for all time sequences $\{t_1, \ldots, t_N\}$. A stochastic process is termed a Gaussian process if the joint probability distribution function in Equation $(D.14)$ is Gaussian for all time sequences $\{t_1, \ldots, t_N\}$. Likewise, a Gaussian process may be defined through the joint probability density function given in Equation $(D.15)$ for all time sequences $\{t_1, \ldots, t_N\}$, if it exists.

D.2.2 Statistics

Having reviewed the definition of a stochastic process, some common statistics used with stochastic process are now presented. The *mean* of $\mathbf{x}(\cdot, \cdot)$ is defined for all $t \in \mathbb{R}^1$ as

$$\begin{aligned} \boldsymbol{\mu}_x(t) &\triangleq E\left\{\mathbf{x}(t, \cdot)\right\} && \text{(D.16)} \\ &= \int_{\mathbb{R}^n} \boldsymbol{\xi} f_{\mathbf{x}(t,\cdot)}(\boldsymbol{\xi})\, d\boldsymbol{\xi} && \text{(D.17)} \end{aligned}$$

As indicated, $\boldsymbol{\mu}_x(t)$ is, in general, time-varying. The *covariance kernel* of $\mathbf{x}(\cdot, \cdot)$ is defined for all $t_1, t_2 \in \mathbb{R}^1$ as

$$\begin{aligned} \mathbf{P}_{xx}(t_1, t_2) &\triangleq E\left\{\left[\mathbf{x}(t_1, \cdot) - \boldsymbol{\mu}_x(t_1)\right]\left[\mathbf{x}(t_2, \cdot) - \boldsymbol{\mu}_x(t_2)\right]^T\right\} && \text{(D.18)} \\ &= \int_{\mathbb{R}^n \times \mathbb{R}^n} \Big\{\left[\boldsymbol{\xi}_1 - \boldsymbol{\mu}_x(t_1)\right]\left[\boldsymbol{\xi}_2 - \boldsymbol{\mu}_x(t_2)\right]^T \cdot \\ &\qquad f_{\mathbf{x}(t_1,\cdot),\mathbf{x}(t_2,\cdot)}(\boldsymbol{\xi}_1, \boldsymbol{\xi}_2)\Big\}\, d\boldsymbol{\xi}_1 d\boldsymbol{\xi}_2 && \text{(D.19)} \end{aligned}$$

When $t_1 = t_2$, the second central moment, or *covariance matrix*, is

$$\mathbf{P}_{xx}(t) = \mathbf{P}_{xx}(t,t) \tag{D.20}$$

The *correlation kernel* of $\mathbf{x}(t,\cdot)$ is defined for all $t_1, t_2 \in \mathbb{R}^1$ as

$$\mathbf{\Psi}_{xx}(t_1,t_2) \triangleq E\left\{\mathbf{x}(t_1,\cdot)\,\mathbf{x}(t_2,\cdot)^T\right\} \tag{D.21}$$

When $t_1 = t_2$, the second non-central moment, or *correlation matrix*, is

$$\mathbf{\Psi}_{xx}(t) = \mathbf{\Psi}_{xx}(t,t) \tag{D.22}$$

The covariance kernel and correlation kernel are related by

$$\mathbf{\Psi}_{xx}(t_1,t_2) = \mathbf{P}_{xx}(t_1,t_2) + \boldsymbol{\mu}_x(t_1)\,\boldsymbol{\mu}_x(t_2)^T \tag{D.23}$$

These definitions can be generalized to two stochastic processes, denoted by $\mathbf{x}(\cdot,\cdot)$ and $\mathbf{y}(\cdot,\cdot)$. The *cross-covariance kernel* is defined for all $t_1, t_2 \in \mathbb{R}^1$ as

$$\mathbf{P}_{xy}(t_1,t_2) \triangleq E\left\{\left[\mathbf{x}(t_1,\cdot) - \boldsymbol{\mu}_x(t_1)\right]\left[\mathbf{y}(t_2,\cdot) - \boldsymbol{\mu}_y(t_2)\right]^T\right\} \tag{D.24}$$

and the *cross-covariance matrix* is defined for all $t \in \mathbb{R}^1$ as

$$\mathbf{P}_{xy}(t) \triangleq \mathbf{P}_{xy}(t,t) \tag{D.25}$$

The *cross-correlation kernel* is defined for all $t_1, t_2 \in \mathbb{R}^1$ as

$$\mathbf{\Psi}_{xy}(t_1,t_2) \triangleq E\left\{\mathbf{x}(t_1,\cdot)\,\mathbf{y}(t_2,\cdot)^T\right\} \tag{D.26}$$

and the *cross-correlation matrix* is defined for all $t \in \mathbb{R}^1$ as

$$\mathbf{\Psi}_{xy}(t) \triangleq \mathbf{\Psi}_{xy}(t,t) \tag{D.27}$$

D.2.3 Stationarity

A stochastic process, $\mathbf{x}(\cdot,\cdot)$, is said to be *strict-sense stationary* (SSS) (or sometimes called strictly stationary, completely stationary, or strongly stationary) if, for all admissible sets $\{t_1,\ldots,t_N\}$ and any τ (such that all sets $\{t_1+\tau,\ldots,t_N+\tau\}$ are admissible), the joint probability distribution functions satisfy the condition

$$F_{\mathbf{x}(t_1,\cdot),\ldots,\mathbf{x}(t_N,\cdot)}(\boldsymbol{\xi}_1,\ldots,\boldsymbol{\xi}_N) = F_{\mathbf{x}(t_1+\tau,\cdot),\ldots,\mathbf{x}(t_N+\tau,\cdot)}(\boldsymbol{\xi}_1,\ldots,\boldsymbol{\xi}_N) \tag{D.28}$$

for all

$$(\boldsymbol{\xi}_1,\ldots,\boldsymbol{\xi}_N) \subset \underbrace{\mathbb{R}^n \times \cdots \times \mathbb{R}^n}_{N} \tag{D.29}$$

Essentially, a process is SSS if the joint probability distribution function is invariant with respect to a shift of the absolute time scale.

A stochastic process, $\mathbf{x}(\cdot,\cdot)$, is said to be *wide-sense stationary* (WSS) (or stationary up to order 2 or weakly stationary) if the following are met:

1. $\boldsymbol{\mu}_x(t)$ is time-invariant, denoted by the constant vector $\boldsymbol{\mu}_x$;
2. $\boldsymbol{\Psi}_{xx}(t)$ is finite and time-invariant, denoted by the constant matrix $\boldsymbol{\Psi}_{xx}(0)$;
3. $\boldsymbol{\Psi}_{xx}(t_1,t_2)$ is a function of $\tau \triangleq t_1 - t_2$ only, denoted by $\boldsymbol{\Psi}_{xx}(\tau)$.

A SSS process is WSS; however, the converse is not true. (A notable exception is that a WSS, Gaussian stochastic process is also a SSS process.) It follows from the definition of a WSS stochastic process that the covariance matrix is finite and time-invariant, denoted by the constant matrix $\mathbf{P}_{xx}$, and the covariance kernel is a function of the time difference only, denoted by $\mathbf{P}_{xx}(\tau)$. A single argument on $\mathbf{P}_{xx}$

and $\boldsymbol{\Psi}_{xx}$ may indicate the covariance kernel and correlation kernel, respectively, of a WSS process, or the covariance matrix and correlation matrix, respectively, of a *non*-WSS process.

D.2.4 Ergodicity

Ergodicity permits averages over time to be used to indicate ensemble averages over realizations. Given one particular realization of the stationary random process, $\mathbf{x}(\cdot, \boldsymbol{\xi})$, ergodicity implies

$$\boldsymbol{\mu}_x = \lim_{T\to\infty} \frac{1}{T} \int_{-\frac{T}{2}}^{+\frac{T}{2}} \mathbf{x}(t, \boldsymbol{\xi})\, dt \tag{D.30}$$

$$\boldsymbol{\Psi}_{xx}(\tau) = \lim_{T\to\infty} \frac{1}{T} \int_{-\frac{T}{2}}^{+\frac{T}{2}} \mathbf{x}(t, \boldsymbol{\xi})\, \mathbf{x}(t+\tau, \boldsymbol{\xi})\, dt \tag{D.31}$$

For realizations of two stationary random processes, denoted by $\mathbf{x}(\cdot, \boldsymbol{\xi})$ and $\mathbf{y}(\cdot, \boldsymbol{\rho})$, ergodicity implies, in addition to the previous implications for the individual processes, that

$$\boldsymbol{\Psi}_{xy}(\tau) = \lim_{T\to\infty} \frac{1}{T} \int_{-\frac{T}{2}}^{+\frac{T}{2}} \mathbf{x}(t, \boldsymbol{\xi})\, \mathbf{y}(t+\tau, \boldsymbol{\rho})\, dt \tag{D.32}$$

In practice, the stationarity of a process is validated under the assumption of ergodicity. A process is ergodic *only if* it is stationary. In this document (unless indicated otherwise), when a process is assumed to be stationary, it is assumed to be both wide-sense stationary and ergodic.

D.2.5 Continuity

For a particular realization, the continuity of $x(\cdot, \xi)$ is defined in the ordinary sense. A stochastic process, $x(\cdot, \cdot)$, is stochastically continuous or "mean-square

continuous" at $t = t_0$ if

$$\underset{t \to t_0}{\text{l.i.m.}}\; x(t, \cdot) = x(t_0, \cdot) \tag{D.33}$$

where l.i.m. denotes the "limit in the mean-square sense." The condition "*if* Equation $(D.33)$" may be interpreted as *if and only if*

$$\lim_{t \to t_0} E\left\{[x(t, \cdot) - x(t_0, \cdot)]^2\right\} = 0 \tag{D.34}$$

A stochastic process which is stochastically continuous at $t = t_0$ for all t_0 is said to be stochastically continuous everywhere (or simply described as a "stochastically continuous process"). Note that stochastic continuity is defined over all realizations; in general, this condition does not imply continuity (in the ordinary sense) for any particular realization.

For a stationary, stochastic process, $x(\cdot, \cdot)$, by definition, (1) $E\left\{[x(t, \cdot)]^2\right\}$ is time-invariant, that is,

$$E\left\{[x(t, \cdot)]^2\right\} \triangleq \Psi_{xx}(0) = \text{constant} \tag{D.35}$$

for all $t \in \mathbb{R}^1$, and (2) $E\{x(t, \cdot)\, x(t_0, \cdot)\}$ is a function of the time-difference $t - t_0$ only, and

$$\Psi_{xx}(t - t_0) \triangleq E\{x(t, \cdot)\, x(t_0, \cdot)\} \tag{D.36}$$

Thus, under the assumption of stationarity and using

$$\begin{aligned} E\left\{[x(t, \cdot) - x(t_0, \cdot)]^2\right\} &= E\left\{[x(t, \cdot)]^2\right\} + E\left\{[x(t_0, \cdot)]^2\right\} \\ &\quad -2E\{x(t, \cdot)\, x(t_0, \cdot)\} \end{aligned} \tag{D.37}$$

Equation $(D.34)$ becomes

$$\lim_{t \to t_0} \left[2\Psi_{xx}(0) - 2\Psi_{xx}(t - t_0) \right] = 0 \tag{D.38}$$

$$\lim_{t \to t_0} \Psi_{xx}(t - t_0) = \Psi_{xx}(0) \tag{D.39}$$

Using $\tau \triangleq t - t_0$, this condition may be rewritten as

$$\lim_{\tau \to 0} \Psi_{xx}(\tau) = \Psi_{xx}(0) \tag{D.40}$$

Therefore, a stationary, stochastic process, $x(\cdot, \cdot)$, is stochastically continuous at $t = t_0$ if and only if $\Psi_{xx}(\tau)$ is continuous (in the ordinary sense) at $\tau = 0$. Under the stationarity assumption, the following also hold [59]: (1) If $\Psi_{xx}(\tau)$ is continuous (in the ordinary sense) at $\tau = 0$, then $\Psi_{xx}(\tau)$ is continuous (in the ordinary sense) everywhere (for all $\tau \in \mathbb{R}^1$), (2) $x(\cdot, \cdot)$ is stochastically continuous everywhere if and only if $x(\cdot, \cdot)$ is stochastically continuous at $t = t_0$, and (3) $x(\cdot, \cdot)$ is stochastically continuous everywhere if and only if $\Psi_{xx}(\tau)$ is continuous (in the ordinary sense) at $\tau = 0$.

D.3 Stochastic Fourier Analysis

In this section, the definition of the Fourier transform of a stochastic process is presented. The aim of stochastic Fourier analysis is to characterize the spectral properties of a stationary, stochastic process. Care must be taken to ensure the results are meaningful. The first approach details the (non-stochastic) Fourier transform of a stationary stochastic process. The second, more elegant, approach introduces the Fourier Stieltjes transform [59] to describe the spectral properties of a stationary stochastic process. These descriptions are presented for the scalar case; the vector

case is a natural extension of these results. Finally, brief mention is made to a method whereby stochastic Fourier analysis may be applied without assuming stationarity.

D.3.1 Fourier Transform

Consider the stationary, stochastic process $x(\cdot,\cdot)$. Ideally, the Fourier transform of $x(t,\cdot)$ for all $t \in \mathbb{R}^1$ would be found over all realizations through

$$\tilde{x}(\omega,\cdot) = \int_{-\infty}^{+\infty} x(t,\cdot)\, e^{-j\omega t} dt \tag{D.41}$$

In general, a particular realization, $x(\cdot,\xi)$, is not periodic in time, nor is there any guarantee that the Fourier existence conditions are met. In fact, it may seem as though an impasse is met where stationary processes imply a sense of steady-state behavior over time, while the Fourier existence conditions imply a function decays as $|t| \to \infty$. The following discussion is a rigorous treatment of this conflict.

Given the stationary, stochastic process $x(\cdot,\cdot)$ and the time interval $T > 0$, let $x_T(t,\cdot)$ be defined for all admissible t as

$$x_T(t,\cdot) \triangleq \begin{cases} x(t,\cdot) & -\frac{T}{2} \le t \le \frac{T}{2} \\ 0 & \text{otherwise} \end{cases} \tag{D.42}$$

Assuming $x(t,\cdot)$ is continuous (and, consequently, $x_T(t,\cdot)$ satisfies the Fourier existence conditions), let $x_T(t,\cdot)$ be described through its Fourier transform, $\tilde{x}_T(\omega,\cdot)$, as

$$x_T(t,\cdot) = \frac{1}{\sqrt{2\pi}} \int_{-\infty}^{+\infty} \tilde{x}_T(\omega,\cdot)\, e^{j\omega t} d\omega \tag{D.43}$$

where, for all $\omega \in \mathbb{R}^1$,

$$\tilde{x}_T(\omega,\cdot) = \frac{1}{\sqrt{2\pi}} \int_{-\infty}^{+\infty} x_T(t,\cdot)\, e^{-j\omega t} dt \tag{D.44}$$

$\tilde{x}_T(\omega, \cdot)$ may be expressed in terms of the original process as

$$\tilde{x}_T(\omega, \cdot) = \frac{1}{\sqrt{2\pi}} \int_{-\frac{T}{2}}^{+\frac{T}{2}} x(t, \cdot) e^{-j\omega t} dt \tag{D.45}$$

Consider the total energy in some small frequency increment, $d\omega$:

$$\left|\tilde{x}_T(\omega, \cdot)\right|^2 d\omega \tag{D.46}$$

It is tempting to let $T \to \infty$ so that $x_T(t, \cdot)$ and $x(t, \cdot)$ are identical for all t. Then,

$$\lim_{T \to \infty} \left|\tilde{x}_T(\omega, \cdot)\right|^2 \tag{D.47}$$

would describe the energy of $x(t, \cdot)$ over ω. However, this limit does not exist for a stationary process. As may be done for the Fourier transform of periodic functions, consider the signal power, or energy per unit of time, in some small frequency increment, $d\omega$, as

$$\frac{\left|\tilde{x}_T(\omega, \cdot)\right|^2}{T} d\omega \tag{D.48}$$

Then, the limit

$$\lim_{T \to \infty} \frac{\left|\tilde{x}_T(\omega, \cdot)\right|^2}{T} \tag{D.49}$$

may exist and may be interpreted as the power density.

If this limit exists for all realizations, then the stochastic process $\tilde{x}_T(\omega, \cdot)$ could be constructed. An alternate approach is to consider $\tilde{x}_T(\omega, \cdot)$ over the average of all realizations. Assuming the limit in Equation $(D.49)$ exists (which permits the order in which the limits are taken to be interchanged; consider the Fubini theorem

sufficient conditions [64]), define

$$s(\omega) \triangleq \lim_{T\to\infty} E\left\{\frac{|\tilde{x}_T(\omega,\cdot)|^2}{T}\right\} \tag{D.50}$$

If it exists, $s(\omega)\,d\omega$ may be interpreted as the average (over all realizations) power contributed by $x(t,\cdot)$ for all $t \in \mathbb{R}^1$ in some small increment, $d\omega$; consequently, $s(\omega)$ is called the *power spectral density function* of $x(\cdot,\cdot)$. The following theorem and corollary present conditions when $s(\omega)$ exists.

Theorem 11

Let $x(\cdot,\cdot)$ be a zero-mean, continuous stationary process with the power spectral density function, $s_{xx}(\omega)$, which exists for all ω, and autocorrelation function, $\Psi_{xx}(\tau)$. Then, $s_{xx}(\omega)$ is the Fourier transform of $\Psi_{xx}(\tau)$, i.e.,

$$s_{xx}(\omega) = \frac{1}{2\pi}\int_{-\infty}^{+\infty} \Psi_{xx}(\tau)\, e^{-j\omega\tau} d\tau \tag{D.51}$$

Proof: *See [59].* ■

Theorem 12

A sufficient condition for $s_{xx}(\omega)$ to exist for all $\omega \in \mathbb{R}^1$ is that $\Psi_{xx}(\tau)$ possesses a Fourier transform, i.e., $\Psi_{xx}(\tau)$ is absolutely integrable:

$$\int_{-\infty}^{+\infty} |\Psi_{xx}(\tau)|\, d\tau < \infty \tag{D.52}$$

Proof: *See [59].* ■

Additionally, the following property may be found.

Theorem 13

If $\Psi_{xx}(\tau)$ *is absolutely integrable and is continuous at* $\tau = 0$*, then*

$$\Psi_{xx}(\tau) = \int_{-\infty}^{+\infty} s_{xx}(\omega)\, e^{+j\omega\tau} d\omega \tag{D.53}$$

Proof: *See [59].* ■

The analysis thus far applies to real-valued and complex-valued processes. The following corollary provides some simplification for real-valued processes.

Theorem 14

For the real-valued process $x(\cdot,\cdot)$*,* $\Psi_{xx}(\tau)$ *is an even function in* τ*. Additionally, if* $\Psi_{xx}(\tau)$ *is absolutely integrable, then* $s_{xx}(\omega)$ *is an even function in* ω *and may be expressed as*

$$s_{xx}(\omega) = \frac{1}{2\pi} \int_{-\infty}^{+\infty} \Psi_{xx}(\tau) \cos(\omega\tau)\, d\tau \tag{D.54}$$

Proof: *See [59].* ■

D.3.2 The Fourier Stieltjes Transform

In general, a stochastic process is neither periodic nor non-periodic with finite energy; therefore, a (non-stochastic) Fourier transform of the stochastic process does not exist. In the previous section, the Fourier transform of a stochastic process was rigorously described using the Fourier transform of a time-windowed version of the stochastic process followed by averaging the result over all realizations. A more general Fourier transform, called the Fourier Stieltjes transform, may be used to capture a complete realization (without taking the limit of a time-windowed version)

and does not require averaging over realizations. The following theorem presents formally the properties of the Fourier Stieltjes transform.

Theorem 15 (Fourier Stieltjes Transform Theorem)

Let $x(\cdot,\cdot)$ be a zero-mean, stochastically continuous, stationary random process. Then there exists an orthogonal process, $Z(\cdot,\cdot)$, such that, for all t, $x(t,\cdot)$ may be written in the form

$$x(t,\cdot) = \int_{-\infty}^{+\infty} e^{j\omega t} dZ(\omega,\cdot) \tag{D.55}$$

where the integral is defined in the mean-square sense. The process $Z(\cdot,\cdot)$ has the following properties:

$$E\{dZ(\omega,\cdot)\} = 0 \quad \text{for all } \omega \tag{D.56}$$

$$E\left\{|dZ(\omega,\cdot)|^2\right\} = dS_{xx}(\omega) \quad \text{for all } \omega \tag{D.57}$$

$$E\{dZ^*(\omega,\cdot)\, dZ(\omega',\cdot)\} = 0 \quad \text{for any } \omega, \omega' \text{ such that } \omega \neq \omega' \tag{D.58}$$

Proof: *See [6] or [59].* ■

When $x(\cdot,\cdot)$ has a continuous spectrum, the *integrated power spectral density function*, $S_{xx}(\omega)$, may be defined as

$$S_{xx}(\omega) \triangleq \int_{-\infty}^{\omega} s_{xx}(\eta)\, d\eta \tag{D.59}$$

so that the differentials are related by

$$dS_{xx}(\omega) = s_{xx}(\omega)\, d\omega \tag{D.60}$$

In this case, Equation $(D.57)$ may be rewritten as

$$E\left\{\left|dZ(\omega,\cdot)\right|^2\right\} = s_{xx}(\omega)\, d\omega \quad \text{for all } \omega \in \mathbb{R}^1 \tag{D.61}$$

The *Fourier Stieltjes transform* defines the spectral representation of the stationary stochastic process, $x(\cdot,\cdot)$, in Equation $(D.55)$. For each realization of $x(\cdot,\cdot)$, $dZ(\cdot,\cdot)$ takes on a different realization. Furthermore, for a particular ω, $dZ(\omega,\cdot)$ is a random variable. If, for all ω, $dZ(\omega,\cdot)$ were differentiable, i.e., the following exists:

$$\frac{dZ(\omega,\cdot)}{d\omega} = \tilde{x}(\omega,\cdot) \tag{D.62}$$

then the Fourier Stieltjes transform is reduced to an ordinary Fourier transform. However, $dZ(\omega,\cdot)$ is not differentiable as a stochastic process based upon the same principles that an ordinary Fourier transform does not exist for a stochastic process. The structure of $dZ(\omega,\cdot)$ in the stochastic integral permits consideration of the spectral properties of $x(\cdot,\cdot)$ when the ordinary Fourier transform does not exist.

The Fourier Stieltjes transform permits $x(t,\cdot)$, for all admissible t, to be represented as (the limit of) the sum of sines and cosines with random coefficients, $dZ(\cdot,\cdot)$, or more precisely, with random magnitudes, $|dZ(\cdot,\cdot)|$ and random phases, $\arg\{dZ(\cdot,\cdot)\}$. Define the random process $Z(\omega,\cdot)$ for all ω as

$$Z(\omega,\cdot) \triangleq \int_{-\infty}^{\omega} dZ(\eta,\cdot) \tag{D.63}$$

where the integral is a stochastic integral defined in the mean-square sense. From Equation $(D.58)$, the increments of $Z(\omega, \cdot)$ at different values of ω are uncorrelated. (Thus, $Z(\cdot, \cdot)$ is called an orthogonal process). Furthermore, the properties of $Z(\cdot, \cdot)$ are related to the spectral properties of $x(\cdot, \cdot)$, where, in a formal sense, the stochastic derivative of $Z(\cdot, \cdot)$ plays the role of the Fourier transform for $x(\cdot, \cdot)$.

Finally, by defining two additional terms, the Wiener-Khintchine Theorem may be used to relate the autocorrelation and power spectral density functions [59]. (This is a generalization of Theorem 11.) Let the *normalized power spectral density function* of $x(\cdot, \cdot)$, denoted by $f_{xx}(\omega)$, be defined as

$$f_{xx}(\omega) \triangleq \frac{s_{xx}(\omega)}{\int_{-\infty}^{+\infty} s_{xx}(\omega)\, d\omega} \tag{D.64}$$

or,

$$f_{xx}(\omega) = \frac{s_{xx}(\omega)}{\Psi_{xx}(0)} \tag{D.65}$$

It is assumed $\Psi_{xx}(0) \neq 0$, since $\Psi_{xx}(0) = 0$ is the trivial case that $x(\cdot, \cdot)$ is deterministic. Let the *integrated normalized power spectral density function*, $F_{xx}(\omega)$, be defined as

$$F_{xx}(\omega) \triangleq \int_{-\infty}^{\omega} f_{xx}(\eta)\, d\eta \tag{D.66}$$

so that the differentials are related by

$$dF_{xx}(\omega) = f_{xx}(\omega)\, d\omega \tag{D.67}$$

Theorem 16 (Wiener-Khintchine Theorem)

A necessary and sufficient condition for $\Psi_{xx}(\tau)$ *to be the autocorrelation function of some stochastically continuous stationary process,* $x(\cdot,\cdot)$*, is that there exists a function,* $F_{xx}(\cdot)$*, having the properties of a distribution function on* $\omega \in (-\infty, +\infty)$*, (i.e.,* $F_{xx}(-\infty) = 0$*,* $F_{xx}(+\infty) = 1$*, and* $F_{xx}(\cdot)$ *non-decreasing), such that, for all* τ*,* $\Psi_{xx}(\tau)$ *may be expressed in the form,*

$$\frac{\Psi_{xx}(\tau)}{\Psi_{xx}(0)} = \int_{-\infty}^{+\infty} e^{j\omega\tau} dF_{xx}(\omega) \tag{D.68}$$

where the integral is the taken in the mean-square sense and

$$\Psi_{xx}(0) \neq 0 \tag{D.69}$$

Furthermore,

$$\Psi_{xx}(\tau) = \int_{-\infty}^{+\infty} e^{j\omega\tau} dS_{xx}(\omega) \tag{D.70}$$

where the integral is the taken in the mean-square sense.

Proof: *See [59].* ■

Theorems 15 and 16 holds true for both real-valued and complex-valued processes. The results of Theorem 15 for a *real-valued*, zero-mean, stochastically continuous, stationary process, $x(\cdot,\cdot)$, become

$$E\{dU(\omega,\cdot)\, dU(\omega',\cdot)\} = 0 \quad \text{for any } \omega, \omega' \text{ such that } \omega \neq \omega' \tag{D.71}$$

$$E\{dV(\omega,\cdot)\, dV(\omega',\cdot)\} = 0 \quad \text{for any } \omega, \omega' \text{ such that } \omega \neq \omega' \tag{D.72}$$

$$E\left\{\left|dU\left(\omega,\cdot\right)\right|^2\right\} = E\left\{\left|dV\left(\omega,\cdot\right)\right|^2\right\} = dH_{x^+}\left(\omega\right) \tag{D.73}$$

where

$$dU\left(\cdot,\cdot\right) = \mathrm{Re}\left\{dZ\left(\cdot,\cdot\right)\right\} \tag{D.74}$$

$$dV\left(\cdot,\cdot\right) = -\,\mathrm{Im}\left\{dZ\left(\cdot,\cdot\right)\right\} \tag{D.75}$$

and $H_{xx^+}\left(\omega\right)$ is the integrated spectrum for positive frequencies only[15]. Furthermore, $dU\left(\cdot,\cdot\right)$ and $dV\left(\cdot,\cdot\right)$ are cross-orthogonal, i.e.,

$$E\left\{dU\left(\omega,\cdot\right)dV\left(\omega',\cdot\right)\right\} = 0 \quad \text{for all } \omega,\omega' \tag{D.76}$$

D.3.3 The General Orthogonal Expansion

Throughout this analysis, WSS processes have been assumed. This assumption permits "in the mean-square sense" definitions (such as stochastic continuity, the stochastic derivative, and the stochastic integral) to be properly defined. The *general orthogonal expansion* avoids these expressions while maintaining rigor. While the details are beyond the scope of this research, the results are a generalization of the Fourier Stieltjes transform that include processes for which stationarity is not assumed [6].

D.4 Summary

This appendix presented Fourier analysis, stochastic processes, and the application of Fourier analysis to stochastic processes. Two main theorems provide the

[15] It can be shown that $H_{xx^+}\left(\omega\right) = \frac{2}{\pi}\int_0^{\omega}\frac{\sin(\tau\omega)}{\tau}\Psi_{xx}\left(\tau\right)d\tau$ [59].

background for stochastic Fourier analysis. The Fourier Stieltjes transform, or the spectral representation of the stationary stochastic process, $x(\cdot,\cdot)$, is given for all admissible t in Equation $(D.55)$ and repeated here as

$$x(t,\cdot) = \int_{-\infty}^{+\infty} e^{j\omega t} dZ(\omega,\cdot) \tag{D.55}$$

From the Fourier Stieltjes transform theorem given in Theorem 15, when $x(\cdot,\cdot)$ is a zero-mean, stochastically continuous, stationary random process, the process $Z(\omega,\cdot)$ as defined using Equations $(D.55)$ and $(D.63)$ has the following properties:

$$E\{dZ(\omega,\cdot)\} = 0 \quad \text{for all } \omega \tag{D.56}$$

$$E\left\{|dZ(\omega,\cdot)|^2\right\} = dS_{xx}(\omega) \quad \text{for all } \omega \tag{D.57}$$

$$E\{dZ^*(\omega,\cdot)\, dZ(\omega',\cdot)\} = 0 \quad \text{for any } \omega,\omega' \text{ such that } \omega \neq \omega' \tag{D.58}$$

From the Wiener-Khintchine theorem given in Theorem 16, when $x(\cdot,\cdot)$ is a zero-mean, stochastically continuous, stationary random process, the autocorrelation function of $x(\cdot,\cdot)$, $\Psi_{xx}(\tau)$, may be expressed in terms of the integrated power spectral density function, $S_{xx}(\omega)$, through Equation $(D.70)$, repeated here as

$$\Psi_{xx}(\tau) = \int_{-\infty}^{+\infty} e^{j\omega\tau} dS_{xx}(\omega) \tag{D.70}$$

The Fourier Stieltjes transform may be reduced to the Fourier transform when $dZ(\cdot,\cdot)$ and $dS_{xx}(\cdot)$ are differentiable for all ω, i.e., Equations $(D.62)$ and $(D.60)$ are

meaningful for all ω as

$$dZ(\omega, \cdot) = \tilde{x}(\omega, \cdot)\, d\omega \tag{D.62}$$

$$dS_{xx}(\omega) = s_{xx}(\omega)\, d\omega \tag{D.60}$$

APPENDIX E - Finite-Timelength Observation Autocorrelation Kernel Theorem

In this appendix, the autocorrelation kernel for a finite-timelength observation of a stochastic process is found in terms of the autocorrelation kernel for the entire stochastic process. Appendix D provides the theory for Fourier analysis of stochastic processes. Under certain restrictions, the autocorrelation kernel of a stationary process may be expressed in terms of the power spectral density of the process. In this appendix, a single realization of a stochastic process is observed over some finite time interval, T. Under the assumptions of ergodicity and stationarity, the results herein enable the autocorrelation kernel for a finite timelength observation to be expressed in terms of the power spectral density function of the original stochastic process. The remainder of this appendix presents a theorem which states this more formally, a proof of the theorem, and a few remarks.

Theorem 17

Let $\mathbf{x}(\cdot,\cdot)$ *be an arbitrary zero-mean, wide-sense stationary, ergodic, Gaussian stochastic process (in time) for which the power spectral density function,* $\tilde{\mathbf{s}}_{xx}(f)$*, exists and is given element-wise as*

$$\Psi_{x_k x_l}(\tau) \overset{\mathcal{F}}{\Longleftrightarrow} \tilde{s}_{x_k x_l}(f) \tag{E.1}$$

Let the Gaussian stochastic process (in frequency), $\tilde{\mathbf{z}}(\cdot,\cdot)$*, be formed as the Fourier transform of a time-gated observation of* $\mathbf{x}(\cdot,\cdot)$*, i.e.,* $\tilde{\mathbf{z}}(\cdot,\cdot)$ *is given for all* f *as*

$$\tilde{\mathbf{z}}(f,\cdot) \triangleq \mathcal{F}\left\{\mathbf{x}(t,\cdot)\prod(t,T)\right\} \tag{E.2}$$

where $\prod(t,T)$ *is a window with height* $\frac{1}{T}$ *and duration* T*:*

$$\prod(t,T) \triangleq \begin{cases} \frac{1}{T} & t \in [t_0, t_0+T] \\ \\ 0 & \text{otherwise} \end{cases} \tag{E.3}$$

Then, the autocorrelation kernel of $\tilde{\mathbf{z}}(\cdot,\cdot)$ *is given element-wise for all* f *as*

$$E\left\{\tilde{z}_k(f,\cdot)\,\tilde{z}_l^*(f-\epsilon,\cdot)\right\} \approx \frac{1}{T}\tilde{s}_{x_k x_l}(f)\,\delta_\kappa(\epsilon) \tag{E.4}$$

where $\tilde{z}_k$ *is the* k^{th} *component of* $\tilde{\mathbf{z}}$*,* $\tilde{z}_l$ *is the* l^{th} *component of* $\tilde{\mathbf{z}}$*, and* $\delta_\kappa(\epsilon)$ *is a modified Kronecker delta function (not a Dirac delta function) defined as*

$$\delta_\kappa(\epsilon) \triangleq \begin{cases} 1 & \epsilon = 0 \\ \\ 0 & \text{otherwise} \end{cases} \tag{E.5}$$

Proof: *The* k,l *element of* $E\left\{\tilde{\mathbf{z}}(\cdot,\cdot)\,\tilde{\mathbf{z}}^*(\cdot,\cdot)\right\}$ *for some arbitrary* f_1 *and* f_2 *is*

$$\begin{aligned} E\left\{\tilde{z}_k(f_1,\cdot)\,\tilde{z}_l^*(f_2,\cdot)\right\} &= E\left\{\int_{-\infty}^{+\infty} x_k(u,\cdot)\prod(u,T)\,e^{-j2\pi f_1 u}du \bullet \right. \\ &\qquad \left. \int_{-\infty}^{+\infty} x_l(v,\cdot)\prod(v,T)\,e^{+j2\pi f_2 v}dv\right\} \end{aligned} \tag{E.6}$$

Recalling the definition of $\prod$ *in Equation (E.3),*

$$\begin{aligned} E\left\{\tilde{z}_k(f_1,\cdot)\,\tilde{z}_l^*(f_2,\cdot)\right\} &= E\left\{\left[\frac{1}{T}\int_{-\frac{T}{2}}^{+\frac{T}{2}} x_k(u,\cdot)\,e^{-j2\pi f_1 u}du\right]\bullet \right. \\ &\qquad \left.\left[\frac{1}{T}\int_{-\frac{T}{2}}^{+\frac{T}{2}} x_l(v,\cdot)\,e^{+j2\pi f_2 v}dv\right]\right\} \end{aligned} \tag{E.7}$$

$$= \frac{1}{T^2}\int_{-\frac{T}{2}}^{+\frac{T}{2}}\int_{-\frac{T}{2}}^{+\frac{T}{2}} E\left\{x_k(u,\cdot)\,x_l(v,\cdot)\right\}e^{-j2\pi(f_1 u - f_2 v)}dudv \tag{E.8}$$

so that

$$E\left\{\tilde{z}_k\left(f_1,\cdot\right)\tilde{z}_l^*\left(f_2,\cdot\right)\right\}=\frac{1}{T^2}\int_{-\frac{T}{2}}^{+\frac{T}{2}}\int_{-\frac{T}{2}}^{+\frac{T}{2}}R_{x_kx_l}\left(u-v\right)e^{-j2\pi(f_1u-f_2v)}dudv \tag{E.9}$$

Using the Wiener-Khintchine Theorem,

$$\Psi_{x_kx_l}\left(\tau\right)=\int_{-\infty}^{+\infty}\tilde{s}_{x_kx_l}\left(f\right)e^{j2\pi f\tau}d\tau \tag{E.10}$$

Equation (E.9) becomes

$$\begin{aligned}E\left\{\tilde{z}_k\left(f_1,\cdot\right)\tilde{z}_l^*\left(f_2,\cdot\right)\right\} &= \frac{1}{T^2}\int_{-\frac{T}{2}}^{+\frac{T}{2}}\int_{-\frac{T}{2}}^{+\frac{T}{2}}\left[\int_{-\infty}^{+\infty}\tilde{s}_{x_kx_l}\left(f\right)e^{+j2\pi f(u-v)}df\right]\cdot \\ &\qquad e^{-j2\pi(f_1u-f_2v)}dudv \end{aligned} \tag{E.11}$$

$$\begin{aligned}&= \frac{1}{T^2}\int_{-\infty}^{+\infty}\int_{-\frac{T}{2}}^{+\frac{T}{2}}\int_{-\frac{T}{2}}^{+\frac{T}{2}}\tilde{s}_{x_kx_l}\left(f\right)e^{+j2\pi f(u-v)}\cdot \\ &\qquad e^{-j2\pi(f_1u-f_2v)}dudvdf \end{aligned} \tag{E.12}$$

$$\begin{aligned}&= \frac{1}{T^2}\int_{-\infty}^{+\infty}\tilde{s}_{x_kx_l}\left(f\right)\left[\int_{-\frac{T}{2}}^{+\frac{T}{2}}e^{+j2\pi u(f-f_1)}du\right]\cdot \\ &\qquad \left[\int_{-\frac{T}{2}}^{+\frac{T}{2}}e^{-j2\pi v(f-f_2)}dv\right]df \end{aligned} \tag{E.13}$$

Integrating the inner integrals,

$$E\left\{\tilde{z}_k\left(f_1,\cdot\right)\tilde{z}_l^*\left(f_2,\cdot\right)\right\} = \frac{1}{T^2}\int_{-\infty}^{+\infty}\tilde{s}_{x_kx_l}\left(f\right)\left[\frac{1}{j2\pi\left(f-f_1\right)}e^{+j2\pi u(f-f_1)}\right]_{-\frac{T}{2}}^{+\frac{T}{2}}\cdot \left[\frac{1}{-j2\pi\left(f-f_2\right)}e^{-j2\pi v(f-f_2)}\right]_{-\frac{T}{2}}^{+\frac{T}{2}}df \tag{E.14}$$

$$= \frac{1}{T^2}\int_{-\infty}^{+\infty}\tilde{s}_{x_kx_l}\left(f\right)\left(\frac{e^{+j\pi T(f-f_1)}-e^{-j\pi T(f-f_1)}}{j2\pi\left(f-f_1\right)}\right)\cdot \left(\frac{e^{+j\pi T(f-f_2)}-e^{-j\pi T(f-f_2)}}{j2\pi\left(f-f_2\right)}\right)df \tag{E.15}$$

Using Euler's Identity, Equation $(E.15)$ *becomes*

$$E\left\{\tilde{z}_k\left(f_1,\cdot\right)\tilde{z}_l^*\left(f_2,\cdot\right)\right\} = \frac{1}{T^2}\int_{-\infty}^{+\infty}\tilde{s}_{x_kx_l}\left(f\right)\left(\frac{j2\sin\left[\pi T\left(f-f_1\right)\right]}{j2\pi\left(f-f_1\right)}\right)\cdot \left(\frac{j2\sin\left[\pi T\left(f-f_2\right)\right]}{j2\pi\left(f-f_2\right)}\right)df \tag{E.16}$$

$$= \int_{-\infty}^{+\infty}\tilde{s}_{x_kx_l}\left(f\right)\left(\frac{\sin\left[\pi T\left(f-f_1\right)\right]}{\pi T\left(f-f_1\right)}\right)\cdot \left(\frac{\sin\left[\pi T\left(f-f_2\right)\right]}{\pi T\left(f-f_2\right)}\right)df \tag{E.17}$$

The two sinc functions can be approximated as zero outside a region on the order of $\frac{1}{T}$*. Within the non-zero region, the two sinc functions are essentially orthogonal so that*

$$E\left\{\tilde{z}_k\left(f_1,\cdot\right)\tilde{z}_l^*\left(f_2,\cdot\right)\right\} = \begin{cases} \int_{-\infty}^{+\infty}\tilde{s}_{x_kx_l}\left(f\right)\left(\frac{\sin[\pi T(f-f_1)]}{\pi T(f-f_1)}\right)\left(\frac{\sin[\pi T(f-f_2)]}{\pi T(f-f_2)}\right)df & f_1=f_2 \\ 0 & f_1\neq f_2 \end{cases} \tag{E.18}$$

But, for $f_1 = f_2$*,*

$$E\left\{\tilde{z}_k\left(f_1,\cdot\right)\tilde{z}_l^*\left(f_1,\cdot\right)\right\} = \int_{-\infty}^{+\infty}\tilde{s}_{x_kx_l}\left(f\right)\left(\frac{\sin\left[\pi T\left(f-f_1\right)\right]}{\pi T\left(f-f_1\right)}\right)^2 df \tag{E.19}$$

Assuming $\tilde{s}_{x_k x_l}(f)$ *can be approximated as a constant if it does not vary significantly over frequency ranges of the order* $\frac{1}{T}$ *rad/sec (i.e., the correlation time of* $\Psi_{x_k x_l}(\tau)$ *is short compared with* T*) and using*

$$\int_{-\infty}^{+\infty} \left(\frac{\sin\left[\pi T\left(f - f_1\right)\right]}{\pi T\left(f - f_1\right)} \right)^2 df = \frac{1}{T} \tag{E.20}$$

Equation $(E.19)$ *becomes*

$$E\left\{\tilde{z}_k\left(f_1, \cdot\right) \tilde{z}_l^*\left(f_1, \cdot\right)\right\} \approx \frac{1}{T} \tilde{s}_{x_k x_l}\left(f_1\right) \tag{E.21}$$

Substituting Equation $(E.21)$ *into Equation* $(E.18)$ *and choosing* $f_1 = f$ *and* $f_2 = f - \epsilon$*, the desired result is obtained.* ■

A notable result is that $\tilde{\mathbf{z}}(\cdot, \cdot)$ is an orthogonal process and is not stationary. (These results were not assumed; they are a consequence of $\mathbf{x}(\cdot, \cdot)$ being stationary.) Similar results can be found by assuming $\mathbf{x}(\cdot, \cdot)$ is periodic, $\tilde{\mathbf{z}}(f_k, \cdot)$ is the k^{th} Fourier coefficient found over one period T. Then, the autocorrelation kernel is found by letting the number of Fourier coefficients taken be large and the spacing between Fourier coefficient frequencies be small [45]. The time-gate function, $\prod$, defined in Equation $(E.3)$ includes a scaling factor of $\frac{1}{T}$, so that the results presented herein are consistent with that of previous research.

BIBLIOGRAPHY

[1] Abel, J. S. "A Divide and Conquer Approach to Least-Squares Estimation," *IEEE Transactions on Aerospace and Electronic Systems*, Vol. 26, No. 2, pp. 423-427, March 1990.

[2] Aloi, D. N. and F. Van Graas. "Ground-Multipath Mitigation via Polarization Steering of GPS Signal," *IEEE Transactions on Aerospace and Electronic Systems*, Vol. 40, No. 2, pp. 536-552, April 2004.

[3] Baniak, J., G. Baker, A. Cunningham, L. Martin. *Lockheed Martin Mission Systems Silent Sentry*$^{\text{TM}}$ *Passive Surveillance*, Gaithersburg, MD, June 1999.

[4] Bard, J. D. and F. M. Ham. "Time Difference of Arrival Dilution of Precision and Applications," *IEEE Transactions on Signal Processing*, Vol. 47, No. 2, pp. 521-523, 1999.

[5] Bard, J. D., F. M. Ham, and W. L. Jones. "An Algebraic Solution to the Time Difference of Arrival Equations," *Proceedings of the IEEE Southeastern Conference*, Tampa, FL, April 1996.

[6] Bartlett, M. S. *An Introduction to Stochastic Processes with Special References to Methods and Applications*, 1^{st} Edition, Cambridge University Press, London, 1955.

[7] Belove, C. *Handbook of Modern Electronics and Electrical Engineering*, John Wiley and Sons, 1986.

[8] Brockwell, P. J. and R. A. Davis. *Time Series: Theory and Methods*, 2^{nd} Ed., Springer-Verlag, NY, 1991.

[9] Carter, G. C, C. H. Knapp, and A. H. Nuttall. "Estimation of the Magnitude-Squared Coherence Function via Overlapped Fast Fourier Transform Processing," *IEEE Transactions on Audio Electro-Acoustics*, Vol. AU-21, pp. 337-344, August 1976.

[10] Cazzani, L., C. Colesanti, D. Leva, G. Nesti, C. Prati, F. Rocca, D. Tarchi. "A Ground-Based Parasitic SAR Experiment," *IEEE Transactions on Geoscience and Remote Sensing*, Vol. 38, No. 5, September 2000.

[11] Chan, Y. T. and K. C. Ho. "A Simple and Efficient Estimator for Hyperbolic Location," *IEEE Transactions on Signal Processing*, Vol. 42, pp. 1905-1915, August 1994.

[12] Cornwall, J. et al. *Non-GPS Methods of Geolocation*, The MITRE Corporation, Report to the Defense Advanced Research Projects Agency (DARPA), McLean, VA, January 2002.

[13] Counselman, C. C. III, *Method and System for Determining Position Using Signals from Satellites*, U. S. Patent No. 4,667,203, May 1987.

[14] Counselman, C. C. III, et al., "Miniature Interferometer Terminals for Earth Surveying: Ambiguity and Multipath with Global Positioning System," *IEEE Transactions on Geoscience & Remote Sensing*, Vol. GE-19, No. 4, pp. 244-52, October 1981.

[15] Davenport, W. B., Jr. *Probability and Random Processes*, McGraw-Hill, New York, NY, 1970.

[16] Doob, J. L. *Stochastic Processes*, John Wiley and Sons, New York, NY, 1953.

[17] Downs, G. *Interplanetary Navigation Using Pulsating Radio Sources*, NASA TR N74-34150, Pasadena, CA, October 1974.

[18] Eggert, R. J. *Evaluating the Navigation Potential of the National Television System Committee Broadcast Signal*, M.S. Thesis, Air Force Institute of Technology, Wright-Patterson AFB, OH, March 2004.

[19] Eggert, R. J. and J. F. Raquet, "Evaluating the Navigation Potential of the NTSC Analog Television Broadcast Signal," *2004 International Symposium on GPS/GNSS*, Sydney, Australia, December 2004.

[20] Fang, B. T. "Simple Solutions for Hyperbolic and Related Position Fixes," *IEEE Transactions on Aerospace and Electronic Systems*, Vol. 26, No. 5, pp. 748-753, September 1990.

[21] *Federal Communications Commission (FCC) Rules and Regulations*, Code of Federal Regulations, Government Printing Office, Vol. 3, Part 73, Subpart A, Washington, DC, 2002.

[22] *Federal Communications Commission (FCC) Rules and Regulations*, Code of Federal Regulations, Government Printing Office, Vol. 3, Part 73, Subparts B and C, Washington, DC, 2002.

[23] *Federal Communications Commission (FCC) Rules and Regulations*, Code of Federal Regulations, Government Printing Office, Section 73.319, Washington, DC, 2002.

[24] Federal Communications Commission (FCC) and the National Telecommunications and Information Administration (NITA), *Manual of Regulations and Procedures for Federal Radio Frequency Management,* available at `www.ntia.doc.gov`

[25] Fink, D. G. *Television Engineering*, 2^{nd} Ed., McGraw-Hill, New York, NY, 1952.

[26] Fisher, K. A. *Enhanced 911: Emergency Location and Indoor Global Position System*, Report to Michael A. Temple,, EENG 673 Air Force Institute of Technology, Wright-Patterson AFB, OH, Fall 2002.

[27] Foy, W. H. "Position Location Solutions by Taylor-Series Estimation," *IEEE Transactions on Aerospace and Electronic Systems*, Vol. 12, No. 2, pp. 187-194, March 1976.

[28] Friedlander, B. "On the Cramer-Rao Bound for Time Delay and Doppler Estimation," *IEEE Transactions on Information Theory*, Vol. IT-30, No. 3, May 1984.

[29] Globalstar Information Website: `http://www.ee.surrey.ac.uk/Personal···/L.Wood/constellations/globalstar.html`

[30] Globalstar Website: `www.globalstar.com`

[31] Goldman, S. *Frequency Analysis, Modulation and Noise*, McGraw-Hill, New York, NY, 1948.

[32] Griffiths, H.D., N.R.W. "Long, Television Based Bistatic Radar," *IEE Proceedings*, Part F, Vol. 133, No. 7, December 1996.

[33] Guner, A. *Ambiguity Function Analysis and Direct-Path Signal Filtering of the Digital Audio Broadcast (DAB) Waveform for Passive Coherent Location (PCL)*, M.S. Thesis, Air Force Institute of Technology, Wright-Patterson AFB, OH, March 2002.

[34] Hall, T. D., C. C. Counselman, and P. Misra. "Instantaneous Radiolocation Using AM Broadcast Signals," *Proceedings of ION-NTM*, Long Beach, CA, pp. 93-99, January 2001.

[35] Hall, T. D. *Radiolocation Using AM Broadcast Signals*, Ph.D. Dissertation, Massachusetts Institute of Technology, Cambridge, MA, September 2002.

[36] Haykin, S. *Communication Systems*, 3^{rd} Ed., John Wiley and Sons, New York, NY, 1994.

[37] Ho, K. C. and Y. T. Chan. "Solution and Performance Analysis of Geolocation by TDOA," *IEEE Transactions on Aerospace and Electronic Systems*, Vol. 29, No. 4, pp. 1311-1322, October 1993.

[38] Ho, K. C. and Y. T. Chan. "Geolocation of a Known Altitiude Object From TDOA and FDOA Measurements," *IEEE Transactions on Aerospace and Electronic Systems*, Vol. 33, No. 3, pp. 770-782, July 1997.

[39] Howland, P. E. "Target Tracking Using Television-based Bistatic Radar," *IEE Proceedings — Radar, Sonar, and Navigation*, Vol. 146, No. 3, June 1999.

[40] Howland, P. E. *Television Based Bistatic Radar*, Ph.D. Dissertation, School of Electronic and Electrical Engineering, University of Birmingham, England, September 1997.

[41] ICO Website: `www.ico.com`

[42] Iridium Satellite LLC Website: `www.iridium.com`.

[43] Kay, Steven M. *Fundamentals of Signal Processing–Estimation Theory*, Prentice Hall, 1993.

[44] Knapp, C. H. and G. C. Carter. "The Generalized Cross Correlation Method for Estimation of Time Delay," *IEEE Transactions on Acoustics, Speech, and Signal Processing*, Vol. ASSP-24, No. 4, pp. 320-327, August 1976.

[45] MacDonald, V. H. and P. M. Schultheiss. "Optimum Passive Bearing Estimation in a Spatially Incoherent Noise Environment," *The Journal of the Acoustical Society of America*, Vol. 46, No. 1-1, pp. 37-43, 1969.

[46] Maybeck, P. S. *Combined Estimation of States and Parameters for On-Line Applications*, Ph.D. Dissertation, Massachusetts Institute of Technology, Cambridge, MA, February 1972. Rep. T-557

[47] Maybeck, P. S. *Stochastic Models, Estimation, and Control*, Vol. 1, Navtech Book and Software Store, Arlington, VA, 1994.

[48] Maybeck, P. S. *Stochastic Models, Estimation, and Control*, Vol. 2, Navtech Book and Software Store, Arlington, VA, 1994.

[49] Mellen, G. T. *Simulation and Analysis of a Time Difference of Arrival GPS Jammer Location System*, M.S. Thesis, Air Force Institute of Technology, Wright-Patterson AFB, OH, March 2000. AFIT/GE/ENG/00M-11

[50] Mellen, G., M. Pachter, and J. Raquet. "Closed-Form Solution for Determining Emitter Location Using Time Difference of Arrival Measurements," *IEEE Transactions on Aerospace and Electronic Systems*, Vol. 39, No. 3, pp. 1056-1058, July 2003.

[51] Middleton, W. M. *Reference Data for Engineers: Radio, Electronics, Computer, and Communications*, 9^{th} Ed., Butterworth-Heinemann, 2002. ISBN: 0-7506-7291-9

[52] Miller, G. M. *Modern Electronic Communication*, Prentice Hall, 1988.

[53] Misra, P., and Per Enge. *Global Positioning System: Signals, Measurements, and Performance*, Ganga-Jamuna Press, Lincoln, MA, 2001.

[54] Pachter, M. and T. Nguyen. "An Efficient GPS Position Determination

Algorithm," *Navigation: Journal of the Institute of Navigation*, Vol. 50, No. 2, pp. 131-141, Summer 2003.

[55] Panter, P. F. *Modulation, Noise, and Spectral Analysis – Applied to Information Transmission*, McGraw-Hill, New York, NY, 1965.

[56] Papoulis, A. *Probability, Random Variables, and Stochastic Process*, 3^{rd} Ed., McGraw-Hill, New York, NY, 1991.

[57] Parkinson, B. W. and P. Axelrad. "Autonomous GPS Integrity Monitoring Using the Pseudorange Residual," *Navigation: Journal of the Institute of Navigation*, Vol. 35, No. 2, pp. 255-274, 1988.

[58] Parkinson, B. W. and J. J. Spilker. *Global Positioning System: Theory and Applications*, Vol. 1, American Institute of Aeronautics and Astronautics, Inc., Washington, DC, 1996.

[59] Priestley, M. B. *Spectral Analysis*, Vols. 1 and 2, Academic Press, NY, 1991.

[60] Raquet, J. F. *Advanced GPS Theory and Applications*, Classnotes, EENG 633, Air Force Institute of Technology, Wright-Patterson AFB, OH, p. 11-147, Summer 2002.

[61] Ringer, M.A., G.J. Frazer, S.J. Anderson. *Waveform Analysis of Transmitters of Opportunity for Passive Radar*, DSTO Electronics and Surveillance Research Laboratory, Salisbury, Australia, June 1999.

[62] Rabinowitz, M. and J. Spilker. *Positioning Using the ATSC Digital Television Signal*, Whitepaper, Rosum Corporation, Redwood City, CA, August 2001.

[63] Rabinowitz, M. and J. Spilker. "The Rosum Television Positioning Technology," *ION 59th Annual Meeting/CIGTF 22nd Guidance Test Symposium*, Albuquerque, NM, pp. 528-541, June 2003.

[64] Rudin, W. *Real and Complex Analysis*, 3^{rd} Ed., McGraw-Hill, New York, NY, pg. 164, 1986.

[65] Sahr, J. D., F. D. Lind. "The Manatash Ridge Radar: A Passive Bistatic Radar for Upper Atmospheric Radio Science," *URSI 96*, Preprint, University of Washington, Seattle, WA, 1996.

[66] Satellite Constellation Visualization Website: `http://savi.sourceforge.net/`

[67] Scales, W. C. and R. Swanson. "Air and Sea Rescue via Satellite Systems," *IEEE Spectrum*, pp. 48-52, March 1984.

[68] Shanmugan, K. S. and A. M. Breipohl. *Random Signals: Detection, Estimation, and Data Analysis*, John Wiley and Sons, 1988.

[69] Sheikh, S. I., et al. "The Use of x-Ray Pulsars for Spacecraft Navigation," *14^{th} AAS/AIAA Space Flight Mechanics Conference*, Paper #04-109, Maui, HI, February, 2004.

[70] Sklar, B. *Digital Communications—Fundamentals and Applications*, 2^{nd} Ed., Prentice Hall PTR, NJ, 2001.

[71] Skolnik, M. *Introduction to Radar Systems*, 3^{rd} Ed., McGraw-Hill, New York, NY, 2000.

[72] Smith, J. O. and J. S. Abel. "Closed-form Least Squares Location Estimation from Range-Difference Measurements," *IEEE Transactions on Acoustics, Speech, and Signal Processing*, Vol. 35, pp. 1661-1669, December 1987.

[73] Swokowski, E. W. *Calculus*, 5^{th} Ed., PWS-Kent Publishing Company, Boston, MA, pg. 752, 1991.

[74] Taylor, J. and M. Ryba. "High Precision Timing of Millisecond Pulsars," *The Astrophysical Journal*, Vol. 371, 1991.

[75] Titchmarsh, E. C. *Introduction to the Theory of Fourier Integrals*, Oxford University Press, London, 1948.

[76] Titterton, D. H. and J.L. Weston. *Strapdown Inertial Navigation Technology*, IEE Books, Peter Peregrinus Ltd, UK, 1997.

[77] Torrieri, D. J. "Statistical Theory of Passive Location Systems," *IEEE Transactions on Aerospace and Electronic Systems*, Vol. 20, pp. 183-198, March 1984.

[78] Van Trees, H. L. *Detection, Estimation, and Modulation Theory*, John Wiley and Sons, New York, NY, 1968.

[79] Veth, M. and J. Raquet. "Precision Navigation Using Optical Images and INS," *2005 Joint Navigation Conference, 30th JSDE Conference*, Orlando, FL, April 2005.

[80] White, S. C. and N. C. Beaulieu. "On the Application of the Cramer Rao and Detection Theory Bounds to Mean Square Error of Symbol Timing Recovery," *IEEE Transactions on Communications*, Vol. 40, No. 10, pp. 1635-1643, October 1992.

[81] Willis, N. J. *Bistatic Radar*, Artech House, 1991.

[82] Zeira, A. and A. Nehorai. "Frequency Domain Cramer-Rao Bound for Gaussian Processes," *IEEE Transactions on Acoustics, Speech, and Signal Processing*, Vol. 38, No. 6, June 1990.

[83] Zeira, A. and P. M. Schultheiss. "Realizable Lower Bounds for Time Delay Estimation," *IEEE Transactions on Signal Processing*, Vol. 41, No. 11, pp. 3102-3113, November 1993.

[84] Zeira, A. and P. M. Schultheiss. "Realizable Lower Bounds for Time Delay Estimation: Part 2—Threshold Phenomena," *IEEE Transactions on Signal Processing*, Vol. 42, No. 5, pp. 1001-1007, May 1994.

Vita

Captain Kenneth A. Fisher received the degree of Bachelor of Science in Electrical Engineering from Ohio Northern University in May 1997. He received his commission through the Air Force ROTC program in May 1997 and reported directly to the Air Force Institute of Technology (AFIT). In March 1999, he was awarded the Masters of Science in Electrical Engineering from AFIT and published a thesis entitled, "Multiple Model Adaptive Estimation with Filter Spawning." Captain Fisher then worked as a spectral analyst in developing and testing hyperspectral algorithms for the Advanced Branch, MASINT Division, National Air Intelligence Center (NAIC), Wright-Patterson AFB, OH. In September 2001, he returned to AFIT in pursuit of his Doctor of Philosophy degree.